QUANTIFYING SALINIZATION OF THE RIO GRANDE USING ENVIRONMENTAL TRACERS

by

Suzanne Kemp Mills

Submitted in Partial Fulfillment
of the Requirements for the Degree of
Master of Science in Earth and Environmental Science
with Thesis in Hydrology

New Mexico Institute of Mining and Technology
Socorro, New Mexico
December, 2003

ABSTRACT

The Rio Grande has undergone a consistent pattern of salinization with distance downstream for the past century, but its causes have remained elusive. To reveal the causes of this salinization, 100 years of historical data as well as data from high-spatial-resolution synoptic sampling campaigns from 2000-2003 were analyzed. During these three years, Rio Grande salinization was manifested by a 50-fold increase in total dissolved solids between the river headwaters in Colorado and the U.S. - Mexico border. Environmental tracer data from August 2001 and January 2002, including $\delta^{18}O$ and δD, chloride and bromide concentrations, and the $^{36}Cl/Cl$ ratio, indicate that a significant percentage of Rio Grande salinization is due to inflow of deep sedimentary brines. A simple chloride and bromide instantaneous mass balance model for August 2001 emphasizes the significance of salt input due to deep brine discharge to the river, particularly at the downstream ends of local sedimentary basins of the Rio Grande rift. Two water- and salt- instantaneous mass balance models of the Rio Grande for August 2001 and January 2002 including major tributaries and agricultural return flows suggest that inflow of natural tributaries, deep brine, and wastewater treatment plant effluent and Elephant Butte Reservoir dynamics account for 25%, 37%, 26% and 9% of the chloride burden increase

between the headwaters and Ft. Quitman, TX, respectively. These models also indicate that evapotranspiration accounts for 55% of increase in chloride concentration, with natural tributaries, deep brines, and wastewater treatment plant effluent respectively accounting for 3%, 30% and 13% of the chloride concentration increase along this distance. Historical analysis and environmental tracer data suggest that the role of the irrigated agricultural systems in influencing salinization of the Rio Grande is their interception of deep basin brines, rather than flushing of shallow saline ground water or evapotranspirative concentration as previously thought. This indicates that Rio Grande salinization is geologically controlled by structures serving as brine conduits, and is anthropogenically facilitated by agricultural drains as well as reservoir operations and inflow of wastewater effluent.

ACKNOWLEDGMENT

The author would first like to acknowledge Sustainability of semiArid Hydrology and Riparian Areas (SAHRA), a National Science Foundation Science and Technology Center, for providing funding for this research. Many thanks and much appreciation are also given to all the professionals at federal, state and local agencies who provided access to data and information for this research. In particular the author would like to thank Scott Anderholm (USGS), Steve Baer (CDWR), Steve Baumgarn (NMED), Linda Beal (USGS), Laura Bexfield (USGS), Jeff Burkett (RRWWTP), Craig Cotton (CDWR), Danny Carrillo (EBID), Angel Colon (EPID), David Garcia (NWWWTP), David Gensler (MRGCD), Steve Glass (SWRP), Javier Grajeda (USBR), John Hawley, Ella Mae Herrera (USBR), Ed Kandl (USBR), Jay Kline (HCCRD), James Narvaez (EBID), Mike Landis (USBR), William Quinn (EPU), Travis Smith (SLVID), Gail Stockton (USACE), Des Stuart (LCWWTP), Terry Thomas (NMBGMR), and Kurian Varughese (LCWWTP). The author would also like to thank the masters advisory committee including Fred Phillips, Jan Hendrickx, James Hogan, and Rob Bowman for providing valuable help in the research process. Samples were analyzed by the New Mexico Bureau of Geology and Mineral Resources, PRIME Lab at Purdue University, and at the University of Arizona.

This thesis was typeset with LaTeX[1] by the author.

[1] LaTeX document preparation system was developed by Leslie Lamport as a special version of Donald Knuth's TeX program for computer typesetting. TeX is a trademark of the American Mathematical Society. The LaTeX macro package for the New Mexico Institute of Mining and Technology thesis format was adapted from Gerald Arnold's modification of the LaTeX macro package for The University of Texas at Austin by Khe-Sing The.

TABLE OF CONTENTS

LIST OF TABLES

LIST OF FIGURES

This thesis is accepted on behalf of the faculty of the Institute by the following committee:

_____

Fred M. Phillips, Advisor

_____

_____

_____

_____

Suzanne Kemp Mills Date

CHAPTER 1

INTRODUCTION

1.1 The problem of river salinization

Semiarid and arid region rivers worldwide suffer from salinization between their headwaters and downstream areas, often exhibiting over an order of magnitude increase in total dissolved solids (TDS) concentration [*Fattah and Baki*, 1980; *Ghassemi et al.*, 1995]. Many of these rivers are used for irrigation, and river salinization brings the attendant threat of salinization of irrigated lands. This may result in lowered crop yields or even necessitate removing agricultural land from use. Understanding causes of salinization is therefore essential to protecting vulnerable yet important irrigated land, which accounts for 85% of worldwide crop production but amounts to only 15% of the world's total agricultural land [*Postel*, 1999].

The Rio Grande is one such river that runs through the semiarid southwestern United States. It experiences a two-order-of-magnitude salinity increase between its headwaters in the San Juan mountains of Colorado and the U. S. - Mexico border region near Ft. Quitman, Texas [*Phillips et al.*, 2003]. Along much of this nearly 1200 km of river length, irrigated farms depend on river water. Yet in the Mesilla valley, one of New Mexico's most productive agricultural regions, the TDS concentration of the Rio Grande is often near 1000 mg L^{-1}, more than an order of magnitude higher than headwaters con-

centrations [*Lippincott*, 1939; *Wilcox*, 1957; *Hendrickx*, 1998]. Furthermore, large urban areas like Albuquerque and El Paso rely on river water for municipal and industrial purposes. These surface water needs are rapidly increasing with the depletion of groundwater that has supplied these cities in the past. These manifold uses of the river make its water quality of significant concern to Rio Grande valley residents.

1.2 Salt inputs and outputs of a typical river system

Salt movement through a river system is governed by many hydrogeologic and anthropogenic processes [*Berner and Berner*, 1996]. Salinization occurs both by salt addition and by concentration of salts due to water removal (Figure 1.1).

Cyclic salts are contributed continuously and diffusely across a river basin by ongoing natural processes. Processes that contribute cyclic salts include mineral weathering and atmospheric deposition. Atmospheric deposition occurs by both wet and dry precipitation. Geologic processes that contribute salts more locally include upwelling of subsurface saline brines or geothermal waters.

Salt may also be added anthropogenically to the surface water system. Wastewater treatment plant effluent, which contains dietary salts, enters a river at the point of effluent discharge. Road salts and fertilizers are generally applied over a large area of urban or agricultural land, and enter the surface water system over a broad area as well. Industrial salts may also contribute to river salinization and may be contributed locally or diffusely.

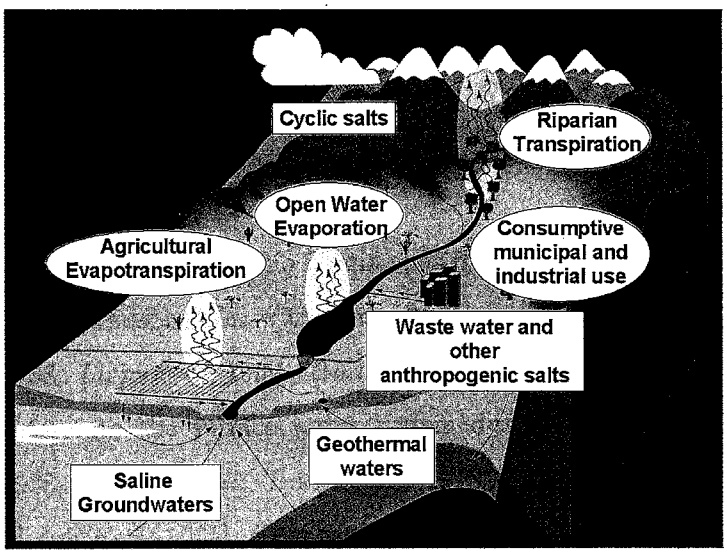

Figure 1.1: Sources of salts and processes that concentrate them within a typical river system. Salt sources are outlined with rectangles and processes that concentrate salts are outlined with ovals. Figure courtesy of James Hogan, University of Arizona.

Processes that remove water from the river concentrate these added salts. Evapotranspiration in riparian and agricultural areas, municipal consumptive use and industrial consumptive use of water increase salinization in this way. Anthropogenic manipulation of a river system can aid salinization by exacerbating natural salinizing processes. Large reservoirs and irrigation canal and drainage systems increase evaporation from the river. An irrigation system also modifies movement of water and salts in the river system by increasing the surface area for interaction between surface and ground waters.

1.3 Purpose and scope of thesis

Salinization of the Rio Grande has previously been attributed to progressive evapotranspiration with agricultural use and re-use of river waters [*NRC*, 1938; *Lippincott*, 1939; *Trock et al.*, 1978], flushing of shallow saline groundwater into the surface water system during the process of irrigation [*NRC*, 1938; *Wilcox*, 1957; *Trock et al.*, 1978], and erosional processes [*van-Denburgh and Feth*, 1965]. This thesis investigates the alternative hypothesis that a significant part of river salinization is in fact geologically controlled, and can be ascribed to localized deep brine fluxes controlled by geologic structures and perhaps by geothermal activity [*Phillips et al.*, 2003].

In order to test this hypothesis and to investigate the movement of water and salts through the Rio Grande system during both the irrigation and non-irrigation seasons, during every January and August since the year 2000 researchers from New Mexico Tech and the University of Arizona conducted a synoptic sampling of the Rio Grande. These trips included sampling of major drains and tributaries. Between the headwaters in Colorado and Ft. Quitman,

TX, samples for water quality analysis were collected at a high spatial resolution of about 10 km. As well as being analyzed for standard parameters in the field, samples were analyzed in the lab for a wide variety of isotopes and dissolved inorganic and organic constituents. This study focuses on analyzing and modeling data collected for conservative environmental tracers including chloride, bromide, chlorine isotopes, and stable isotopes of hydrogen and oxygen.

This thesis first explains the natural hydrogeologic setting of the Rio Grande basin, followed by a description of anthropogenic alterations of the hydrologic system. Next, previous studies of salinization of the Rio Grande are summarized and then historical discharge, chloride concentration, and chloride burden data are analyzed and briefly compared with field data. After a discussion of the theory of conservative environmental tracers, the chloride, bromide, and isotope data from one week in August 2001 and one week in January 2002 are analyzed in detail. Following that, a simple chloride and bromide mass-balance model for August 2001 is introduced to gain a general understanding of the pattern of salinization due to deep ground water addition. Then a detailed water, chloride, and bromide mass balance model is explained and analyzed for both August 2001 and January 2002, and deep ground water discharges and salt fluxes are calculated based on this model. Finally, basin-scale estimates of salt concentration and contribution from major salinizing processes are calculated in order to show the relative role of deep ground water in Rio Grande salinization.

CHAPTER 2

DESCRIPTION OF HYDROGEOLOGIC AND BIOLOGIC FEATURES OF THE RIO GRANDE BASIN

2.1 General basin characteristics

Within the study area, the Rio Grande drains over 118,880 km^2 of southern Colorado, New Mexico, and western Texas. Average annual precipitation ranges from less than 20 cm in the semiarid valley floor to more than 120 cm in the headwaters mountains. Rio Grande water is derived mostly from spring snowmelt in the southern Rocky mountain ranges between April and May, though heavy storms during the summer monsoon season in July and August also contribute runoff [*Levings et al.*, 1998]. Snowmelt runoff originates in the 4300-meter-high San Juan mountains of southern Colorado as well as in the Sangre de Cristo and the Jemez mountains of northern New Mexico (Figure 2.1). Major gaged tributaries of the Rio Grande in southern Colorado include Goose Creek, the South Fork of the Rio Grande, Pinos Creek, and the Conejos River. Gaged tributaries in northern and central New Mexico include Costilla Creek, the Red River, the Rio Pueblo de Taos, the Rio Hondo, Embudo Creek, the Rio Chama, the Santa Cruz River, the Santa Fe River, Galisteo Creek, the Jemez River, the Rio Puerco, and the Rio Salado. The latter two tributaries are ephemeral and tend to run dry at times other than the spring runoff and the summer monsoon seasons. Between the Rio Salado

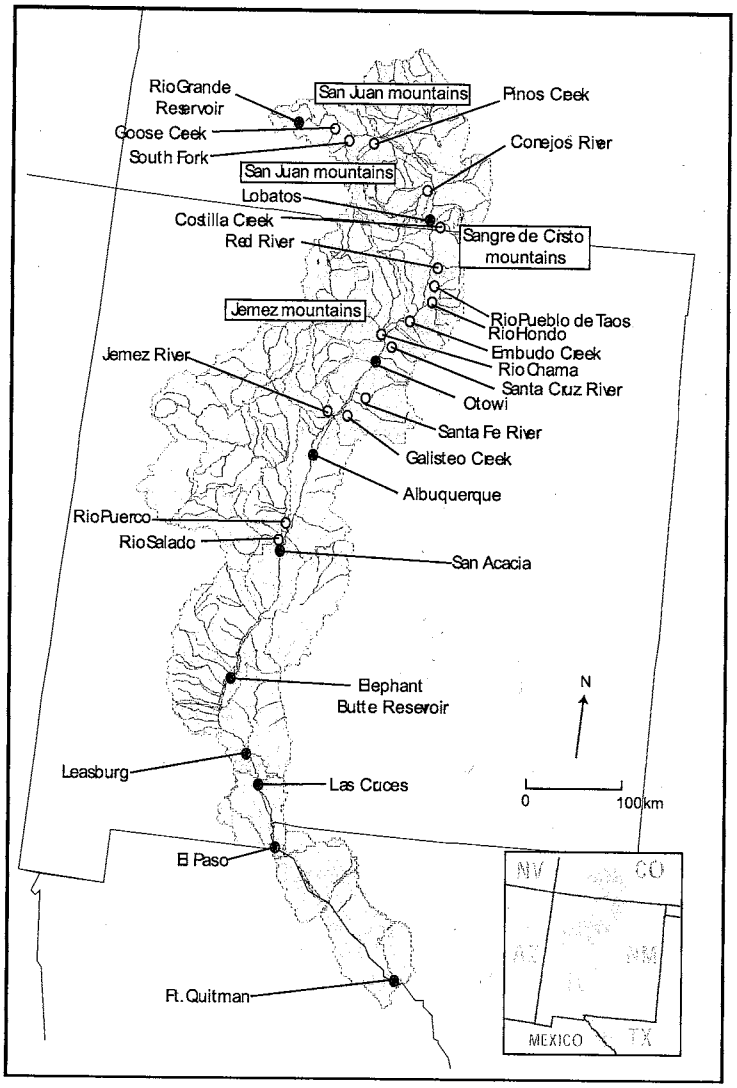

Figure 2.1: Major snowmelt-producing headwaters mountain ranges and gaged tributaries of the Rio Grande, headwaters - Ft. Quitman, Texas. Yellow circles indicate locations of tributary gages; blue circles show locations of some main stem Rio Grande gaging stations for reference.

and the downstream end of the study area at Ft. Quitman, Texas, the Rio Grande does not have any natural tributaries that run frequently enough to be gaged.

The Rio Grande valley is characterized by riparian, urban, and agricultural land use. Riparian evapotranspiration (ET) is poorly quantified, though between Otowi and Elephant Butte Reservoir ET is thought to consume an average of 8.9 m^3 s^{-1}, which is 37% of total river depletions [*Papadopulos and Associates*, 2000]. *Veenhuis* [2002] estimated winter ET loss to be 0.06 - 0.12 m^3 s^{-1} between Bernalillo and the Rio Bravo bridge in Albuquerque, and summer ET loss to be 0.23 - 1.5 m^3 s^{-1} between Bernalillo and Isleta.

2.2 Hydrogeologic setting

The Rio Grande flows through the Rio Grande rift, a 26-million-year-old fault-bounded structure characterized by uplifted blocks on its east and west sides and down-dropped alluvial-filled grabens in the center (Figure 2.2). The alluvial basins and their bounding blocks are arranged en echelon, with each basin and uplift offset to the east of the basin to its south. Accommodation zones between basins are characterized by bedrock surface outcrops, through which the Rio Grande has carved narrow channels. Rifting is still active and is accompanied by high heat flow and geothermal activity [*Wilkins*, 1998].

The rift is bounded on the north, east, and west by Paleozoic and Mesozoic sedimentary rocks and Tertiary and Quaternary volcanics. These rocks are generally much less permeable than the rift basin fill. The thousands of feet of Miocene to Holocene sediments and volcanics that fill the basin com-

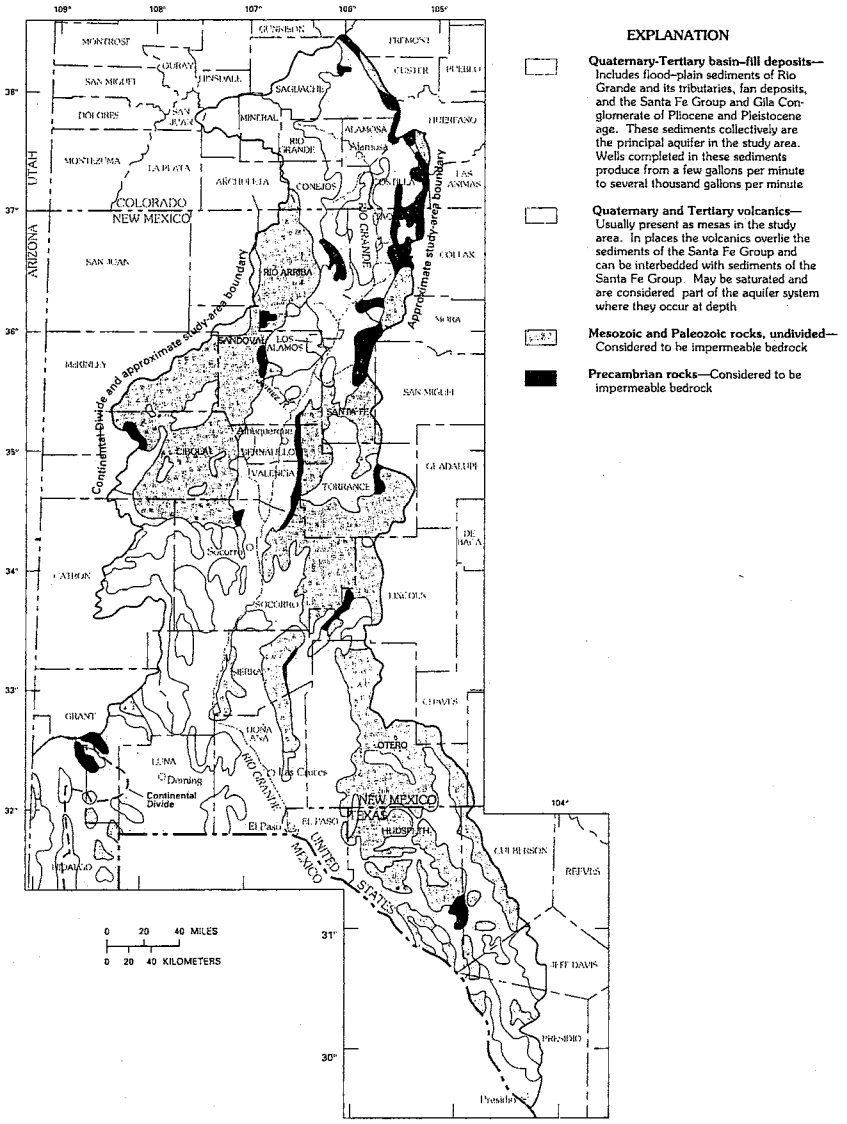

Figure 2.2: Geology of the Rio Grande rift. From *Wilkins* [1998].

prise the early-rifting Popotosa Formation and the Santa Fe Group. Santa Fe Group sediments are unconsolidated to moderately consolidated, ranging from very coarse- to very fine-grained lithologies. The Santa Fe Group, along with younger basin-edge fan deposits and river valley alluvium, forms the major basin-fill aquifer, which is hydraulically connected, anisotropic, and heterogeneous [*Wilkins*, 1998].

Six major basins underpin the structure of the study area: the San Luis basin, the Española basin, the Albuquerque basin, the Socorro basin, the Palomas basin, and the Mesilla basin (Figure 2.3). Of these basins, the San Luis basin is one of the deepest, extending 6.4 km into the subsurface near basin-bounding faults. In the vicinity of the river, basin depths range from 3500 m near Alamosa to less than 2500 m toward the distal end of the basin [*Keller and Cather*, 1994]. East of the Rio Grande at the distal end of the San Luis basin, *Hanna and Harmon* [1989] observed that the Paleozoic and Precambrian bedrock rises from about 1000 m depth to only 300 m depth near the Conejos River. The northern part of the San Luis basin (the San Luis Closed basin) is hydraulically closed in terms of both surface and ground water [*Wilkins*, 1998].

The Taos plateau, composed of several hundred feet of volcanics, separates the San Luis basin from the Española basin to the south. The depth of the Española basin is unknown, though it has been suggested that there is unquantified significant subsurface geohydrologic connection between the southern end of the Española basin and the Albuquerque basin to the south [*McAda and Barroll*, 2002]. The La Bajada escarpment and a narrow bedrock constric-

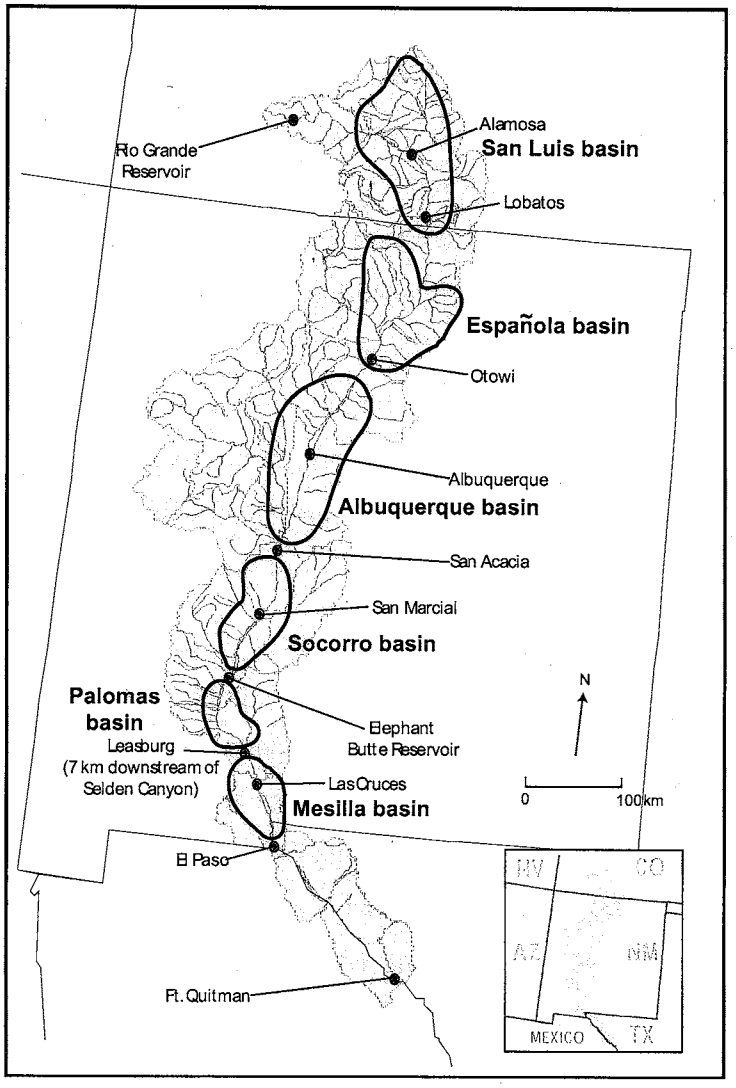

Figure 2.3: Basins of the Rio Grande rift, Colorado, New Mexico, and Texas. Basin boundaries in thick black lines are estimated from *Wilkins* [1998]. Blue circles show main stem Rio Grande gaging stations.

tion at Embudo mark the distal end of the Española basin and the northern end of the Albuquerque basin. Albuquerque basin fill reaches 4300 - 5500 m in thickness locally [*McAda and Barroll*, 2002; *Wilkins*, 1998]; at the distal end of the basin the depth to Precambrian rocks decreases from 3000 m to near land surface at San Acacia [*Wilkins*, 1998]. San Acacia marks the convergence of faults and bedrock highs that form the constriction between the Albuquerque and Socorro basins, across which *Wilkins* [1998] observed a small amount of groundwater flow. *Reiter* [2003] noted a high temperature anomaly in a well near the southern end of the Albuquerque basin that is indicative of ground water movement to the surface, perhaps from great depth. *Anderholm* [1987] reported high-chloride ground waters at the southern end of the Albuquerque basin that discharge to the Rio Grande and/or to the Socorro basin to the south.

The Socorro basin shares a structure similar to the other alluvial basins. The depth to Precambrian bedrock in the basin is deepest near the basin center and decreases with distance downstream until the distal end of the basin at the narrows above Elephant Butte Reservoir [*Anderholm*, 1987]. The depth of the Socorro basin is unknown. High chloride concentrations in northern Socorro basin ground water are attributed to inflow of deep ground waters from the Albuquerque basin [*Anderholm*, 1987]. Ground waters in the middle Socorro basin are relatively dilute due to mixing with infiltrated irrigation water, and due to inflow of dilute waters from the La Jencia basin to the west. High-chloride, high-sodium ground water is also found at the southern end of the Socorro basin. It has been suggested that this water originates from geothermal sources in the Socorro Peak area or as a deep-basin

brine[*Anderholm*, 1987]. The bedrock constriction at the narrows above Elephant Butte Reservoir marks the distal end of the Socorro basin and the northern end of the Palomas basin. The Palomas basin, which underlies the Rincon valley, has an unknown depth but is assumed to be similar to the adjacent Mesilla basin to the south.

The southernmost basin in the study area, the Mesilla basin, extends from the bedrock constriction at Selden canyon (the distal end of the Palomas basin) to the El Paso narrows. The depth of the basin-fill sediments in the Mesilla basin decreases from about 2000 m in the deepest part of the basin to 1000 m at its shallower distal end [*Hawley and Lozinsky*, 1992]. *Wilkins* [1998] noted a downward hydraulic gradient at the northern end of the basin and an upward gradient at the southern end. *Frenzel et al.* [105 pp. plus plates, 1992] and *Wilson et al.* [1981] also documented an upward movement of ground water at the southern end of the Mesilla valley.

Throughout most of the study area, the Rio Grande is hydraulically connected to the shallow aquifer of the river floodplain as well as the deeper basin-fill aquifer formed by the Santa Fe Group. In gaining reaches of the river, water is added to the river by seepage from the shallow aquifer. *Winograd* [1959] identified a gain of 2.7 $m^3\ s^{-1}$ to the river from groundwater seepage between Lobatos and the mouth of the Red River. *Wilson et al.* [1981] identified a gain of 0.62 $m^3\ s^{-1}$ between the outlet of Caballo Reservoir and Hatch, and a small unquantified gain at the southern end of Selden canyon.

Water is removed from the river by seepage to the shallow aquifer in several places, notably between Bernalillo and San Marcial as well as in the

Mesilla valley. This water is either intercepted by the agricultural drains that return the water to the river further downstream, or is lost to the surface water and shallow aquifer system entirely and recharges the deeper Santa Fe aquifer. *Veenhuis* [2002] reported an average winter loss of 6 m^3 s^{-1} between Bernalillo and the Rio Bravo bridge in Albuquerque, of which 2.5 m^3 s^{-1} is lost to the deep aquifer. *Veenhuis* [2002] also statistically summarized previous studies, calculating flow losses to the deep aquifer of 1.9 - 7.0 % in the winter and 5.9 - 6.4 % in the summer. Further downstream, *Papadopulos and Associates* [2002a] measured a summer seepage loss from the river between San Acacia and San Marcial of 7-10 m^3 s^{-1}, and found no relationship between the magnitude of river discharge and the seepage rate. Near the southern end of the study area, *Wilson et al.* [1981] noted winter seepage losses from the river of 0.9 m^3 s^{-1} between Las Cruces and the Mesilla diversion dam and of 0.6 m^3 s^{-1} between the return points of the Del Rio and Montoya drains to the river.

CHAPTER 3

DESCRIPTION OF THE ANTHROPOGENIC FEATURES OF THE RIO GRANDE

3.1 Chapter summary

The following chapter first summarizes water rights and the history of water use in the Rio Grande basin, and then describes the man-made structures and systems on the Rio Grande from north to south, starting at the headwaters. This description also indicates the spatial availability of gaging data for agricultural diversions and return flows along the river. This thesis does not discuss dams, diversion structures, or other man-made constructions on tributaries of the Rio Grande.

3.2 Water rights and water appropriation in the Rio Grande basin

In general, the right to use water in the Rio Grande valley today is determined by the doctrine of prior appropriation, summarized by the catchphrase "first in time, first in right." Under this doctrine, the first person to divert water from the river and put it to beneficial use has the most senior water right. Those that arrive later to use water may claim junior water rights. By the doctrine of prior appropriation, the most senior water user is entitled to his entire water right before any water is delivered to junior water users. Each water right claimant is assigned a "priority date" corresponding to the first time of beneficial use, and each water user is theoretically entitled to a certain

amount of water. However, adjudication, the process by which this amount is legally confirmed, requires land surveys and installation of flow gages and is therefore time-consuming and costly. The state of Colorado has invested heavily in adjudication, and as a result major agricultural diversions from the river have been gaged for over 50 years and water rights are fully adjudicated. In contrast, it is estimated that over 85% of agricultural water rights in New Mexico remain unadjudicated today, in part due to lack of gage installation and flow measurements [*Johnson and Shomaker*, 2002]. The extent of adjudication directly reflects the data availability in the valley, as will be discussed further in following sections.

Though individual water rights describe small-scale transfers of water out of the river, water appropriation at the basin-scale is governed by interstate and international agreements. The most widely reaching of these is the Rio Grande Compact, a 1938 agreement between Colorado, New Mexico, Texas, and Mexico. This compact calls for a flexible system of water deliveries between the three states and two nations based on annual river discharge at index gaging stations. Colorado is responsible for delivering a varying percentage of water in the Rio Grande at Del Norte and in Costilla Creek at Mogote to New Mexico depending on the climatic conditions. Similarly, New Mexico must deliver a varying percentage of water to stakeholders downstream of Elephant Butte Reservoir based on flow of the Rio Grande at Otowi [*Johnson and Shomaker*, 2002]. Water quality requirements of the compact are vague.

3.3 Summary of irrigation systems, dams, and reservoirs on the main stem Rio Grande

Manipulation of Rio Grande water for anthropogenic purposes probably began around the year 1300 during a period of drought, which spurred a mass migration of Native Americans to the floodplains of the river and its tributaries [*Scurlock*, 1998]. The pueblo culture that sprang up around the Rio Grande depended in part on farming, involving limited-scale use of man-made ditches and canals. With the Spanish conquest of New Mexico beginning in the 16^{th} century, agricultural activities expanded and complex irrigation networks including diversion dams were constructed throughout arable lands along the river. These systems, called acequias, were operated in the traditional Spanish manner of fairly equitable water-sharing among parciantes, or stakeholders, regulated by a head administrator called a mayordomo [*Scurlock*, 1998]. These systems continue to operate on the Rio Grande today, particularly in northern New Mexico between the Colorado border and Cochiti Lake. The current large-scale system of water diversion and storage on the main stem Rio Grande did not begin until 1915, when the United States Bureau of Reclamation (USBR) began storing water behind Elephant Butte dam. Today, one dam owned by an irrigation district (Rio Grande Reservoir) and three major federally owned dams on the main stem Rio Grande (Cochiti, Elephant Butte, and Caballo) store and release water for irrigation and flood prevention. Furthermore, six diversion dams owned and operated by local irrigation districts (Angostura, Isleta, San Acacia, Percha, Leasburg, and Mesilla) control diversions from the Rio Grande into the surrounding agricultural lands. Two more diversion dams (American and International) operated by the Interna-

tional Boundary and Water Commission (IBWC) partition Rio Grande waters between the United States and Mexico. These districts gage most of their diversions from the river; however, there are still a large number of ungaged river diversions, particularly in unadjudicated areas of New Mexico. Furthermore, agricultural return flows are unregulated by water right appropriations along the entire length of the river, and therefore are not often gaged.

3.3.1 Headwaters to Colorado-New Mexico state line

Spanning the river high in the headwaters and above all major settlement and agricultural development, the Rio Grande Reservoir dam is the oldest and most upstream major dam on the main stem Rio Grande. Construction began on this dam in 1908, and water storage behind the dam began in 1911. The capacity of Rio Grande Reservoir itself is 52,000 acre-feet (64 million m^3). The dam is owned and operated by the San Luis Valley Irrigation District (SLVID), an organization that was created by Colorado state statute in 1905. During the winter from November through March, the SLVID stores runoff for release during the irrigation season between April 1^{st} and October 31^{st}. Transmountain flows piped from the western side of the continental divide are also stored behind Rio Grande Reservoir dam. The SLVID operates Rio Grande Reservoir in agreement with the six major mutual ditch companies in the San Luis valley, the U. S. Fish and Wildlife Service (which runs the Alamosa National Wildlife Refuge), and other water users [*Travis Smith, SLVID,* personal communication 2003].

The San Luis Valley Project is the only federally mandated water project on the Rio Grande in Colorado. Authorized by Congress in 1940,

its main purposes are to assist Colorado in meeting its Rio Grande Compact obligations to New Mexico and Texas as well as to help the United States meet its commitments to Mexico under the Treaty of 1906. In terms of flows directly into the Rio Grande today, the most relevant part of the San Luis Valley Project is the Closed Basin Division, authorized by Congress in 1972. This system of wells and canals pump and divert water from the Closed Basin into the Rio Grande via the Closed Basin Canal, also called the Franklin Eddy Canal [*CDWR*, 2003]. As well as assisting fulfillment of compact and treaty obligations, the Closed Basin Project allows recovery of shallow ground water that would otherwise be lost to evapotranspiration [*Ella Mae Herrera, USBR,* personal communication 2003]. In order to be included as a water delivery to New Mexico under the Rio Grande Compact, water discharged from the Closed Basin Canal must have a TDS concentration not exceeding 350 mg L^{-1} [*Powell*, 1958]. The Closed Basin Canal is gaged by the Colorado Division of Water Resources (CDWR) and water quality data is collected by the USBR.

An extensive network of agricultural canals and drains crisscrosses the San Luis valley. Various independent parts of this network are operated by the SLVID and the six mutual ditch companies mentioned above, though the CDWR has been responsible for gaging them since the 1950's. Currently, gaged diversions include (upstream to downstream) the Anaconda Ditch, the Minor Ditch, the Rio Grande Canal, the Prairie Ditch, the Monte Vista Canal, the Rio Grande and Piedra Valley Ditch, the Centennial Ditch, the Excelsior Ditch, the Westside Ditch, and the Chicago Ditch. Several other diversions were monitored historically but are no longer monitored. Return flows in the San Luis valley remain ungaged.

3.3.2 Colorado - New Mexico state line to Cochiti Lake

Just downstream of the Colorado-New Mexico state line, the Rio Grande enters the 150-m-deep Rio Grande gorge. From here until the terminus of the gorge near Española, the river flows naturally without manipulation by man. From the gorge terminus to just downstream of the confluence of the Rio Grande and the Rio Chama, river diversions are controlled by numerous small, independent acequia associations. These associations have oldest priority dates in the state, with water rights dating back to the Spanish conquest. Immediately downstream of these historically Hispanic agricultural areas, a series of Native American Pueblos lines the Rio Grande until the remote and unirrigated White Rock canyon just upstream of Cochiti Lake. Many water rights in northern New Mexico remain unadjudicated [*OSE*, 2003], and acequia and Native American diversions and return flows are ungaged.

3.3.3 Cochiti Lake to Elephant Butte Reservoir

Completed in 1970 with money appropriated by Congress in the late 1940's, Cochiti dam is owned and operated by the United States Army Corps of Engineers (USACE). This 76.5-m high, 8-km long earthfill dam was created for the purpose of regulating floodwater and sediment flushed downstream from spring headwater snowmelt [*USACE*, 2003]. Additionally, some water piped from the west side of the continental divide by the USBR for Albuquerque (San Juan-Chama project water) is stored behind Cochiti dam to maintain a recreational lake with a 1200-acre (4356 m^2) surface area [*USBR*, 2003a]. The long-term residence time of Cochiti Lake (calculated by dividing average monthly storage by average monthly discharge from the reservoir) from 1974 -

Table 3.1: Average residence times of Cochiti Lake, Elephant Butte reservoir, and Caballo reservoir. Residence times are in days except where otherwise noted. Average residence times were calculated for the entire period of record for each reservoir, as well as for 2001-2002, January's of 2001-2002, and August's of 2001-2002. It should be kept in mind that these residence time calculations are calculated from averages of transient reservoir conditions and allow only a qualitative look at the relative effects of reservoir storage and release on the movement of water and salts. See Appendix A for residence time calculations.

reservoir	historical	2001-2002	Jan 01+Jan 02	Aug 01+Aug 02
Cochiti	22	32	45	32
Elephant Butte	1.33 years	1.29 years	8.1 years	273
Caballo	46	20	21 years	11

2002 was 22 days (Table 3.1). Furthermore, data from 2001 and 2002 (Table 3.1) indicate that the average residence time of Cochiti Lake was 45 days in January, 32 days in August, and 32 days annually, confirming that it is essentially a flow-through reservoir in both winter and summer, and that recent reservoir conditions are representative of the historical record. The Middle Rio Grande Conservancy District (MRGCD), founded in 1923, oversees the agricultural system and flood management downstream of Cochiti dam to San Marcial at the head of Elephant Butte Reservoir (see Appendix B for a schematic of the MRGCD system). Four diversion dams in the MRGCD administrative region were constructed by 1935 [*MRGCD*, 2003]. However, Cochiti diversion dam, at the northernmost end of the region, was inundated upon construction of Cochiti Lake. Now the USACE controls diversions into Sili Main Canal and the Cochiti Main Canal, which have maximum capacities of 2.7 and 5.0 m^3 s^{-1} (96 and 175 cfs), respectively. Below Cochiti dam and 1.6 km above the confluence of the Jemez River and the Rio Grande, Angostura diversion dam

supplies a maximum of 11.3 m^3 s^{-1} (400 cfs) to the Albuquerque Main Canal. Further downstream and 1.6 km west of Isleta Pueblo, the Isleta diversion dam provides water to the Belen Highline Canal with a maximum capacity of 22.0 m^3 s^{-1} (775.7 cfs), and to the Peralta Main Canal with a capacity of 7.8 m^3 s^{-1} (275 cfs). The most downstream diversion point in the MRGCD is the San Acacia diversion dam, located 1.6 km upstream of the town of San Acacia. Here a maximum of 8.0 m^3 s^{-1} (283 cfs) is diverted into the Socorro Main Canal [*MRGCD,* personal communication 2003]. *Bullard and Wells* [1992] provide further information on the construction of the diversion structures, canals, laterals, and drains of the middle Rio Grande region.

Built during the severe drought period of the 1950's, the low-flow Conveyance Channel extends from San Acacia to Elephant Butte Reservoir. In order to better fulfill Rio Grande Compact water delivery requirements to the reservoir, river water was diverted from the wide, slow-moving Rio Grande in this region into the narrow, deep Conveyance Channel where it would be conveyed directly to Elephant Butte Reservoir with as few evapotranspirative and seepage losses as possible. The Conveyance Channel probably also succeeded in draining stored shallow ground water during the period immediately after it was built. Diversions into the channel ceased in the 1980's, and today the Conveyance Channel acts as a drain, picking up shallow seepage from the Rio Grande and surrounding drains and continuing to feed its contents into the narrows above Elephant Butte Reservoir. As the lowest point in the surface drainage system, the existence of the Conveyance Channel results in a hydraulic gradient away from the river toward the west and increases natural movement of water out of the riverbed. Unfortunately, river fauna cannot fol-

low the path of the water. During periods of low flow, water is pumped from the Conveyance Channel into the Rio Grande at several locations in order to maintain river flows for the endangered Rio Grande silvery minnow.

The Conveyance Channel has been gaged by the USGS in two locations since its construction. Gages were installed by the MRGCD on most diversions between 1954 and 1974, and more recently the MRGCD began gaging their drains. *Papadopulos and Associates* [2002a] provide the clearly drawn schematic of the MRGCD system shown in this chapter as well as an overview of historically available gaging data. A similar schematic with real-time data is available in two parts online [*USBR*, 2003b].

3.3.4 Elephant Butte Reservoir to El Paso County - Hudspeth County line

In 1905, Congress authorized the Rio Grande Reclamation Project and thus the construction of Elephant Butte Reservoir in order to store runoff for irrigation purposes. These Rio Grande Project waters were to benefit the Rio Grande valley in southern New Mexico and west Texas to the El Paso County - Hudspeth County line. By 1916, the USBR had completed the dam, a 91.7-m high, 510-m long concrete dam capable of impounding 2,210,290 acre-feet (2.7 billion m^3) of water. However, flooding continued to thwart agricultural development in the El Paso valley. In 1933, the U. S. and Mexican governments jointly agreed to develop the Rio Grande Rectification project, which straightened 248 km of river along the international border in order to assist in flood control [*IBWC*, 2003a]. (Since then, the Treaty of 1970 called for minimizing anthropogenic changes in the river channel.) Additionally, in 1936

a second major dam with a reservoir was added to the Rio Grande Project: Caballo dam, a 29.3-m high, 1399-m long earthfill structure with a capacity of 343,900 acre-feet (424 million m^3). By 1938 Caballo dam was completed, allowing further control over releases from Elephant Butte dam, expansion of agriculture in the El Paso valley, and a recovery of storage lost in Elephant Butte dam due to silt deposition. Today, Caballo dam also stores winter releases from Elephant Butte dam hydropower generation and stores them for summer irrigation use [*USBR*, 2003c]. The long-term residence time of Elephant Butte Reservoir was calculated to be 1.33 years (1915 - 2002); the long-term residence time of Caballo Reservoir (1939 - 2002) was calculated to be 46 days (Table 3.1). These calculations show that water remains in Elephant Butte Reservoir much longer than in Caballo Reservoir, the latter of which is basically a flow-through reservoir like Cochiti Lake. Calculations from 2001 and 2002 (Table 3.1) indicate that annual average residence time of the water in Elephant Butte Reservoir was about 1.29 years, seasonally ranging from just under one year in August to 8.1 years in January. Residence time in Caballo Reservoir during 2001 - 2002 annually averaged about 20 days, with the residence time during August averaging about 11 days and in January averaging 21 years. The long winter residence times reflect the temporary, seasonal condition of reservoir storage during the non-irrigation season. Residence times are significantly shorter during the summer when water is released for irrigation. These calculations suggest that all water stored in Caballo Reservoir during a single winter leaves the reservoir by the end of following the irrigation season. On the other hand, water remains in Elephant Butte Reservoir for multiple seasons. Annual average residence times for the two reservoirs from 2001 - 2002

are smaller than the historical averages, probably due to decline in reservoir storage during this period due to drought conditions.

Rio Grande Project diversions begin as far north as Caballo Reservoir itself. Water is diverted directly from the outlet of Caballo Reservoir into the Bonita Lateral for the agricultural community near the reservoir. Immediately downstream of Caballo Reservoir is the Percha diversion dam. Constructed in the late 1910's, it is the most northerly diversion dam in the Project area. This concrete structure diverts water into the Rincon Valley Main Canal, carrying water for 16,260 acres of agricultural land in the Rincon valley. The Rincon Valley Main Canal is 45 km long and has an initial capacity of 9.9 m^3 s^{-1} (350 cfs). Ninety-nine kilometers north of El Paso at the head of the Mesilla Valley, the Leasburg diversion dam was completed in 1908 and has been diverting water into the Leasburg Canal ever since. The Leasburg Canal is 21.9 km long and has an initial capacity of 17.7 m^3 s^{-1} (625 cfs), transporting water to 31,600 acres in the Mesilla valley. Thirty-five kilometers downstream, the Mesilla diversion dam is a 6.7-m high concrete weir built between 1914 and 1919. It diverts water into the East Side and West Side Canals, providing water to 53,650 acres of the Mesilla valley. The East Side Canal is 21.6 km long and has an initial capacity of 8.5 m^3 s^{-1} (300 cfs). The West Side Canal is 37.6 km long and has an initial capacity of 18.4 m^3 s^{-1} (650 cfs).

The southernmost diversion point in the Rio Grande Project is the Riverside diversion dam. Twenty-four kilometers southeast of El Paso, the Riverside diversion dam was formerly used to divert water into the Riverside Canal. However, the dam failed in 1996 and a temporary rockfill structure was

built to replace it. Since May of 1998, the Riverside Canal has been fed by the newly built American Canal extension rather than by diversions directly from the Rio Grande [*EPID*, 2003]. The Riverside Canal is 27.5 m long with an initial capacity of 25.5 m^3 s^{-1} (900 cfs). It serves 39,000 acres in the lower El Paso valley. Surplus water is carried from the drains in the Riverside Canal system to the Hudspeth County Conservation and Reclamation District No. 1 [*USBR*, 2003c].

The IBWC owns one diversion dam in the Rio Grande Project. The American diversion dam, 3 km upstream of El Paso and immediately above the point where the Rio Grande becomes the international boundary, diverts irrigation water into the IBWC-owned American Canal. The dam is an 5.5-m high radial-gate structure between earthfill dikes and is operated by the American Section of the IBWC. The American Canal has an initial capacity of 34 m^3 s^{-1} (1200 cfs) and carries water 3.4 km to the head of the Franklin Canal. In turn, the Franklin Canal conveys irrigation water to 17,000 acres in the upper El Paso valley. The Franklin Canal is 28.4 miles long and has an initial capacity of 9.2 m^3 s^{-1} (325 cfs). It was privately constructed in 1889 by the El Paso Irrigation Company, and was later bought by the USBR in 1912 [*USBR*, 2003c].

Before the American dam began operating in 1933, diversions of United States and Mexican waters from the Rio Grande occurred several miles downstream at the International dam. This dam is now owned by the USBR and facilitates only Mexican diversions into the Acequia Madre, owned by Mexico [*Manny Rubio, IBWC,* personal communication 2003]. By the Treaty

of 1906 between the U. S. and Mexico, the U. S. must deliver 60,000 acre-feet annually to the head of the Acequia Madre [*IBWC*, 2003a].

Construction of a drainage system for the Rio Grande project began in 1916. A dramatic rise in the shallow groundwater table by 1918 expedited drain construction. By 1930 the canal and drain system as it exists today had been constructed, with nearly 960 km of canals and laterals and 745 km of drains. These irrigation systems were operated by the USBR until 1980. At that time, the Elephant Butte Irrigation District (EBID) in New Mexico and the El Paso County Water Improvement District No. 1 (EPID) in west Texas began to oversee operations. As recently as 1996, ownership of the canal and drainage system changed hands from the USBR to the EBID and EPID, though dam operation remains in the hands of the USBR. Along with ownership, gaging responsibilities have been transferred to the local irrigation districts [*USBR*, 2003c]. Today, canals at all diversion dams in the Rio Grande Project area are gaged. Gaged drains include the Garfield, Hatch, Del Rio, La Mesa, East, and Montoya Drains, though at least 15 drains and wasteways remain ungaged. Ungaged drains typically return only a minor amount of water to the river, either because they drain a small area or because the majority of their water is consumptively used [*James Narvaez, EBID,* personal communication 2003].

3.3.5 Hudspeth County line to Ft. Quitman

Downstream of the Rio Grande Project, the Hudspeth County Conservation and Reclamation District No. 1 (HCCRD) regulates irrigation water for 18,300 acres on the U. S. side of the Rio Grande [*USBR*, 2003c]. Though the district is capable of diverting water directly from the river, this hap-

pens rarely, only when the river carries excess Elephant Butte water that is unused by Rio Grande Project lands [*Jay Kline, HCCRD,* personal communication 2003]. Most HCCRD water originates as drain flows of the EPID system upstream. The drain flows of the Riverside Canal system are diverted directly in the Tornillo Canal, which is owned by the HCCRD, and are then distributed throughout the Hudspeth County system [*Javier Grajeda, USBR,* personal communication 2003]. HCCRD waters often suffer from high salinity levels; *Trock et al.* [1978] reported a nearly 50% decrease in the amount of irrigated land devoted to cotton between 1950 and 1974 due to soil and water salinization.

3.4 Wastewater treatment plants

Many pueblos, towns, cities, and industries in the Rio Grande basin contribute wastewater to the Rio Grande. Of the 35 permitted dischargers in New Mexico and the three wastewater treatment facilities in El Paso, only nine effluent streams averaged over one million gallons per day (0.044 $m^3 s^{-1}$) in August 2001 (Table 3.2). Of these nine, only four discharge directly to the river: the Rio Rancho wastewater treatment plant (including effluent streams no. 2 and no. 3), the Southside Water Reclamation Plant (SWRP) of Albuquerque, the Jacob Hands wastewater treatment plant in Las Cruces, and the Northwest wastewater treatment plant in El Paso. The others discharge wastewater to a nearby tributary or agricultural drain. Historical data [*Kelly and Taylor*, 1996] and measurements during August 2001 and January 2002 (Appendix F) at these four locations indicate that effluent chloride concentrations are typically one or two times that of local river water. Assuming that these measurements

Table 3.2: Permitted wastewater dischargers in the Rio Grande valley, New Mexico and Texas. Average and maximum flows for August 2001 are specified in $m^3\ s^{-1}$. The year the discharger was established is in parentheses next to the discharger name where available. Not included are six zero-dischargers and non-reporting dischargers for August 2001. New Mexico data from Steve Baumgarn, New Mexico Environment Department; El Paso data from the El Paso Water Utility, http://www.epwu.org.

Discharger	Average Flow	Maximum Flow
Elephant Butte SP	0.0001	0.0002
Gadsden School	0.0005	0.0031
Bosque Farms	0.0050	0.0060
Los Lunas Pen	0.0070	0.0079
LA County White Rock	0.0079	0.0189
Rio Communities	0.0094	0.0103
Hatch	0.0109	0.0120
Taos Ski Valley	0.0136	0.0256
Red River	0.0209	0.0243
Santa Teresa	0.0212	0.0272
El Paso Elec	0.0215	0.0668
Anthony	0.0216	0.0241
Rio Rancho no. 3	0.0253	0.0329
LANL	0.0269	0.0311
LA County Bayo	0.0326	0.0619
Socorro	0.0361	0.0469
Sunland Park	0.0364	0.0456
T or C	0.0377	0.0417
Belen	0.0394	0.0438
Española	0.0400	0.0482
Los Lunas	0.0412	0.0477
Taos	0.0451	0.0548
PNM Reeves	0.0470	0.0894
Rio Rancho no. 2	0.0831	0.1029
Santa Fe	0.1577	0.2190
Las Cruces	0.3635	0.3986
Albuquerque Southside WWTP (1962)	2.2951	2.4221
El Paso Northwest WWTP (1984)	na	0.7665
El Paso Haskell Street WWTP (1923)	na	1.2133
El Paso Roberto Bustamante WWTP (1991)	na	1.7082

reflect regulatory requirements and are representative of most effluent streams in the Rio Grande basin, and given that one million gallons per day is typically less than one percent of river flow, it is unlikely that smaller effluent streams have much effect on river salinity. The Rio Grande valley in Colorado has no population centers as large as the significant wastewater dischargers in New Mexico and Texas, so no effluent streams in that state were considered.

3.5 Chapter 3 conclusions

The Rio Grande is highly engineered, and human activity has a significant effect on water and salt movement through the river system. Wastewater treatment plants add salts to the river; irrigation networks re-route water and salts and increase evapotranspiration. For most of the past century, studies have attributed salinization of the Rio Grande to the effects of anthropogenic manipulation of the hydrologic system, in particular to irrigated agriculture. The next chapter summarizes these previous studies. However, investigation of salinization using environmental tracers as described in Chapters 6 - 10 shows that significant river salinization may in fact be due to geologic rather than anthropogenic factors.

CHAPTER 4

PREVIOUS SALINIZATION STUDIES

The progressive salinization of the Rio Grande with distance downstream has been under investigation for most of the 20^{th} century. In general, salinization has been attributed to the effects of irrigated agriculture [*NRC*, 1938; *Lippincott*, 1939; *Wilcox*, 1957; *Trock et al.*, 1978]. More recently, salinization has been ascribed to factors such as wastewater treatment plant effluent inflow, natural tributary inflows, and saline groundwater input in addition to agricultural return flows [*Moore and Anderholm*, 2002].

4.1 A pre-Elephant Butte Reservoir salinity study at San Marcial and El Paso

Before the construction of Elephant Butte Reservoir or an open drain network in the region, *Stabler* [1911] collected biweekly discharge and chloride concentration data (as well as TDS, carbonate concentration, bicarbonate concentration, and total suspended solids data) at San Marcial and El Paso from 1905 - 1907. Based on this data, the monthly average chloride burden (chloride concentration multiplied by discharge) was calculated to be 110,000 kg dy^{-1} at San Marcial and 145,000 kg dy^{-1} at El Paso from September 1905 - April 1907 (Table 4.5). The average monthly chloride gain of 35,000 kg dy^{-1} between the two stations suggests that chloride addition occurred during this time in this reach of the river independent of the existence of Elephant Butte

Reservoir or drain return flow to the river. At both San Marcial and El Paso, average monthly chloride burdens from 1905 - 1907 were more similar to recent average monthly chloride burden conditions (1962 - 2001) than to chloride burden conditions within the 40 years immediately after the 1920's construction of the agricultural drainage networks (Figure 4.1, Figure 4.2; water quality data available beginning in 1934). *Hendrickx* [1998] suggested that higher chloride burdens persisted for several decades after drain construction due to flushing of shallow saline ground water from agricultural lands. *Hendrickx* [1998] also reported that this process is irrelevant to river salinization now because all saline ground water was flushed by the 1950's or 1960's. At San Marcial, chloride burden data show that recent water quality conditions (1962 - 2001) are indeed similar to pre-drainage conditions from 1905 - 1907. Because the chloride burden from 1905 - 1907 at El Paso is at the lowest end of the burden range, it is possible that the agricultural system between San Marcial and El Paso continues to contribute salts to the river today through some process aside from shallow ground water flushing. Causes of drain salinity are discussed further in Chapter 7.

4.2 Rio Grande salinity studies, 1938 - present

The National Resource Committee (NRC) published an extensive report of the upper Rio Grande basin in 1938. This report included annual average TDS, salt burden (TDS concentration multiplied by discharge), chloride burden, and discharge values for 1936 at Del Norte, for 1934 - 1936 at Otowi and San Marcial, and for 1931 - 1936 in the Rio Grande Project between the outlet of Elephant Butte Reservoir and Ft. Quitman. The NRC

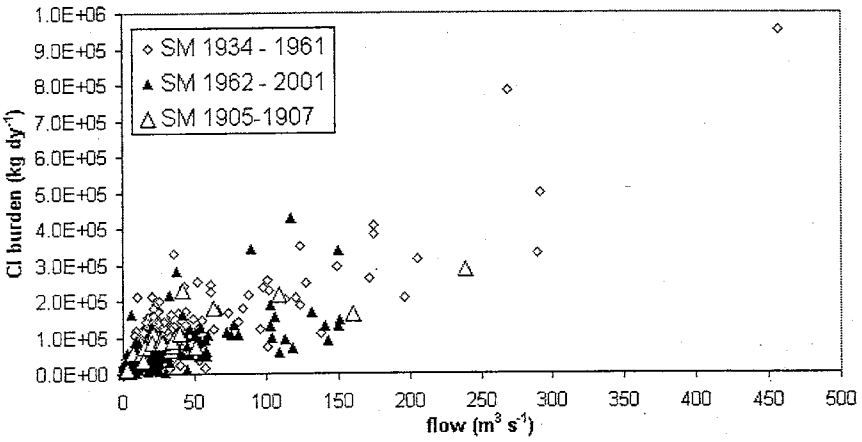

Figure 4.1: Relationship between average monthly chloride burden and average monthly flow at San Marcial from 1905 - 2001.

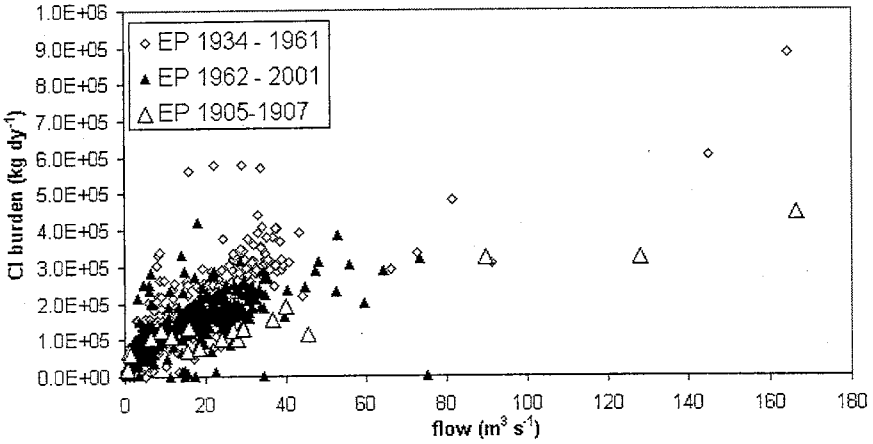

Figure 4.2: Relationship between average monthly chloride burden and average monthly flow at El Paso from 1905 - 2001.

Table 4.1: Comparison of total dissolved solids values (mg L^{-1}) in previous Rio Grande salinization studies.

source: years studied:	NRC (1938) 1931-1936	Lippincott (1939) 1939	Wilcox (1957) 1934-1953	EPA (1978) 1918-1973
Del Norte	81	110	na	below 100
Otowi	253	na	221	200-300
San Marcial	610	427	449	482
EB dam	595	na	478	na
Caballo dam	na	na	515	504
Leasburg	640	na	551	558
El Paso	897	832	787	802
Ft Quitman	2023	2120	1691	1851

Table 4.2: Comparison of discharge values (m^3 s^{-1}) in previous Rio Grande salinization studies.

source: years studied:	Stabler (1911) 1905-1907	NRC (1938) 1931-1936	Wilcox (1957) 1934-1953
Del Norte	na	18	na
Otowi	na	10	42
San Marcial	50	33	33
EB dam	na	30	31
Caballo dam	na	na	31
Leasburg	na	29	29
El Paso	36	20	21
Ft Quitman	na	7	8

Table 4.3: Comparison of total salt burden values (kg dy^{-1}) in previous Rio Grande salinization studies.

source:	NRC (1938)	Wilcox (1957)	Moore and Anderholm (2002)
years studied:	1931-1936	1934-1953	1993-1995
Del Norte	1.29E+05	na	1.28E+05
Otowi	7.28E+05	8.05E+05	8.84E+05
San Marcial	2.22E+06	1.29E+06	na
EB dam	1.54E+06	1.28E+06	na
Caballo dam	na	1.36E+06	na
Leasburg	1.61E+06	1.38E+06	1.02E+06
El Paso	1.59E+06	1.40E+06	1.19E+06
Ft Quitman	1.18E+06	1.16E+06	na

Table 4.4: Comparison of chloride concentration values (mg L^{-1}) in previous Rio Grande salinization studies.

source:	Stabler (1911)	NRC (1938)	Wilcox (1957)
years studied:	1905-1907	1931-1936	1934-1953
Del Norte	na	4	na
Otowi	na	11	7
San Marcial	38	10	32
EB dam	na	54	34
Caballo dam	na	na	41
Leasburg	na	71	45
El Paso	142	159	63
Ft Quitman	na	687	101

Table 4.5: Comparison of chloride burden values (kg dy^{-1}) in previous Rio Grande salinization studies.

source: years studied:	Stabler (1911) 1905-1907	NRC (1938) 1931-1936
Del Norte	na	7.00E+03
Otowi	na	9.00E+03
San Marcial	1.10E+05	2.95E+04
EB dam	na	2.28E+04
Caballo dam	na	na
Leasburg	na	1.80E+05
El Paso	1.45E+05	2.80E+05
Ft Quitman	na	4.00E+05

calculated average TDS values increasing from 81 mg L^{-1} at Del Norte to 2023 mg L^{-1} at Ft. Quitman (Table 4.1). They calculated average total salt burdens ranging from 129,180 kg dy^{-1} to over 1.1 million kg dy^{-1} along the same distance (Table 4.3). They reported an increase in chloride burden from 7,004 kg dy^{-1} to about 400,000 kg dy^{-1} between Del Norte and Ft. Quitman (Table 4.5). Based on their reported discharge values (Table 4.2), this is equivalent to an increase in chloride concentration from 4 - 687 mg L^{-1} (Table 4.4). The large differences between chloride concentration, chloride burden, and total salt burden averages calculated by the NRC and *Stabler* [1911] at San Marcial are probably due to effects of highly variable flow conditions. Daily discharge at San Marcial commonly ranges within 3 orders of magnitude in a single month; USGS data indicate that discharge within just one week of August 1935 ranged from nearly 0 to 311 m^3 s^{-1} (0.9 - 11,500 cfs). Additionally, the calculation of an apparent decrease in average chloride concentration between Otowi and San Marcial from 1934 - 1936 may be due to a typographical error in the reported chloride burden value because it is unlikely that the average chloride

concentration or chloride burden decreased while the average total salt burden increased in this reach.

The *NRC* [1938] also reported the average annual electrical conductivity (EC) of many individual agricultural drains between Otowi and Ft. Quitman. Electrical conductivity, which represents the inverse of water resistance, is related to TDS by a constant that is about 0.66 for the Rio Grande Project area [*Williams*, 2001]. Between Otowi and San Marcial, the NRC noted that most drains have the same conductivity at their distal ends as at their heads where their water was diverted from the river. The drain with the highest percent chloride in the area was observed to be the San Acacia Drain, with 51% chloride and an EC of 303 μS cm^{-1} (equivalent to 303 μS cm^{-1} * 0.66 = 200 mg L^{-1} TDS). The Luis Lopez Drain A had the second-highest percent chloride and EC at 49% and 254 μS cm^{-1} (168 mg L^{-1} TDS), respectively. In the Rio Grande Project region, the NRC reported higher TDS concentrations and percent chloride values in all drains than in the river at their points of diversion. Between Elephant Butte dam and El Paso, the East Drain had the highest EC of 442 μS cm^{-1} (292 mg L^{-1} TDS) as well as the highest percent chloride of 53 %. Drain salinity was thought to be due to percolation of saline soil waters into the drains. The NRC attributed both drain salinity and the addition of an average of 70,000 kg dy^{-1} of salts between the outlet of Elephant Butte Reservoir and El Paso to flushing of shallow saline ground water by agricultural drains. Salinization upstream of San Acacia was reported to be due to input of natural tributaries and evapotranspirative concentration. Salt loss between El Paso and Ft. Quitman was attributed to deposition in the soil.

In 1939, Lippincott noted TDS values of 110 mg L^{-1} at Del Norte, 427 mg L^{-1} at the head of Elephant Butte reservoir, 832 mg L^{-1} at El Paso, and 2120 mg L^{-1} at Ft. Quitman (Table 4.1). It is unclear if these values are averages or represent a single sampling. Lippincott attributed this TDS increase to the cumulative evapotranspirative effect of progressive use and re-use of Rio Grande waters for irrigation with distance downstream.

Wilcox [1957] calculated average Rio Grande TDS values from 1934 - 1953 based on monthly TDS measurements. He noted average TDS concentrations slightly lower than those of the *NRC* [1938] and *Lippincott* [1939], ranging from 221 mg L^{-1} at Otowi to 1691 mg L^{-1} at Ft. Quitman (Table 4.1). He noted an increase in total salt burden of over 25%, from 804,740 - 1,159,900 kg dy^{-1} within the same reach, which is slightly less than that reported by the NRC (Table 4.3). Average chloride concentration values reported by Wilcox range from 7 - 101 mg L^{-1} from Otowi to Ft. Quitman, which are significantly lower than those calculated by the NRC (Table 4.4). The fact that Wilcox and the NRC calculated such differing salinity conditions with distance downstream though they reported similar average discharges (Table 4.2) is probably an indicator of differing proportions of inflows of different salinities. Though the values differ, data from both the NRC and Wilcox showed that the largest increase in total salt burden south of Otowi occurred between Otowi and Elephant Butte Reservoir (Table 4.3). They also reported a slight increase in total salt burden between Elephant Butte Reservoir and El Paso, and a subsequent decrease from El Paso to Ft. Quitman. As observed by both researchers, the TDS more than doubled between Otowi and San Marcial and again between El Paso and Ft. Quitman (Table 4.1). A consistent pattern of change in chloride

concentration between the two data sets is less obvious due to the anomalous value reported by the NRC at San Marcial (Table 4.4). Wilcox attributed downstream river salinization to flushing of shallow saline groundwater into the surface water system during the process of irrigation.

In a simple basin-scale chloride mass balance, *vanDenburgh and Feth* [1965] calculated that only 4.2% of the chloride burden of the Rio Grande enters with precipitation. They deduced that the remainder of the chloride load originates within the basin, entering the river by way of "continental solute erosion."

In 1978, an Environmental Protection Agency (EPA) report by Trock et al. provided discharge-weighted average annual Rio Grande TDS values from 1918 - 1973 (Table 4.1). They noted a three-fold increase in TDS concentration from 504 - 1498 mg L^{-1} between Caballo Reservoir and the Hudspeth County line, which is in agreement with previously published values. *Trock et al.* [1978] observed average annual agricultural drain TDS values between Caballo Reservoir and the Hudspeth County line (drain averages were lumped into three categories based on location in the Rincon, Mesilla, or El Paso valleys) as being 50 - 100% higher than river TDS values. *Trock et al.* [1978] also computed cumulative differences in salt load between gaging stations from Caballo Reservoir to Ft. Quitman from 1934 - 1963. They observed that the net increase in salt load between Caballo Reservoir and Leasburg during this time was about 40,000 kg dy^{-1}. Between Leasburg and El Paso they noted a smaller net salt load increase of about 27,000 kg dy^{-1}. They calculated a similar net salt burden difference between El Paso and the Hudspeth County

line during the same period and considered it to be negligible. Between the Hudspeth County line and Ft. Quitman, they calculated a significant net salt removal of about 275,000 kg dy^{-1}. These accumulation calculations for the same region suggest that net salt addition to the river on the decadal scale is small in comparison to the total salt burden of the river of over 1 million kg dy^{-1} calculated by *Wilcox* [1957]. *Trock et al.* [1978] attributed river salinization to the effects of irrigation. They ascribed the increase in river TDS concentration to evapotranspirative concentration of drain waters; the increase in salt burden was said to be due to displacement flushing of shallow saline ground water through agricultural drains. Salt removal between the Hudspeth County line and Ft. Quitman was attributed to salt buildup in the soil.

Much more recently, *Moore and Anderholm* [2002] analyzed spatial and temporal patterns of discharge and water quality at twelve gaging stations on the main-stem Rio Grande and its tributaries. Using data collected from 1993-1995 as part of the National Water Quality Assessment (NAWQA) Program, they calculated TDS burdens that compare favorably the other values in the literature already cited (Table 4.3). After performing burden calculations, they simultaneously examined variations in TDS burden, discharge, nutrient burden, and suspended solids burdens between main-stem Rio Grande gaging stations. They correlated these variations with major tributaries and diversions, though they did not attempt to quantify these inputs and outputs. They ascribed river salinization in Colorado to inflow of the Closed Basin Canal. Salinization between the Colorado-New Mexico border and Otowi was attributed to the effects of increased discharge due to natural tributary inflow, especially from the Rio Chama. Increase in salt burden south of Otowi was

said to be due to wastewater treatment plant inflow, evapotranspiration (particularly through Elephant Butte and Caballo Reservoirs), agricultural return flows, tributary inflows, and saline groundwater input.

4.3 Chapter 4 conclusions

A consistent pattern of salinization of the Rio Grande with distance downstream has been observed throughout the past century. In general, TDS concentration has increased by an order of magnitude from about 100 mg L^{-1} at the headwaters to about 2000 mg L^{-1} at Ft. Quitman (Table 4.1). Chloride concentration has consistently increased with distance downstream by nearly two orders of magnitude, from about 4 mg L^{-1} to over 100 mg L^{-1} (Table 4.4). Total salt burden along the same distance has increased from about 130,000 kg dy^{-1} to over 1,000,000 kg dy^{-1} (Table 4.3); chloride burden has risen from about 8,000 - 400,000 kg dy^{-1} (Table 4.5). It is apparent that the chloride burden increases from less than 5% of the total salt burden to about 35% by Ft. Quitman. The constancy in the salinization pattern with time suggests that river salinity is controlled by ongoing processes that have been occurring for the previous century. Some of the earliest studies [*Lippincott*, 1939] suggested that evapotranspiration concentrates salts in the river by progressive removal of water. However, it is apparent that not only salt concentrations but also salt burdens increase with distance downstream. Several researchers [*NRC*, 1938; *Wilcox*, 1957; *Trock et al.*, 1978] concluded that salt addition occurs by flushing of shallow ground waters by agricultural drains. Indeed, saline drains have been observed in both the middle Rio Grande and in the Rio Grande Project area [*NRC*, 1938; *Trock et al.*, 1978]. However, the causes of drain salinity have

not been verified and their effects have not been quantified. Furthermore, *Hendrickx* [1998] noted that in the Mesilla valley, all shallow groundwater is flushed about every 25 years. Thus all shallow saline ground water would have been flushed from agricultural soils within the first few decades after drains were constructed in the Rio Grande valley in the 1920's (see Section 4.1). This flushing may be the cause of the difference in average total salt burdens in the Rio Grande Project area reported by the *NRC* [1938] and *Wilcox* [1957] under nearly identical discharge conditions. Assuming other agricultural valleys in the Rio Grande basin are similar to the Mesilla valley, shallow saline ground waters would not be expected to have had an effect on river water quality after the 1950's. Yet river salinization is still seen today [*Moore and Anderholm*, 2002].

In the next chapter, spatial and temporal patterns of salinization are examined in more detail based on discharge and chloride concentration data available from the USGS and the USBR for the past century. Chapters 6 - 10 of this thesis use environmental tracer data and modeling to evaluate the causes of river salinization proposed in this chapter in comparison to the alternative hypothesis that river salinization has a significant geologic component, that of deep saline ground water contribution.

CHAPTER 5

HISTORICAL DATA ANALYSIS AND COMPARISON TO FIELD DATA

5.1 Introduction

In order to examine Rio Grande salinization in more detail than is discussed in the literature (see Chapter 4), this chapter develops a more in-depth spatial and temporal analysis of historical discharge, chloride concentration and chloride burden for the main stem Rio Grande and its major tributaries. The majority of this chapter is dedicated to statistical analysis of historical average monthly parameters for August's and January's using box and whisker graphs. To determine if the conditions in August 2001 and January 2002 represented typical summer and winter conditions in the Rio Grande basin, they are briefly compared to seasonal and monthly historical parameter averages. (Further analysis of August 2001 and January 2002 conditions is left until chapters 7 - 10.) Next,the ranges of annual average values of historical parameters at each location are briefly examined. At the end of this chapter, historical water quality in Elephant Butte Reservoir is investigated.

5.2 Historical data availability

Over 50 gaging stations administered by the USGS, the USBR, the IBWC, and the CDWR on the Rio Grande, its tributaries and diversions have extensive daily flow gaging records dating back to 1889. However, correspond-

Table 5.1: Abbreviations for source agencies used in Tables 5.2 - 5.5.

code	Agency
G	U.S. Geological Survey
N	New Mexico Dept. of Health and Environment
B(L)	U.S. Bureau of Reclamation, Landis (2002)
B(W)	U.S. Bureau of Reclamation, Williams (2001)

Table 5.2: Historical discharge data availability and sources for gaging stations of the main stem Rio Grande. See Table 5.1 for source codes.

label	location	distance (km)	availability	source
A	Lobatos	256.9	7/1/1899 - 2/7/2003	G
B	Taos Junction	359.3	10/1/1925 - 5/27/2003	G
C	Otowi	430.9	2/1/1895 - 5/27/2003	G
D	San Felipe	496.4	1/1/1927 - 5/27/2003	G
E	Bernardo	630.7	10/1/1957 - 5/27/2003	G
F	San Acacia	655.3	10/1/1958 - 5/27/2003	G
G	San Marcial	731.1	1/1/1899 -5/27/2003	G
H	EB dam	801.3	10/1/1916 - 5/27/2003	G
I	Caballo dam	841.0	1/1/1938 - 5/29/2003	G
J	Leasburg	919.5	1/1/1938-12/31/1995	B(L)
K	El Paso	1013.8	1/1/1923-11/30/2002	G
L	Ft. Quitman	1149.0	1/1/1923-12/31/2002	G

ing chloride concentration data exist for fewer than half of these stations. Furthermore, only a third of the stations have sufficient simultaneous flow and chloride data for either all January's or all August's on record (about 10 values) to perform a meaningful statistical analysis of the chloride burden historical record (Table 5.1, Tables 5.2 - 5.5, Figure 5.1, Figure 5.2). On the main stem Rio Grande, stations with sufficient data include: A) Lobatos, B) Taos Junction bridge, C) Otowi, D) San Felipe, E) Bernardo, F) below San Acacia diversion dam, G) San Marcial, H) below Elephant Butte Reservoir, I) below Caballo Reservoir, J) below Leasburg diversion dam, K) El Paso, and L) Ft.

Table 5.3: Historical chloride concentration data availability and sources for gaging stations of the main stem Rio Grande. Dates of data availability do not necessarily imply a continuous historical record. See Table 5.1 for source codes.

label	location	distance (km)	availability	source
A	Lobatos	256.9	10/1/1947 - 8/30/2001	G
B	Taos Junction	359.3	3/19/1974-7/18/2001	G,N
C	Otowi	430.9	10/1/1959-9/12/2001	G,N
D	San Felipe	496.4	6/1/1970 - 7/11/2001	G,N
E	Bernardo	630.7	3/3/1960-7/29/1998	G,N
F	San Acacia	655.3	1/15/1941-8/3/1998	G,B(W)
G	San Marcial	731.1	1/15/1934-8/22/2001	G,B(W)
H	EB dam	801.3	1/15/1934-9/2/1982	G,B(W)
I	Caballo dam	841.0	1/15/1940-7/24/1996	G,B(W)
J	Leasburg	919.5	1/1/1938-12/31/1963	B(L)
K	El Paso	1013.8	1/15/1934-9/28/2001	G,B(W)
L	Ft. Quitman	1149.0	1/15/1934-12/15/1963	B(W)

Table 5.4: Historical discharge data availability and sources for major tributaries of the Rio Grande. See Table 5.1 for source codes.

label	location	distance (km)	availability	source
a	Red River	318.9	8/9/1978 - 5/27/2003	G
b	Rio Pueblo de Taos	356.2	4/1/1957 - 5/27/2003	G
c	Embudo Creek	380.6	10/1/1923 - 5/27/2003	G
d	Rio Chama	409.2	10/1/1912 - 5/27/2003	G
e	Jemez River	507.8	4/1/1936 - 5/27/2003	G
f	Rio Puerco	637.1	11/1/1939 - 9/30/2001	G
g	Rio Salado	650.0	10/1/1947 - 9/30/1984	G
h	Conveyance Channel	731.1	12/1/1951 - 5/27/2003	G

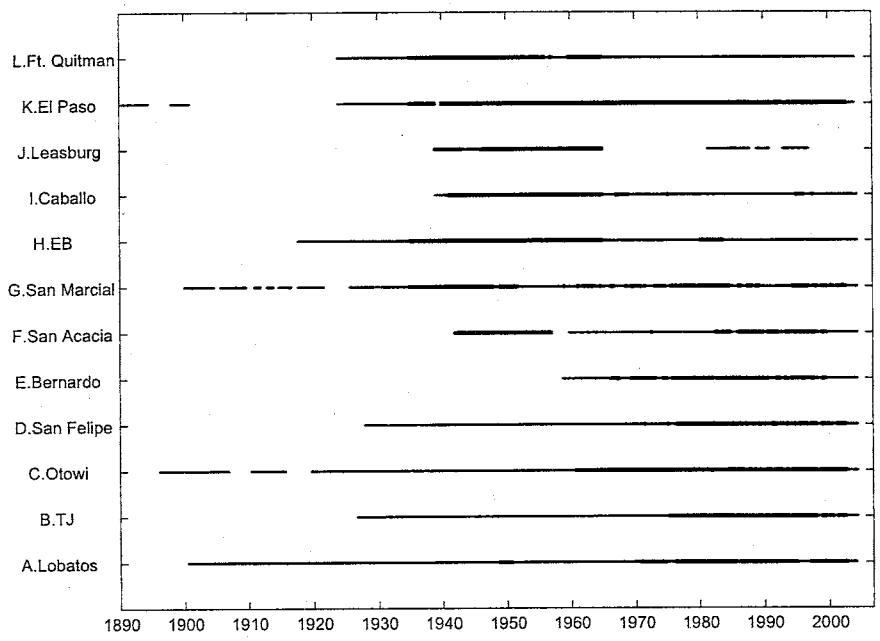

Figure 5.1: Availability of discharge and chloride concentration data from 1890-2003 at all main stem Rio Grande gaging stations with enough historical data to make a meaningful comparison with field data. The thin line indicates dates for which only discharge data is available; the thick line shows dates for which both discharge and chloride concentration data are available. Not shown are dates with chloride concentration data but without discharge data. Data is available at El Paso beginning in May 1889. Stations are identified in Table 5.2.

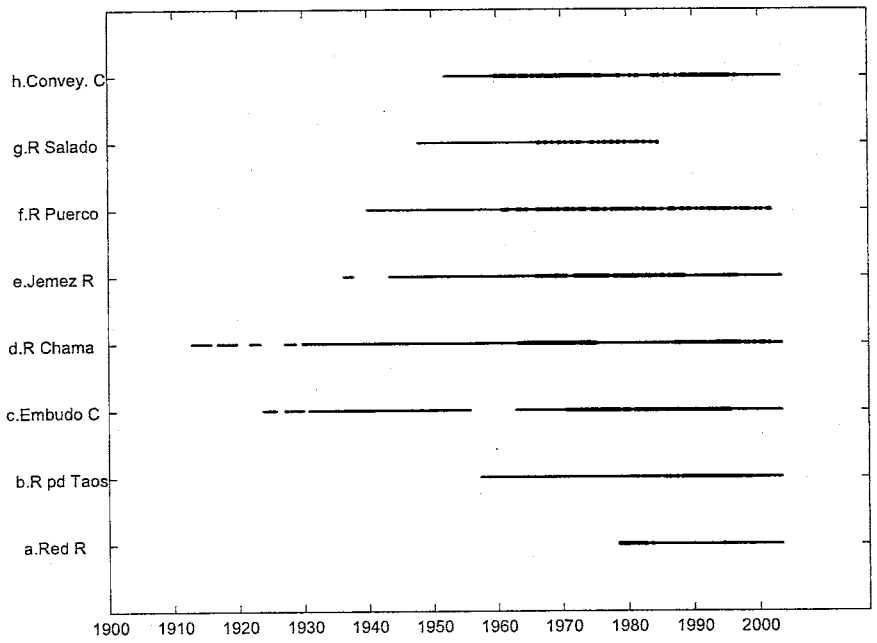

Figure 5.2: Availability of discharge and chloride concentration data from 1900-2003 at all tributary gaging stations with enough historical data to make a meaningful comparison with field data. The thin line indicates dates for which only discharge data is available; the thick line shows dates for which both discharge and chloride concentration data are available. Not shown are dates with chloride concentration data but without discharge data. Stations are identified in Table 5.4.

Table 5.5: Historical chloride concentration data availability and sources for major tributaries of the Rio Grande. Dates of data availability do not necessarily imply a continuous historical record. See Table 5.1 for source codes.

label	location	distance (km)	availability	source
a	Red River	318.9	10/26/1977-8/29/1994	G
b	Rio Pueblo de Taos	356.2	5/21/1981-8/26/1998	G
c	Embudo Creek	380.6	8/24/1970-7/17/1995	G,N
d	Rio Chama	409.2	4/3/1963-7/19/2001	G
e	Jemez River	507.8	2/3/1966-8/27/1996	G
f	Rio Puerco	637.1	10/19/1960-8/15/2001	G
g	Rio Salado	650.0	6/21/1966-8/24/1984	G
h	Conveyance Channel	731.1	10/1/1959-7/23/1996	G

Quitman. Tributaries with such a record include: a) Red River, b) Rio Pueblo de Taos, c) Embudo Creek at Dixon, d) Rio Chama, e) Jemez River, f) Rio Puerco, g) Rio Salado, and h) Conveyance Channel at San Marcial. Though the Conveyance Channel flows into the Rio Grande 40 km downstream of San Marcial, San Marcial is the closest gaging station on this important tributary and so its historical record is analyzed and considered representative of downstream Conveyance Channel conditions. Drain return flows in the Rio Grande Project have been consistently recorded by the USBR since 1938 and drain water quality data was collected as early as 1918, but drain TDS and chloride data have only been recorded for a year or two for each drain since then. No other historical water quality data exists for agricultural diversions or return flows within the field area. Two other tributaries without adequate historical records include the Closed Basin Canal in Colorado and the Southside Water Reclamation Plant (SWRP) in Albuquerque. Since 1986, weekly TDS data has been recorded for the Closed Basin Canal, but chloride concentration data is not recorded for the canal itself (chloride concentration is recorded for the

source wells once per year). The SWRP does not test their main effluent stream for TDS, EC, or chloride; however, since 1999 the SWRP has tested the TDS of filtered effluent that is reused within the plant for dust control and pump lubrication [*Steve Glass, SWRP,* personal communication 2003]. This data is reported in the historical analysis of chloride burden to follow.

5.3 Historical data compilation and computations

To calculate historical chloride burdens, data was compiled from several sources (Tables 5.1 - 5.5). Daily average discharge measurements for all stations listed above were downloaded from the *USGS* [2003] and *USGS* [2003b] websites. Monthly average discharge data for the stations from San Acacia to Ft. Quitman were obtained from the USBR [*Mike Landis, USBR,* personal communication 2002]. Calculations of monthly average discharge from USGS and IBWC daily discharge data nearly exactly matched the USBR monthly average discharges, so the daily USGS and IBWC data were used for all stations in order to be consistent. One exception is at Leasburg, where monthly average discharge data from the USBR was used because no data was available from the USGS or the IBWC.

Daily chloride concentration measurements (USGS water quality parameter 00940) were available from the USGS website for all tributaries and all main stem Rio Grande stations upstream of and including El Paso, except Leasburg. STORET [*EPA*, 2003], an EPA-administered online database of water quality data from non-USGS agencies, also served as a source of chloride data. Data from the New Mexico Department of Health and Environment (NMDHE) was available in STORET for the main stem stations in north-central New

Mexico from Taos Junction bridge to Bernardo as well as for Embudo Creek. Monthly average chloride data from San Acacia to Ft. Quitman was obtained from Mike Landis at the USBR [personal communication 2002] and *Williams* [2001]. Williams' data is based on USBR data, and nearly exactly matches the data provided by Landis. Since Williams' data is more complete, his data was used in favor of Landis' data at all stations between San Acacia and Ft. Quitman. Daily USGS and STORET chloride concentration values were aggregated with Williams' data to compose the most complete historical record possible.

In an effort to create a database that would be useful for future water quality studies, corresponding daily data for electrical conductivity (USGS water quality parameter 00095) and TDS (USGS water quality parameter 70300) were downloaded from the USGS and STORET websites along with the chloride data when possible. These two types of data were also available from the USBR records of *Williams* [2001]. Occasionally, water quality data from multiple agencies was available for a single day. Because duplicate data values were generally within 10% of each other, for simplicity duplicate data was removed rather than averaged. The most complete daily record (with chloride, electrical conductivity, and TDS) was kept in the compiled database. In the case of equally complete data records for a single day, USGS data and Williams' data took precedence over data from the two agencies in the STORET database. USGS and Williams' data rarely overlapped. In the case of two equally complete records for a single day from the same agency, the second record was deleted.

Instantaneous burdens were calculated by multiplying a chloride concentration measurement by its corresponding daily average discharge value. Monthly historical burden values for stations with USGS chloride data were calculated by averaging all available instantaneous chloride burdens for the month. Where Williams' data was used, his monthly average chloride data was assigned to the 15^{th} of the month and was multiplied by the gaged discharge on the 15^{th} to obtain a monthly average burden. Historical chloride burden was analyzed in terms of monthly average burdens due to the data collection method employed by the USBR between San Acacia and Ft. Quitman. At the USBR, monthly chloride concentration measurements for a station were performed on an aggregated collection of daily samples of a standard volume [*Williams*, 2001]. Thus the aggregated sample represented a time-weighted rather than a flow-weighted average of chloride concentration for that particular month. Assuming that flow does not vary much within the given month, this should be a reasonable average.

Close inspection of the historical daily average flow records for the aforementioned gaging stations reveals that 10-25% variation in daily flow is common within any given month of a single year; flow variations of 50% are not uncommon. At the gaging stations immediately below Elephant Butte and Caballo reservoirs, flow variations during January and August were similar to variations at other gaging stations. However, flow routinely varied two to three orders of magnitude during the months at the beginning (Feb - Mar) and the end (Sept - Nov) of irrigation season at these two gaging stations downstream of major reservoirs. At all gaging stations, flow variations between months generally spanned an order of magnitude or more, which is generally a much

greater range of variation than the variation that occurs during a single month. Given that flow variations within each month are much less than variations between months, the calculated average monthly chloride burdens should reflect marked seasonal variations. However, they should not be interpreted as an extremely accurate reconstruction of conditions on the Rio Grande for any single month.

5.4 Visualization of spatial variation of historical data using box and whisker graphs

August and January historical discharges and chloride burdens at each station were primarily analyzed using box and whisker graphs. On each graph, the stations are indicated along the x-axis by the letters by which they were introduced earlier in this section (Tables 5.2 and 5.4). The upper and lower limits of each box represent the first and third quartiles (25^{th} and 75^{th} percentiles, or Q1 and Q3) of each data set, respectively. The single line across each box represents the median. The whiskers extend to adjacent high and low values that fall within 1.5 times the interquartile range (Q3 - Q1). The whisker limits are defined by the following equations:

Lower Limit: Q1 - 1.5 (Q3 - Q1)

Upper Limit: Q3 + 1.5 (Q3 - Q1)

Asterisks indicate outliers that fall beyond 1.5 times the interquartile range. Numbers in parentheses below each box and whisker set indicate the number of values in the historical record for the particular gaging station. In the case of the chloride burden graphs, the numbers in parentheses represent the number of months for which it is possible to calculate an average monthly

burden given the availability of flow and chloride concentration data in the historical record.

Heavy black dots represent conditions during the August 2001 and January 2002 field seasons. On the flow graphs, the dots represent daily average flow obtained from various agencies; on the chloride concentration graphs the dots indicate chloride values measured during August 2001 and January 2002 for this study; on the chloride burden graphs the dots show the chloride burden values calculated from these data. Discharge data for the field seasons were obtained from the USGS, EBID, and IBWC. Chloride concentrations for the Rio Pueblo de Taos and the Jemez River in August 2001 and for the Jemez River in January 2002 were estimated because field measurements were not collected due to inaccessibility. Values resulting from estimated rather than measured values are indicated by a superscript "e" over the station letter on the graph. These estimated chloride concentrations are the seasonal (6-month) mean of all historical chloride measurements (excluding outliers) corresponding to daily discharges between 0 - 2 $m^3 s^{-1}$, the range of flows of these two tributaries during the two field seasons. Chloride burdens for these two tributaries for the August 2001 and January 2002 field seasons were then estimated by multiplying the estimated chloride concentration and the USGS daily discharge measurement. Initially, the field season chloride burdens for these two tributaries were estimated as the averages (means) of their respective August and January historical burdens. However, dividing these estimated burdens by the actual USGS discharge values resulted in unrealistic chloride concentrations. It was decided that estimating chloride burden based on the estimated chloride concentrations was more accurate.

5.5 Analysis of historical data

5.5.1 Historical flow conditions during August and January

The box and whisker graphs of the historical data show that at any single location on the Rio Grande and its tributaries, as well as between adjacent stations, flow varies widely in the historical record within the single month of August or January (Figure 5.3, Figure 5.4, Figure 5.5, and Figure 5.6). At a single station, it often fluctuates by half an order of magnitude, and not uncommonly it varies by one or two orders of magnitude when outliers are considered. In both August (Figure 5.3) and January (Figure 5.5), flow significantly increases on the main stem Rio Grande from Lobatos (A) to Otowi (C), probably due to input of the major mountain tributaries of southern Colorado and northern New Mexico (Figure 5.4, Figure 5.6). In particular, the Rio Chama (d) is the most significant gaged tributary of this reach, entering the Rio Grande between Taos Junction bridge (B) and Otowi (C) (Figure 5.4, Figure 5.6). Main stem flow does not change much between Otowi (C) and San Felipe (D) in either August (Figure 5.3) or January (Figure 5.5). Further downstream, fairly insignificant Jemez River (e) inflow (Figure 5.4, Figure 5.6) does not seem to increase flow significantly between San Felipe (D) and Bernardo (E) (Figure 5.3, Figure 5.5). In fact, flow decreases dramatically between these two stations in August (Figure 5.3). This drop is not as dramatic in the January historical record (Figure 5.5), indicating that loss of flow in August can probably be attributed to summer agricultural diversions. Flow loss due to significant riverbed seepage in the middle Rio Grande probably accounts for the broad range of January flows from Bernardo (E) to San Marcial (G) (Figure 5.5). Riverbed seepage is also significant in the summer, but the August

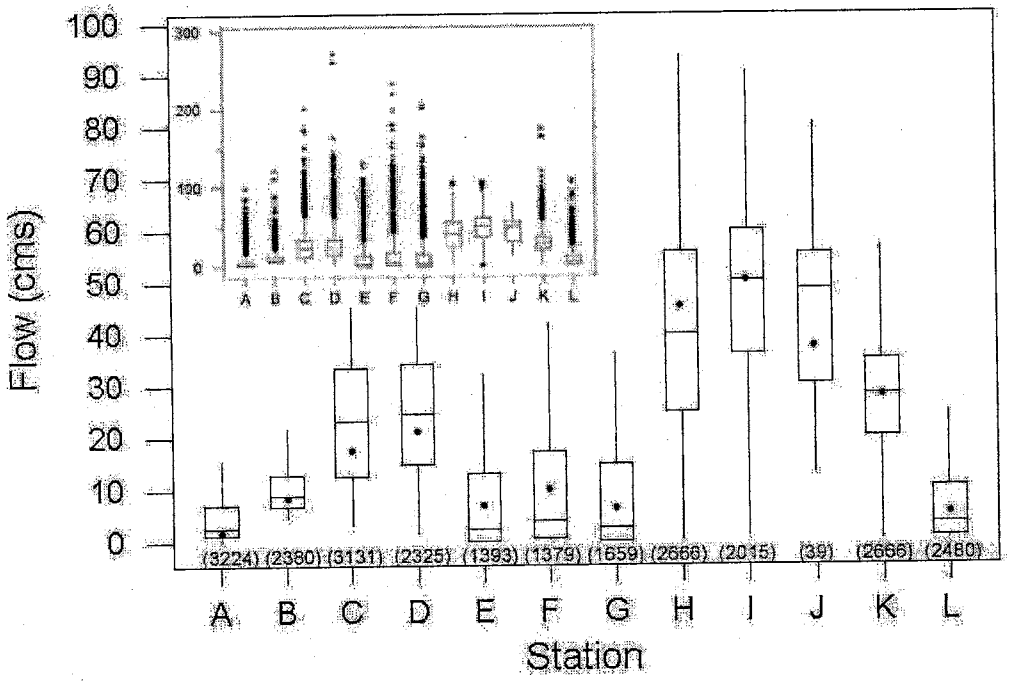

Figure 5.3: Historical August flow of the Rio Grande compared to USGS gaging data for August 2001, Lobatos - Ft. Quitman. Inset shows the full extent of the data with outliers. Stations are identified in Table 5.2. Each box extends across the interquartile range from the 25^{th} to the 75^{th} percentile of the data. The line across the inside of the box represents the median. Whiskers extend to 1.5 times the interquartile range; outliers are shown by asterisks. Heavy black dots represent recent conditions from data collected for this study (August 2001 or January 2002).

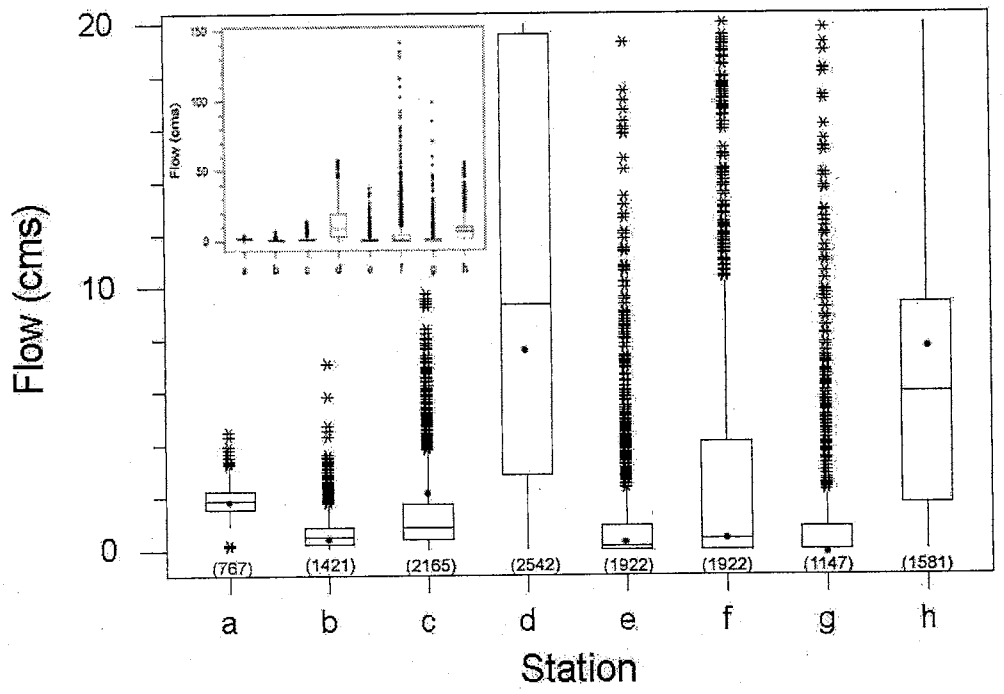

Figure 5.4: Historical August flow of major tributaries of the Rio Grande compared to USGS gaging data for August 2001, Red River - Conveyance Channel at San Marcial. Inset shows the full extent of the data. Stations are identified in Table 5.4. See Figure 5.3 for explanation of box and whisker symbology.

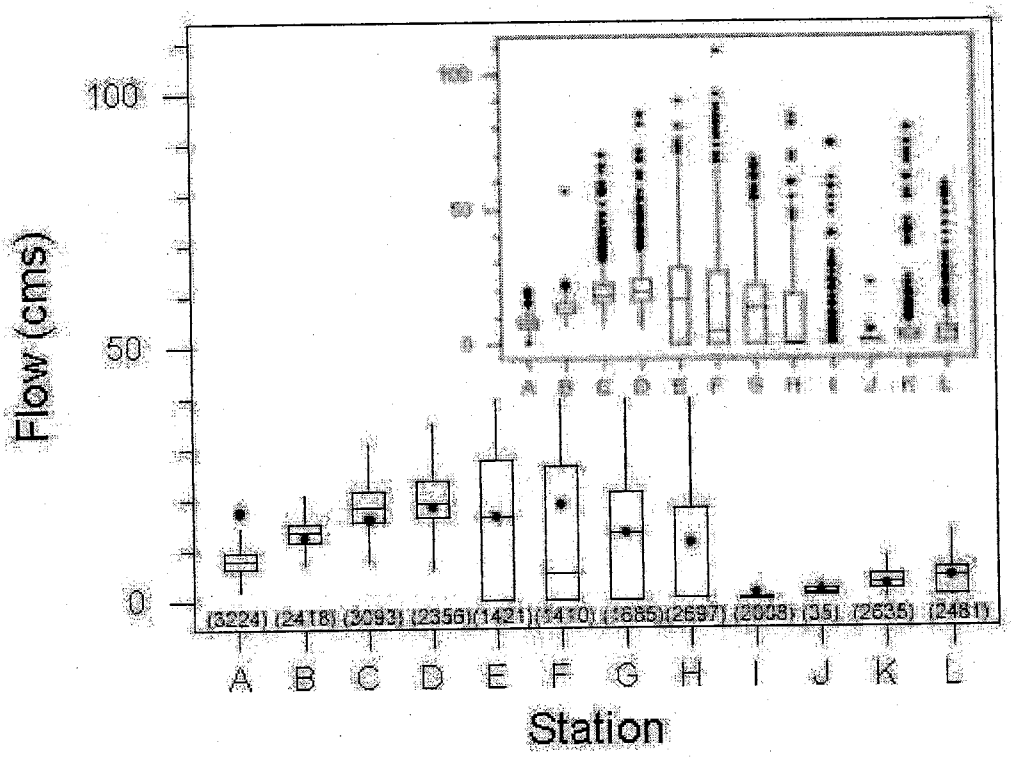

Figure 5.5: Historical January flow of the Rio Grande compared to USGS gaging data for January 2002, Lobatos - Ft. Quitman. The median historical flow below Elephant Butte Reservoir (H) is near zero. Inset shows the full extent of the data with outliers. Stations are identified in Table 5.2. See Figure 5.3 for explanation of box and whisker symbology.

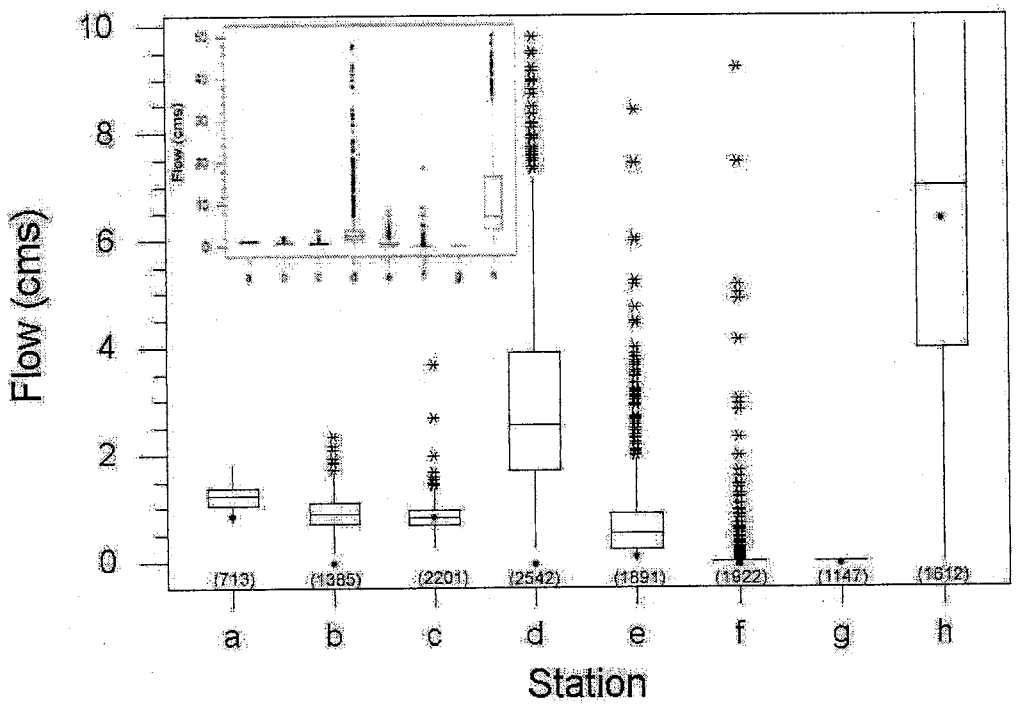

Figure 5.6: Historical January flow of major tributaries of the Rio Grande compared to USGS gaging data for January 2002, Red River - Conveyance Channel at San Marcial. Inset shows the full extent of the data. Stations are identified in Table 5.4. See Figure 5.3 for explanation of box and whisker symbology.

historical record does not reflect such a wide range of flows in this reach because agricultural diversions also remove river flow (Figure 5.3). Natural tributaries in this region, the Rio Puerco (f) and Rio Salado (g), contribute fairly insignificant flows (Figure 5.4, Figure 5.6).

In both seasons a significant change in flow conditions is apparent between San Marcial (G) and the outlet of Elephant Butte Reservoir (H) (Figure 5.3, Figure 5.5). The only major tributary in this region and the southernmost major tributary of the Rio Grande in the field area, the Conveyance Channel (h) contributes significant flow to the river (Figure 5.4,Figure 5.6), but the change in flow in this region is affected more by the operations of Elephant Butte Reservoir. In August (Figure 5.3), water is released for downstream irrigation use, and increased river flow due to these reservoir releases is noticeable through El Paso (K). By Ft. Quitman (L), flow seems to return to a "natural" level similar to river flow above Elephant Butte Reservoir. In January (Figure 5.5), water is stored in Elephant Butte Reservoir with the exception of releases for hydropower production, which are stored in Caballo Reservoir. This results in an almost complete termination of flow in the river below each of the reservoirs. Downstream flow increases are probably due to return flow from drains that continue to return shallow groundwater to the river year-round, as well as from wastewater treatment plant inflows at Las Cruces and El Paso.

5.5.2 Historical chloride concentration conditions during August and January

Similar to flow, chloride concentration on the Rio Grande and its tributaries commonly varies by half an order of magnitude or more at a single

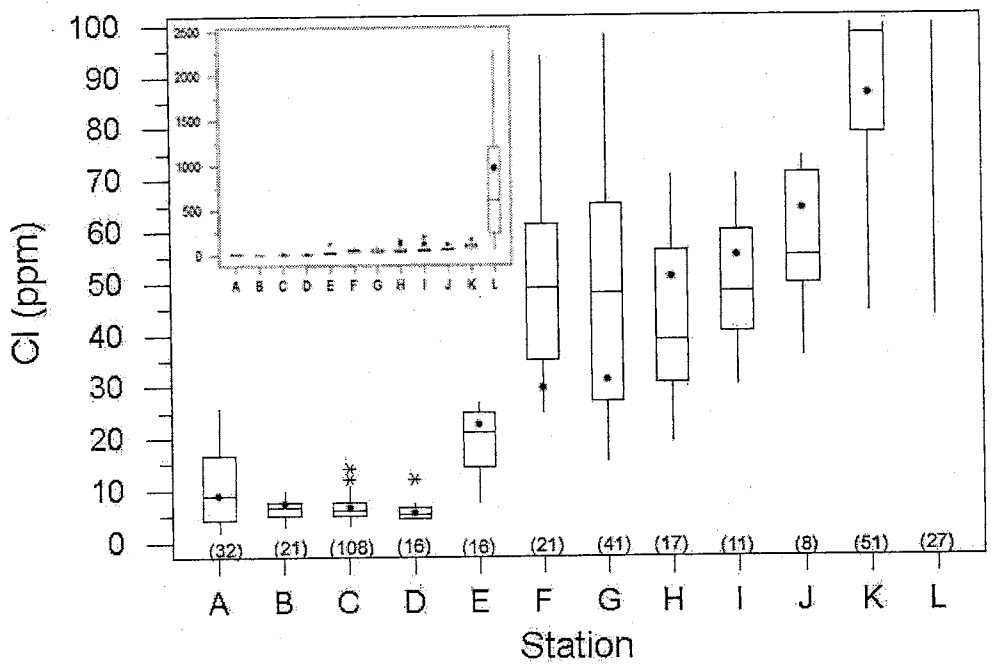

Figure 5.7: Historical August chloride concentration of the Rio Grande compared to August 2001, Lobatos - Ft. Quitman. Inset shows the full extent of the data. Stations are identified in Table 5.2. See Figure 5.3 for explanation of box and whisker symbology.

station, and by two orders of magnitude with distance downstream (Figure 5.7, Figure 5.8, Figure 5.9, Figure 5.10, and Figure 5.11). Significant chloride increases during both the August and January historical records are apparent at Bernardo (E), San Acacia (F), El Paso (K), and Ft. Quitman (L) (Figure 5.7, Figure 5.9, and Figure 5.10). Additionally, a major chloride jump between the outlets of Elephant Butte (H) and Caballo (I) Reservoirs is noticeable in the January record (Figure 5.9). The relatively broad spread of August chloride concentration data at Lobatos (A) (Figure 5.7) is probably due to variable in-

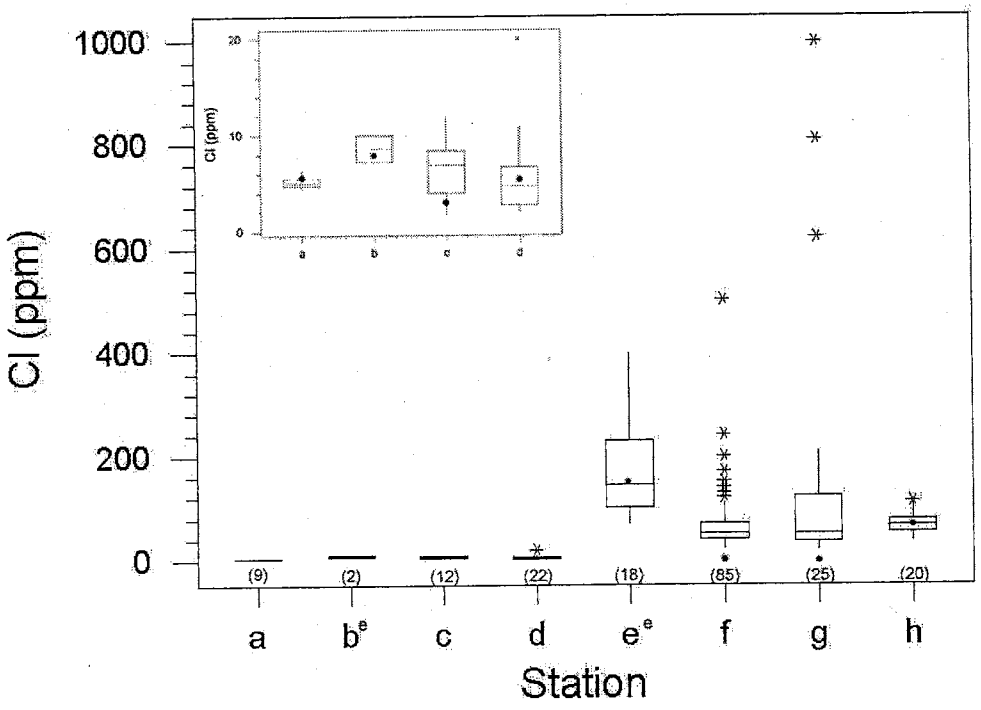

Figure 5.8: Historical August chloride concentration of major tributaries of the Rio Grande compared to August 2001, Red River - Conveyance Channel at San Marcial. Inset shows detail of the region from the Red River to the Rio Chama. The superscript "e" on a station label indicates an estimated rather than measured value. Stations are identified in Table 5.4. See Figure 5.3 for explanation of box and whisker symbology.

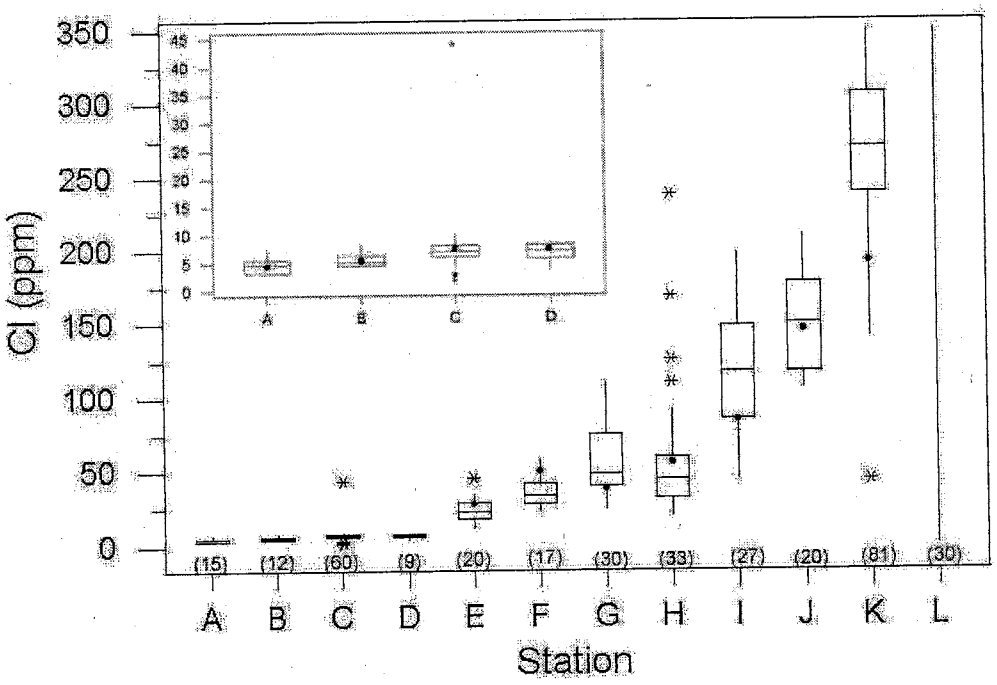

Figure 5.9: Historical January chloride concentration of the Rio Grande compared to January 2002, Lobatos - Ft. Quitman. See Figure 5.10 for full extent of the historical data. Stations are identified in Table 5.2. See Figure 5.3 for explanation of box and whisker symbology.

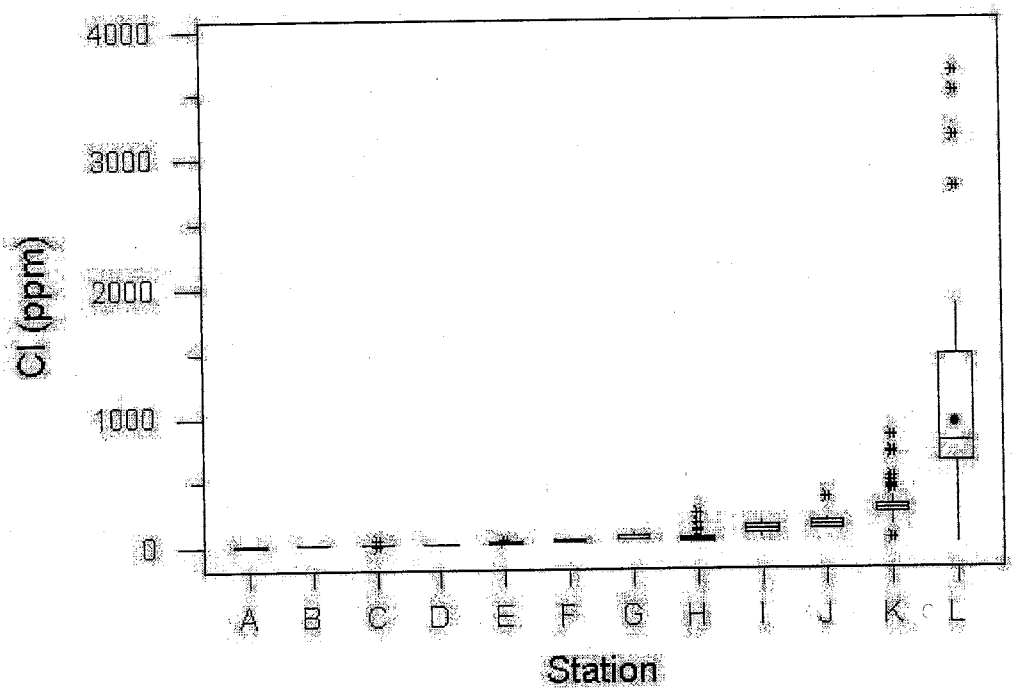

Figure 5.10: Historical January chloride concentration of the Rio Grande compared to January 2002, Lobatos - Ft. Quitman. Graph shows full extent of historical chloride data. Stations are identified in Table 5.2. See Figure 5.3 for explanation of box and whisker symbology.

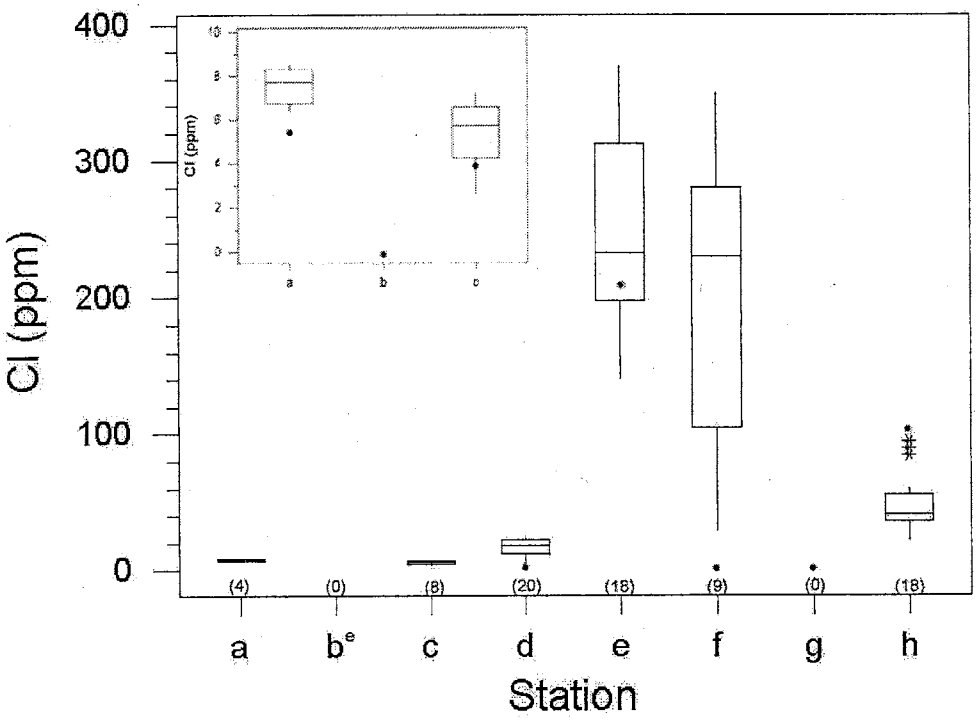

Figure 5.11: Historical January chloride concentration of major tributaries of the Rio Grande compared to January 2002, Red River - Conveyance Channel at San Marcial. Inset shows detail of Red River - Embudo Creek. The superscript "e" on a station label indicates a calculated rather than measured value. Stations are identified in Table 5.4. See Figure 5.3 for explanation of box and whisker symbology.

flow of relatively high-TDS waters from the Closed Basin Canal. Other causes of chloride concentration increase will be investigated using environmental tracers in Chapters 7 - 10. Tributaries that contribute significant chloride include the four southernmost major gaged tributaries: the Jemez River (e), the Rio Puerco (f), the Rio Salado (g), and the Conveyance Channel (h) (Figure 5.8, Figure 5.11). The Jemez River consistently had the highest chloride concentration in the historical record. In general, tributary chloride concentrations are lower in January (Figure 5.11) than in August (Figure 5.8), but river concentrations show the opposite pattern (Figure 5.7, Figure 5.9, and Figure 5.10).

5.5.3 Historical chloride burden conditions during August and January

The chloride burden calculations from the historical record reflect a combination of the historical patterns in flow and chloride data (Figure 5.12, Figure 5.13, Figure 5.14, and Figure 5.15). During August and January in the historical record, chloride burden increases significantly from Lobatos (A) to San Felipe (D) (Figure 5.12, Figure 5.14) just as discharge does (Figure 5.3, Figure 5.5). This indicates that chloride burden increase in the Rio Grande in this reach is due to the same processes that cause flow increase, namely tributary input. Despite the fact that by San Felipe (D) river flow reaches some of its highest values (with the exception of flows due to reservoir releases), the chloride burden at San Felipe remains less than five percent of the total chloride burden at Ft. Quitman (L) (Figure 5.12, Figure 5.14). The natural tributaries contributing to the river in this reach therefore must be very dilute, which is confirmed by the historical record of tributary chloride burden

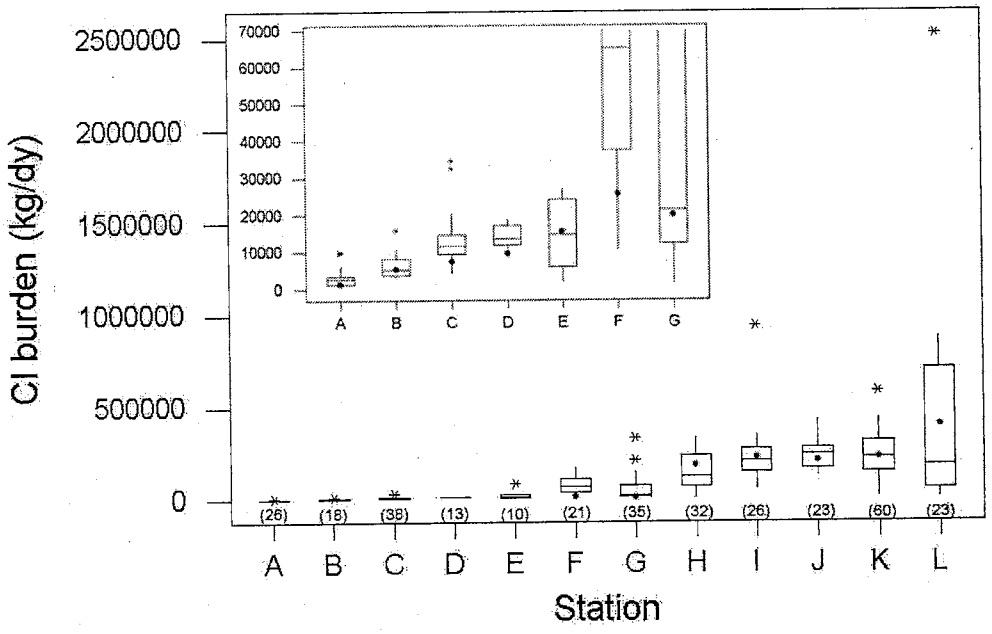

Figure 5.12: Historical August chloride burden of the Rio Grande compared to August 2001, Lobatos - Ft. Quitman. Stations are identified in Table 5.2. See Figure 5.3 for explanation of box and whisker symbology.

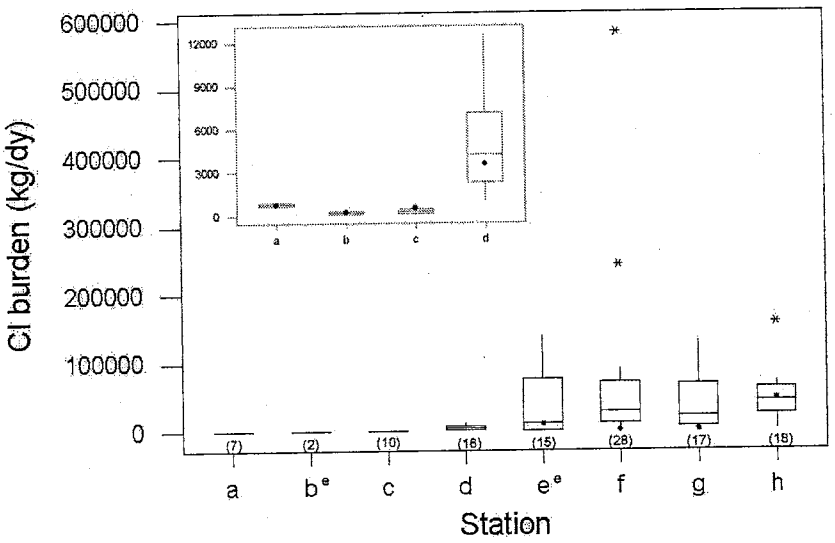

Figure 5.13: Historical August chloride burden of tributaries of the Rio Grande compared to August 2001, Red River - Conveyance Channel at San Marcial. The superscript "e" on a station label indicates the burden calculation is based on a calculated value. Stations are identified in Table 5.4. See Figure 5.3 for explanation of box and whisker symbology.

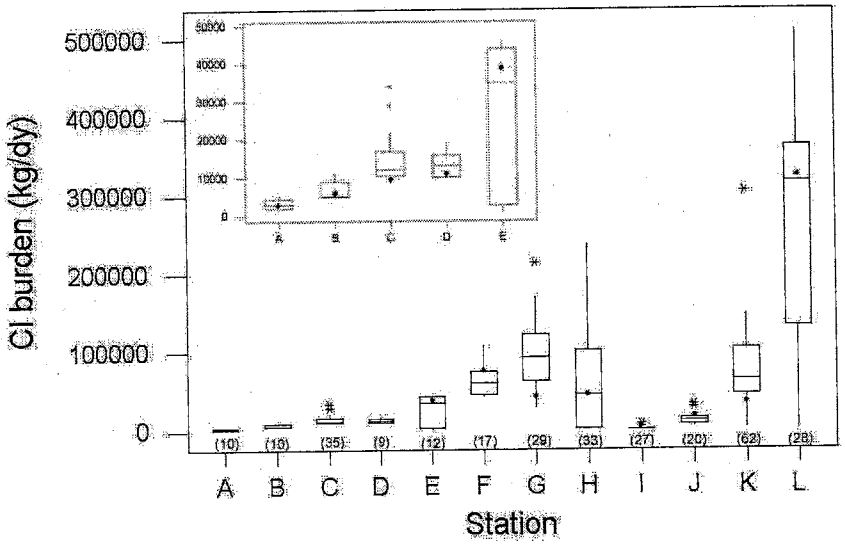

Figure 5.14: Historical January chloride burden of the Rio Grande compared to January 2002, Lobatos - Ft. Quitman. Stations are identified in Table 5.2. See Figure 5.3 for explanation of box and whisker symbology.

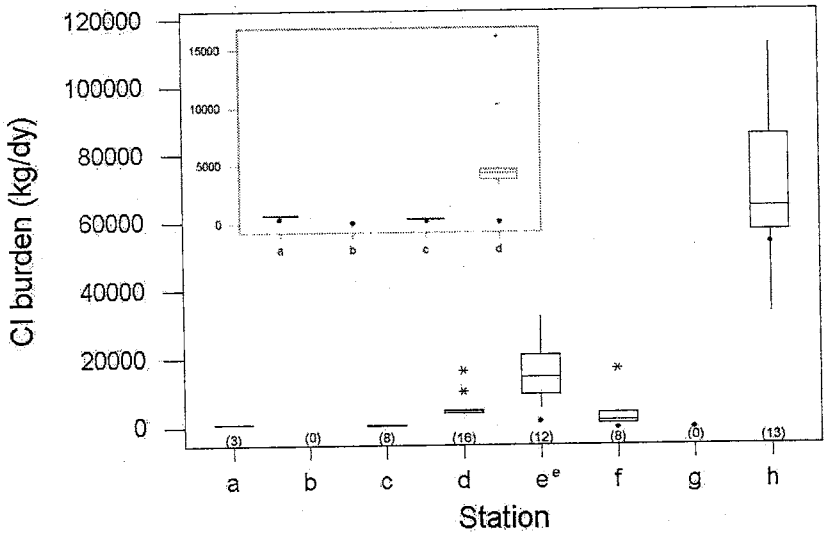

Figure 5.15: Historical January chloride burden of tributaries of the Rio Grande compared to August 2001, Red River - Conveyance Channel at San Marcial. The superscript "e" on a station label indicates the burden calculation is based on a calculated value. Stations are identified in Table 5.4. See Figure 5.3 for explanation of box and whisker symbology.

(Figure 5.13, Figure 5.15). Chloride burden of the main stem Rio Grande significantly increases again at Bernardo (E) during irrigation and non-irrigation season (Figure 5.12, Figure 5.14), corresponding with a major chloride concentration increase (Figure 5.7, Figure 5.9) but not a flow increase (Figure 5.3, Figure 5.5). This indicates the inflow of high-concentration, low-volume inflows between San Felipe (D) and Bernardo (E). The Jemez River (e) is probably one of these inflows; its chloride burden and chloride concentration are also high though its discharge is low. The Southside Water Reclamation Plant in Albuquerque is probably another important high-concentration input. Between 1999 and 2002, TDS values of filtered, reused effluent ranged between 273 - 560 mg L^{-1} [*Steve Glass, SWRP,* personal communication 2003]. Operating within the narrow range of 52 - 53 million gallons per day (2.28 - 2.32 m^3 s^{-1}) during those four years, the monthly salt burden from the SWRP would have been between 53,700 and 112,300 kg dy^{-1}. Assuming a chloride to TDS ratio of 0.2 from a sample collected at the SWRP in July 2002 with a TDS of 530 mg L^{-1} and a chloride concentration of 90 mg L^{-1}, this is equivalent to a chloride burden of 10,700 - 22,500 kg dy^{-1}. In combination with input from the Jemez River, contributions from the SWRP are large enough to explain the historical doubling of chloride burden between San Felipe (D) and Bernardo (E) during the winter (Figure 5.14). It is unclear why the median chloride burden between these two stations does not increase as much during the summer given these high inputs (Figure 5.12).

Rio Grande chloride burden again increases at San Acacia (F) (Figure 5.12, Figure 5.14), in tandem with a chloride concentration increase (Figure 5.7, Figure 5.9) with no significant flow increase (Figure 5.3, Figure 5.5).

Once again, this indicates the existence of high-concentration, low-volume inflows between Bernardo (E) and San Acacia (F). The next significant change in chloride burden occurs below Elephant Butte Reservoir (H). The changes have opposite trends for August (Figure 5.12) and January (Figure 5.14), reflecting the historical flow patterns rather than chloride concentration patterns. The downstream effects of inputs from the Rio Puerco (f), Rio Salado (g), and Conveyance Channel (h) are obscured by Elephant Butte Reservoir operations (Figure 5.13, Figure 5.15). However, it is apparent from the high chloride burdens and high chloride concentrations (Figure 5.8, Figure 5.11) of these three that they each contribute significant salt to the river in the middle Rio Grande. The high chloride burdens of the Rio Puerco (f) and Rio Salado (g) closely reflect their high chloride concentrations, though the high chloride burden of the Conveyance Channel (h) is dependent on its relatively high flow in combination with a moderately high chloride concentration.

In both the August and January historical records, the chloride burden again increases between Elephant Butte (H) and Caballo (I) reservoirs, a reach where there are no major known tributaries (Figure 5.12, Figure 5.14). In the summer this burden increase is accompanied by a slight increase in chloride concentration (Figure 5.7) and in flow (Figure 5.3), but in the winter the burden increase is accompanied by a more pronounced increase in chloride concentration (Figure 5.9) and a drastic decrease in flow (Figure 5.5) due to lack of reservoir releases. In January, the historical chloride burden also increases at El Paso (K) and at Ft. Quitman (L) (Figure 5.14); in the August historical record (Figure 5.12), broadening of the range of burden values is apparent rather than distinct jumps. Comparing these two months, the tempering of

summer burden increases is probably due to agricultural diversion of water, and thus chloride, from the river.

5.5.4 Analysis of temporal variation in historical data using annual parameter averages

In order to evaluate temporal variation of discharge, chloride concentration, and chloride burden with distance downstream, annual averages for these parameters were calculated for the main stem Rio Grande (Figure 5.16, Figure 5.17, and Figure 5.18). Annual averages were calculated as the means of all values available from January to December of a single year. Flow data were typically available for 9 - 12 months of any particular year during which data were collected, but for about 20% of data-collection years, chloride concentration data were available for fewer than six months of the year. In most cases, chloride concentration data were measured at equal time intervals through the year, and they generally represent the full seasonal variability of the particular year in which they were collected. For this reason, years with few chloride concentration measurements were still included in the annual parameter average calculations. Comparing historical annual average flow (Figure 5.16) to historical August (Figure 5.3) and January flow (Figure 5.5) shows that monthly flow conditions commonly vary from annual averages by one half to one order of magnitude, depending on the reach of river considered. Chloride concentrations in August (Figure 5.7) and January (Figure 5.9, Figure 5.10) vary from the annual averages much less than discharge from Lobatos (A) to Bernardo (E), though they vary from the annual average range by up to 50% downstream (Figure 5.17). One exception is the chloride concentration at the outlet of Ele-

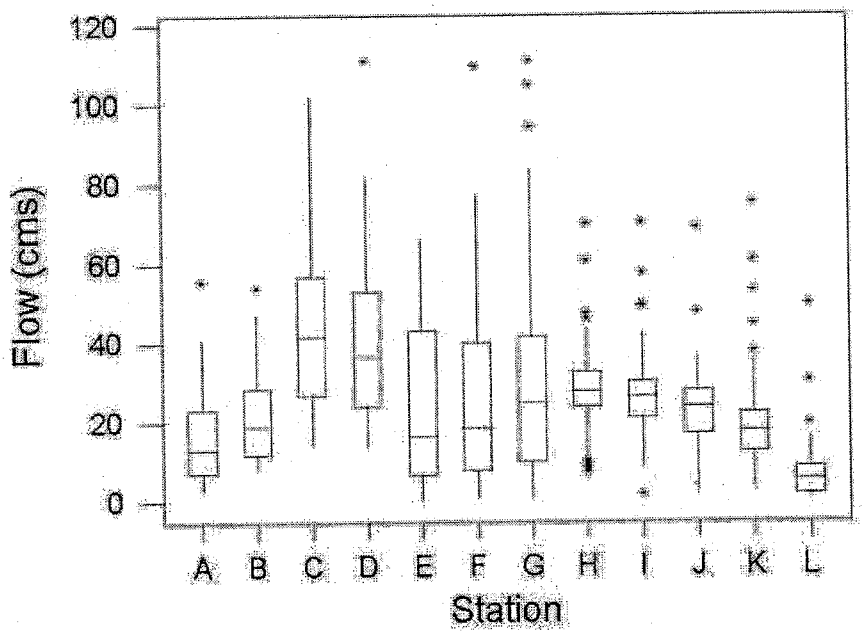

Figure 5.16: Average annual flow of the Rio Grande, Lobatos - Ft. Quitman. Stations are identified in Table 5.2. See Figure 5.3 for explanation of box and whisker symbology. See Figure ?? for temporal range of data for each station.

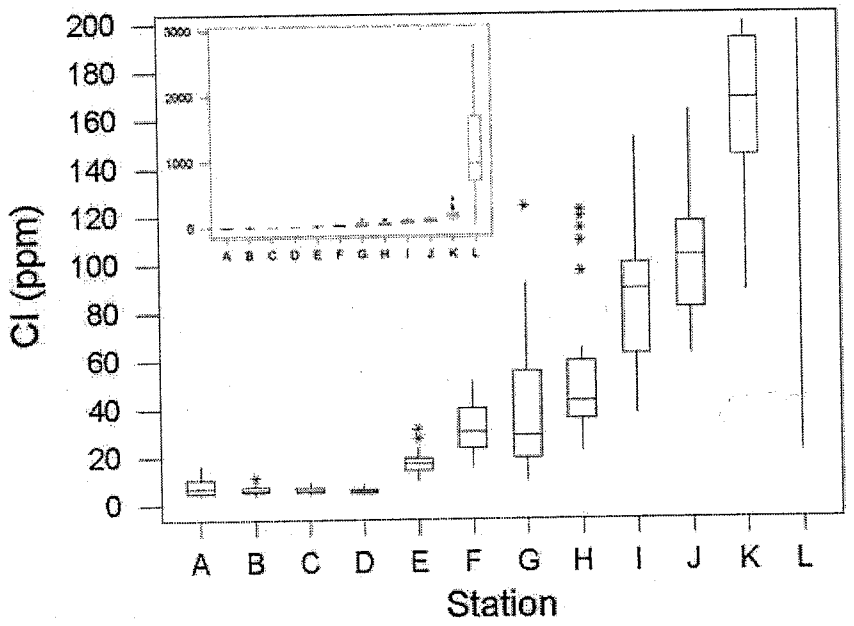

Figure 5.17: Average annual chloride concentration of the Rio Grande, Lobatos - Ft. Quitman. Stations are identified in Table 5.2. See Figure 5.3 for explanation of box and whisker symbology. See Figure ?? for temporal range of data for each station.

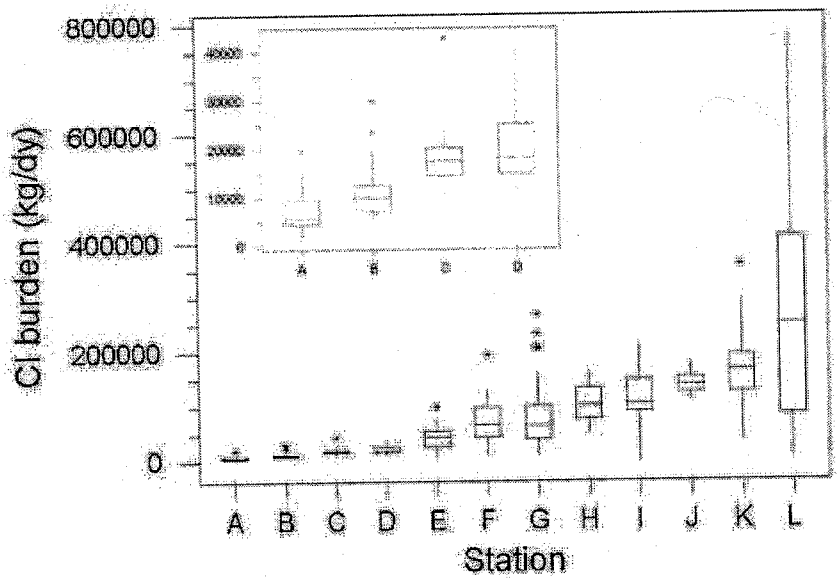

Figure 5.18: Average annual chloride burden of the Rio Grande, Lobatos - Ft. Quitman. Stations are identified in Table 5.2. See Figure 5.3 for explanation of box and whisker symbology. See Figure ?? for temporal range of data for each station.

phant Butte Reservoir (H), which has about the same chloride concentration range annually as monthly. This is most likely due to the integrating effect that the reservoir has on upstream water quality as water sits behind the dam for long periods of time. Historical chloride burdens have ranges similar to the annual averages with distance downstream, except in January when the range of burden values is up to 50% lower than the annual range below Elephant Butte Reservoir to El Paso. These low January values probably reflect the historical attenuation of winter reservoir releases.

This comparison demonstrates that the annual and monthly averages of flow often differ by up to an order of magnitude. Chloride concentration and chloride burden upstream of Elephant Butte Reservoir have about the same range over monthly and annual conditions in the historical record, though conditions downstream of the reservoir vary by up to half an order of magnitude downstream of the reservoir.

5.6 General comparison of historical data with August 2001 and January 2002 data

To get a general idea of how field conditions compare with historical averages, simple line graphs were constructed. Graphs for discharge and chloride burden were plotted with distance downstream to compare August 2001 and January 2002 values with the August and January monthly averages as well as the 6-month seasonal averages at each station (Tables 5.6 - 5.7; Figure 5.19, Figure 5.20, Figure 5.21, Figure 5.22). Because tributaries were each sampled at a single location closest to their point of discharge to the Rio Grande, comparing tributary historical and field conditions with a line graph

Table 5.6: Seasonal and monthly historical average river discharges compared to August 2001 and January 2002 discharges ($m^3\ s^{-1}$). Stations are identified by name in Table 5.2.

station	summer (Apr-Sept)	Aug avg	Aug '01	winter (Oct-Mar)	Jan avg	Jan '02
A	22.4	6.7	1.8	9.5	8.0	17.6
B	27.7	11.8	8.4	14.8	13.6	12.3
C	60.9	26.5	16.6	24.4	19.4	15.8
D	54.9	29.1	21.8	24.9	21.3	17.1
E	31.9	11.5	8.2	16.7	16.6	16.1
F	33.6	16.5	11.2	15.8	15.4	19.8
G	40.7	16.4	7.2	16.4	15.7	13.6
H	42.0	40.0	45.3	14.9	9.2	9.4
I	43.0	48.0	50.7	10.1	2.0	1.0
J	39.5	44.7	35.6	9.6	2.2	1.2
K	28.9	28.3	27.7	8.5	4.6	2.4
L	7.0	8.5	5.1	5.4	4.5	4.6

Table 5.7: Seasonal and monthly historical average river chloride burdens compared to August 2001 and January 2002 burdens (kg dy^{-1}). Stations are identified by name in Table 5.2.

station	summer (Apr-Sept)	Aug avg	Aug '01	winter (Oct-Mar)	Jan avg	Jan '02
A	8.68E+03	3.05E+03	1.38E+03	4.73E+03	3.21E+03	9.95E+04
B	1.22E+04	6.33E+03	5.17E+03	7.95E+03	6.70E+03	2.08E+05
C	2.07E+04	1.33E+04	9.38E+03	1.50E+04	1.44E+04	4.46E+05
D	2.11E+04	1.45E+04	1.00E+04	1.48E+04	1.36E+04	4.23E+05
E	3.90E+04	2.10E+04	1.59E+04	3.22E+04	2.60E+04	8.05E+05
F	9.47E+04	9.14E+04	2.63E+04	7.77E+04	8.56E+04	2.65E+06
G	9.36E+04	5.30E+04	1.90E+04	8.22E+04	9.80E+04	3.04E+06
H	1.52E+05	1.51E+05	2.05E+05	5.65E+04	5.73E+04	1.78E+06
I	1.97E+05	2.37E+05	2.37E+05	4.30E+04	1.21E+03	3.77E+04
J	2.12E+05	2.42E+05	1.93E+05	5.61E+04	1.27E+04	3.93E+05
K	2.10E+05	2.35E+05	2.04E+05	1.05E+05	7.57E+04	2.35E+06
L	3.26E+05	4.09E+05	3.72E+05	2.78E+05	2.73E+05	8.47E+06

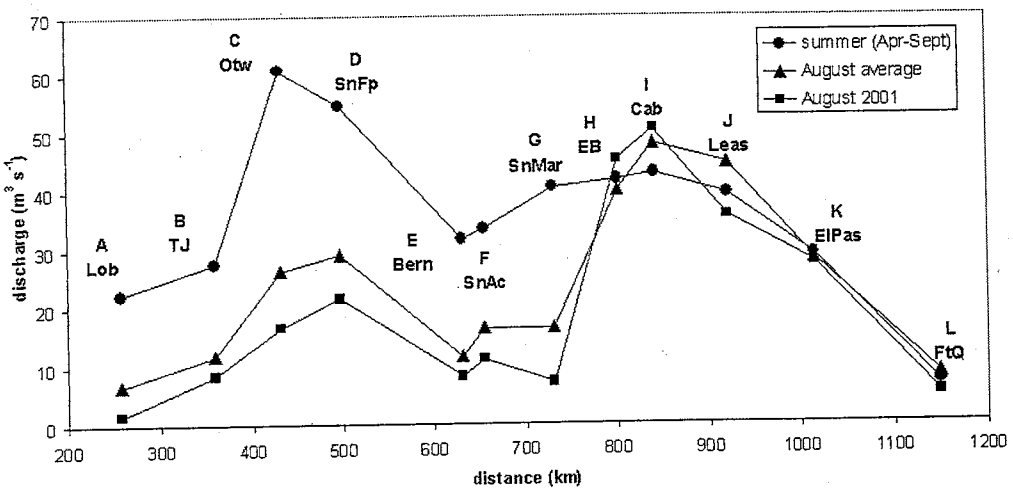

Figure 5.19: August 2001 river discharge compared to historical monthly and seasonal average discharges with distance downstream. Stations are identified in Table 5.2.

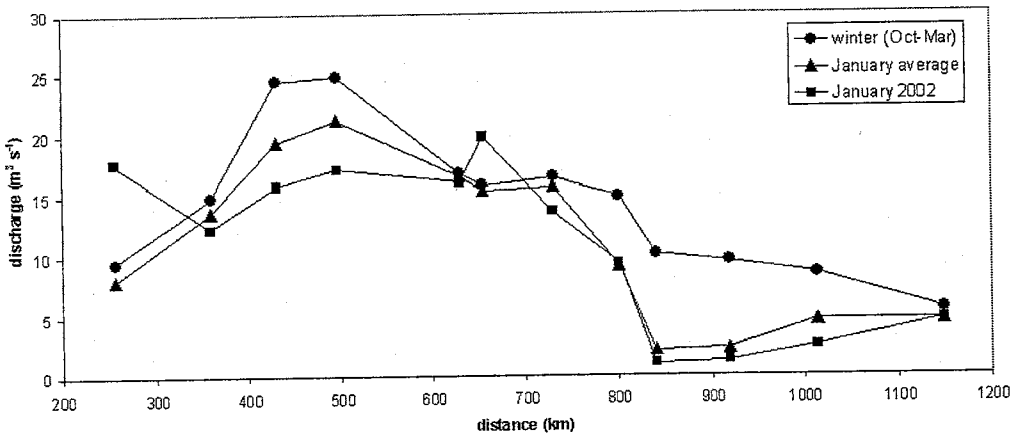

Figure 5.20: January 2002 river discharge compared to historical monthly and seasonal average discharges with distance downstream. Stations are identified in Table 5.2.

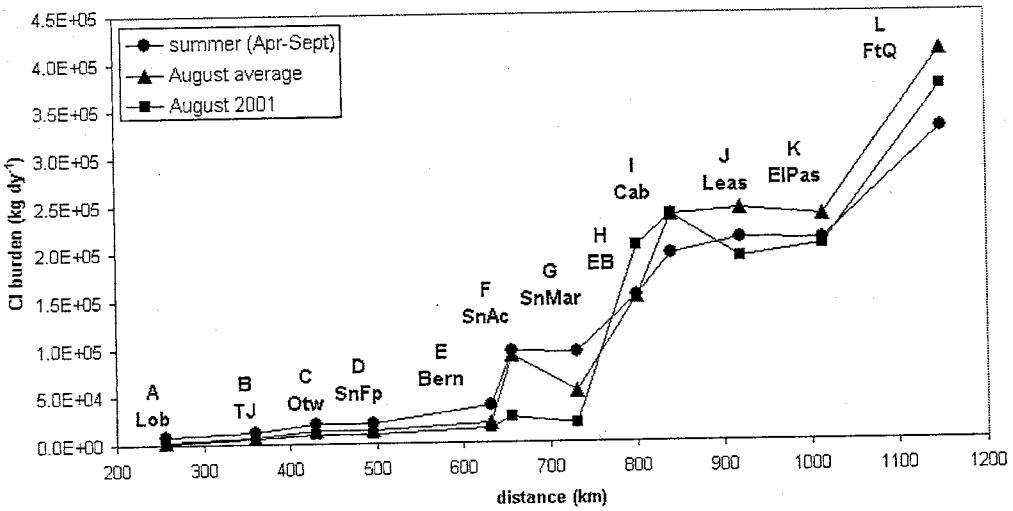

Figure 5.21: August 2001 chloride burden compared to historical monthly and seasonal average discharges with distance downstream. Stations are identified in Table 5.2.

would misleadingly imply a progression of parameters between tributaries. For this reason, line graphs were only constructed for the main stem Rio Grande. Historical averages were calculated as means of average monthly values, such that each point on the monthly average line represents the average of all historical values for the given parameter for that month at that location. Each point on the seasonal average line indicates the average of all historical values at that location for the relevant season, either summer irrigation season (April-September) or the winter non-irrigation season (October-March).

With distance downstream, August 2001 and January 2002 discharge conditions mimic the patterns of the monthly average conditions (Figure 5.19, Figure 5.20). Historical seasonal averages follow a similar pattern, though the

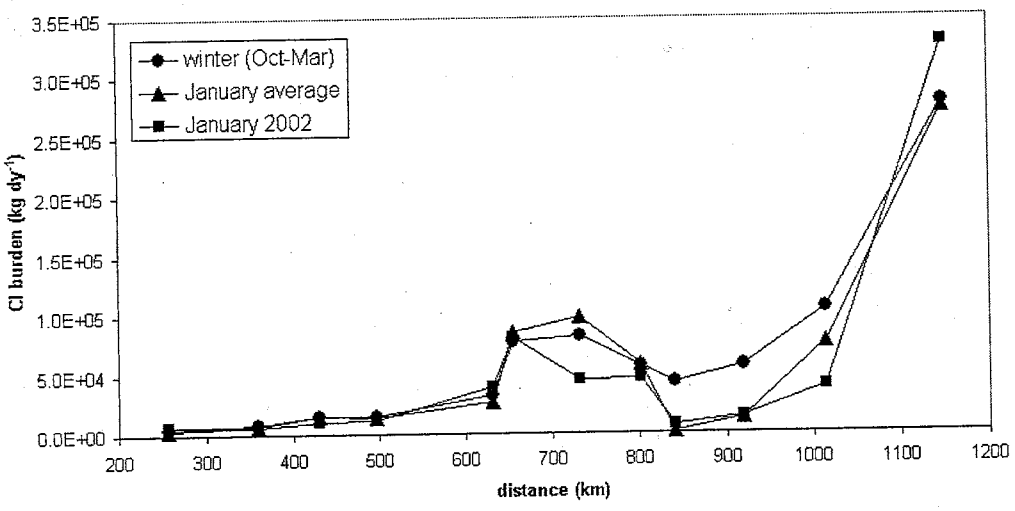

Figure 5.22: January 2002 chloride burden compared to historical monthly and seasonal average discharges with distance downstream. Stations are identified in Table 5.2.

seasonal pattern is not particularly coincident with the monthly pattern nor the August 2001 and January 2002 data. This is not surprising, since it is expected that a wider range of conditions exists on the river during the course of the 6-month-long season that during any single month. The field chloride burden conditions are similar to both the monthly and seasonal averages (Figure 5.21 - Figure 5.22), though August 2001 and January 2002 conditions follow the monthly trend more closely. Because monthly comparisons to data collected for this study seem more meaningful than seasonal comparisons, further historical data analysis was restricted to monthly values.

Table 5.8: Rio Grande discharge values ($m^3\ s^{-1}$) and percentiles for August 2001 and January 2002.

Rio Grande		August 2001		January 2002	
label	location	value	percentile	value	percentile
A	Lobatos	1.78	0.40	17.6	0.997
B	Taos Junction	8.41	0.46	12.3	0.34
C	Otowi	16.6	0.35	15.8	0.29
D	San Felipe	21.8	0.41	17.1	0.33
E	Bernardo	8.15	0.64	16.1	0.49
F	San Acacia	11.2	0.66	19.8	0.61
G	San Marcial	7.19	0.63	13.6	0.52
H	EB dam	45.3	0.61	9.40	0.69
I	Caballo dam	50.7	0.50	1.02	0.82
J	Leasburg	35.6	0.35	1.19	0.62
K	El Paso	27.7	0.48	2.41	0.32
L	Ft. Quitman	5.07	0.59	4.61	0.55

5.7 Comparison of historical data to August 2001 and January 2002 data using percentile calculations

Comparison of historical data with August 2001 and January 2002 data was performed using percentile calculations in EXCEL. Percentiles were calculated using the PERCENTRANK command (Tables 5.8 - 5.13), and the values were graphed as heavy black dots on the box and whisker plots of historical data just discussed. It should be kept in mind that the number of available measurements or calculations for each station significantly affects the percentile calculations. In particular, there are relatively few chloride concentration and chloride burden values in the historical record. The fewer historical values available, the less likely it is that a percentile calculation will correctly reflect the relationship of a field value to actual historical conditions. Additionally, with fewer historical values, it is more likely that a field value will

Table 5.9: Rio Grande chloride concentration values (mg L^{-1}) and percentiles for August 2001 and January 2002.

Rio Grande		X01		W02	
label	location	value	percentile	value	percentile
A	Lobatos	8.97	0.52	4.60	0.45
B	Taos Junction	7.11	0.67	5.61	0.64
C	Otowi	6.53	0.60	7.56	0.61
D	San Felipe	5.34	0.55	7.71	0.63
E	Bernardo	22.6	0.53	27.8	0.71
F	San Acacia	27.1	0.05	47.4	0.83
G	San Marcial	30.5	0.29	38.5	0.20
H	EB dam	52.3	0.71	56.2	0.72
I	Caballo dam	54.3	0.77	83.1	0.23
J	Leasburg	62.7	0.86	139	0.45
K	El Paso	85.3	0.44	187	0.12
L	Ft. Quitman	849	0.65	825	0.54

Table 5.10: Rio Grande chloride burden values (kg dy^{-1}) and percentiles for August 2001 and January 2002.

Rio Grande		X01		W02	
label	location	value	percentile	value	percentile
A	Lobatos	1.38E+03	0.30	2.64E+03	0.40
B	Taos Junction	5.17E+03	0.47	5.97E+03	0.61
C	Otowi	9.38E+03	0.21	1.03E+04	0.24
D	San Felipe	1.00E+04	0.08	1.14E+04	0.37
E	Bernardo	1.59E+04	0.56	3.87E+04	0.65
F	San Acacia	2.63E+04	0.18	8.11E+04	0.81
G	San Marcial	1.90E+04	0.38	4.53E+04	0.07
H	EB dam	2.05E+05	0.70	4.56E+04	0.50
I	Caballo dam	2.37E+05	0.60	7.32E+03	0.96
J	Leasburg	1.93E+05	0.30	1.43E+04	0.76
K	El Paso	2.04E+05	0.44	3.90E+04	0.19
L	Ft. Quitman	3.72E+05	0.62	3.28E+05	0.57

Table 5.11: Major tributary discharge values ($m^3\ s^{-1}$) and percentiles for August 2001 and January 2002.

Tributaries		X01		W02	
label	location	value	percentile	value	percentile
a	Red River	1.87	0.47	0.93	0.074
b	Rio Pueblo de Taos	0.42	0.42	0	0
c	Embudo Creek	2.18	0.80	0.93	0.70
d	Rio Chama	7.70	0.46	0	0
e	Jemez River	0.65	0.69	0.22	0.24
f	Rio Puerco	0.48	0.51	0	0
g	Rio Salado	0	0	0	0
h	Conveyance Channel	8.12	0.65	6.17	0.37

Table 5.12: Major tributary chloride concentration values (mg L^{-1}) and percentiles for August 2001 and January 2002. A superscript "e" indicates a value that based on calculations rather than measured data.

Tributaries		X01		W02	
label	location	value	percentile	value	percentile
a	Red River	5.33	0.78	5.38	0
b	Rio Pueblo de Taos	7.76^e	0.20	0	na
c	Embudo Creek	3.21	0.09	4.05	0.16
d	Rio Chama	5.80	0.61	0	0
e	Jemez River	166^e	0.61	213^e	0.40
f	Rio Puerco	11.0	0	0	0
g	Rio Salado	0	0	0	na
h	Conveyance Channel	67.0	0.54	105	100

Table 5.13: Major tributary chloride burden values (kg dy^{-1}) and percentiles for August 2001 and January 2002. A superscript "e" indicates a value that based on calculations rather than measured data. "Na" indicates that percentile calculation was not possible due to lack of historical data.

Tributaries		X01		W02	
label	location	value	percentile	value	percentile
a	Red River	859	0.62	434	0
b	Rio Pueblo de Taos	285^e	0.87	0	na
c	Embudo Creek	604	0.89	327	0.21
d	Rio Chama	3854	0.42	0	0
e	Jemez River	9335^e	0.44	3955^e	0
f	Rio Puerco	459	0.01	0	0
g	Rio Salado	0	0	0	na
h	Conveyance Channel	47022	0.62	56012	0.12

appear as an outlier, though it may not be. It should also be kept in mind that although box and whisker plots of flow and of chloride concentration show all daily historical values available, chloride burden plots only represent calculations of flow and chloride data that are available on the same day. When more than one simultaneous daily set of flow and chloride data were present for a single month, all daily sets were averaged to derive a monthly burden value in order to be consistent with the method of data collection (see Section 5.3). For this reason, the box and whisker graphs for chloride burden represent a more limited and altered data set than either the flow or chloride concentration plots. This may result in seeming discrepancies between the percentile calculations for flow and chloride versus the percentile calculations for chloride burden, particularly for San Felipe (D) in August 2001 and for San Marcial (G) in January 2002. The percentile calculations here are an attempt to characterize the relationships between the historical and field data, but these caveats should be

kept in mind. This is particularly true for the tributary chloride concentration and chloride burden percentile calculations, since very few historical chloride concentration measurements are available.

Comparison of August 2001 and January 2002 discharge measurements with the historical record (Figure 5.3, Figure 5.5) shows that flow on the main stem Rio Grande between Lobatos (A) and San Felipe (D) generally was lower than average (median), while flow downstream of San Felipe (D) was at or above average for both August 2001 and January 2002. However, in both August 2001 and January 2002 the majority of flows fell between the first and third quartiles for each station, well within the standard flow conditions at each particular station. Tributary flow in August 2001 (Figure 5.4) was average for the Red River (a), the Rio Pueblo de Taos (b), the Jemez River (e), and the Rio Puerco (f); flow was above average for Embudo Creek (c) and the Conveyance Channel (h); flow was below average for the Rio Chama (d). Flow during January 2002 was below average for all major tributaries (Figure 5.6). The Rio Pueblo de Taos (b) and the Rio Puerco (f) were dry in January 2002, and the Rio Salado (g) was dry during both August 2001 and January 2002. Though the Rio Chama (d) was observed to be flowing during January 2002, the gage was frozen and a flow measurement is not available.

Main stem Rio Grande chloride concentrations for August 2001 and January 2002 fell within a varying range of conditions with distance downstream (Figure 5.7, Figure 5.9, Figure 5.10). Values from August 2001 and January 2002 were generally at or above average between Lobatos (A) and San Felipe (D), whereas conditions fluctuated downstream of San Felipe. Generally,

August 2001 and January 2002 values were within the first and third quartiles at each station, though there were a few exceptions. The chloride concentration at San Acacia (F) was particularly low in comparison to the historical record in August 2001 (Figure 5.7), but was particularly high in January 2002 (Figure 5.9). Chloride concentrations below Caballo Reservoir (I) and at El Paso (K) were particularly low in January 2002 (Figure 5.9). Tributary chloride concentration percentiles varied inconsistently with distance downstream in August 2001 (Figure 5.8), though they were all below average in January 2002 (Figure 5.11).

River chloride burdens were generally at or below average during August 2001 (Figure 5.12). Exceptions include below Elephant Butte Reservoir (H) and Ft. Quitman (L), where the chloride burdens were particularly high. In January 2002 (Figure 5.14), river chloride burdens vacillated between above- and below-average conditions with distance downstream. Tributary chloride burdens in August 2001 (Figure 5.13) were above average for Red River (a), Rio Pueblo de Taos (b), Embudo Creek (c), and the Conveyance Channel (h), but were at or below average for the remaining gaged tributaries. January 2002 tributary burdens (Figure 5.15) were consistently below average.

In general, comparison of August 2001 and January 2002 flow, chloride concentration, and chloride burden conditions shows that recent conditions are typical of historical conditions. Further analysis of August 2001 and January 2002 data (see Chapters 7 - 10) should reflect the same salinization patterns that have been present historically.

5.8 Transient salt storage and release in Elephant Butte Reservoir

With a capacity of over 2 million acre-feet (2.7 billion m^3) and a decadal-scale residence time (see Chapter 3, Table 3.1), it can be expected that Elephant Butte Reservoir has a large effect on river salt burden due to long-term transient salt storage and release. To determine the magnitude of this effect, the water quality records immediately above the reservoir at San Marcial (G) and below the reservoir (H) were examined in more detail and compared to USBR reservoir storage records [*Mike Landis, USBR,* personal communication 2002; *Javier Grajeda, USBR,* personal communication 2003]. The longest consecutive overlapping historical monthly chloride records for these two gaging stations are from January 1934 - September 1950. By estimating a linear relationship between chloride concentration at San Marcial and chloride concentration at San Acacia from 1940 - 1950, the historical water quality record at San Marcial was extended an additional 5 years by calculating chloride concentrations at San Marcial for October 1950 - December 1955 based on San Acacia chloride concentration data during that time. (The derived linear relationship did not include high chloride concentration conditions at San Acacia, and thus chloride concentrations at San Marcial may be overestimated from 1950 - 1955.) For a total of 21 years, monthly average chloride burdens were calculated at San Marcial and at the outlet of Elephant Butte Reservoir, and the burden below Elephant Butte was subtracted from the burden at San Marcial to calculate a monthly chloride burden imbalance through the reservoir (Figure 5.23). This imbalance was accumulated to determine the net effect of transient chloride storage and release with the filling and emptying of the reservoir (Figure 5.24). Missing chloride concentration data at San Marcial for

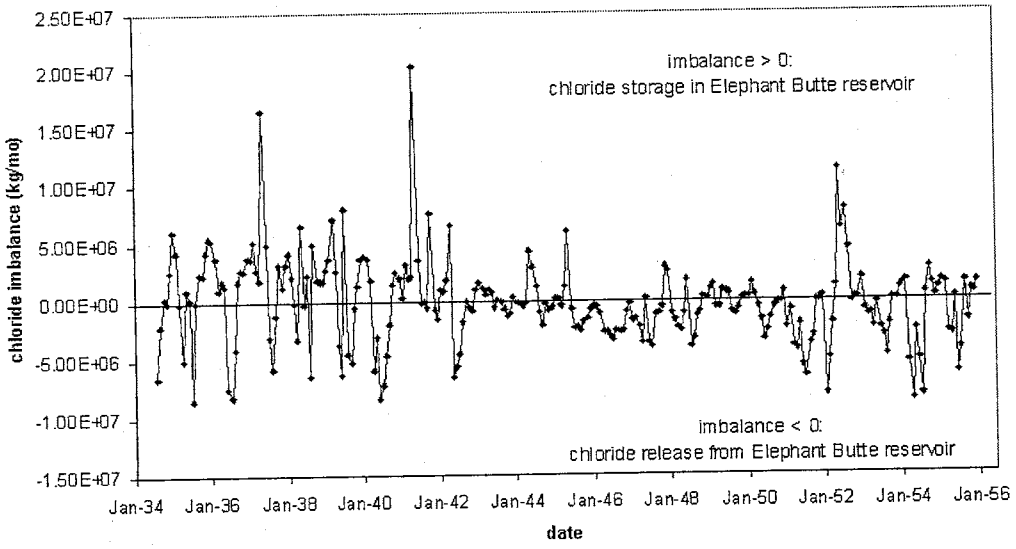

Figure 5.23: Chloride imbalance between San Marcial and the outlet of Elephant Butte Reservoir, Jan. 1934 - Dec. 1955. Chloride imbalance was calculated as the chloride burden at Elephant Butte subtracted from the chloride burden at San Marcial. No gaging data is available for July 1934 at San Marcial. Chloride burdens at San Marcial for the year 1947 and for Oct. 1950 - Dec. 1955 were estimated (see text).

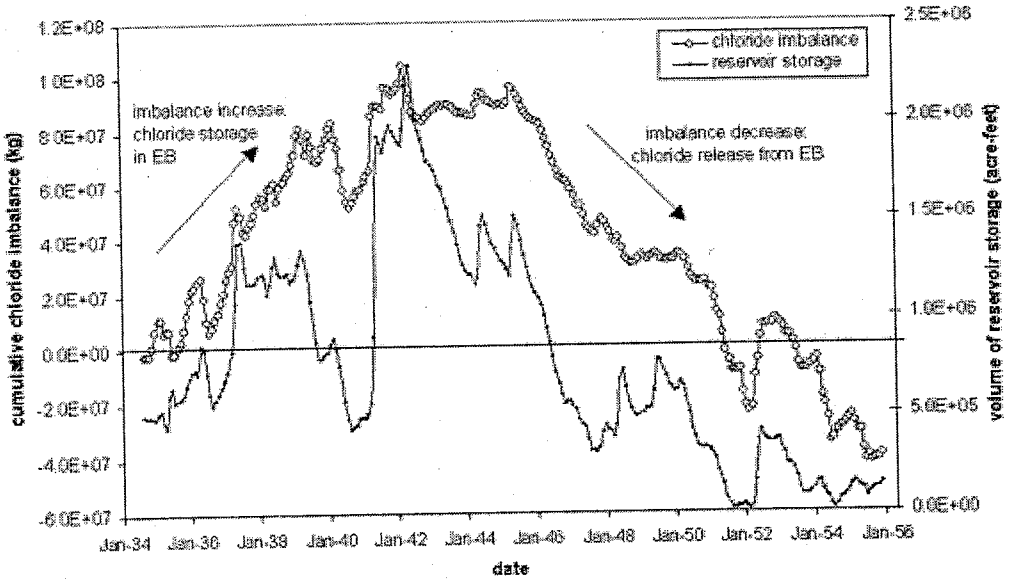

Figure 5.24: Elephant Butte average monthly reservoir storage and cumulative chloride imbalance between San Marcial and the outlet of Elephant Butte Reservoir, Sept. 1934 - Dec. 1955. Chloride burdens at San Marcial for the year 1947 and for Oct. 1950 - Dec. 1955 were estimated (see text).

the year 1947 were estimated by averaging the chloride concentrations at San Marcial in December 1946 and January 1948. From September 1934 - June 1950, the reservoir underwent two major and one minor filling and emptying cycles, ending at about the same reservoir storage at which it started (Figure 5.24). In Sept. 1934, about 500,000 acre-feet were stored behind Elephant Butte dam. From that level, the reservoir filled to about 1,390,000 acre-feet in the summer of 1937 and emptied to about 427,000 acre-feet in September 1940. During this period, the cumulative chloride imbalance increased, indicating net chloride storage in the reservoir. Between September 1940 and April 1947, the reservoir filled to a maximum of about 2.2 million acre-feet in May 1942 after a

record-breaking flood year in 1941. By the time the reservoir level had dropped to about 500,000 acre-feet again in April 1947, the net chloride imbalance was still significantly positive ($5.21 * 10^7$ kg cumulative imbalance in April 1947 from a cumulative imbalance of $5.20 * 10^7$ kg in September 1940), though the net chloride imbalance for these seven years was about zero. From May 1947 - June 1950, the reservoir filled to a maximum volume of about 773,000 acre-feet in August 1949 to about 500,000 acre-feet in June 1950. The reservoir generally exported chloride this entire time, with the chloride imbalance dropping from $5.2 * 10^7$ to $2.87 * 10^7$ kg.

After July 1950, the reservoir continued to empty to a minimum of 33,000 acre-feet. A small filling event in the summer of 1952 increased reservoir storage to about 400,000 acre-feet, but the reservoir dropped to 125,000 acre-feet by the end of 1953 and remained fairly constant through 1955. From 1950 - 1953, the chloride imbalance in Elephant Butte reflected the movement of surface water through the reservoir. The chloride imbalance decreased and became negative as the reservoir initially emptied from 1950 - 1951; the imbalance increased and decreased again corresponding to the minor filling and emptying of 1952 - 1953. However, from 1954 - 1955 the chloride imbalance continued to decrease by an order of magnitude from 400,000 kg to 40 million kg while the reservoir level remained relatively stable.

In general, the periods of salt export from the reservoir correspond with a reduction in reservoir storage, and periods of salt storage correspond with periods of increased water storage. However, the historical data reveal that the cumulative chloride imbalance is highly dependent on previous reservoir

behavior. It is particularly apparent that the reservoir has the capacity to store and release chloride on the decadal scale, evidenced by the long-term effect of flood input to the chloride imbalance of the reservoir. This behavior is probably related to the slow process of water and chloride movement in and out of bank storage. At the end of the historical water quality record of the extended low reservoir level from 1950 - 1955, it is likely that such bank storage of water and salts were released into the reservoir, though it is unknown how long this process takes. It is unclear whether all chloride export from the reservoir from 1954 - 1955 was due to bank storage release or to some other non-Rio Grande salt input directly into the reservoir. Over the 21 - year period from 1934 - 1955, the total chloride imbalance of 40 million kg is about equal to the median annual chloride burden below Elephant Butte Reservoir of 36.5 million kg (Figure 5.18). During these two decades, this averages to an annual addition of about 2 million kg (about 5% of the average annual chloride burden) due to reservoir dynamics. This suggests that it is possible for reservoir dynamics to have a small but still noticeable effect on downstream chloride burden.

5.9 Chapter 5 conclusions

Analysis of historical discharge, chloride concentration, and chloride burden data reveals clues about the salinizing processes that affect the Rio Grande. In the headwaters, this analysis suggests that natural tributary input plays a large role in the chloride burden increase between Lobatos and San Felipe. The chloride burden increase between San Felipe and Bernardo is probably due to inflows from both the Jemez River and wastewater effluent. Between Bernardo and Elephant Butte Reservoir, the Rio Puerco, Rio Sal-

ado, and Conveyance Channel all contribute significant salt to the Rio Grande. During August 2001 and January 2002, the Conveyance Channel was the only significant salt contributor, the other two being dry or nearly so. Salinization through the agricultural valleys downstream of Elephant Butte and Caballo reservoirs during August in the historical record does not follow any obvious pattern, except for a significant chloride concentration and burden increase between El Paso and Ft. Quitman. However, in January the chloride concentration and burden both increase dramatically between each gaging station from Caballo Reservoir to Ft. Quitman. Along with the fact that chloride concentrations and burdens are higher in the Rio Grande in the January historical record than in the August record, this suggests that salinization in this reach is more apparent when flows released from upstream reservoirs are shut off. The historical record also reveals significant salinization patterns during both the irrigation and non-irrigation seasons that remain unexplained due to increases in chloride concentration and/or chloride burden without attendant increases in flow. These include chloride concentration and chloride burden increases at San Acacia as well as a chloride concentration increase between Elephant Butte and Caballo reservoirs. This analysis also shows that chloride burden at the outlet of Elephant Butte Reservoir is highly dependent upon the amount of water released from the reservoir as well as on previous storage of water and salts in the reservoir. Though its rate and amount remain unquantified, the movement of water and salts in and out of bank storage in Elephant Butte due to change in reservoir storage appears to play an important role in downstream salinization.

Comparison of August 2001 and January 2002 data to the historical

record indicates that the 2001 and 2002 data analyzed in the remaining chapters of this thesis is well within the range of typical conditions on the Rio Grande. The analysis of August 2001 and January 2002 salinization patterns to follow in Chapters 7 - 10 should be fairly representative of salinization that has occurred on the Rio Grande for the past century.

CHAPTER 6

THEORY OF ENVIRONMENTAL TRACERS UTILIZED

6.1 Introduction to environmental tracers

Environmental tracers are chemical constituents of the natural environment that can be used to quantify earth processes. They may be naturally occurring or anthropogenically contributed. Useful tracers have a distinct pattern of environmental variability that can be correlated to a limited number of factors, are relatively common in the field area, and require fairly inexpensive analyses. The traditional method of investigating salinization (see chapter 4 of this thesis) relies on computing chloride burdens from chloride concentration and discharge data. This limits these studies to the spatial resolution of the gaging stations, which is 20-50 km. Use of tracers such as chloride and bromide concentrations, chloride-bromide ratios, chlorine-36, and the stable isotopes of hydrogen and oxygen is advantageous because they can be measured easily and cheaply at a high spatial resolution, such as 10 km in this study. Employing multiple tracers simultaneously further helps to establish and quantify causes of Rio Grande salinity.

6.2 Chloride and bromide

Chloride and bromide, the anions Cl^- and Br^-, rarely participate in oxidation-reduction or other chemical reactions in the natural environment.

Due to their negative charge, they also tend not to adsorb to or react with geologic media [*Phillips*, 2000]. Thus they generally are considered conservative, and both Cl^- and the Cl/Br ratio are commonly used as tracers [*Feth*, 36 pp., 1981; *Flury and Papritz*, 1993; *Davis et al.*, 1998].

Gerritse and George [1988] observed changes in the Cl/Br ratio of water as it moved through soil due to interaction with organic matter. They noticed a decrease in Cl/Br ratio in rain water that percolated through a laboratory soil column, though in the field they observed increases and decreases in Cl/Br ratio between rain water and shallow ground water at various locations in Australia. The variation in Cl/Br ratio of soil organic matter presumably is due to variation in uptake of chloride and bromide by the organic matter when it was living. This uptake of chloride and bromide by living matter and release during its decay is a process that likely occurs in agricultural and riparian areas of the Rio Grande valley. It is possible that systematic differential uptake of chloride and bromide may occur in areas where plants die but do not decay, such as in riparian areas with a buildup of dead material under the living canopy. In most riparian areas and agricultural areas, however, the chloride and bromide uptake process can be considered to be at steady state.

Waters of different sources have easily distinguishable chemical signatures in terms of chloride and bromide: meteoric waters tend to have a low Cl^- concentration and a Cl/Br ratio less than 150; wastewater tends to have a much higher Cl^- concentration and a Cl/Br ratio of 300 to 600; deep ground waters and geothermal waters commonly have high chloride concentrations and Cl/Br ratios of 1000 or greater [*Davis et al.*, 1998].

6.3 Chlorine-36

Chlorine-36 (^{36}Cl) is a rare isotope of chlorine that has the same conservative chemical behavior as the more common chloride isotopes. In addition, it is radiogenic and has a relatively long half-life of 301,000 +/- 4000 years. It is produced in the atmosphere by spallation reactions when a nucleus with a proton number larger than that of Cl, namely ^{40}Ar, interacts with high energy cosmic rays. A minor amount of ^{36}Cl is atmospherically produced by ^{35}Cl thermal neutron capture as well. Chlorine-36 is also produced in the subsurface by ^{35}Cl capture of thermal neutrons from radioactive decay of U and Th. Because much of the subsurface ^{36}Cl is produced by ^{35}Cl thermal neutron capture, ^{36}Cl production is generally proportional to the Cl^- concentration. For this reason, ^{36}Cl measurements are usually reported in terms of the $^{36}Cl/Cl$ ratio [*Phillips*, 2000].

Atmospheric ^{36}Cl production is much greater than subsurface production, so meteoric and surface waters tend to have a high $^{36}Cl/Cl$ ratio. As meteoric water infiltrates, its $^{36}Cl/Cl$ ratio decreases as ^{36}Cl decays and is not replenished by atmospheric production. Subsurface waters thus have a low $^{36}Cl/Cl$ ratio that approaches secular equilibrium with ^{36}Cl production in the host rock.

6.4 $\delta^{18}O$ and δD values

Surface water systems commonly are subject to transpiration and evaporation. These two processes have very different effects on the isotopic composition of water molecules. Transpiration, the movement of water through

plants, does not affect the chemical composition of the water molecules it acts upon. Water uptake through roots and its movement through the rest of the plant is advective, does not involve a phase change or chemical reaction, and is thus non-fractionating. Water exits plants through the leaves and stem, where it is completely evaporated. This results in no net fractionation [*Clark and Fritz*, 1997]. On the other hand, evaporation acting directly on a water body rarely results in a phase change of the entire body, and thus it fractionates water molecules between the liquid and gas phases based on the molecular weights of their constituent atoms. Water molecules containing the common heavy isotope of oxygen (^{18}O) and/or of hydrogen (^{2}H, or deuterium, D) preferentially remain in the liquid phase of water during the process of evaporation, while the molecules containing the light isotopes (^{16}O and ^{1}H) fractionate into the vapor phase [*Dansgaard*, 1964]. Because the natural atomic abundance of ^{18}O is only 0.1995% and that of ^{2}H is a mere 0.0156% [*Campbell and Larson*, 1998], their concentrations are commonly expressed as the ratio δ relative to standard mean ocean water (SMOW):

$$\delta_i = \left[\frac{R_{sample}}{R_{SMOW}} - 1\right] * 10^3 \tag{6.1}$$

where

$$R = \frac{moles, heavyisotope}{moles, lightisotope} \tag{6.2}$$

where δ_i is the isotopic enrichment or depletion in units per thousand (per mille), R_{sample} is the molar ratio of heavy to light isotopes of constituent i in the sample, and R_{SMOW} is the molar ratio of heavy to light isotopes of

constituent i in the standard. A negative delta value indicates the sample is isotopically lighter than, or depleted in, the heavy isotope with respect to the standard; a positive value indicates the sample isotopically heavier than, or enriched in, the heavy isotope with respect to the standard. Evaporative fractionation of isotopes is dependent on temperature as well as on the fraction of water that has been converted between phases, and can be described by Rayleigh distillation:

$$\delta_{i,f} = \delta_{i,o} - \varepsilon_i \ln f \tag{6.3}$$

where $\delta_{i,f}$ is the final value of constituent i in the liquid phase, $\delta_{i,o}$ is the initial value of the same constituent in the liquid phase; ε_i is the temperature-dependent fractionation factor of i, and f is the fraction remaining in the liquid phase. A convenient derivation of the Rayleigh equation can be found in *Campbell and Larson* [1998].

In fact, all precipitation worldwide falls along a Rayleigh distillation curve dependent mainly on global-scale changes in the isotopic fractionation factors of oxygen and hydrogen due to elevation-and altitude-induced changes in temperature. When plotted on a graph of δD vs. δ^{18}O, this curve is nearly linear and is known as the global meteoric water line [*Craig*, 1961]. The meteoric water line has a slope of about 8. Deviations from the meteoric water line in surface waters indicate that localized fractionation processes are acting. For example, waters subject to open-water evaporation tend to fall along lines with slopes between 5 and 8 [*IAEA*, 1983].

Surface water δ^{18}O and δD values also may be affected by mixing

with waters of different isotope concentrations, such as by ground water contribution. The stable isotope concentrations of ground water depend upon the composition of precipitation and thus the climatic conditions during the time it was recharged. Though estimates of paleoprecipitation composition vary, *Desaulniers et al.* [1981] noted that ground water recharged in North America during the Pleistocene ice age is 6 per mille $\delta^{18}O$ lighter than ground water recharged recently. Furthermore, isotopes in ground water can be fractionated by various water-rock chemical interactions, though these reactions only make a difference over long time scales. One such example in geothermally active areas is enrichment of ground water $\delta^{18}O$ values by high-temperature water-rock interaction with oxygen-bearing minerals [*IAEA*, 1983].

61

CHAPTER 7

DATA COLLECTION AND ANALYSIS

7.1 Sample collection and laboratory analysis

Every August and January between the years 2000 and 2003, surface water samples were collected from the Rio Grande, the Conveyance Channel, major drains, and major tributaries between the headwaters in Colorado and Ft. Quitman, Texas. Field sampling periods were chosen to be far from the beginning and end of the irrigation season when reservoir and diversion dam operations fluctuate the most. Field seasons were also chosen to avoid the spring, when diurnal fluctuation of snowmelt occurs. Samples were collected at a 10 km interval between January 2000 and January 2002, though during subsequent seasons they were collected at a 40 km interval. Using a plastic bucket, samples were collected from the fastest moving part of the water body of interest to ensure a well-mixed sample representative of the local chemistry. However, at some locations, samples had to be taken from the bank of the water body. Particularly through Elephant Butte and Caballo Reservoirs, it was not possible to sample the most well-mixed part of the reservoir. The TDS, electrical conductivity (EC), pH, and temperature of each sample were measured and recorded in the field immediately after sample collection. During the August 2001 and January 2002 sampling seasons, a 500-mL sample was collected in a TraceClean (acid-washed) HDPE bottle to be transported to the lab for dissolved constituent and chlorine isotope analysis; another sample was

collected in a 60-mL HDPE bottle for stable isotope analysis. Samples were labeled according to their distance from the outlet of the Rio Grande Reservoir, determined digitally with the software TopoUSA produced by DeLorme. Each sample was given a prefix indicating whether it was from the Rio Grande, a tributary, a drain, or the Conveyance Channel. Samples were also given a suffix to indicate the sampling season, with "X" indicating summer field season and "W" indicating winter field seasons. The suffix "-X01" indicates August 2001, "-W02" indicates January 2002, etc.

At the completion of the August 2001 field season and again at the end of the January 2002 field season, all samples (122 in August 2001; 116 in January 2002) were analyzed for Cl^- and Br^- by ion chromatography at the University of Arizona in Tucson, AZ. Eleven headwaters samples from each field season had bromide concentrations below the instrument detection threshold of 0.01 mg L^{-1}. To obtain bromide concentrations, these samples were concentrated by evaporation and re-analyzed. The bromide concentrations of the original samples were calculated from the new measured concentrations and the degree of evaporative concentration. Additionally, all August 2001 samples and about half of the January 2002 samples were analyzed at the University of Arizona for $\delta^{18}O$ and δD using a Finnigan Delta E gas source isotope ratio mass spectrometer. Furthermore, sixteen samples from August 2001 were prepared at New Mexico Tech for $^{36}Cl/Cl$ ratio analysis following the techniques reported in Appendix C. Samples in the headwaters region had chloride concentrations that were too low to allow for accurate $^{36}Cl/Cl$ analysis, even after attempting to collect large (5 L) samples and evaporatively concentrate them. Between the headwaters and Albuquerque, chloride concentrations were still so

low that collected samples had to be combined to obtain a sample suitable for analysis. Samples with adjacent locations and similar chloride concentrations and Cl/Br ratios were combined under the assumption that these samples had similar geochemical origins and thus similar $^{36}Cl/Cl$ ratios. Final $^{36}Cl/Cl$ accelerator mass spectrometer analysis was performed at the Purdue Rare Isotope (PRIME) laboratory at Purdue University in West Lafayette, Indiana.

In March 2002, a saline pool was discovered just north of the diversion dam at San Acacia, New Mexico. An additional sample was collected this pond in order to determine whether it was a surface exposure of deep brine upwelling or simply irrigation water that had seeped from the adjacent Unit 7 Drain. The pool was analyzed for TDS, EC, pH, major cations and anions, and the $^{36}Cl/Cl$ ratio. All data for field season samples from 2000 - 2003 and from the San Acacia pool can be found in Appendices I-J.

7.2 Total dissolved solids in the Rio Grande

The total dissolved solids (TDS) of the Rio Grande show distinct trends during the summer and winter sampling seasons (Figure 7.1). During both seasons, the TDS increases by over two orders of magnitude between the headwaters and Ft. Quitman, TX. Along this distance, the TDS increases occur at distinct jumps, with a relatively constant TDS between jumps. Particularly notable are the TDS increases downstream of Elephant Butte Reservoir during the winter, when the base flow of the river is relatively undiluted by reservoir releases. During the winter, TDS increases at Elephant Butte Reservoir, Selden Canyon, and El Paso are apparent. Also obvious is a TDS increase in southern Colorado during the summers. During both seasons a dramatic TDS increase

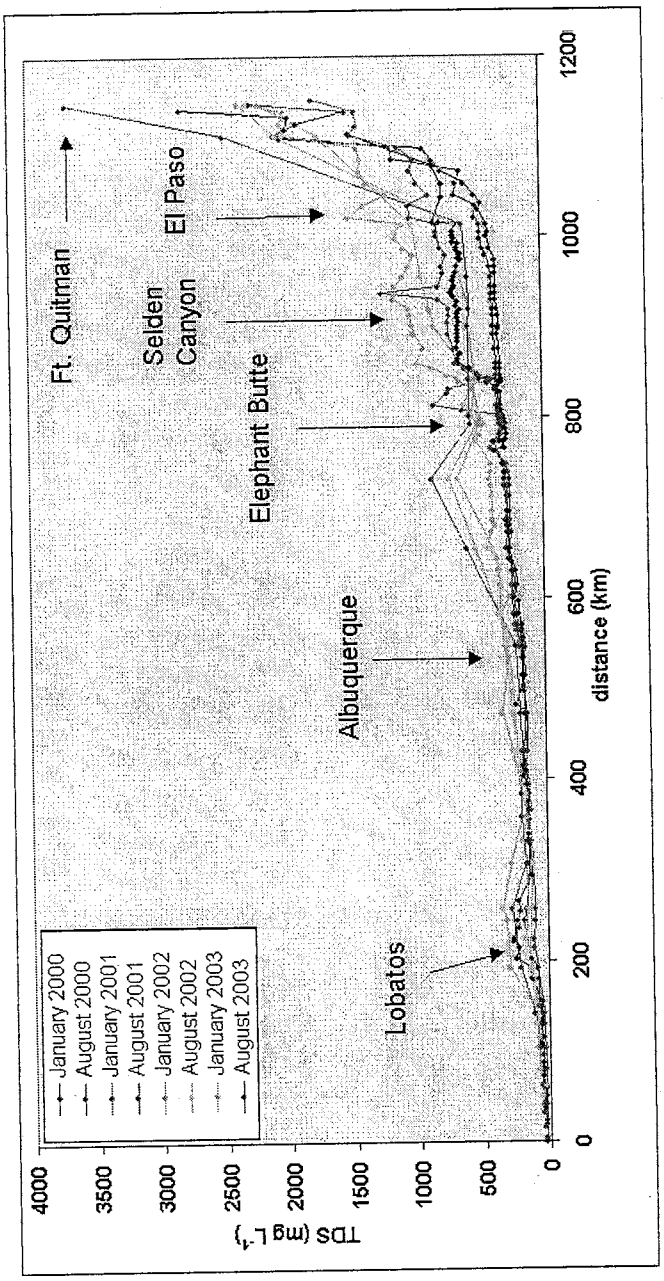

Figure 7.1: Total dissolved solids of the Rio Grande during summer and winter sampling seasons from the years 2000 to 2003. Note the two order of magnitude increase in salinity between the river headwaters in Colorado the U.S. - Mexico border region 1200 km downstream. The TDS jump just upstream of Elephant Butte in the August 2002, January 2003, and August 2003 seasons are probably due to pumping of Conveyance Channel water with a higher TDS into the Rio Grande to maintain river flows for the endangered silvery minnow.

about 100 km downstream of El Paso is evident.

TDS concentrations (Table 7.1, Figure 7.2) during August 2001 were consistently lower than TDS concentrations reported by the *NRC* [1938]; *Lippincott* [1939]; *Wilcox* [1957], and *Trock et al.* [1978] with the exception of Ft. Quitman, where August 2001 TDS values were higher. January 2002 TDS values were very similar to other reported values upstream of Elephant Butte Reservoir, though below the reservoir outlet January 2002 values were significantly higher. These differences may be due to the fact that the other reported values are annual averages and thus do no represent the seasonal variation reflected in the August 2001 and January 2002 data.

Similarly, the August 2001 and January 2002 discharge conditions (Table 7.3, Figure 7.3) reflect distinct seasonal patterns resulting from high headwaters discharge and high flow downstream of Elephant Butte Reservoir during the summer and low headwaters discharge and low flow downstream of the reservoir during the winter when reservoir flows are minimized. The annual averages reported by the *NRC* [1938] and *Wilcox* [1957] do not show such extreme seasonality, though it is clear that the 1930's was a period of lower average headwaters discharge and that 1934 - 1953 was a period of higher average headwaters discharge in comparison with the August 2001 and January 2002 values.

Total salt burden (Table 7.2, Figure 7.4) in August 2001 and January 2002 was almost invariably lower than all other reported conditions in the 20^{th} century, which probably reflects climatic variability. For example, *Wilcox* [1957] noted an increase in total salt burden between Otowi and Ft. Quitman

of over 25%, from 804,740 kg dy^{-1} to over 1.16 million kg dy^{-1}. In the August 2001 field season, the salt burden increased from 250,600 kg dy^{-1} to 985,610 kg dy^{-1} in that same stretch of river; in the January 2002 field season, the salt burden increased from 302,350 kg dy^{-1} to 908,130 kg dy^{-1}. Given that the TDS concentrations reported by Wilcox are similar to August 2001 and January 2002 conditions, the differences in their total salt burden calculations are most likely due to the fact that the instantaneous flow conditions during the two field seasons are significantly lower than the average flow values for 1934-1953 that Wilcox used. In particular, the high-flow year 1941 (with subsequent continued high flows south of Elephant Butte Reservoir into 1942) most likely biases Wilcox's calculations toward a higher-than-average flow and thus a higher-than-average salt burden (given similar TDS values). This bias particularly affects the salt burden calculations above Elephant Butte Reservoir, when no dams existed on the main-stem Rio Grande above Elephant Butte to damp the high flows during that time.

Table 7.1: Comparison of Rio Grande TDS concentrations from previous studies to August 2001 and January 2002. In mg L^{-1}.

source: years studied:	NRC (1938) 1931-1936	Lippincott (1939) 1939	Wilcox (1957) 1934-1953	EPA (1978) 1918-1973	X01 Aug 2001	W02 Jan 2002
Del Norte	81	110	na	100	36	83
Otowi	253	na	221	na	174	222
San Marcial	610	427	449	482	296	412
EB dam	595	na	478	na	338	481
Caballo dam	na	na	515	504	349	653
Leasburg	640	na	551	558	375	1020
El Paso	897	832	787	802	463	1070
Ft Quitman	2023	2120	1691	1851	2250	2280

Table 7.2: Comparison of Rio Grande total salt burdens from previous studies to August 2001 and January 2002. In kg dy^{-1}.

source: years studied:	NRC (1938) 1931-1936	Wilcox (1957) 1934-1953	Moore and Anderholm (2002) 1993-1995	X01 Aug 2001	W02 Jan 2002
Del Norte	1.29E+05	na	1.28E+05	7.92E+04	3.23E+04
Otowi	7.28E+05	8.05E+05	8.84E+05	2.51E+05	3.02E+05
San Marcial	2.22E+06	1.29E+06	na	1.84E+05	4.85E+05
EB dam	1.54E+06	1.28E+06	na	1.32E+06	3.91E+05
Caballo dam	na	1.36E+06	na	1.53E+06	5.75E+04
Leasburg	1.61E+06	1.38E+06	1.02E+06	1.15E+06	1.05E+05
El Paso	1.59E+06	1.40E+06	1.19E+06	1.11E+06	2.23E+05
Ft Quitman	1.18E+06	1.16E+06	na	9.86E+05	9.08E+05

Table 7.3: Comparison of Rio Grande discharges from previous studies to August 2001 and January 2002. In $m^3\ s^{-1}$.

source: years studied:	NRC (1938) 1931-1936	Wilcox (1957) 1934-1953	X01 Aug 2001	W02 Jan 2002
Del Norte	18	na	25	5
Otowi	10	42	17	16
San Marcial	33	33	7	14
EB dam	30	31	45	9
Caballo dam	na	31	51	1
Leasburg	29	29	36	1
El Paso	20	21	28	2
Ft Quitman	7	8	5	5

Because data from August 2001 and January 2002 field seasons had the highest spatial resolution, they were fairly representative of historical conditions (see also Chapter 5), and together they represented both the irrigation and non-irrigation seasons, both seasons were chosen for detailed study using environmental tracers.

7.3 Stable isotopes of hydrogen and oxygen in the Rio Grande

Stable isotope data for Rio Grande waters in August 2001 and January 2002 were compared to the global meteoric water line (Figure 7.5 and Figure 7.6). During both seasons, Rio Grande waters fall along a line with a slope of about 5. This slope is significantly less than that of the meteoric water line, and is characteristic of open-water evaporation [*IAEA*, 1983]. Tributary values are more similar to meteoric water than to river water. Drain water and river water have $\delta^{18}O$ and δD values that are similar to each other. The implications of these similarities are discussed below.

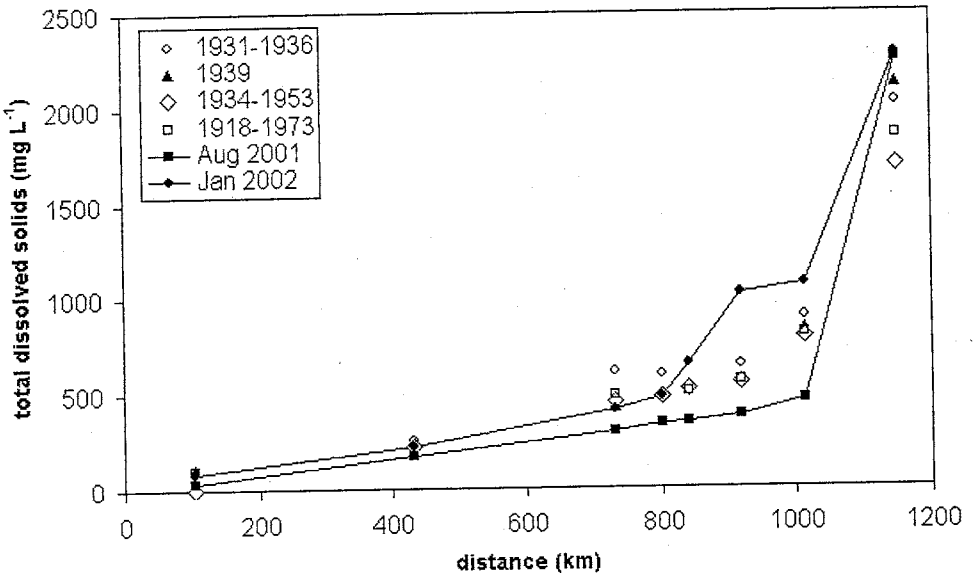

Figure 7.2: Comparison of Rio Grande TDS concentration from previous studies to August 2001 and January 2002.

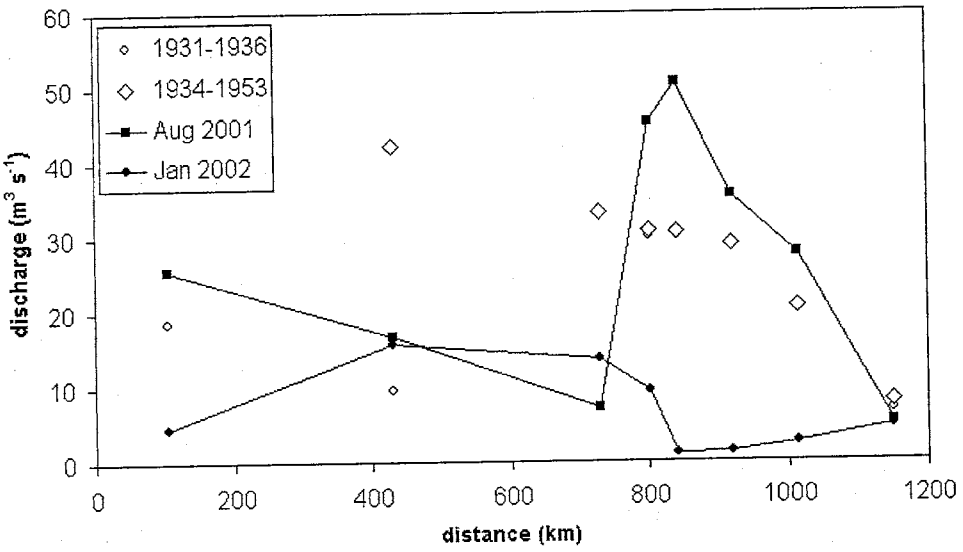

Figure 7.3: Comparison of Rio Grande discharge from previous studies to August 2001 and January 2002.

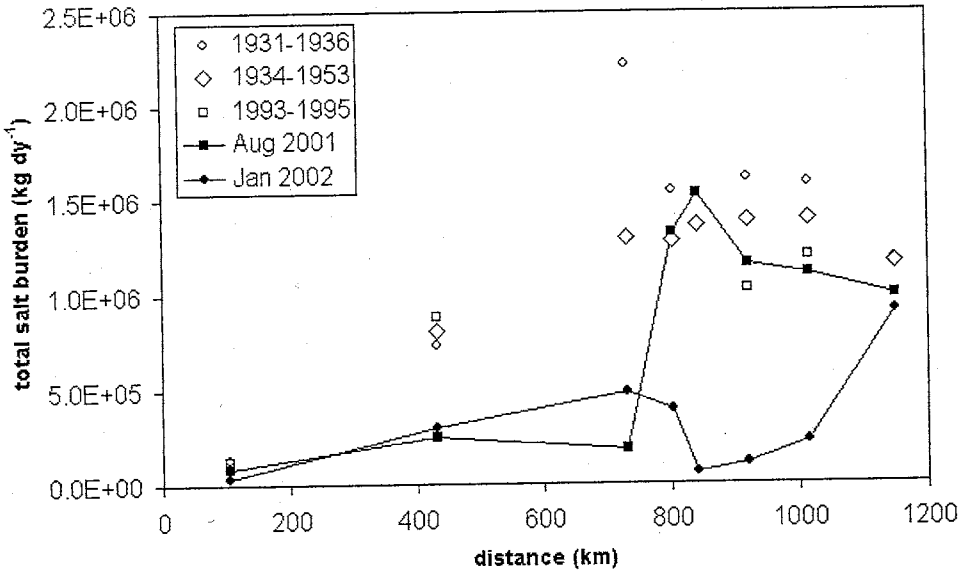

Figure 7.4: Comparison of Rio Grande total salt burden from previous studies to August 2001 and January 2002.

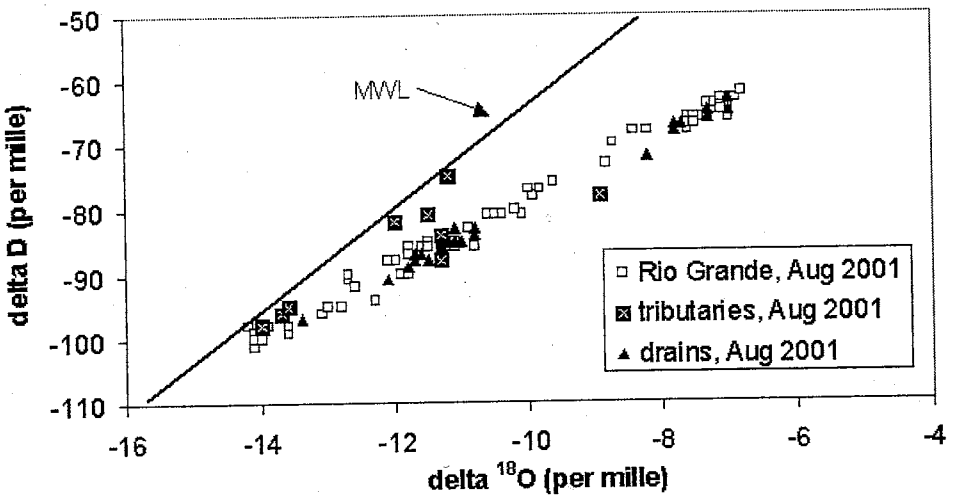

Figure 7.5: Comparison of $\delta^{18}O$ and δD values for the Rio Grande, its major tributaries and drains to the meteoric water line (MWL), August 2001.

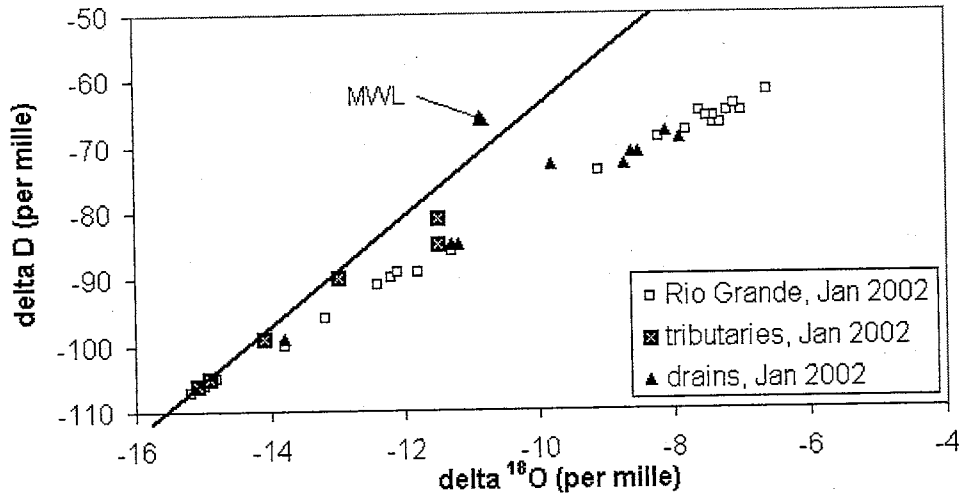

Figure 7.6: Comparison of $\delta^{18}O$ and δD values for the Rio Grande, its major tributaries and drains to the meteoric water line (MWL), January 2002.

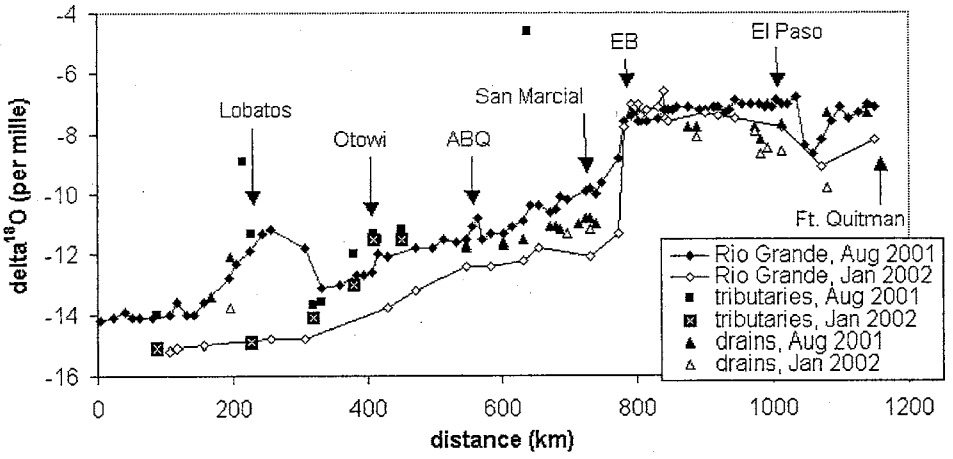

Figure 7.7: Delta ^{18}O values with flow distance for the Rio Grande, its major tributaries and drains for August 2001 and January 2002. ABQ= Albuquerque, EB= Elephant Butte Reservoir.

Though data from January 2002 are more sparse than August 2001 data, Rio Grande δ^{18}O values reveal processes occurring with distance downstream during both the irrigation and non-irrigation seasons. During both seasons (Figure 7.7), δ^{18}O values become progressively more enriched with distance downstream, ranging from about -15 to -6 per mille. The most dramatic enrichment is through Elephant Butte Reservoir, most likely due to strong evaporation. The main stem data also shows enrichment and depletion in response to mixing with enriched or depleted tributaries. During August 2001 (Figure 7.8), main stem δ^{18}O values increase dramatically near Lobatos in response to inputs from the Closed Basin Canal, La Jara Creek, the Conejos River, and perhaps other enriched headwaters streams. Depleted inflows in northern New Mexico from the Red River and the Rio Hondo cause a drop in river δ^{18}O values, though the river becomes enriched again due inputs from

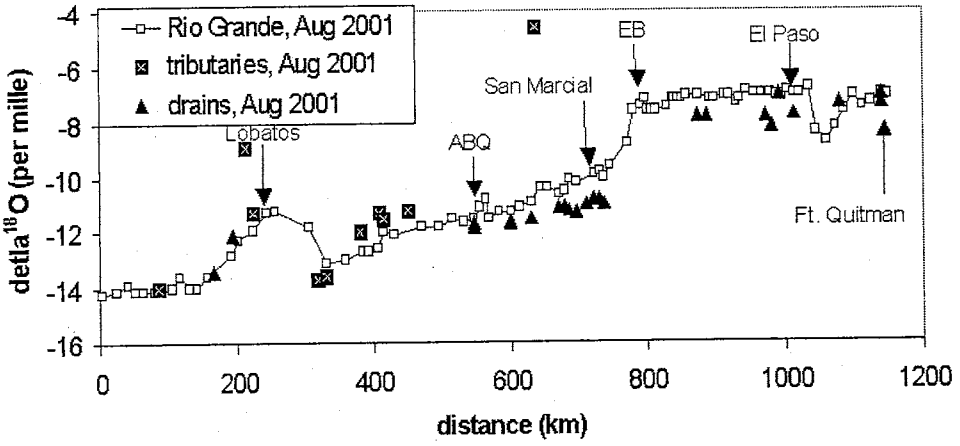

Figure 7.8: Delta ^{18}O values with flow distance for the Rio Grande, its major tributaries and drains, August 2001. ABQ= Albuquerque, EB= Elephant Butte Reservoir.

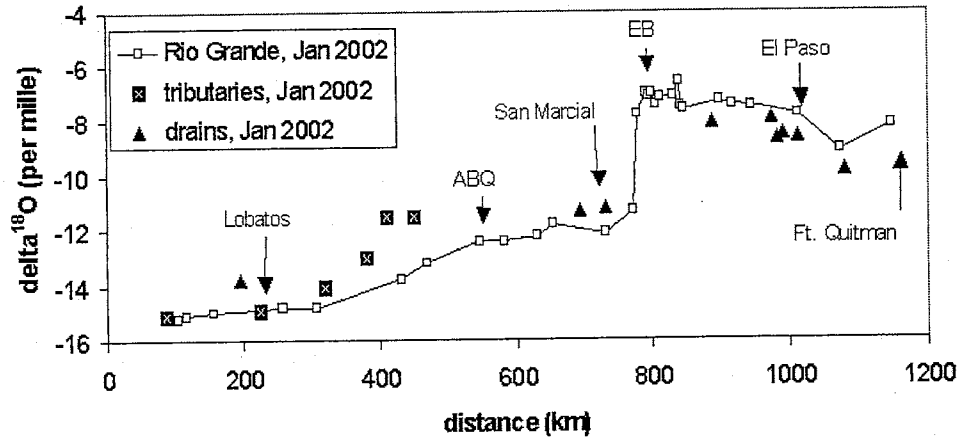

Figure 7.9: Delta ^{18}O values with flow distance for the Rio Grande, its major tributaries and drains, January 2002. ABQ= Albuquerque, EB= Elephant Butte Reservoir.

Embudo Creek, the Rio Chama, the Santa Cruz River, and the Rito de los Frijoles. January 2002 river $\delta^{18}O$ values (Figure 7.9) between Del Norte and Cochiti also reflect tributary input. The river becomes more enriched during the winter with addition of the previously mentioned headwaters tributaries. These tributaries are more depleted in the winter, as would be expected from the temperature dependence of the isotopic enrichment factor of oxygen, and their inflows do not result in as much of an enrichment in river $\delta^{18}O$ values in the winter as in the summer. Except for the Red River and the Rio Hondo in August 2001, headwaters tributaries have an enriching effect on river $\delta^{18}O$ values.

In August 2001, enrichment of $\delta^{18}O$ values at Albuquerque is probably due to input of Southside Wastewater Reclamation Plant (SWRP) effluent (Figure 7.8). Effluent from the SWRP has undergone domestic and municipal use, and it is expected to be more evaporated than river water. Furthermore, water used by city residents is pumped ground water, which most likely has a different $\delta^{18}O$ signature than river water. Though Las Cruces and El Paso also pump ground water for municipal use and release it into the river via wastewater treatment plants, their effluent streams do not have a noticeable effect on river chemistry because their discharges are much smaller that that of the SWRP. No increase in $\delta^{18}O$ values is noted at Albuquerque in January 2002 due to the coarser spatial resolution of the data during that field season.

The main stem Rio Grande seems relatively unaffected by drain input during both seasons, except at the southern end of the field area in the winter where mixing with depleted drain waters decreases river $\delta^{18}O$ values

(Figure 7.9). The steady enrichment of $\delta^{18}O$ values through northern and central New Mexico in both summer and winter (Figure 7.7) shows the continued effects of evaporation, whereas the relative lack of $\delta^{18}O$ change south of Elephant Butte suggests that in this major agricultural area, transpiration rather than evaporation is the cause of most water removal.

To estimate the magnitude of evaporation on the Rio Grande, a simple Rayleigh distillation calculation was applied to the August 2001 $\delta^{18}O$ main stem river samples (see Chapter 6 of this thesis for equation). This calculation assumes a low relative humidity, thus neglecting condensation back-flux of evaporated water. The initial $\delta^{18}O$ value was assumed to be -14.2 per mille, the measurement just below Rio Grande Reservoir in Colorado (RG-3.2-X01). The final $\delta^{18}O$ value was taken to be -7.1 per mille, the measurement at Ft. Quitman (RG-1149.0-X01). The Rio Grande system was assumed to be at steady state. Using a fractionation factor for ^{18}O of -17.68 per mille from the liquid to the vapor phase, it was calculated that 33 m^3 s^{-1} of river water has been evaporated along that 1200 km distance (Table 7.4). The Rayleigh distillation calculation was then applied to the river in four sections, separated by major changes in slope of the $\delta^{18}O$ versus distance curve. The fractions remaining in the liquid phase in each section were all multiplied to obtain the fraction remaining for the entire river. From this second model, the river is calculated to be 42% evaporated. The first model assumes a linear trend in $\delta^{18}O$ between the headwaters and Ft. Quitman, when in reality the trend is much steeper, particularly upstream of Lobatos and through Elephant Butte Reservoir. For this reason, the second model results in calculation of a higher evaporated fraction. However, the steep enrichment of $\delta^{18}O$ values north of Lobatos is more

Table 7.4: Rayleigh distillation calculations for August 2001 $\delta^{18}O$ data. Model 1 assumes a linear trend in $\delta^{18}O$ between the headwaters and Ft. Quitman, TX. Model 2 divides the river into four sections for the evaporation calculation, based on breaks in slope in the $\delta^{18}O$ curve. Model 3 is the same as model 2, but assumes the local $\delta^{18}O$ peak near Lobatos is due to tributary inflow rather than evaporation and ignores it. Locations are in distance downstream from the outlet of Rio Grande Reservoir (km).

	initial location	final location	initial $\delta^{18}O$	final $\delta^{18}O$	fraction remaining	fraction evap'd
model 1	3.2	1149.0	-14.2	-7.1	0.67	**0.33**
model 2	3.2	256.9	-14.2	-11.2	0.84	
	332.5	731.1	-13.1	-9.8	0.83	
	738.8	797.2	-10.0	-7.2	0.85	
	801.1	1149.0	-7.6	-7.1	0.97	
				TOTAL:	0.58	**0.42**
model 3	3.2	332.5	-14.2	-13.1	0.94	
	359.3	731.1	-13.0	-9.8	0.83	
	738.8	797.2	-10.0	-7.2	0.85	
	801.1	1149.0	-7.6	-7.1	0.97	
				TOTAL:	0.65	**0.35**

likely dominated by mixing with enriched tributaries rather than due to pure evaporation. If the local $\delta^{18}O$ high near Lobatos is ignored in Rayleigh calculations, a third model again dividing the river into four sections indicates that the river undergoes 35% evaporation. Gaging data for the August 2001 field season show that flow at Wagon Wheel Gap, CO was 21.1 $m^3\ s^{-1}$, flow at Del Norte, CO was 25.5 $m^3\ s^{-1}$, and flow at Ft. Quitman, TX was 5.1 $m^3\ s^{-1}$. Neglecting reservoir effects and assuming all water diverted from the river that is not consumptively lost is returned, this indicates that the river lost 75-80% of its water within the field area to evaporation and transpiration combined. Since transpiration is non-fractionating and Rayleigh calculations show that evaporation accounts for about a 35% loss, the remaining 35-40% water loss is estimated to be due to transpiration. Such a 75% evapotranspirative concentration would result in a four-fold increase in chloride concentration. Despite this strong degree of evapotranspiration, it cannot account for the observed two order of magnitude TDS increase observed in the Rio Grande. It is apparent that salts must be added to the river with distance downstream in order to cause such salinization. The chloride concentration, Cl/Br ratio, and $^{36}Cl/Cl$ ratio data are examined next with this in mind.

7.4 Chloride and bromide in the Rio Grande

The chloride concentration of the Rio Grande during August 2001 and January 2002 follows a pattern similar to that of the TDS, increasing at distinct locations (Figure 7.10 and Figure 7.11). Similar to TDS concentration, chloride concentrations (Table 7.5, Figure 7.12) during August 2001 were lower than chloride concentrations during January 2002. January

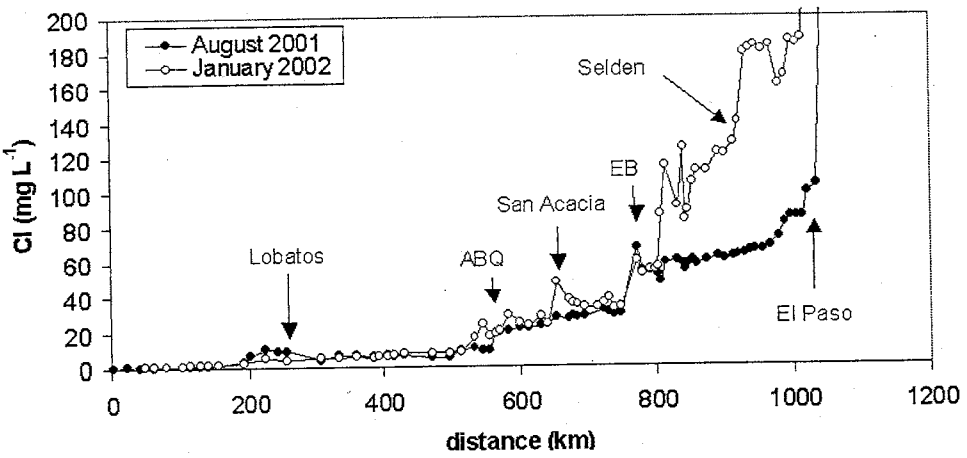

Figure 7.10: Chloride concentration of the Rio Grande during August 2001 and January 2002. Note chloride jumps at Lobatos, CO; Albuquerque (ABQ); San Acacia; Elephant Butte Reservoir (EB); Selden canyon and El Paso. See Figure 7.11 for full extent of the data.

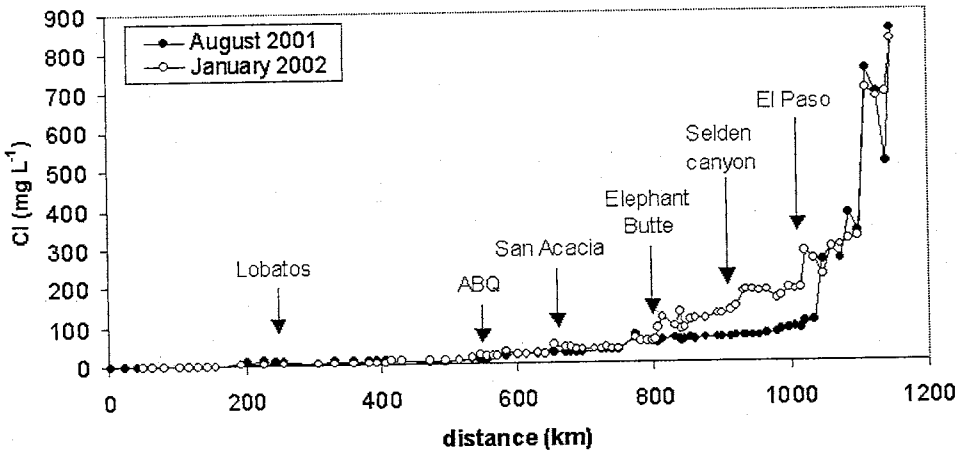

Figure 7.11: Chloride concentration of the Rio Grande during August 2001 and January 2002. ABQ = Albuquerque. Graph shows full concentration range of chloride.

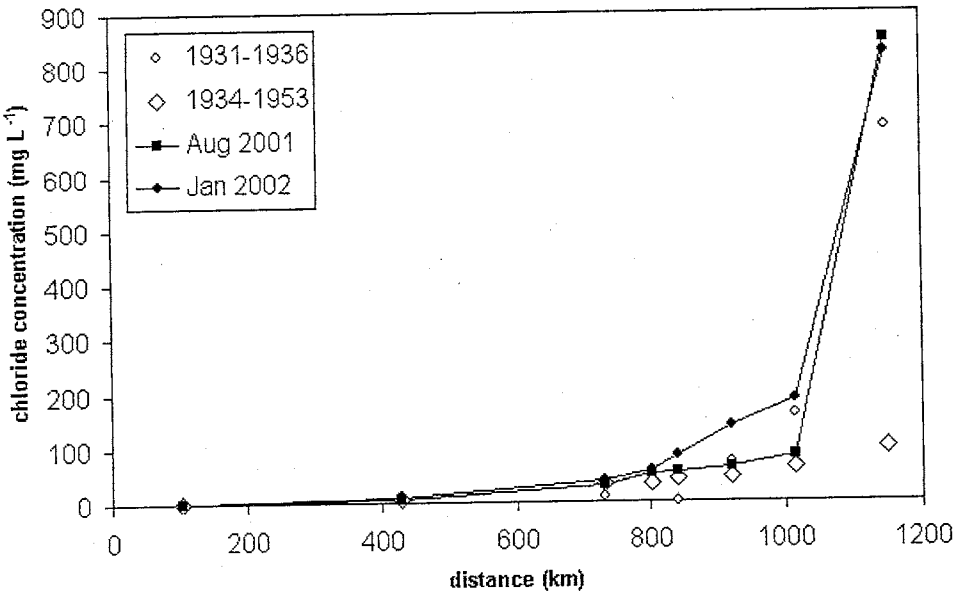

Figure 7.12: Comparison of Rio Grande chloride concentration from previous studies to August 2001 and January 2002.

Table 7.5: Comparison of Rio Grande chloride concentrations from previous studies to August 2001 and January 2002. In mg L^{-1}.

source: years studied:	NRC (1938) 1931-1936	Wilcox (1957) 1934-1953	X01 Aug 2001	W02 Jan 2002
Del Norte	4	na	1	1
Otowi	11	7	7	8
San Marcial	10	32	31	38
EB dam	54	34	52	56
Caballo dam	na	41	54	83
Leasburg	71	45	63	139
El Paso	159	63	85	187
Ft Quitman	687	101	849	825

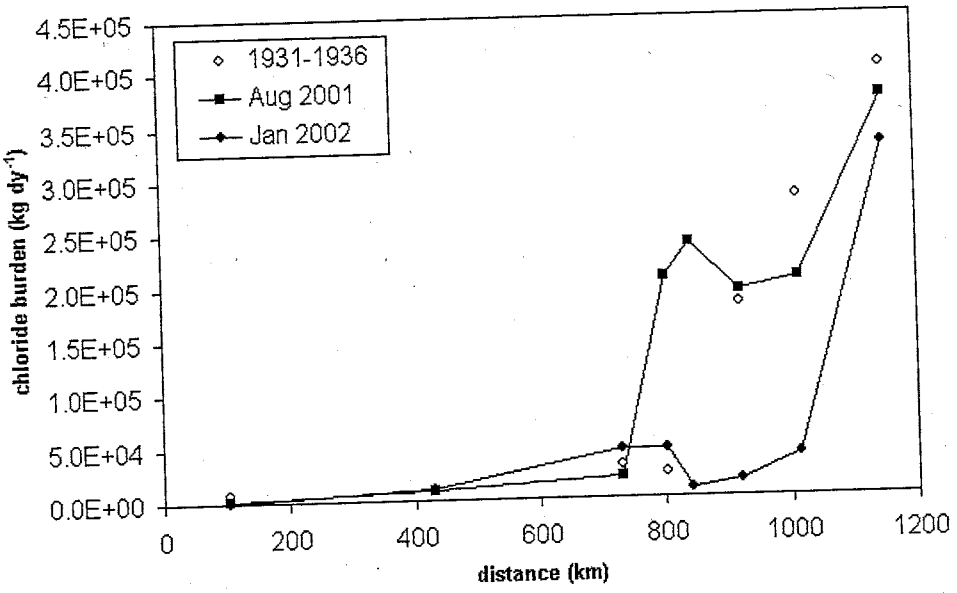

Figure 7.13: Comparison of Rio Grande chloride burden from previous studies to August 2001 and January 2002.

Table 7.6: Comparison of Rio Grande chloride burdens from previous studies to August 2001 and January 2002. In kg dy^{-1}.

source: years studied:	NRC (1938) 1931-1936	X01 Aug 2001	W02 Jan 2002
Del Norte	7.00E+03	1.49E+03	4.93E+02
Otowi	9.00E+03	9.38E+03	1.03E+04
San Marcial	2.95E+04	1.90E+04	4.53E+04
EB dam	2.28E+04	2.05E+05	4.56E+04
Caballo dam	na	2.38E+05	7.32E+03
Leasburg	1.80E+05	1.93E+05	1.43E+04
El Paso	2.80E+05	2.04E+05	3.90E+04
Ft Quitman	4.00E+05	3.72E+05	3.28E+05

2002 chloride concentrations were higher than values reported by the *NRC* [1938] and *Wilcox* [1957], particularly below Elephant Butte Reservoir. August 2001 values were slightly higher than values calculated by Wilcox, though they were both higher and lower than NRC values. August 2001 and January 2002 chloride concentrations were both higher than earlier reported concentrations.

In both August 2001 and January 2002, the chloride concentration increases in distinct jumps at Albuquerque, San Acacia, the north end of Elephant Butte Reservoir, and El Paso. The chloride concentration also significantly increases north of Lobatos in August 2001 as well as south of Caballo Reservoir and through Selden Canyon in January 2002. This pattern implies chloride addition to the river occurs at distinct locations, as evapotranspirative concentration of chloride would result in a linear increase in chloride with distance downstream. South of El Paso there is a large, relatively sustained increase in chloride concentration that may be due to transpirative concentration (the stable isotopes do not get enriched in this region, see previous section). Chloride concentration increase south of El Paso may also be due to salt addition at Ft. Hancock, where there is a major chloride increase in both August 2001 and January 2002.

The chloride burdens in August 2001 and January 2002 (Table 7.6, Figure 7.13) follow distinct seasonal patterns reflecting the river discharge during these times. The August 2001 values do match the burdens reported by the *NRC* [1938] fairly well, though it is unclear why the average chloride burden reported by the NRC at Elephant Butte Reservoir is so low in comparison to 2001 and 2002 conditions.

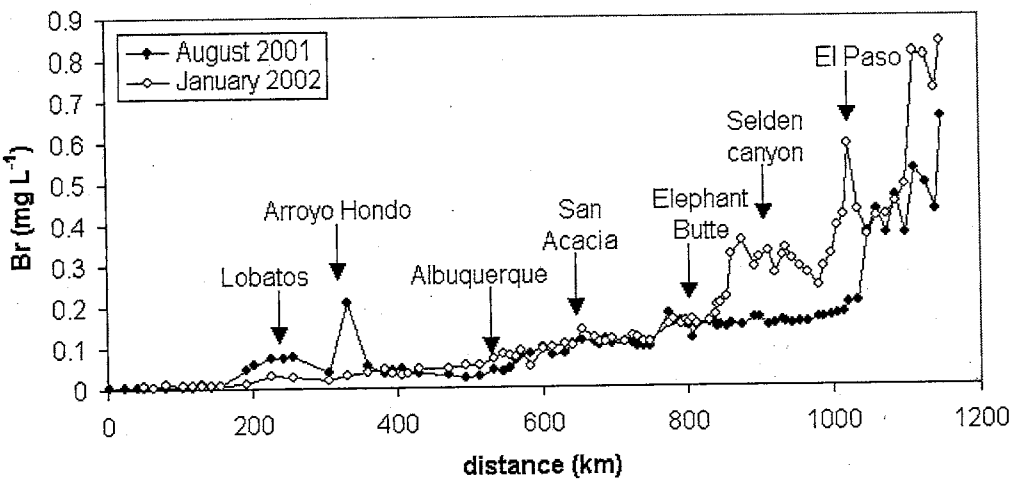

Figure 7.14: Bromide concentration of the Rio Grande during August 2001 and January 2002. EB = Elephant Butte Reservoir.

Like chloride concentration, the bromide concentration (Figure 7.14) increases by over two orders of magnitude with distance downstream, and it follows a pattern similar to that of the chloride concentration. The anomalously high value at the confluence of the Arroyo Hondo and the Rio Grande may be due to local input of high-bromide geothermal waters, such as those within 30 km at Ojo Caliente noted by *Witcher* [1995]. This bromide anomaly results in an anomalous Cl/Br ratio at Arroyo Hondo (Figure 7.15). An anomalous Cl/Br value is also observed at Los Lunas (Figure 7.15), which is probably due to analytical error in the bromide analysis. Otherwise, the chloride-bromide ratio of the river follows a similar pattern to that of the chloride concentration (Figure 7.15). Although there is no notable change in the Cl/Br ratio in the headwaters region in either season, there are distinct Cl/Br increases in Albuquerque, at San Acacia, south of Elephant Butte Reservoir, through

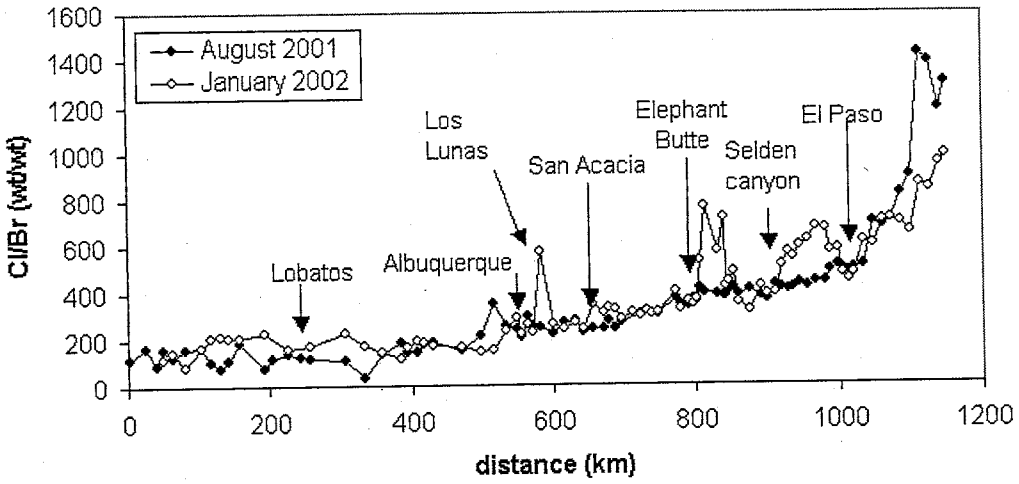

Figure 7.15: Chloride-bromide mass ratio of the Rio Grande during August 2001 and January 2002. Note jumps at Albuquerque, San Acacia, below Elephant Butte Reservoir, downstream of Selden canyon, and south of El Paso.

and downstream of Selden Canyon, and south of El Paso. These Cl/Br ratio jumps further suggest that input of high Cl/Br waters occurs at point sources or within narrow regions.

7.4.1 Chloride concentration and Cl/Br ratio of agricultural drains

Comparison of the Cl/Br ratio and chloride concentrations of drain waters to main stem river waters in August 2001 (Figure 7.16) shows that in the San Luis, Albuquerque, and Socorro basins, drain waters have similar chemistries to that of the river. Drains do not appear to contribute significant salts to the Rio Grande in these basins, with the exception of the Socorro Drain. In the Palomas and Mesilla basins, drains had much higher chloride

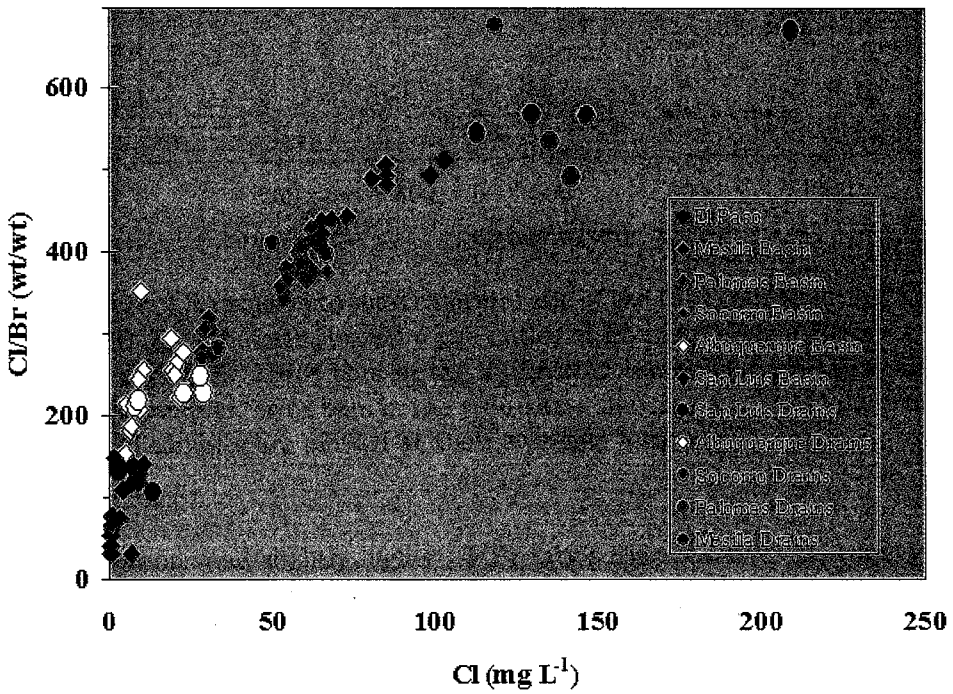

Figure 7.16: Comparison of chloride-bromide ratio vs. chloride concentration in drains and main stem river samples during August 2001. Drains have similar chemistries to the river in the San Luis, Albuquerque, and Socorro basins. The Socorro Drain and drains in the Palomas and Mesilla basins have elevated chloride concentrations and Cl/Br ratios relative to local river waters.

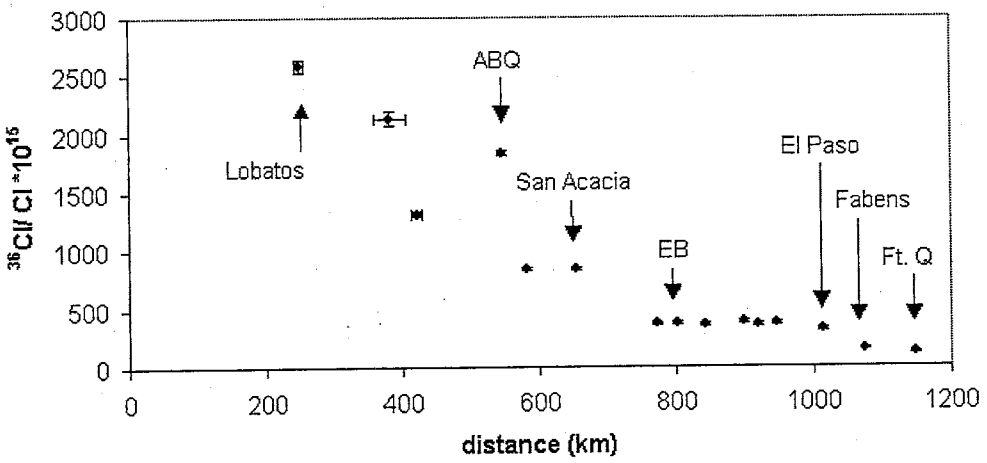

Figure 7.17: Chlorine-36 to total chlorine ratio of the Rio Grande during August 2001. ABQ= Albuquerque, EB= the outlet of Elephant Butte Reservoir, Ft. Q= Ft. Quitman. Error bars in the x-direction represent uncertainty due to combined samples; error bars in the y-direction indicate analytical uncertainty. Combined samples are plotted at their averaged location.

concentrations and slightly higher Cl/Br ratios than the river in August 2001 and January 2002 (Figure 7.16). Both the *NRC* [1938] and *Trock et al.* [1978] observed that Rio Grande Project drains were more saline than the river as well. The possible causes of drain salinity are discussed in detail in Chapter 10.

7.5 Chlorine-36 in the Rio Grande

Generally, the $^{36}Cl/Cl$ ratio decreases with distance downstream in August 2001 (Figure 7.17). The only major exception to this pattern is the sample at Albuquerque (547.5 km), which is thought to be anomalously high due to analytical errors in $^{36}Cl/Cl$ analysis. Excluding this one sample, the $^{36}Cl/Cl$ ra-

tio progressively diminishes between the headwaters and Albuquerque. It drops at two distinct locations: between San Acacia and Elephant Butte Reservoir, and between El Paso and Fabens, TX. It also decreases again, though less obviously, between Fabens and Ft. Quitman. Although the lower spatial resolution of the $^{36}Cl/Cl$ analyses makes it less straightforward to pinpoint the location of ^{36}Cl entry into the river, the change in both ratios at relatively the same locations suggests local inputs of high Cl/Br, low $^{36}Cl/Cl$ waters, such as sedimentary brines.

7.6 Comparison of Cl, Cl/Br, and Chlorine-36 Rio Grande data to theoretical assumptions

Comparing Rio Grande waters with end member compositions of the aforementioned tracers should help identify the most likely sources of salt to the river. First, Rio Grande samples from the August 2001 field season were compared with meteoric, geothermal, and sedimentary brine end members (Table 7.7; Figure 7.18, Figure 7.19, and Figure 7.20). Young ground waters of meteoric origin in the San Juan basin in northwest New Mexico [*Plummer*, 1996] have the low chloride concentration, low Cl/Br ratio, and high $^{36}Cl/Cl$ expected of meteoric waters. Furthermore, these ground waters have chemistries similar to those of the Rio Grande headwaters, where most water (and therefore the accompanying salts) also originates as precipitation. All Rio Grande samples north of Otowi, NM (25 with chloride and bromide data; 3 with $^{36}Cl/Cl$ data) are included in Figure 7.18 and Figure 7.20 to show this similarity. However, natural meteoric waters typically have a $^{36}Cl/Cl$ ratio of about 700. The fact that the Rio Grande headwaters have higher $^{36}Cl/Cl$ ratios probably indicates

Table 7.7: End members compared with Rio Grande waters in graphs and mixing calculations. G=geothermal (Jemez Mountains); M=meteoric (San Juan basin); S=sedimentary brine (Permian basin). Geothermal $^{36}Cl/Cl$ data from *Rao et al.* [1996]; geothermal Cl/Br data from *LANL* [1987]. Meteoric data from *Plummer* [1996], except for the Rio Grande headwaters data, which is from the August 2001 sampling for this study. Sedimentary brine data from *Stueber et al.* [1998], except for San Acacia pool data, which is from a March 2002 sampling for this study. The ^{36}Cl /Cl ratio of RG-3.2-X01 is assumed from the most upstream Rio Grande ^{36}Cl /Cl analysis.

type	location	$^{36}Cl/Cl * 10^{15}$ (unitless)	Cl (mg L^{-1})	Br (mg L^{-1})	Cl/Br (wt/wt)
G	Baca well no. 13	35	2594	7.01	370
G	Travertine Mound spring	26	910	2.60	350
G	Soda dam spring	17	1520	3.84	396
G	Hidden Warm spring	21	1240	4.11	302
G	Main Jemez spring	11	926	2.86	324
M	NM-5	1293	6.1	0.088	69
M	NM-6	1088	8.8	0.102	86
M	NM-8	1262	2.6	0.03	87
M	NM9	1004	3.5	0.059	59
M	NM-16	912	5.7	0.16	36
M	Rio Grande headwaters, RG-3.2-X01	2586	0.28	0.0024	119
S	San Andres no. 1	na	21800	39	559
S	San Andres no. 2	na	25200	37	681
S	San Andres no. 3	na	26000	42	619
S	San Andres no. 4	na	26300	30	877
S	San Andres no. 5	na	33200	60	553
S	San Acacia pool	35	32300	28	1154

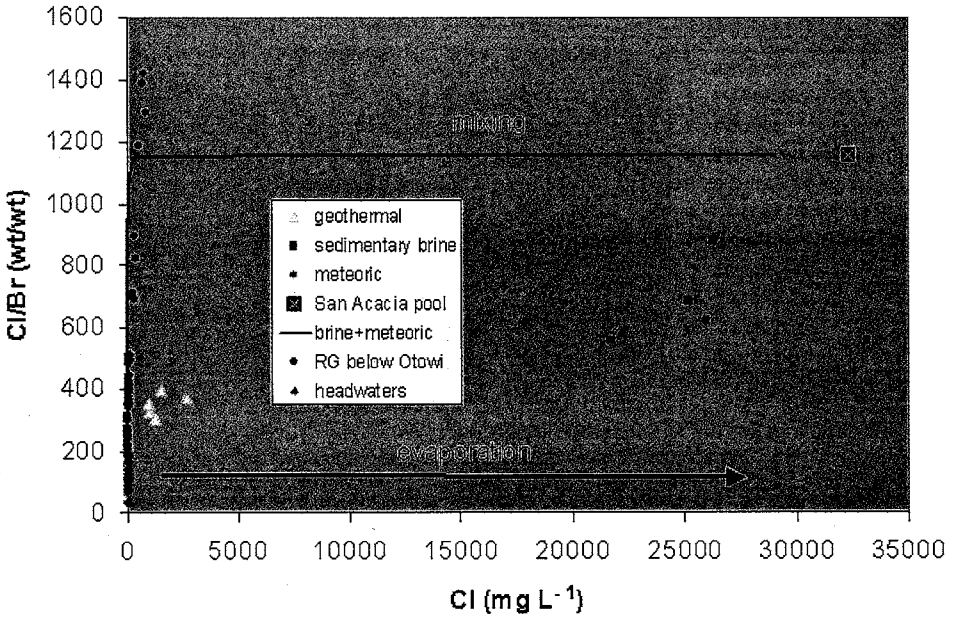

Figure 7.18: Comparison of Rio Grande waters to meteoric waters, geothermal waters, and sedimentary brines with respect to chloride concentration and the Cl/Br ratio. Rio Grande waters closely follow a mixing curve been meteoric waters and sedimentary brines (represented by the San Acacia salty pool), suggesting the importance of brine upwelling in river salinization. See Figure 7.19 for detail of the Rio Grande samples; see Appendix D for a table of mixing calculation data.

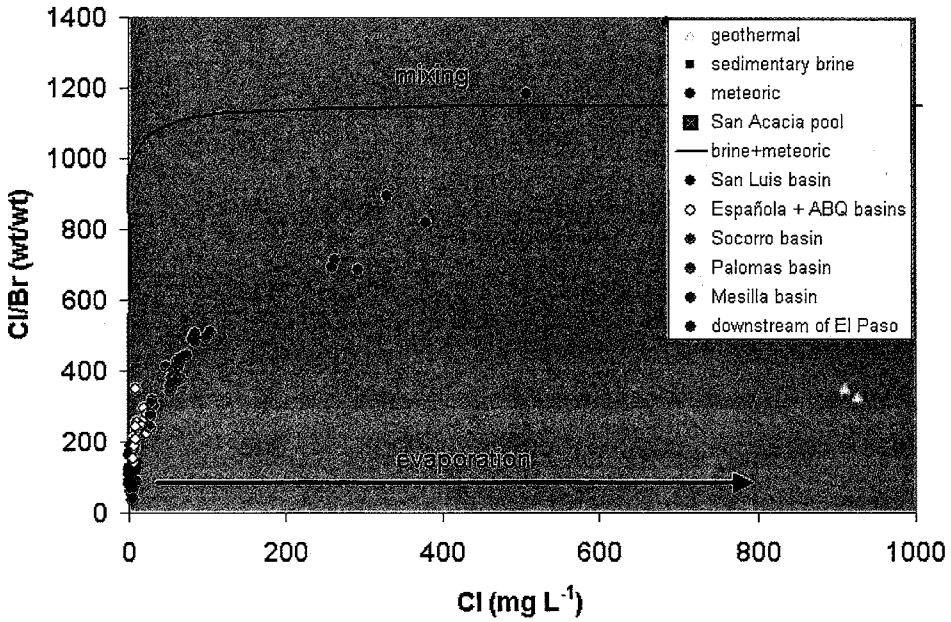

Figure 7.19: Comparison of Rio Grande waters to meteoric waters, geothermal waters, and sedimentary brines with respect to chloride concentration and the Cl/Br ratio, detail of Rio Grande waters. Rio Grande samples are color-coded by basin as in Figure 7.16. See Appendix D for a table of mixing calculation data.

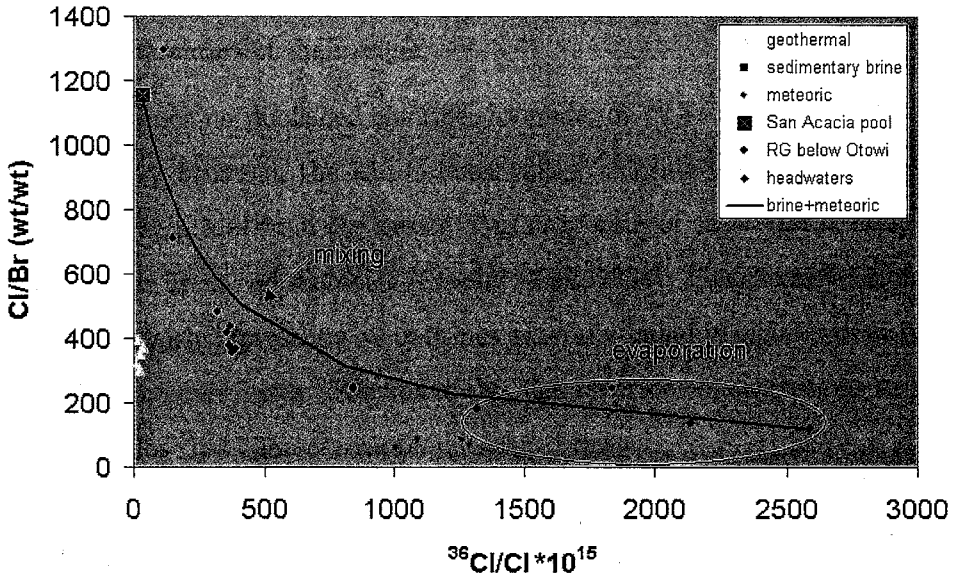

Figure 7.20: Comparison of Rio Grande waters with meteoric waters, geothermal waters, and sedimentary brines (represented by the San Acacia salty pool) in terms of the Cl/Br and ^{36}Cl/Cl ratios. There is pronounced similarity between the progression of Rio Grande chemistry with distance downstream and a calculated mixing curve between the river headwaters chemistry and sedimentary brines (represented by the San Acacia salty pool). The Rio Grande headwaters probably have higher ^{36}Cl/Cl ratios than the meteoric end members because of continued radioactive atmospheric ^{36}Cl fallout from 1950's and 1960's thermonuclear testing. See Appendix D for a table of mixing calculation data.

the lingering atmospheric and biospheric presence of ^{36}Cl from the thermonuclear weapons testing of the mid-20th century [*Cornett et al.*, 1997]. Geothermal waters of the Jemez mountains in northern New Mexico [*LANL*, 1987] have the moderately high chloride concentrations, Cl/Br ratios, and $^{36}Cl/Cl$ ratios expected of waters of their origin.

Since no published chloride, bromide, or $^{36}Cl/Cl$ data was found for sedimentary brines in the Rio Grande valley, chloride and bromide data for sedimentary brines from the nearby Permian basin of east-central Texas were assumed as brine end members [*Stueber et al.*, 1998]. The chemistries of these brines are fairly representative of brines generally found in oilfields of southeast New Mexico and Texas. They have the high chloride concentrations and high Cl/Br ratios that characterize sedimentary brines.

Two mixing curves were calculated between possible end members in order to quantitatively estimate mixing of waters in the Rio Grande. The first mixing curve (Figure 7.18 and Figure 7.19) was derived to describe the chloride concentration and Cl/Br ratio evolution of meteoric waters progressively mixed with brine. A second curve (Figure 7.20) describes the evolution of the Cl/Br and $^{36}Cl/Cl$ ratios due to progressive brine mixing. For both curves, the northernmost August 2001 field sample (RG-3.2-X01) was used as the meteoric end member. This location was assumed to have the same $^{36}Cl/Cl$ ratio as the northernmost August 2001 sample analyzed for the $^{36}Cl/Cl$ (a combination of RG-243.5-X01 and RG-256.9-X01). Upon analysis of the San Acacia pool sample mentioned in the introductory paragraphs of this chapter, the pool was found to have the high chloride concentration, high Cl/Br ratio, and

low $^{36}Cl/Cl$ ratio characteristic of sedimentary brines. Due to its similarity to known brines in terms of chloride concentration and Cl/Br ratio, its local origin and the lack of published $^{36}Cl/Cl$ brine data, the chemistry of this salty pool was assumed as the brine end member in calculations used to derive both mixing curves. It is likely that the San Acacia pool water is evaporated and that its chloride and bromide concentrations are higher than those of actual local discharging ground waters (which are probably a mixture of upwelling brine and shallow ground water).

In terms of chloride concentration, Cl/Br ratio, and $^{36}Cl/Cl$ ratio, Rio Grande samples show trends very similar to the theoretical calculated mixing curves between meteoric waters and sedimentary brines (Figure 7.18, Figure 7.19, and Figure 7.20). Calculations (Appendix D) indicate that a total contribution of only 1% sedimentary brine to a meteoric water can cause the total observed Cl/Br ratio increase and most of the observed Cl concentration increase between the headwaters and Ft. Quitman. Similarly, mixing calculations for the Cl/Br and $^{36}Cl/Cl$ ratios (Appendix D) show that a 1-2% brine addition to a meteoric water can account for the change in $^{36}Cl/Cl$ ratio and most of the change in chloride concentration observed along this 1200 km stretch of river. This suggests that at locations of brine discharge to the river, large increases in chloride concentration and chloride burden may occur with no significant increase in river flow.

7.7 Chlorine-36 mixing calculations

Calculations were performed to account for the observed changes in both the chloride concentration and $^{36}Cl/Cl$ ratio during August 2001. These

calculations attempt to track total chloride and non-radioactive chloride additions from brine mixing as well as evaporative concentration of chloride with distance downstream, such that the following equation was solved at each point with $^{36}Cl/Cl$ data:

$$R_{obs} = \frac{eC_mR_m + C_bR_b}{e(1-f) + C_bf} \tag{7.1}$$

where R_{obs} is the observed $^{36}Cl/Cl$ ratio, R_m is the $^{36}Cl/Cl$ ratio of river water at the station immediately upstream, R_b is the $^{36}Cl/Cl$ ratio of the brine end member, C_m is the chloride concentration at the upstream station (the meteoric chloride contribution), C_b is the chloride concentration of the brine end member, and f is the fraction of brine added since the upstream station. The term e accounts for evapotranspirative concentration, i.e., it is equivalent to V_o/V_x where V_o is the volume of water at the upstream station and V_x is the volume remaining at some distance x down the river, assuming no inputs or outputs of water other than by evapotranspiration. To make sense, it should be a number greater than 1. Once again, the San Acacia pool was assumed as the brine end member. At each station, both e and f are unknown. However, e and f can be checked against the actual measured chloride concentration at the station of interest using the following simple mass balance:

$$C_a = eC_m(1-f) + C_bf \tag{7.2}$$

where C_a is the actual chloride concentration of interest. Attempting to simultaneously solve both equations was uninstructive, resulting in calculations of f that were equal to 1, greater than 1, or unsolvable. Using estimates of evapotranspirative loss from a detailed mass balance model (described in Chapter 9 of this thesis) as values for e resulted in brine fractions greater than 1. In

Table 7.8: Calculation of brine fraction added, f, based on changes in chloride concentration and $^{36}Cl/Cl$ ratio due to brine mixing and evapotranspiration (e) with distance downstream. The unitless fractions e and f were estimated in order to estimate the measured chloride concentration as closely as possible. The negative values of e indicate that the results of these calculations are unrealistic. Starred samples are averages based on combinations of samples otherwise too dilute for $^{36}Cl/Cl$ analysis.

distance (km)	Cl (mg L^{-1})	$^{36}Cl/Cl$ *10^{15} (atoms)	f	e	estimated Cl (mg L^{-1})
250.2*	9.06	2587			
383.4*	6.64	2136	0.00251	-8.3	6.39
423.1*	6.40	1318	0.00163	-7.0	6.49
547.5	9.07	1840	0.00000	12.1	77.37
582.9	20.08	844	0.00182	-4.3	20.16
655.3	27.06	844	0.02474	-39.4	27.57
772.4	66.92	369	0.00455	-3.0	66.75
801.3	52.34	376	0.04941	-24.3	52.69
841.0	54.26	364	0.03420	-20.7	58.48
899.4	60.56	391	0.00000	27.6	1496.39
919.5	62.68	356	0.02329	-11.7	62.57
944.7	65.39	372	0.00000	40.3	2523.44
1013.8	85.31	324	0.02072	-9.1	85.22
1072.9	262.03	151	0.01470	-2.5	262.17
1149.0	848.96	118	0.05138	-3.3	848.93
		cumulative brine added:	**0.23**		

a second attempt to solve these equations realistically, f was estimated in the Equation 7.1 in order to solve for e. These two variables were then plugged into Equation 7.2 to solve for C_a. This estimation of f was repeated to attain the closest possible agreement between the actual measured chloride concentration and C_a (Table 7.8). These equations show the greatest additions of brine in Elephant Butte Reservoir, between the outlet of Elephant Butte Reservoir and Caballo Reservoir, and between Fabens and Ft. Quitman. Additionally, the

sum of the best-fit f values suggests that 23% of salts are derived from brines between the headwaters (250.2 km) and Ft. Quitman (1149.0 km). However, the results of these calculations are not entirely realistic because all of the e values are negative, which does not make sense if e truly represents evapotranspirative concentration of chloride. Looking at the data, it is clear that this simple model cannot account for some important river processes. For example, it is difficult to explain by evapotranspiration and brine mixing alone how the $^{36}Cl/Cl$ ratio drops by nearly 100% between samples 383.4 and 423.1, yet the chloride concentration remains the nearly the same. Nevertheless, these equations are informative in that they give a general idea of where most "dead" chloride is being added to the river.

7.8 Brief analysis of major anion and cation chemistry of the Rio Grande

The environmental tracer data make it clear that most of the salinization of the Rio Grande is due to salt addition that occurs at distinct locations. This salt most likely originates from high Cl/Br ratio, low $^{36}Cl/Cl$ ratio sources such as sedimentary brines. Figure 7.21 shows a Piper diagram comparison of major cations and anions of the August 2001 main stem Rio Grande with geothermal and brine end members. These end members include local geothermal waters from the Jemez mountains, Radium Springs, and Truth or Consequences [*Witcher*, 1995] as well as sedimentary brines and brine-influenced waters, represented by the San Acacia pool and ground waters discharging at the distal end of the Albuquerque basin [*Bexfield*, 2001] where brine discharge is hypothesized. With distance downstream, Rio Grande wa-

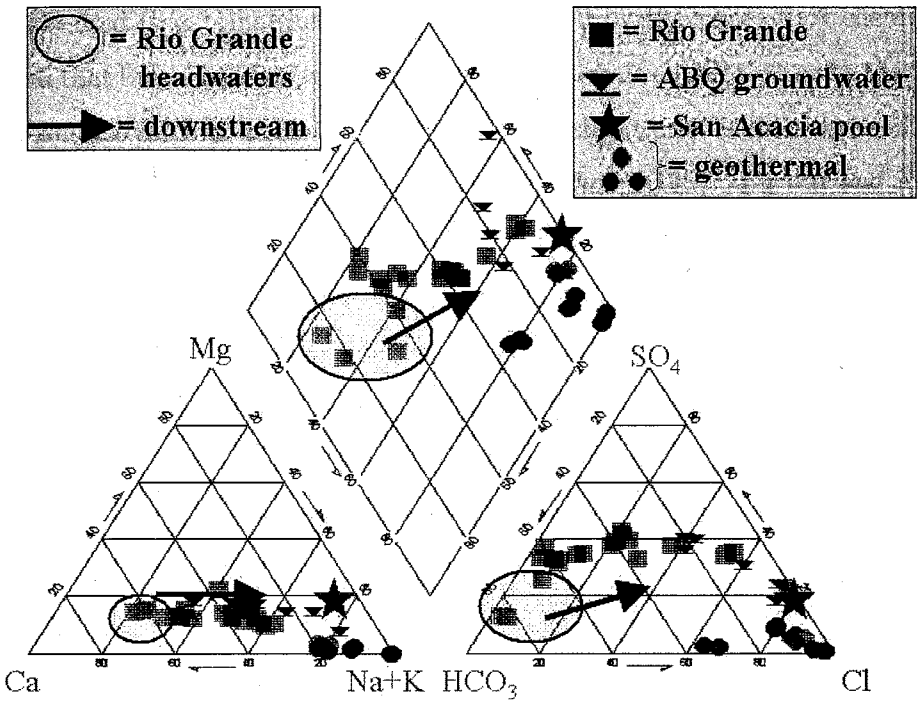

Figure 7.21: Piper diagram comparing chemical evolution with distance downstream of August 2001 main stem Rio Grande waters with local geothermal and sedimentary brine end members. Geothermal end members [*Witcher*, 1995] are from the Jemez mountains (red), Truth or Consequences (pink), and Radium Springs (orange). Sedimentary brine-influenced waters are represented by the San Acacia pool and ground waters discharging at the distal end of the Albuquerque basin [*Bexfield*, 2001].

ters become sodium- and chloride-dominated, their chemistries evolving toward that of the San Acacia pool and several of the brine-influenced Albuquerque ground waters are sodium- and chloride-dominated as well. *Hanor* [1994] hypothesized that brine chemistries are controlled by their host rock chemistry, such that brine chemistries approach thermodynamic equilibrium with the local subsurface mineral assemblages. In the southern Socorro basin where sodium-rich deep ground waters were noted by *Anderholm* [1987], *Barroll and Reiter* [1995] observed that local well logs indicate the presence of salt beds at 596 m depth, immediately below the main aquifer system. These evaporite beds may be a source of sodium and chloride to deep ground waters in the Socorro basin. The chemical composition of lithologies at depth may play a role in determining brine chemistry throughout the Rio Grande basin. Additionally, the progressive enrichment of sodium in Rio Grande waters may be due to interception of sodium-rich brines that are influenced by local sodium-dominated geothermal waters. In an active rift zone like the Rio Grande valley, it is not unlikely that deep sedimentary brines may be recirculated under the influence of geothermal systems. These systems probably influence brine chemistry and perhaps further facilitate brine movement to the surface.

CHAPTER 8

ANALYSIS OF CHLORIDE AND BROMIDE DATA USING A SIMPLE MASS BALANCE MODEL

8.1 Model description

To help pinpoint and quantify brine input to the Rio Grande, a simple mass balance model based on the main stem chloride and bromide concentration data from August 2001 was developed. This model assumes all salinization is due to evapotranspirative concentration of salts and brine addition, using the following equations:

$$m_{Cl} = e\left[m_{Cl,groundwater} \bullet f + m_{Cl,river}(1-f)\right] \tag{8.1}$$

$$m_{Br} = e\left[m_{Br,groundwater} \bullet f + m_{Br,river}(1-f)\right] \tag{8.2}$$

Here m_x is the constituent mass at the sampling station in mg L^{-1}, $m_{x,groundwater}$ is the constituent mass contributed by deep ground water at the sampling station in mg L^{-1}, and $m_{x,river}$ is the mass at the sampling station immediately upstream in mg L^{-1}. The fraction of constituent added by deep ground water is denoted by f, which is dimensionless. The dimensionless variable e is the inverse evaporated fraction of water between the two sampling stations, just as in the chloride concentration and $^{36}Cl/Cl$ mixing calculations in Chapter 7. The variable e is defined in the following way:

$$e = \frac{V_o}{V_x} \tag{8.3}$$

where V_o is the volume of water at the upstream sampling station and V_x is the volume remaining at the downstream sampling station x, assuming that evapotranspiration accounts for all change in water volume between these two stations. The deep ground water end member was assumed to have the chemistry of a ground water discharging at the distal end of the Albuquerque basin, with a chloride concentration of 280 mg L^{-1}, a bromide concentration of 0.5 mg L^{-1} and a Cl/Br ratio of 560 [*Bexfield*, 2001]. The San Acacia pool was not used as an end member because it was thought that its extremely high chloride concentration, which is probably influenced by evaporative concentration, may not be representative of brine end members throughout the Rio Grande basin. Furthermore, the model is oversensitive to changes in river chloride concentration when the chloride concentration of the San Acacia pool (32,300 mg L^{-1}) is used as an end member. This results in calculation of brine addition fractions that are negative and/or fluctuate wildly, which does not present an effective picture of basin-scale river salinization.

The two mass balance equations were solved simultaneously at each sampling station for the unknowns e and f. As an example, the two equations are solved at Rincon (891.3 km) for August 2001. m_{Cl} was equal to the chloride concentration at Rincon, 62.5 mg L^{-1}. $m_{Cl,groundwater}$ was equal to the chloride concentration of the deep ground water end member, 280 mg L^{-1}. $m_{Cl,river}$ was equivalent to 59.2 mg L^{-1}, the chloride concentration at the upstream sampling station, Placitas (874.3 km). Similarly, m_{Br} was the bromide concentration at Rincon, 0.17 mg L^{-1}. $m_{Br,groundwater}$ was the bromide concentration of the ground water end member, 0.5 mg L^{-1}. $m_{Br,river}$ was equal to the bromide concentration at the upstream sampling station, 0.15 mg L^{-1}. Using these

values, the two mass balance equations were solved simultaneously to determine the evapotranspirative concentration of constituents e and the fraction of deep ground water f added between Placitas and Rincon. Solving the equations for this example results in an e value of 1.29 and an f value of 0.098.

In order to determine locations of greatest relative brine addition, the f terms were successively accumulated with distance downstream and normalized by the accumulation at El Paso. Data that caused the accumulation to become anomalously high or low were removed. Such data include points at Alamosa (192.8 km), near Arroyo Hondo (332.5 - 384.5 km), and at Alameda (533.4 km) where the Cl/Br ratio dropped by over 30% and the drops were not sustained downstream. South of El Paso (1021.6 km), the August 2001 river chloride concentration rose above the chloride concentration of the ground water end member, causing anomalies in the accumulation that were best dealt with by removing these points as well.

8.2 Model interpretation

This model indicates that during August 2001, the most notable high Cl^-, high Cl/Br additions occurred south of Alamosa, in the south valley of Albuquerque, at San Acacia, in the narrows above Elephant Butte Reservoir, in Selden Canyon, and at El Paso (Figure 8.1). The addition of high Cl/Br water south of Alamosa is probably due to input of the Closed Basin Canal, which has a significant ground water component that has a higher Cl/Br ratio than local surface water. High Cl/Br addition in Albuquerque is most likely effluent from the Southside Water Reclamation Plant, which has a high Cl/Br ratio characteristic of wastewater. Comparing the remaining four locations to

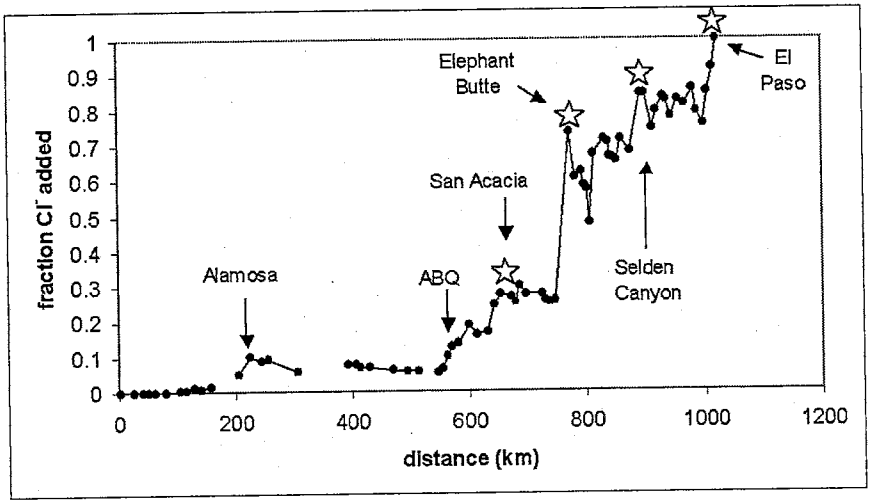

Figure 8.1: Results of the simple chloride and bromide mass balance model for the Rio Grande in August 2001. This model assumes all river salinization is due to evapotranspirative concentration of salts and addition of a high Cl^-, high Cl/Br ratio brine. Additions at Alamosa and Albuquerque (ABQ) correspond to input of the Closed Basin Canal and effluent from the Southside Water Reclamation Plant, respectively. Stars correspond to locations of greatest brine addition and to locations of southern termini of sedimentary basins on the hydrogeologic cross section (Figure 8.3).

the structure of the Rio Grande rift (Figure 8.2), it is apparent that these locations coincide with the shallow southern termini of major sedimentary basins: San Acacia is at the southern end of the Albuquerque basin; Elephant Butte Reservoir is at the distal end of the Socorro basin; Selden Canyon is at the terminus of the Palomas basin; and El Paso is at the southern end of the Mesilla basin.

To further investigate the structural influence on brine upwelling, a hydrogeologic cross-section based on work by *Keller and Cather* [1994], *Wilkins* [1998], *Anderholm* [1987], and *Hawley and Lozinsky* [1992] was constructed parallel to the river path (Figure 8.3). This cross-section suggests that deep brines are being forced to the surface where the bedrock elevation shallows. Other structural features such as faults may control brine discharge at the distal basin ends. These locations of deep ground water upwelling are consistent with work by *Anderholm* [1987], *Wilson et al.* [1981], and *Frenzel et al.* [105 pp. plus plates, 1992] that confirm ground water discharge at the distal ends of the Albuquerque, Socorro, Palomas, and Mesilla basins (see Chapter 2 of this thesis). Furthermore, this model is consistent with the location of the briney San Acacia pool, which is found at the distal end of the Albuquerque basin.

Although this simple model successfully illustrates the overall pattern of Rio Grande salinization, it is necessary to employ a more complex mass balance model in order to account for inflows to and outflows from the river. Additionally, it is necessary to explicitly take water mass balance into account. This more detailed model is described in the next chapter.

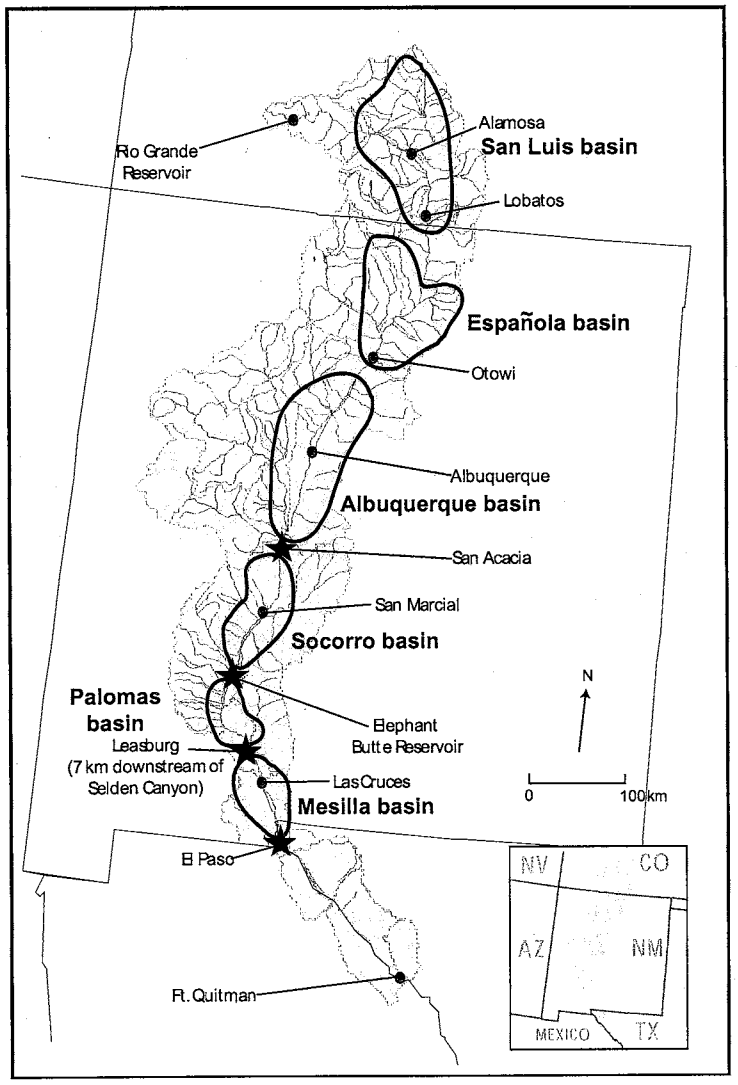

Figure 8.2: Sedimentary basins of the Rio Grande rift with locations of inferred deep brine upwelling at the distal ends of the basins. Red stars indicate basin termini. Blue circles indicate gaging stations for reference. Basin shapes determined from *Wilkins* [1998].

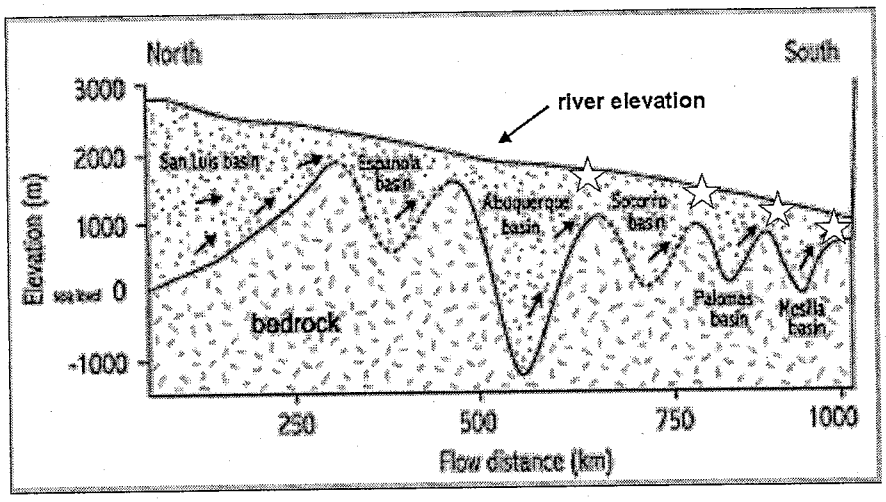

Figure 8.3: Hydrogeologic cross section of the Rio Grande rift, drawn parallel to river path. Basin depths and shapes were determined from *Keller and Cather* [1994], *Wilkins* [1998], *Anderholm* [1987], and *Hawley and Lozinsky* [1992]. The top line indicates river elevation. Basin depth is dashed where inferred. Stars indicate sedimentary basin termini.

CHAPTER 9

DESCRIPTION OF THE DETAILED CHLORIDE, BROMIDE, AND WATER MASS BALANCE MODEL

9.1 Modeling schematic

To improve upon the simple mass balance model described above, two detailed instantaneous chloride, bromide and water mass balance models were developed. Both models use the same equations, though the first is based on August 2001 data and the second on January 2002 data. At each sampling station, the water balance equation was written in terms of the gaging interval and the constituent mass balance equations were written in terms of the sampling interval (Figure 9.1).

9.2 Water mass balance

Since discharge data was not collected in the field but rather obtained from governmental agencies and irrigation districts, the water mass balance equation at the station of interest, b ((Figure 9.1), was written in terms of the interval of the available gaging data, which averages about 40 km:

$$V_2 = V_1 - \sum V_{div} + \sum V_{trib} - V_N \tag{9.1}$$

All terms are in units of cubic meters per second ($m^3\ s^{-1}$). Here V_1 is the discharge at the gaging station upstream of b and V_2 is the discharge at gaging station 2 downstream of b. Between the two gaging stations, $\sum V_{div}$ is the sum

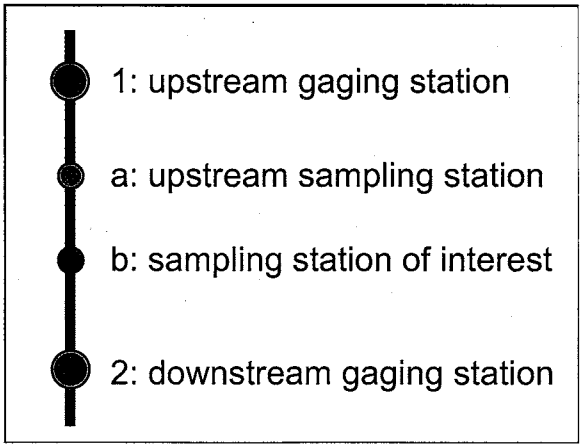

Figure 9.1: Schematic of the river system used for the detailed water and constituent mass balance equations. The small red circle represents the sampling station of interest (b) where the mass balance equations are being solved; the small yellow circle represents the sampling station immediately upstream (a) of the sampling station of interest; the large green circles represent the upstream (1) and downstream (2) gaging stations. In reality, there may be more or fewer sampling stations upstream and downstream of the sampling station within a single gaging interval.

of water fluxes removed by agricultural diversion and riverbed seepage; $\sum V_{trib}$ is the sum of fluxes added by natural tributaries, riverbed seepage, irrigation return flow, and wastewater outfall. V_N is the net water imbalance which is attributed to evapotranspirative loss, though in application this term may be dominated by the effects of ungaged water gains or losses within the gaging interval.

Since the Cl^- concentration and Cl/Br ratio of deep ground water contributions were assumed to be very high, it was expected that the ground water discharge necessary to cause the observed salinity jumps would be low in comparison to the total flow of the river. Following from this, the ground water contribution was assumed to be negligible in terms of the water mass balance, allowing analytical solution of the water and constituent mass balance equations. A precipitation term was not included in the water mass balance because precipitation during both the August 2001 and January 2002 sampling seasons was negligible.

In the case of the three gaging intervals with a reservoir at their downstream ends, it was assumed that evapotranspirative loss through the interval was dominated by evaporation from the reservoir. For these intervals, V_N was calculated using daily pan evaporation and reservoir surface area data [*Ed Kandl, USBR,* personal communication 2003]. An additional term V_s was added to the water mass balance at these three stations to represent water storage in or release from the reservoir:

$$V_2 = V_1 - \sum V_{div} + \sum V_{trib} - V_N + V_s \tag{9.2}$$

Here the storage term V_s is positive when there is net release from a reservoir

(i.e., discharge exceeds inflow) and is negative when there is net storage.

9.3 Constituent mass balance

The constituent mass balance equations were based on changes in constituent burdens between sampling stations. The constituent burden was calculated by multiplying constituent concentration in mg L^{-1} by discharge in m^3 s^{-1}. At the sampling station of interest, b:

$$C_{b,x}V_b = C_{a,x}V_a + \Sigma C_{trib,x}V_{trib} - \Sigma C_{div,x}V_{div} + I \tag{9.3}$$

If the sampling station of interest is immediately below a reservoir, the mass balance becomes:

$$C_{b,x}V_b = C_{a,x}V_a + \Sigma C_{trib,x}V_{trib} - \Sigma C_{div,x}V_{div} + C_{s,x}V_s + I \tag{9.4}$$

In both equations, $C_{b,x}$ is the constituent concentration at the sampling station of interest and $C_{a,x}$ is the constituent concentration at the sampling station immediately upstream, both in mg L^{-1}. The terms $\sum C_{trib,x}V_{trib}$ and $\sum C_{div,x}V_{div}$ are the sums of the constituent burdens of inflows to and outflows from the river within the sampling interval, respectively. Both have dimensions of mass per time, reported as kg dy^{-1}. The term $C_{s,x}V_s$, also with dimensions of mass per time and reported in units of kg dy^{-1}, represents the constituent burden added to or removed from reservoir storage. V_a is the discharge at the previous sampling station and V_b is the discharge at the sampling station of interest, both in m^3 s^{-1}. V_b is either gaged or is calculated based on the water mass balance within the sampling interval using the following equation:

$$V_b = \frac{V_a + V_{trib} - V_{div}}{e} \tag{9.5}$$

Similar to other evapotranspirative terms used in this thesis, the coefficient e represents the inverse evapotranspired fraction of water between the two sampling stations. In fact, it is the reciprocal of the water remaining "after" evapotranspiration. It is calculated by normalizing V_N to the sampling interval, since V_N is calculated based on the gaging interval:

$$e = \frac{V_1}{V_1 - (V_N/L \bullet d)} \tag{9.6}$$

where L is the distance between the upstream gaging station 1 and the downstream gaging station 2. The variable d is the distance between the sampling station of interest b and the upstream sampling station a (Figure 9.1). This equation equally partitions the evapotranspirative water loss with distance along the gaging interval.

Finally, I is the salt imbalance term. It represents the constituent flux not accounted for by the known river inputs and outputs. The equation is written such that if $I > 0$, the mass balance is incomplete with the available data, and an addition of salt to the system is necessary to satisfy the mass balance. On the other hand, if $I < 0$, the available data have over-accounted for salt at the sampling station. Overall, the salt imbalance term lumps inaccuracies in the water and salt balances due to data unavailability with the effects of real but unquantified river processes such as deep groundwater discharge to the river and riverbed seepage. It is these calculated salt imbalances, in conjunction with end member constituent concentrations found in the literature, that were employed to solve for both the chloride burden and the flux of deep ground water at the locations of deep ground water discharge that were noted in Chapter 8.

9.4 Application of mass balance equations to the detailed model

To use these equations, first the water mass balance equation was solved for V_N at the sampling station of interest:

$$V_N = V_1 - V_2 - \sum V_{div} + \sum V_{trib} \tag{9.7}$$

For example, at Rincon (891.3 km) in August 2001, V_1 was equal to 50.7 m^3 s^{-1}, the discharge at the nearest upstream gaging station at Caballo Reservoir. V_2 was equal to 43.5 m^3 s^{-1}, the discharge at the nearest downstream gaging station at Haynor Ranch. $\sum V_{div}$ was the total flow removed from the river between Caballo Reservoir and Haynor Ranch, equivalent to 7.1 m^3 s^{-1} diverted from the river at Percha diversion dam. $\sum V_{trib}$ was the total flow added to the river within the same gaging interval, equal to 0.6 m^3 s^{-1} contributed by the Garfield and Hatch drains. Thus, V_N was equal to 0.65 m^3 s^{-1} at Rincon.

This V_N value was used to calculated the evapotranspirative variable e using Equation (9.6). Continuing with the example at Rincon started above, V_1 was equal to 50.7 m^3 s^{-1}, the discharge at the upstream gaging station at Caballo Reservoir. V_N equaled 0.65 m^3 s^{-1} as determined in the previous paragraph. L was equal to 58.4 km, the distance between Caballo Reservoir and Haynor Ranch (e.g. the distance between the upstream gaging station and the downstream gaging station). With a value of 17 km, the term d was equivalent to the distance between Rincon and and the upstream sampling station at Placitas (874.3 km). With these values, e at Rincon was determined to be 1.00 (a unitless fraction), which indicates that no evaporation occurred over this segment of the river.

This value for e subsequently was used in Equation (9.5) to solve for V_b, the discharge at the sampling station of interest. Substituting the values at Rincon into this equation, V_a was equal to the discharge at the immediately upstream sampling station Placitas, or 43.3 $m^3\ s^{-1}$ (which was calculated from the water and chloride mass balance equations solved at Placitas); V_{trib} was the inflow of water to the river between Placitas and Rincon, which was equal to 0.6 $m^3\ s^{-1}$ inflow from the Garfield and Hatch drains; V_{div} was the outflow of water from the river between Placitas and Rincon, which was 0 $m^3\ s^{-1}$; e was equal to 1.00 as determined in the previous paragraph. With those variables, the discharge V_b at Rincon was calculated to be 43.5 $m^3\ s^{-1}$. Where V_b was known (where a sampling station coincided with a gaging station), it was not necessary to employ Equation (9.5) nor Equation (9.6). In either case, V_b then was substituted into the chloride mass balance equation to solve for the chloride imbalance I at the sampling station of interest:

$$I = C_{b,Cl}V_b - C_{a,Cl}V_a - \Sigma C_{trib,Cl}V_{trib} + \Sigma C_{div,Cl}V_{div} \tag{9.8}$$

At Rincon in August 2001, V_b and V_a were the calculated discharges at Rincon and at the upstream sampling station Placitas and were equal to 43.5 and 43.3 $m^3\ s^{-1}$, respectively. $C_{b,Cl}$, the chloride concentration at Rincon, was equal to 62.5 mg L^{-1}. $C_{a,Cl}$, the chloride concentration at the upstream sampling station Placitas, was equal to 59.2 mg L^{-1}. $\sum C_{trib,Cl}V_{trib}$ was equal to the sum of the chloride burdens of the two inflows to the river between Placitas and Rincon, the Garfield and Hatch drains. The Garfield drain had a discharge of 0.2 $m^3\ s^{-1}$ and a chloride concentration of 142 mg L^{-1} in August 2001. Multiplying the two results in a chloride burden of 28.2 g s^{-1}. In August 2001 the Hatch

drain had a discharge of 0.4 m^3 s^{-1} and a chloride concentration of 136 mg L^{-1}, resulting in a chloride burden of 53.9 g s^{-1}. Adding the chloride burdens of both drains, the term $\sum C_{trib,Cl} V_{trib}$ becomes 82.1 g s^{-1}. $\sum C_{div,Cl} V_{div}$ was equal to 0 because there were no diversions in the sampling interval in August 2001. Using these variables in the equation, the chloride imbalance at Rincon was calculated to be 86.3 g s^{-1}, which was then converted to 7458 kg dy^{-1} for comparison to other chloride burdens. The fact that the imbalance was greater than zero indicates that the mass balance equations do not account for all chloride that entered the river between Placitas and Rincon in August 2001. However, 7458 kg dy^{-1} was only 3% of the river chloride burden at Haynor Ranch 8 km downstream (the nearest river gaging station and thus the nearest location at which chloride burden could be calculated). This is only 1% more than the error in the chloride measurements determined by check standards and replicates (2%).

Calculations were repeated in this way at each successive sampling station. In the case of stations immediately below reservoirs, the value for V_N was derived from pan evaporation data, the water balance was closed by solving for the storage term V_s (see Equation (9.2)), and the constituent mass balance included the constituent burden $C_{s,x} V_s$ contributed within the reservoir (see Equation (9.4)). At sampling stations that coincide with gaging stations, gaging data was substituted into the model for the V_b term in the water balance; gaging data was substituted into the V_a term at stations immediately downstream from gaging stations. This effectively reset the water balance at each gaging station. Carrying a single water balance through the entire model results in an increase in salt imbalances by 2-5 orders of magnitude at many

sampling stations. The bromide constituent mass balance equation was only used at locations of suspected deep ground water inflow, as will be described in Chapter 10.

It was assumed that discharge was relatively constant throughout each day of field sampling. It was also assumed that the river was well-mixed, such that diversions removed water with a representative river chemistry, and that tributaries mixed instantaneously with river water. In fact, the Rio Grande is observed to be a poorly mixed river in some locations. For example, during both August 2001 and January 2002 neither the river chloride concentration nor the Cl/Br ratio increased immediately downstream (555.6 km) of effluent inflow from the Southside Water Reclamation Plant (at 550.0 km). Instead, the elevated chloride and Cl/Br signal was not observed in the data for another 10 km downstream (564.9 km) in August 2001 and for another 30 km (582.9 km) in January 2002. The SWRP releases effluent from the east bank of the river, and it is likely that if sampling did not occur on the same side of the river, the effluent signal was not observed. Elephant Butte Reservoir is also known to be poorly mixed [*NRC*, 1938], and the other smaller reservoirs probably have similar though less-pronounced behavior. However, effects of variable mixing could not be examined given the limitations of the data collected.

9.5 Calculation of tributary and diversion mass fluxes

To calculate tributary and diversion chloride mass fluxes, discharge and chemical data were obtained from a variety of sources (Appendix E). Tributary and diversion gaging data were obtained from various local, state, and federal agencies. Riverbed seepage flows were obtained from the literature.

Riverbed seepage values calculated for the Upper Rio Grande Water Operations Model (URGWOM) were not immediately available for the August 2001 and January 2002 field seasons. Furthermore, though the method for determining riverbed seepage for the URGWOM is quite detailed, it remains very approximate due to lack of data [*Gail Stockton, USACE,* personal communication 2003]. It was thought that introducing this method into the mass balance models would make salt imbalance calculations less transparent and unnecessarily complicated.

To calculate a diversion mass flux, the chemistry of the diversion was assumed to be the same as the chemistry of the nearest reasonable river sampling location during the same field season. Similarly, the chemistry of riverbed seepage out of the river was assumed to be the same as local river chemistry. Assuming a close connection between the river and the shallow aquifer, shallow groundwater seepage into the river was assumed to have a chemistry similar to the local river samples as well.

For tributaries and drain return flows that were sampled during August 2001 and January 2002, sampled chemistries were paired with gaging data to calculate tributary mass fluxes. Tributaries that were not sampled during the field seasons were assumed to have the same chemistry as a similar tributary that was actually sampled. For example, unsampled headwaters streams were assumed to have the same chloride and bromide concentrations as nearby sampled headwaters streams, and unsampled drain return flows were assumed to have the same concentrations as sampled return flows within the same basin. Two exceptions are the Rio Pueblo de Taos and the Jemez River. Their chloride

concentrations were estimated from the historical record (see Chapter 5).

9.5.1 Wastewater treatment effluent data collection

Though all wastewater treatment facilities measure daily average discharge, most do not test for chloride. Effluent samples were collected after the synoptic sampling seasons from the three major plants in Albuquerque (July 2002), Las Cruces (March 2003), and El Paso (March 2003). Assuming that these measurements reflect regulatory requirements and in some cases noting their similarity with other reported values [*Kelly and Taylor*, 1996], the chemistries observed for these samples were assumed to be similar to that of effluent during the field seasons.

The two Rio Rancho wastewater treatment plant effluent streams that discharge to the Rio Grande (no. 2 and no. 3) are tested monthly for chloride concentration. For this reason, the chloride concentration values for the models were derived from the August 2001 and January 2002 monthly chloride data collected by the Rio Rancho plant. Between May 2001 and May 2002, the chloride concentration of effluent no. 2 varied between 43 - 58 mg L^{-1} with a single outlier value of 84 mg L^{-1} in May 2001. The chloride concentration of effluent no. 3 varied between 96 - 410 mg L^{-1} in the same time period [*Jeff Burkett, RRWWTP,* personal communication 2003]. Both effluent streams are derived mainly from domestic users, and the causes of variation in chloride concentration are unknown. Due to a change in management at the Rio Rancho wastewater treatment plant within the past 5 years, the accessible historical record of effluent chloride concentrations does not extend further back in time than the management change. However, it is thought that this record is repre-

sentative of historical conditions. Furthermore, it should be kept in mind that the combined effluent streams comprise about 1% of river flow, and that the higher TDS discharge of effluent stream no. 3 was 70 - 75% smaller than the more dilute discharge of effluent no. 2 in both August 2001 and January 2002. This suggests that variations in chloride concentration in the historical record, particularly for effluent no. 3, probably do not have a large effect on the river.

9.6 Figures and data for modeled flow and chloride burden conditions in August 2001 and January 2002

A color schematic diagram of the modeled river system comprises Figure 9.2, Figure 9.3, Figure 9.4, Figure 9.5, and Figure 9.6. Pipe diagrams of flow (Figure 9.7 and Figure 9.8) and chloride burden (Figure 9.9, Figure 9.10, Figure 9.11, and Figure 9.12) for August 2001 and January 2002 show the calculated inputs and outputs to the river as well as main stem parameters measured at gaging stations. Smaller-scale chloride burden pipe diagrams are presented in Appendix F. Diversion and tributary data sources, chloride, bromide, and flow data, and calculated chloride burdens for August 2001 and January 2002 are reported in Appendix E. River discharges, river chloride burdens, cumulative water and chloride imbalances, and cumulative water and chloride burden percent imbalances are reported by gaging interval for both sampling seasons in Appendix G. Chloride imbalances for each sampling station for both the summer and the winter model are reported in Appendix G. The next chapter examines both the collected data and the chloride imbalances resulting from the model in order to develop a coherent picture of the most important salinizing processes in the Rio Grande.

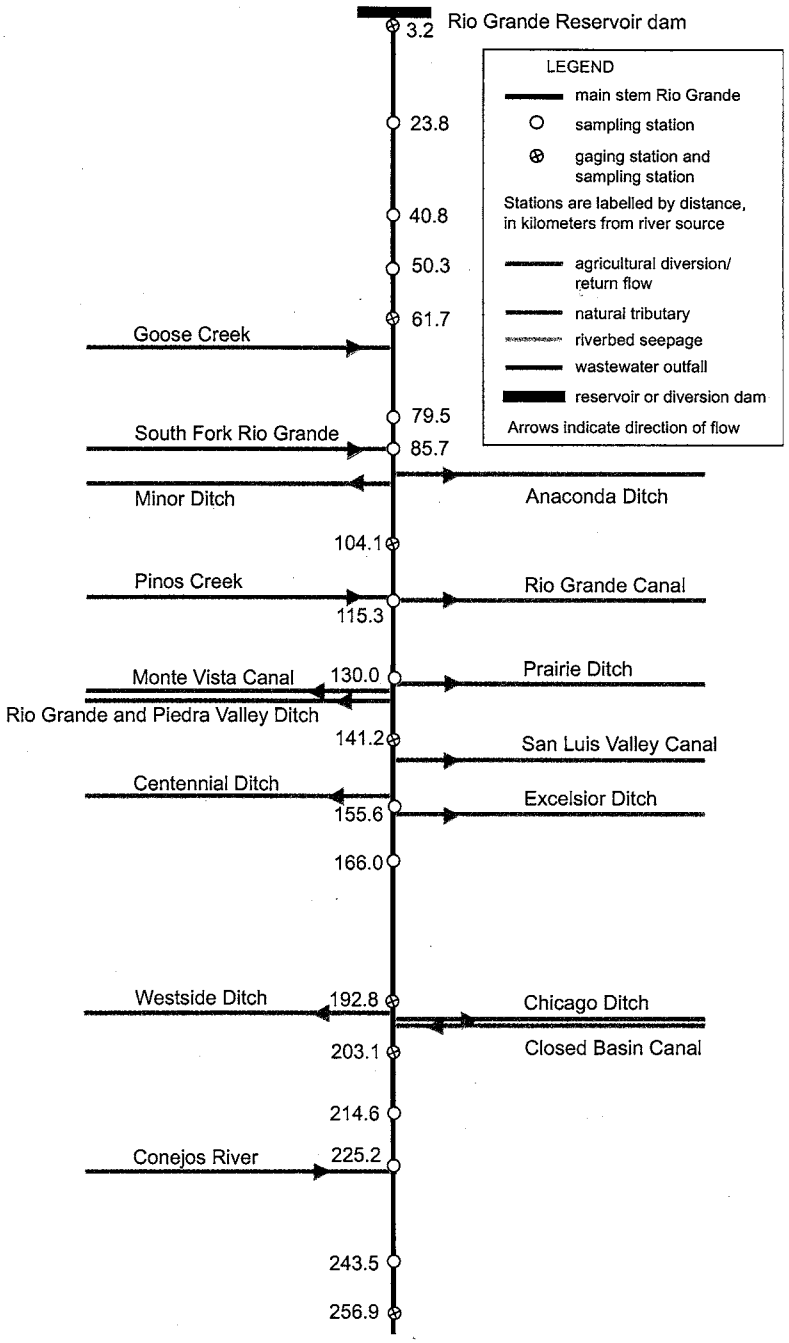

Figure 9.2: Detailed schematic of Rio Grande system including gaging stations, sampling stations, and modeled tributaries and diversions, river kilometers 3.2 - 256.9. River distances are to a 1:100,000 scale.

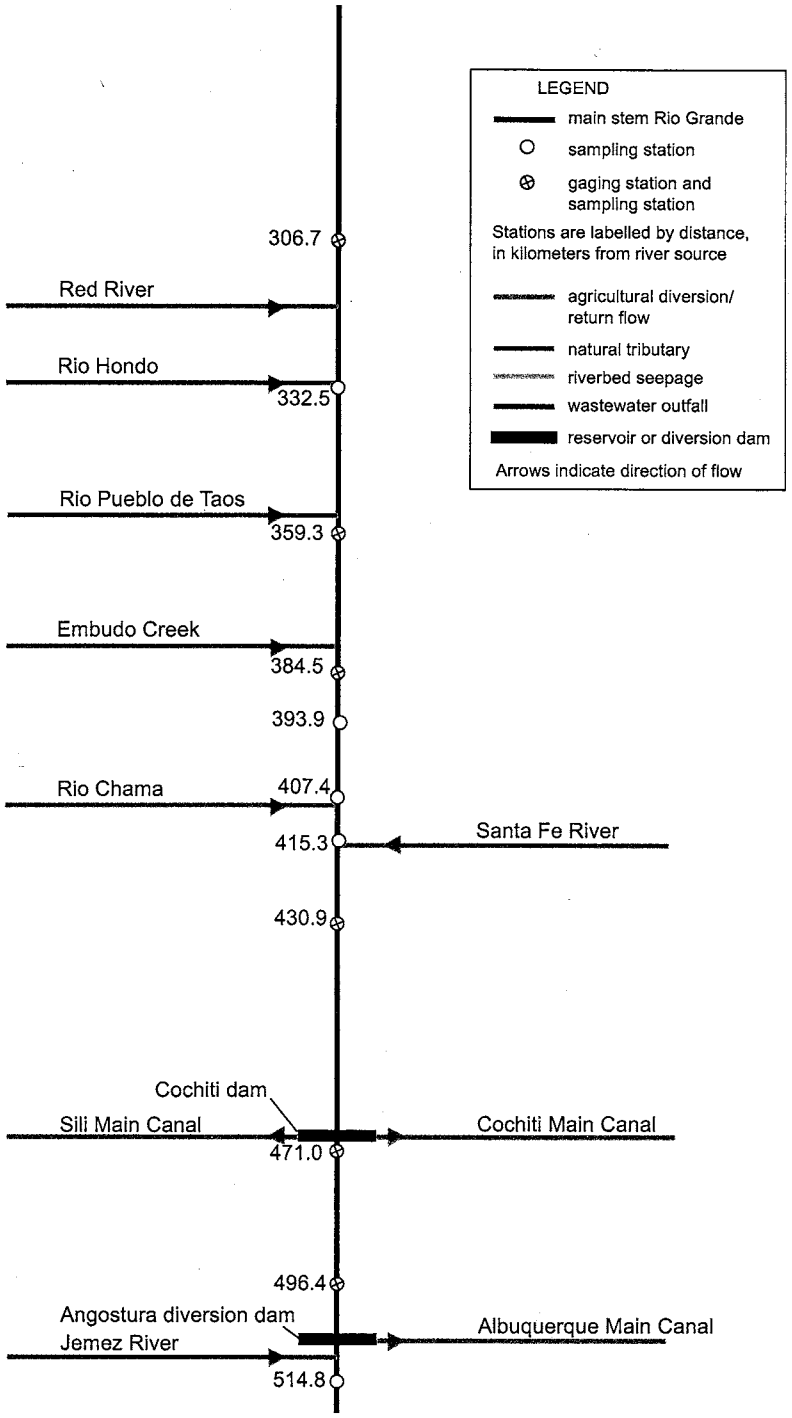

Figure 9.3: Detailed schematic of Rio Grande system including gaging stations, sampling stations, and modeled tributaries and diversions, river kilometers 264.0 - 514.8. River distances are to a 1:100,000 scale.

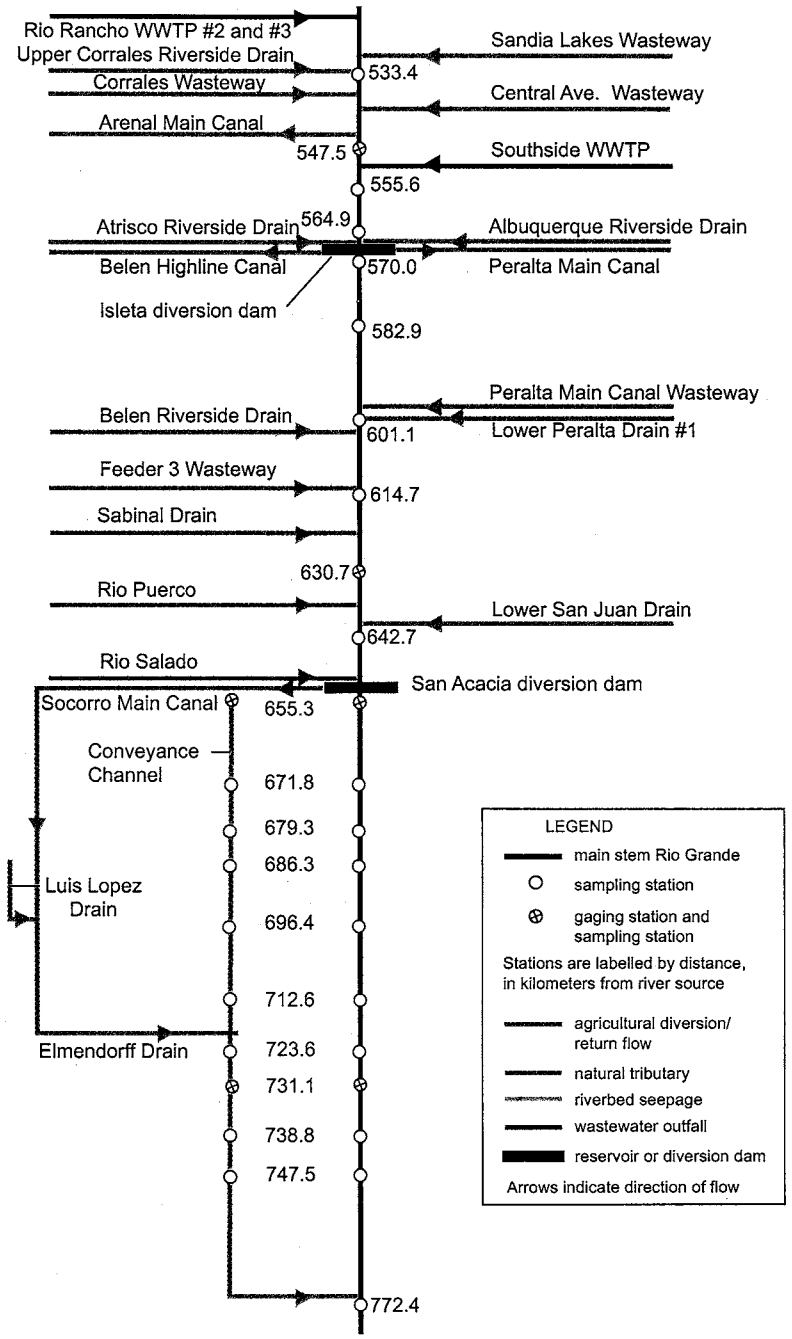

Figure 9.4: Detailed schematic of Rio Grande system including gaging stations, sampling stations, and modeled tributaries and diversions, river kilometers 522.5 - 772.4. River distances are to a 1:100,000 scale.

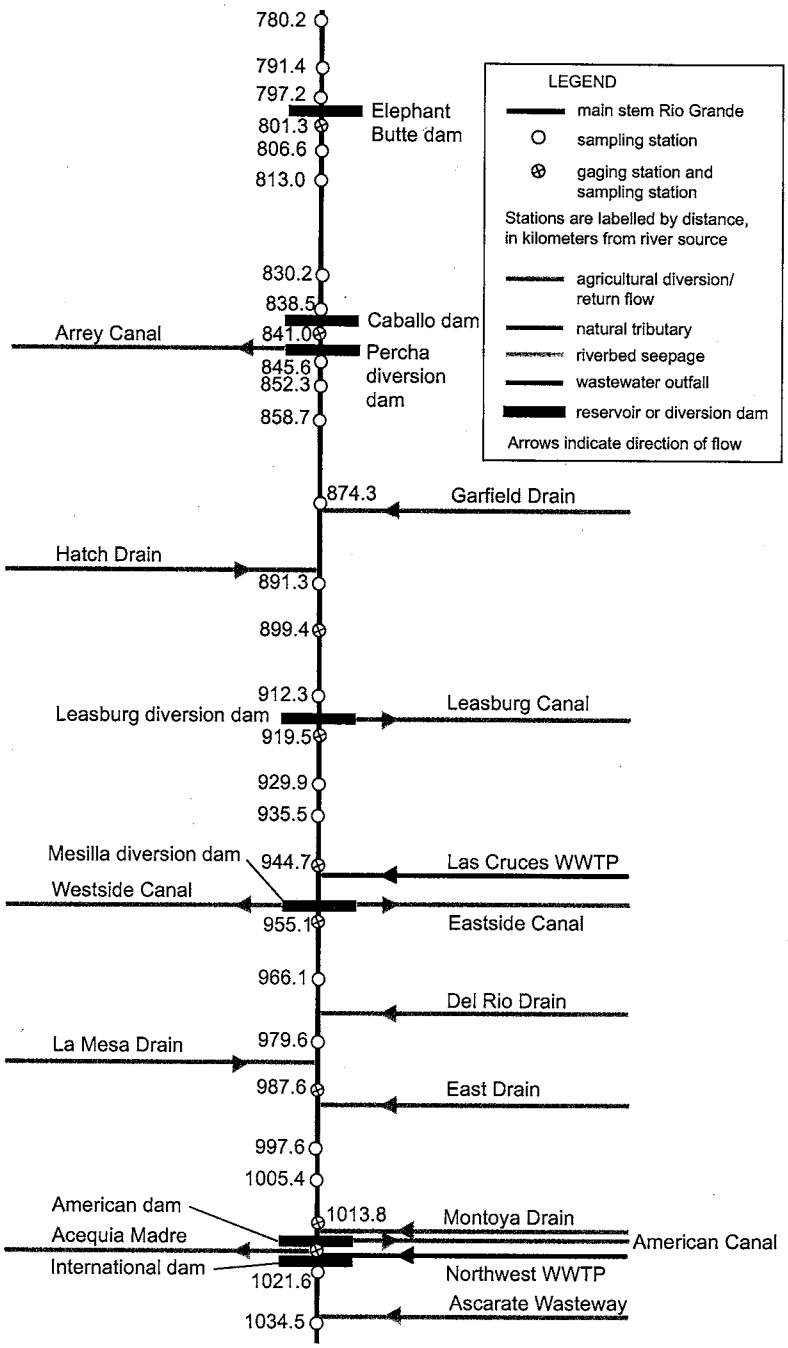

Figure 9.5: Detailed schematic of Rio Grande system including gaging stations, sampling stations, and modeled tributaries and diversions, river kilometers 780.0 - 1040.0. River distances are to a 1:100,000 scale.

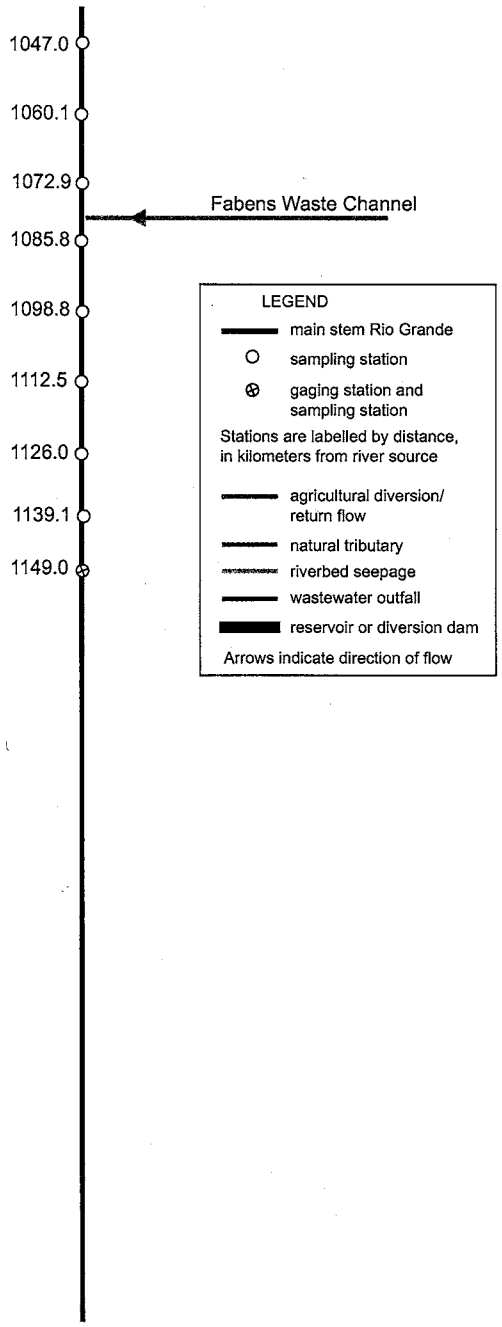

Figure 9.6: Detailed schematic of Rio Grande system including gaging stations, sampling stations, and modeled tributaries and diversions, river kilometers 1040.0 - 1149.0. River distances are to a 1:100,000 scale.

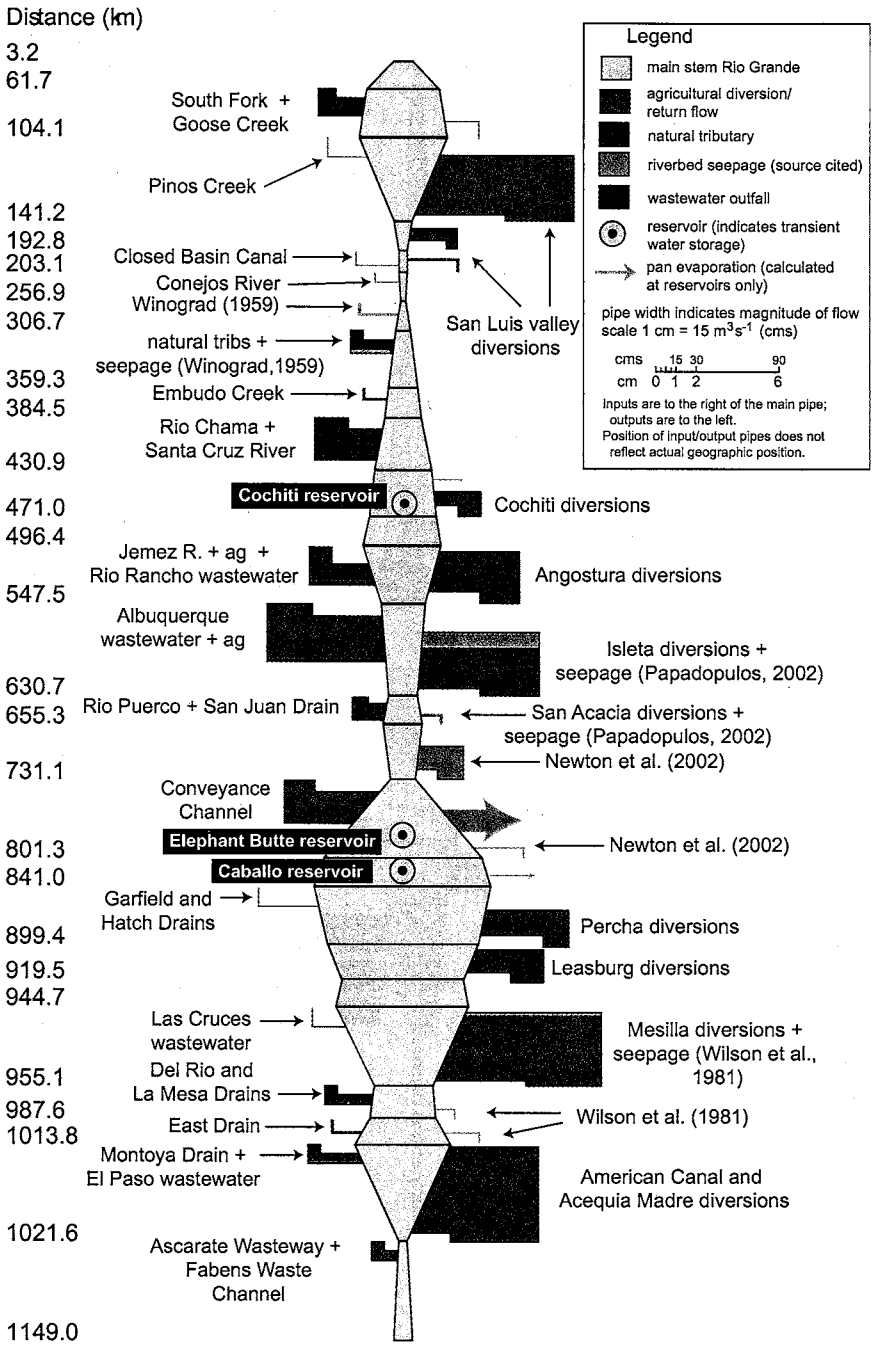

Figure 9.7: Pipe diagram of flow of the Rio Grande, its modeled tributaries and diversions, August 2001 ($m^3\ s^{-1}$).

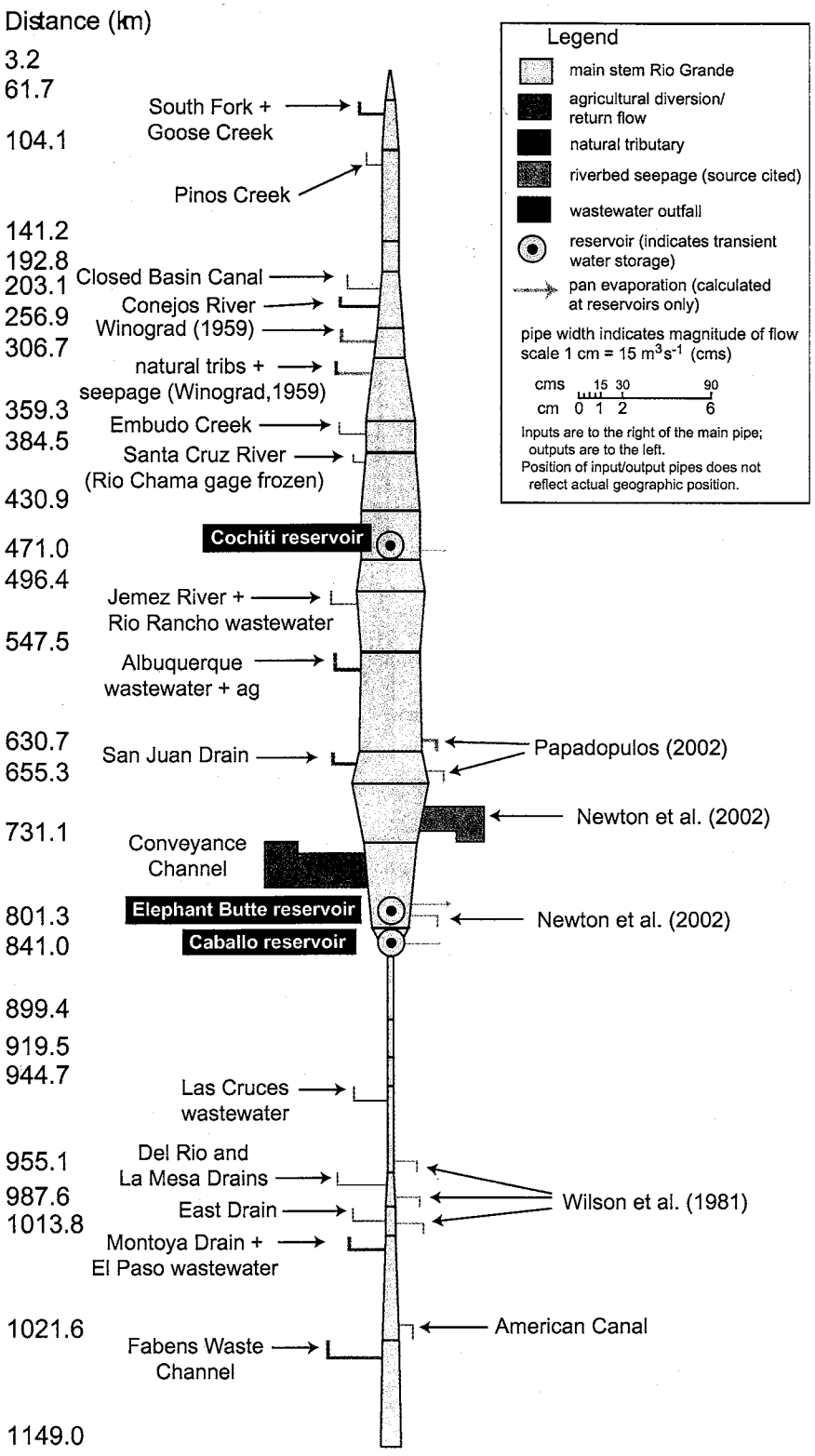

Figure 9.8: Pipe diagram of flow of the Rio Grande, its modeled tributaries and diversions, January 2002 ($m^3\ s^{-1}$).

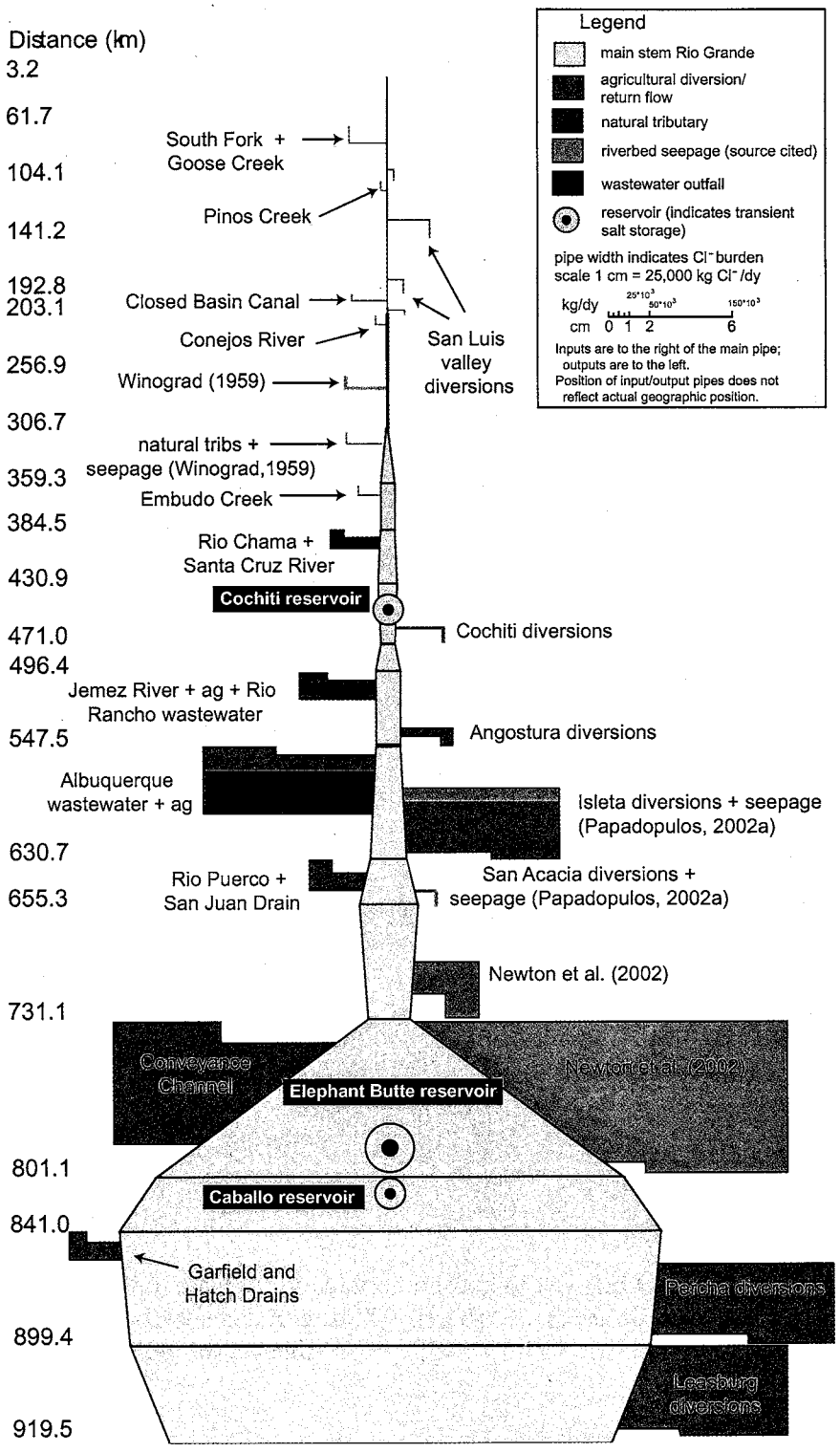

Figure 9.9: Pipe diagram of chloride burden of the Rio Grande, its modeled tributaries and diversions, August 2001 (kg dy^{-1}). River distance 3.2 - 919.5 km.

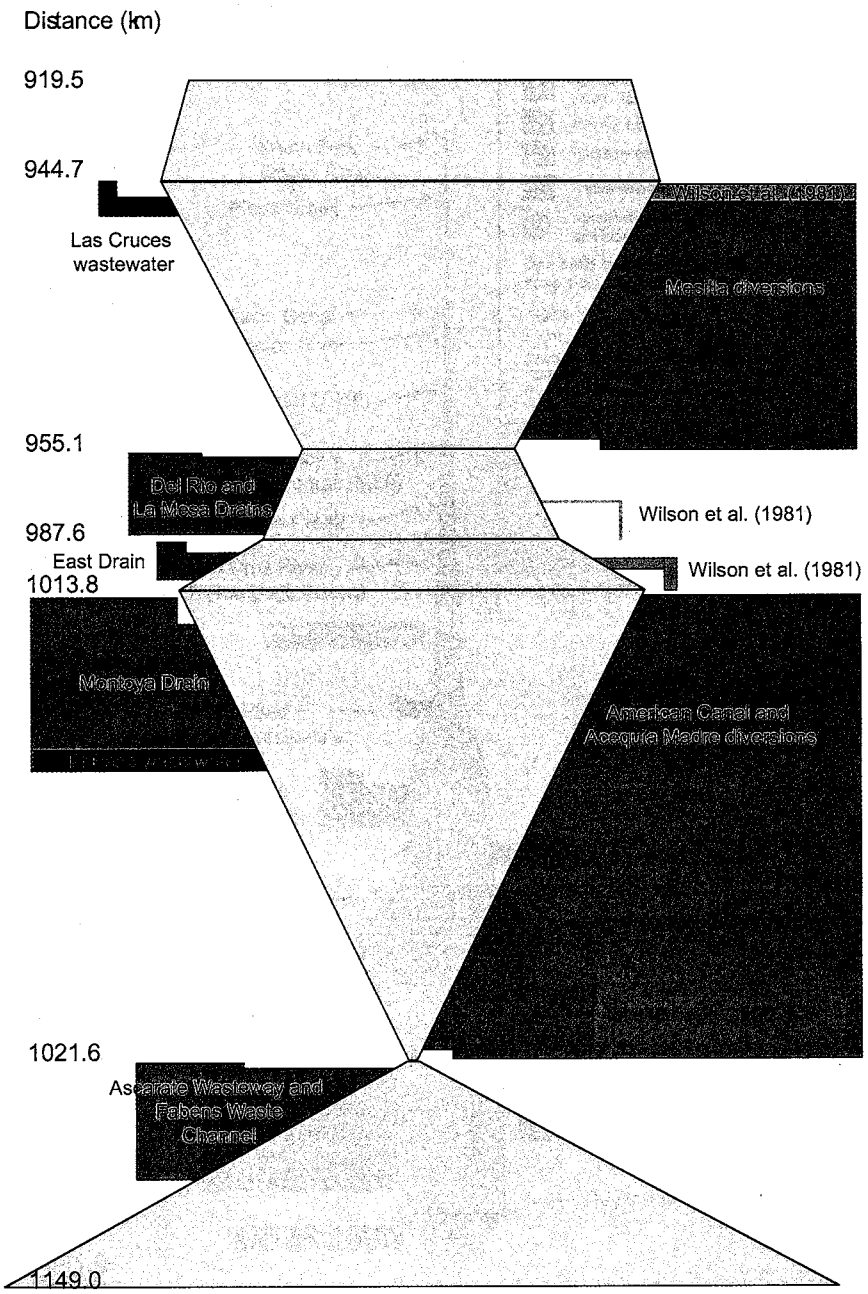

Figure 9.10: Pipe diagram of chloride burden of the Rio Grande, its modeled tributaries and diversions, August 2001 (kg dy^{-1}). River distance 919.5 - 1149.0 km. See Figure 9.9 for legend.

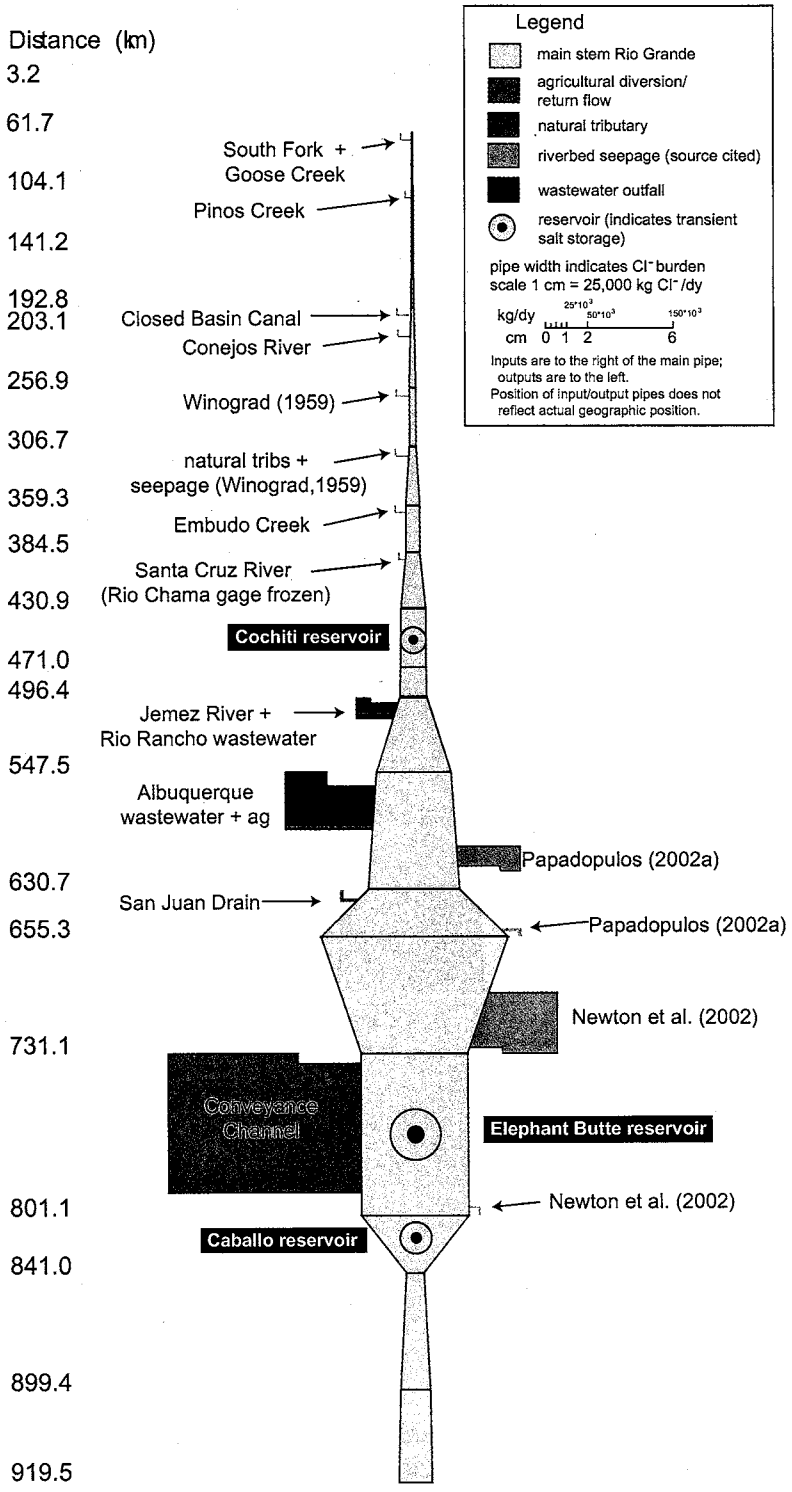

Figure 9.11: Pipe diagram of chloride burden of the Rio Grande, its modeled tributaries and diversions, January 2002 (kg dy^{-1}). River distance 3.2 - 919.5 km. Diagrammed locations of river distances match those of Figure 9.9.

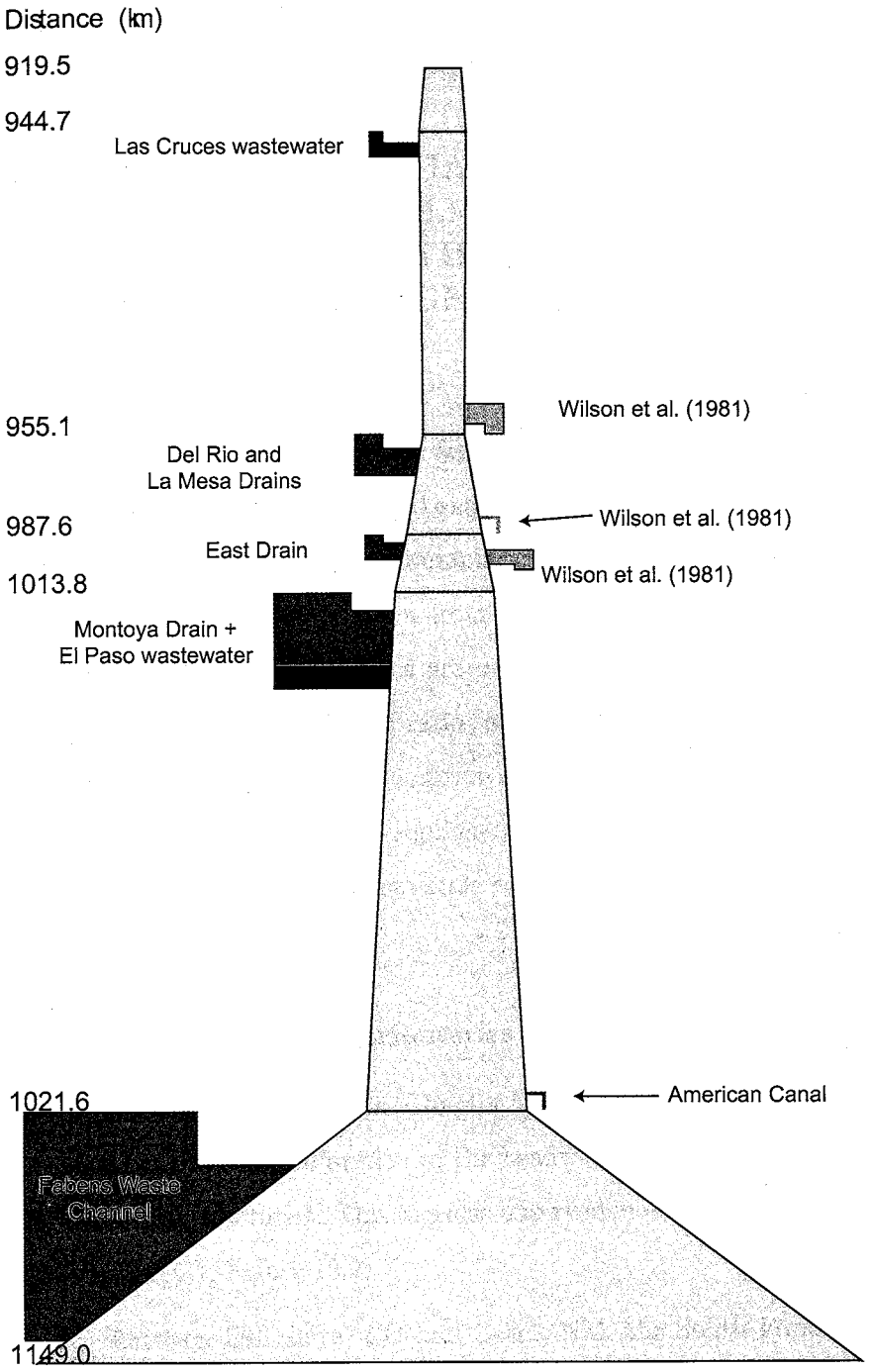

Figure 9.12: Pipe diagram of chloride burden of the Rio Grande, its modeled tributaries and diversions, January 2002 (kg dy^{-1}). River distance 919.5 - 1149.0 km. See Figure 9.11 for legend. Diagrammed locations of river distances match those of Figure 9.10.

CHAPTER 10

EVALUATION AND QUANTIFICATION OF THE MOST IMPORTANT SALINIZING PROCESSES ON THE RIO GRANDE

Based on the data collected for the detailed mass balance models, the mass balance models themselves, and analyses and literature reviews performed earlier in this thesis, this section summarizes the most important salinizing processes in the Rio Grande basin from the headwaters in Colorado to Ft. Quitman, TX. Salinizing processes are described in terms of their effects on the chloride concentration, Cl/Br ratio, and chloride burden. Following that, estimations of deep ground water addition directly to the river are provided. At the end of the chapter, the most significant salinizing processes are quantified in terms of their cumulative basin-scale effects on river chloride burden and chloride concentration.

10.1 Influence of natural tributaries

Historical data analysis (Chapter 5) suggests that increases in chloride concentration and chloride burden in the headwaters region are mainly due to input of natural tributaries. This was also observed in August 2001 and January 2002 (Figure 10.1, Figure 10.2).

Between Del Norte, CO and Cerro, NM, the South Fork of the Rio

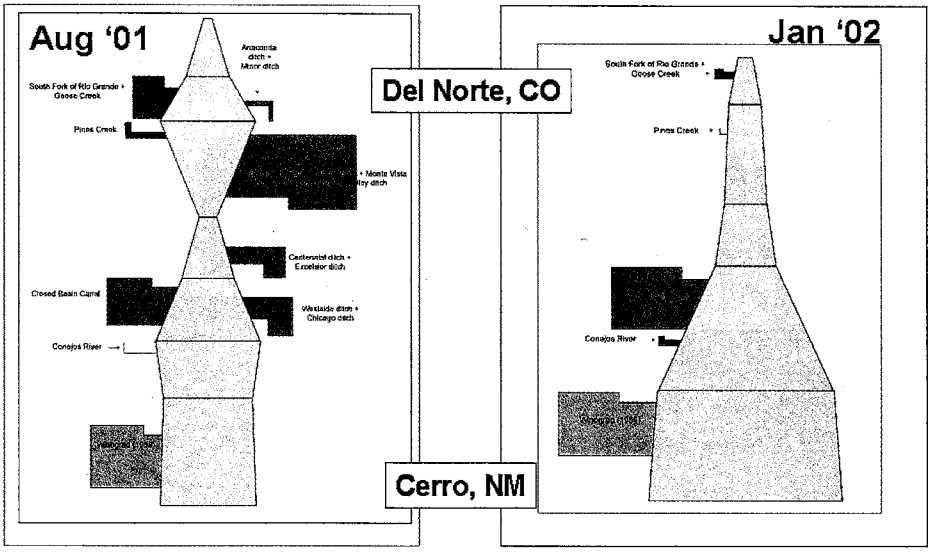

Figure 10.1: Chloride burden inputs to and outputs from the Rio Grande in August 2001 and January 2002, Del Norte, CO - Cerro, NM. Natural tributaries and the Closed Basin Canal are the significant salt contributors in this region. See Appendix F for a larger version of these diagrams and a pipe diagram explanation.

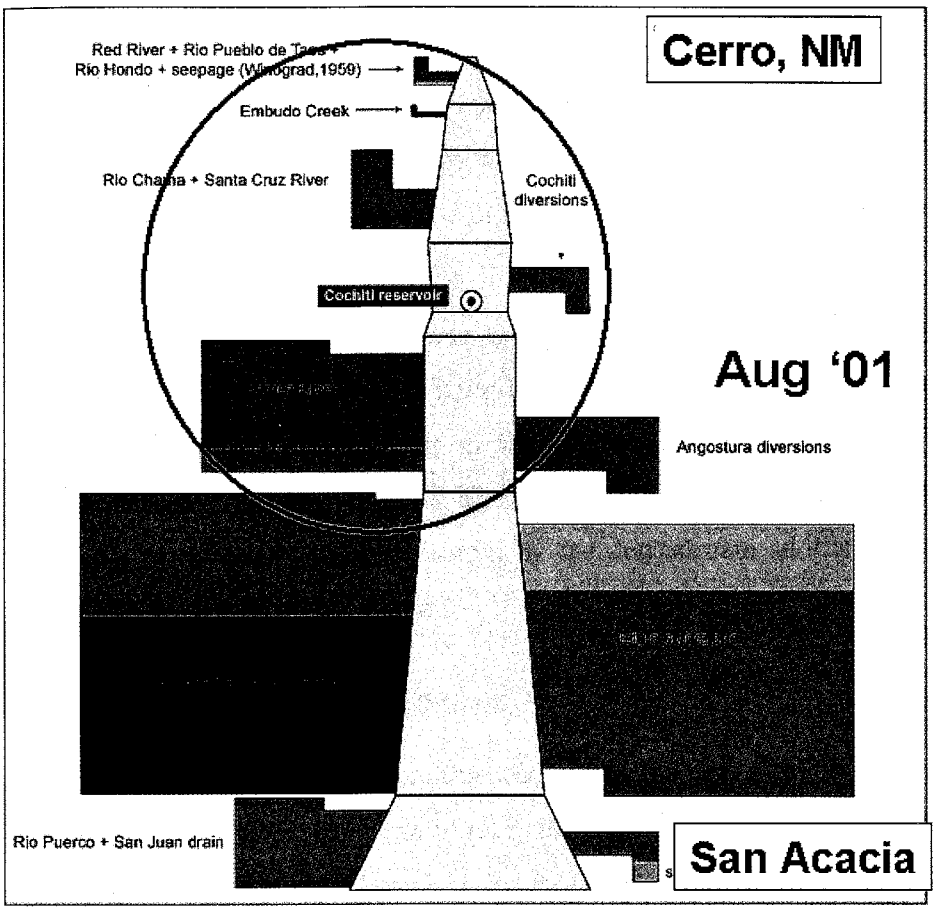

Figure 10.2: Chloride burden inputs to and outputs from the Rio Grande in August 2001, Cerro - San Acacia. Natural tributaries are important chloride contributors north of Albuquerque (inside black circle), but their influence is dwarfed by other inputs downstream such as wastewater effluent (noted in pink). January 2002 pipe diagrams show a similar pattern. See Appendix F for a larger version of this diagram and a pipe diagram explanation.

Grande, Goose Creek, and Pinos Creek are the main natural chloride inputs. However, they are relatively small in comparison with the input of chloride from the Closed Basin Canal, which is the most important gaged chloride contributor in the reach. Seepage into the river may also add significant salt [*Winograd*, 1959], though the amount of seepage was only estimated here for the model (See Appendix F for detailed chloride burden pipe diagrams of the headwaters region including seepage estimates).

Natural tributaries continue to be important chloride contributors between Cerro and Albuquerque (Figure 10.2). The Rio Chama and the Jemez River contribute the most chloride in this segment of river, as observed in analysis of historical data (Chapter 5). However, the contribution of natural tributaries in the headwaters is dwarfed by the downstream addition of salts from other sources discussed below.

10.2 Inflow of wastewater effluent

Moving downstream from the headwaters, the next most obvious chloride contribution comes from the SWRP, the Albuquerque wastewater treatment plant (Figure 10.2). As calculated in Chapter 5, the SWRP typically adds a highly concentrated, low-volume effluent stream with a chloride burden that is about equal to the burden of the entire river in Albuquerque. The chloride burden at the next gaging station downstream, Bernardo, did not reflect this salt addition during August 2001, probably due to agricultural diversions that removed the salt from the river through this reach. Seepage of water and chloride out of the riverbed between Albuquerque and Bernardo may explain the lack of expected chloride burden increase in January 2002.

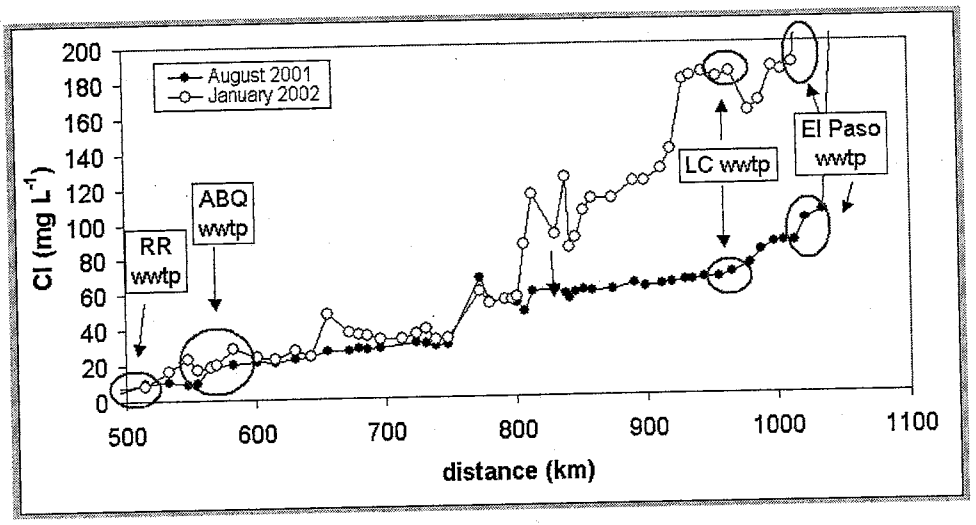

Figure 10.3: Rio Grande chloride concentration with distance downstream, August 2001 and January 2002. Inputs of wastewater effluent at Rio Rancho (RR), Albuquerque (ABQ), Las Cruces (LC) and El Paso are marked along with the corresponding increases in chloride concentration they effect. The Albuquerque wastewater treatment plant (SWRP) causes the largest increase in river chloride concentration. The increase in chloride concentration from the SWRP is not noted until several tens of kilometers downstream of the actual effluent input point due to lack of mixing in the river.

The Rio Rancho, Las Cruces and El Paso (Northwest) wastewater treatment plants also release high chloride concentration water to the river. However, the discharges of these effluent streams are only a fraction of the SWRP effluent, and their effects on river salinization are minor (Figure 10.3).

10.3 Chloride contribution by drains intercepting deep basin salts

It has already been observed (see Chapter 7) that agricultural drains in general do not contribute to salinization of the Rio Grande. One notable

exception is the Socorro Drain, which had higher chloride concentration and Cl/Br ratio than other local drains and river water in August 2001 and January 2002. The source of salinity in the Socorro Drain was determined by three events of field sampling that confirmed that the source of the saline Socorro Drain waters is the Luis Lopez Drain A (Table 10.1). The Luis Lopez Drain A, a 9-km long drain which passes exclusively through agricultural fields, has a TDS that is about 1200 mg L^{-1} along its entire length during both the irrigation and non-irrigation season. This is 4 times as high as the river in the same area. In November 2003, the chloride concentration of the Luis Lopez Drain A was 232 mg L^{-1} and its Cl/Br ratio was 839, clearly indicating that its salinity is due to processes other than evapotranspiration. The Luis Lopez Drain A has a history of being saline as well. As mentioned in Chapter 4 of this thesis, the *NRC* [1938] noted that in the 1930's, the Luis Lopez Drain A had the second-highest EC of any drain between Otowi and San Marcial. With no salt source evident at the surface, high Cl/Br-ratio water, and a historically consistent high salinity, it is probable that the Luis Lopez Drain A intercepts locally upwelling deep brines.

Table 10.1: Chemistry of the Luis Lopez Drain A (LLDA) and the Socorro Drain for three sampling events in March 2002, July 2002, and November 2003. The March 2002 and November 2003 sampling events determined that the LLDA is the source of salt to the Socorro Drain; the July 2002 sampling event determined that the LLDA is saline along its entire length between its outflow to the Socorro Drain and its origin in the town of Luis Lopez. March 2002 and July 2002 TDS measurements were taken in the field; the November 2003 TDS value was obtained in the laboratory because the field instrument malfunctioned. The anomalously low TDS value at the mouth of the LLDA in July 2002 may be due to the accidental sampling of the adjacent San Antonio ditch. The Socorro Drain sampling location corresponds with the synoptic sampling location. The LLDA mouth is located at latitude N 33° 55.5' and longitude W 106° 51.5'.

location	TDS (mg L^{-1})	Cl (mg L^{-1})	Br (mg L^{-1})	Cl/Br (wt/wt)
March 18 2002				
mouth of LLDA	1510			
Socorro Drain 40 m above LLDA	638			
Socorro Drain below LLDA (696.4 km)	769			
July 2 2002				
mouth of LLDA	565			
Socorro Drain below LLDA (696.4 km)	675			
LLDA 15 m upstream of siphon under Mosely Lateral	1210			
LLDA at Windys Farm Road	1330			
LLDA at railroad crossing in town of Luis Lopez	1040			
November 12 2003				
mouth of LLDA	1260	232	0.27	859
Socorro Drain 40 m above LLDA	710	62	0.16	388
Socorro Drain below LLDA (696.4 km)	610	77	0.16	481

Furthermore, in both August 2001 and January 2002, jumps in the chloride concentrations and the Cl/Br ratios of the Conveyance Channel and of the river correspond closely to the probable pathway of water originating from the Luis Lopez Drain A (Figure 10.4). Data from both seasons indicate that between San Acacia (655.3 km) and San Antonio (696.4 km), the chloride concentration of the Conveyance Channel was fairly constant and was similar to that of the river. However, in both August 2001 and January 2002 the chloride concentration of the Conveyance Channel doubled and the Cl/Br ratio increased by 30% between the towns of Luis Lopez (686.3 km) and San Marcial (731.1 km). This fits well with the known pathway of water through the local irrigation system: the Luis Lopez Drain A empties into the Socorro Drain from just upstream of Route 380 as mentioned in the previous paragraph. The Socorro Drain is routed into the Elmendorff Drain, which empties into the Conveyance Channel at Tiffany (723.6 km), just upstream of San Marcial. The Conveyance Channel delivers its water to the river at the Elephant Butte narrows, which doubled the river chloride concentration and increased the river Cl/Br ratio by 30% in both August 2001 and January 2002. Despite their progressive dilution with movement through the surface water system, the salts contributed by the Luis Lopez Drain A apparently cause significant salinization of the river. As the regional low point in the southern Socorro basin, the Conveyance Channel appears to pick up these high chloride, high Cl/Br waters. These saline waters may enter the channel from other local drains as well. In August 2001, the chloride concentration and Cl/Br ratio of the Conveyance Channel increased about 30% above the input of the Elmendorff Drain as well as increasing below its input. This suggests that saline waters may also seep

into the Conveyance Channel directly. The existence and location of such saline waters is consistent with the mixing of geothermal or other deep waters with La Jencia basin ground waters that upwell in the southern Socorro basin [*Anderholm*, 1987].

As noted in Chapter 7, Palomas and Mesilla basin drains also had much higher chloride concentrations and slightly higher Cl/Br ratios than the river in August 2001 and January 2002 (Figure 10.5). Historically, both the *NRC* [1938] and *Trock et al.* [1978] observed that Rio Grande Project drains were more saline than the river. Though these two sources attributed high drain salinity to flushing of shallow ground water, *Hendrickx* [1998] noted that stored salts and shallow saline ground waters in the Mesilla valley have long since been flushed by the drainage system. Instead, the high chloride concentrations of these drains can probably be attributed to concentration through transpiration, since stable isotope data indicate that drains and the river were equally evaporated in August 2001 and January 2002 (see Chapter 7, Figure 7.7). The slightly higher Cl/Br ratios of these drains suggest that they pick up brine in these two basins just as the Socorro Drain picks up brines in the Socorro basin. In particular, the East Drain and the Montoya Drain had elevated chloride concentrations and Cl/Br ratios relative to the river in both August 2001 and January 2002. Downstream of the return points of both drains, river chloride concentration and Cl/Br ratio increased in both seasons, confirming their small salinizing effect on the river (Figure 10.5). Like the Luis Lopez Drain A, the East Drain in particular has a longstanding record of poor water quality [*NRC*, 1938; *Hendrickx*, 1998]. The water quality of both of these drains is most likely controlled by faults or other geologic features that serve as brine conduits near

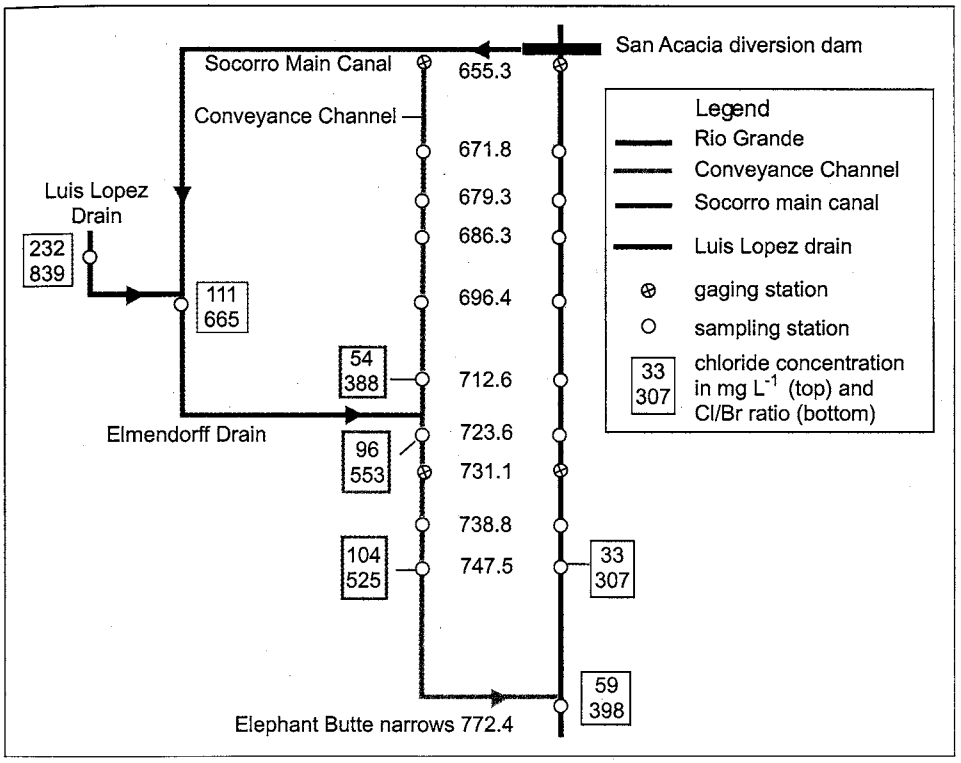

Figure 10.4: Simple schematic of the Socorro basin surface water system showing salinization of the river due to saline water originating from the Luis Lopez Drain A moving through the irrigation system and Conveyance Channel to the river. Boxed sets of numbers indicate chloride concentration (top) and Cl/Br ratio (bottom) at various locations. Data for the Luis Lopez Drain A is from November 2003; all other data is from January 2002. Data from August 2001 show similar trends. Unboxed numbers indicate river distances in kilometers. Diagram to scale north-south but not to scale east-west.

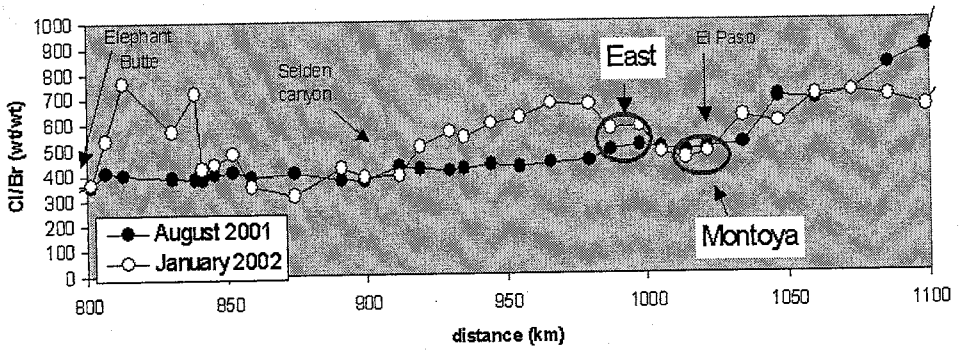

Figure 10.5: Chloride-bromide ratio of the river during August 2001 and January 2002. Locations of inputs of East and Montoya Drains and the increases in river Cl/Br downstream of their inflows are shown. The relatively high Cl/Br ratios of these drains indicates they may intercept deep ground water.

these drains.

10.4 Effects of Elephant Butte Reservoir

Based on two decades of monthly chloride burden data from 1934 - 1955, the effect of transient salt storage in Elephant Butte Reservoir has already been discussed in detail in Chapter 5. This analysis determined that in general, chloride is stored in the reservoir during times of reservoir water storage increase and is released from the reservoir during periods of water storage decline. Though no long-term consecutive overlapping water quality records exist for the San Marcial and Elephant Butte gaging stations after 1950, the effect of Elephant Butte Reservoir during the August 2001 and January 2002 field seasons can be examined in terms of reservoir water storage. The storage record (Figure 10.6) indicates that the reservoir has been decreasing in volume since February 2000, suggesting that a net export of stored salts from the

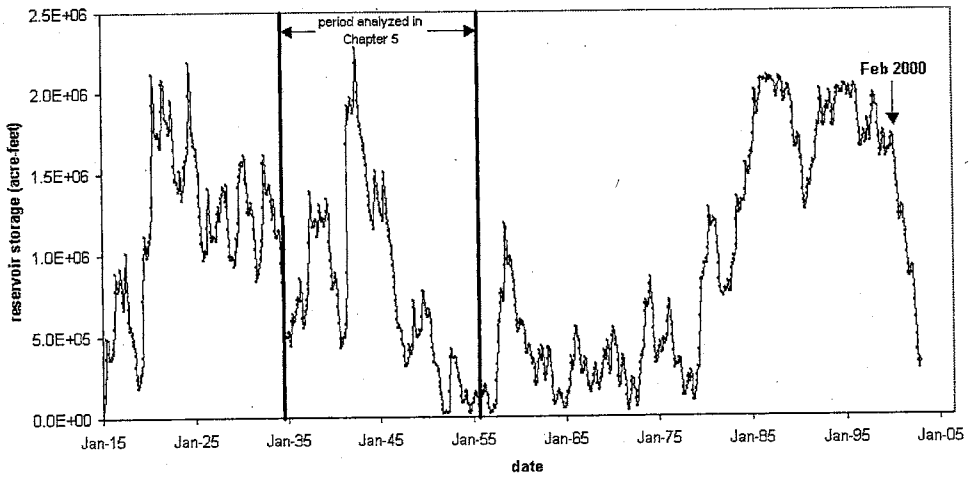

Figure 10.6: Elephant Butte average monthly reservoir storage, March 1915 - December 2002. Reservoir storage has been decreasing since February 2000, suggesting that the reservoir added salts during August 2001 and January 2002.

reservoir has occurred since then. The greater than 100% increase in chloride burden between San Marcial and the outlet of Elephant Butte Reservoir during August 2001 indicates that salts released from the reservoir had a large effect on river chloride burden during that season.

10.5 Estimation of direct addition of deep brine chloride to the river

Using the detailed water and chloride mass balance model described in Chapter 9, chloride imbalances were determined for each sampling station with distance downstream (Appendix G). Mainly due to lack of constraint on the water balance over certain gaging intervals and the corresponding poor calculations of evapotranspirative water loss from the river, high calculated chloride imbalances do not necessarily indicate an actual chloride imbalance due

to deep ground water input as hypothesized. In order to determine probable locations of ground water discharge, it was necessary 1) to closely examine changes in the river chloride concentration and Cl/Br ratio for August 2001 and January 2002; 2) to look closely at the simple mass balance model (Chapter 8); and 3) to refer to the hydrogeologic literature (Chapter 2). Pulling all of this information together, four major locations of probable deep ground water discharge directly to the river were identified as San Acacia, Truth or Consequences (T or C)/Williamsburg, Selden Canyon/Leasburg, and El Paso. Significant chloride concentration and Cl/Br ratio increases were observed at these locations during August 2001 and/or January 2002; these locations also correspond to the distal ends of sedimentary basins or to known locations of geothermal springs (T or C). Ground water end member chemistries were estimated from the literature (Figure 10.7), and ground water chloride burdens and fluxes were calculated (Figure 10.8). The methodology for such calculations is described in Appendix H, which also describes the chloride imbalances of the mass balance models in detail. The estimated ground water chloride burden contributions range from a fairly insignificant 2% of river chloride burden at Selden Canyon/Leasburg, to half of the river chloride burden at San Acacia in January 2002. In all cases, the estimated discharge of deep ground water was less than 5% of local river flow.

10.6 Cumulative effect of important salinization processes on river chloride burden, August 2001

It has been demonstrated in this thesis that the major sources of salt to the Rio Grande within the study area include natural tributaries, wastewater

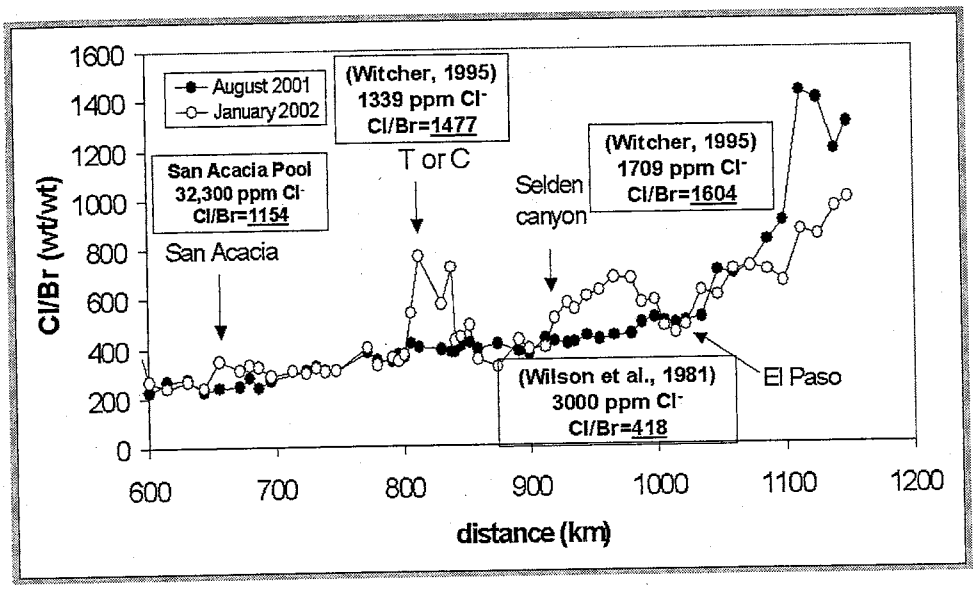

Figure 10.7: End member chemistries used to calculate deep ground water input to the river at San Acacia, Truth or Consequences, Selden Canyon, and El Paso.

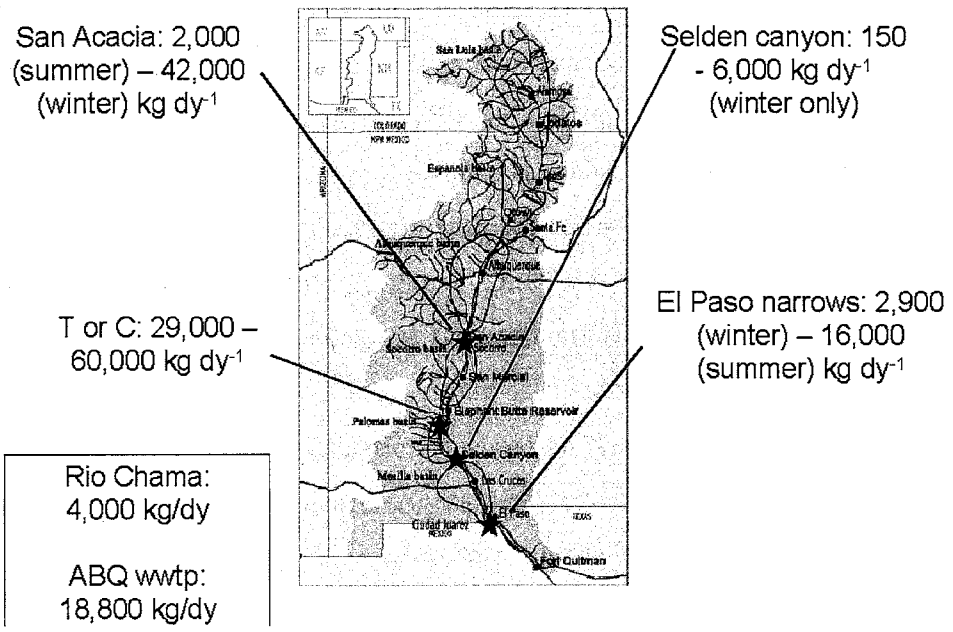

Figure 10.8: Estimated ranges of chloride burden contributed by deep ground water input directly to the river at San Acacia, Truth or Consequences, Selden Canyon, and El Paso for August 2001 and January 2002. The Rio Chama and the Albuquerque wastewater effluent chloride burdens are included for comparison. Estimates were performed using the detailed water, chloride, and bromide mass balance model (see Appendix H for methodology).

effluent, salts released from Elephant Butte Reservoir due to transient reservoir dynamics, and deep ground water (Tables 10.3 - 10.4). In order to determine their relative effects, increases in chloride burden during August 2001 were attributed to one of these four processes and accumulated by category at each gaging station with distance downstream. The El Paso - Ft. Quitman reach was not included because so little is known about the large chloride burden increases in that region. Though all river and most tributary chloride burdens were calculated from data from a single sampling week, the increases in river burden do not correspond exactly with the measured tributary burden inputs because the sampling was not actually instantaneous. This is also true for the detailed mass balance model, but the assumption of instantaneity can be particularly misleading in the generalizing calculations described in this section. For this reason, these calculations focused on the river chloride burdens. Attempting to use the measured tributary chloride burdens would result in more complex seepage calculations, which was not the focus of this study. Measured tributary chloride burdens were attributed to the three salt source categories where appropriate. At other locations, the chloride burdens attributed to these categories were estimated based on changes in river burden and the known local relative importance of each of the salt sources.

Table 10.2: River and diversion chloride concentrations, discharges, and total chloride burdens use for cumulative chloride burden calculations, headwaters - El Paso, August 2001.

distance (km)	Cl (mg L^{-1})	discharge (m^3 s^{-1})	diversions (m^3 s^{-1})	total flow (m3 s^{-1})	Cl burden (kg dy^{-1})
3.2	0.28	5.8		5.8	142
61.7	0.37	21.1		21.1	667
104.1	0.68	25.5	0.9	26.4	1538
141.2	0.65	5.1	18.3	23.4	1323
192.8	3.44	2.7	2.7	5.4	1605
203.1	6.98	2.7	1.2	3.9	2350
256.9	8.97	1.8		1.8	1382
306.7	4.22	4.0		4.0	1474
359.3	7.11	8.4		8.4	5165
384.5	6.37	10.4		10.4	5745
430.9	6.53	16.6		16.6	9384
471.0	4.87	19.2	5.9	25.1	10557
496.4	5.34	21.8		21.8	10038
547.5	9.07	12.4	10.9	23.3	18257
630.7	22.6	8.2	15.7	23.9	46610
655.3	27.1	11.2	0.6	11.8	27579
731.1	48.0	7.2	8.1	15.3	63403
801.3	52.3	45.3		45.3	2.05E+05
841.0	54.3	50.7		50.7	2.37E+05
899.4	60.6	43.5	7.1	50.6	2.65E+05
919.5	62.7	35.6	8.7	44.3	2.40E+05
955.1	65.2	16.8	19.2	36.0	2.03E+05
987.6	80.4	18.8		18.8	1.30E+05
1013.8	85.3	27.7		27.7	2.04E+05
1021.6	98.7	0.3	24.0	24.3	2.07E+05

Table 10.3: Cummulative effects of natural tributaries (nat), deep ground water (gw), wastewater effluent (wwtp), transient reservoir dynamics of Elephant Butte Reservoir (res), and riverbed seepage loss on chloride burden of the Rio Grande in August 2001, headwaters - San Marcial. Chloride burdens of major tributaries used in accumulation calculations are on the left side of the table. The river chloride burden is that calculated from the sum of the cumulative chloride burdens of the five sources/processes. Italicized values in the chloride burden column represent values that could not be properly estimated. Italicized values in the "gw" column indicate estimates.

distance	major tributaries Cl burden (kg dy^{-1})			river Cl burden	major salinization sources/processes cummulative Cl burdens (kg dy^{-1})				
(km)	gw	wwtp	seep	(kg dy-1)	nat	gw	wwtp	res	seep
3.2				142	142				
61.7				667	667				
104.1				1538	1538				
141.2				1323	1538				216
192.8				1605	1820				216
203.1	683			2350	1883	683			216
256.9				1382	1883	683			1184
306.7				1474	1975	683			1184
359.3				5165	5666	683			1184
384.5				5745	6246	683			1184
430.9				9384	9885	683			1184
471.0				10557	11058	683			1184
496.4				10038	11058	683			1703
547.5		1434		18257	17842	683	1434		1703
630.7		18801		46610	27394	683	20235		1703
655.3	3600		22631	27579	27394	4283	20235		24333
731.1	23511		10317	*36490*	27394	23511	20235		34651

Table 10.4: Cummulative effects of natural tributaries (nat), deep ground water (gw), wastewater effluent (wwtp), transient reservoir dynamics of Elephant Butte Reservoir (res), and riverbed seepage loss on chloride burden of the Rio Grande in August 2001, Elephant Butte Reservoir - El Paso. Chloride burdens of major tributaries used in accumulation calculations are on the left side of the table. The river chloride burden is that calculated from the sum of the cumulative chloride burdens of the five sources/processes. Italicized values in the chloride burden column represent values that could not be properly estimated. Italicized values in the "gw" column indicate estimates.

distance	major tributaries Cl burden (kg dy^{-1})			river Cl burden	major salinization sources/processes cummulative Cl burdens (kg dy^{-1})				
(km)	gw	wwtp	seep	(kg dy^{-1})	nat	gw	wwtp	res	seep
801.3				2.05E+05	82183	70532	60705	25996	34651
841.0	*32732*			2.37E+05	82183	1.03E+05	60705	25996	34651
899.4				*2.65E+05*					
919.5	*2365*			2.40E+05	82183	1.06E+05	60705	25996	34651
955.1		6585	43491	2.03E+05	82183	1.06E+05	67290	25996	78142
987.6				*1.30E+05*					
1013.8	*1224*			2.04E+05	82183	1.07E+05	67290	25996	78142
1021.6		8773	5799	2.07E+05	82183	1.07E+05	76063	25996	83941
				% TOTALS:	28	37	26	9	

Though the basin-scale trend with distance downstream obviously follows a pattern of increasing chloride burden, the river chloride burden does decrease locally. These chloride burden decreases were attributed to loss by riverbed seepage. Though this term helped explain river chloride burden decreases at most relevant locations, calculations at San Marcial (731.1 km), Haynor Ranch (899.4 km), and Anthony (987.6) were problematic. The seepage and the chloride input terms could not be adequately determined independently at San Marcial, resulting in an underestimated total chloride burden value. Attributing the chloride burden decreases to riverbed seepage below Haynor Ranch and at Anthony resulted in calculations of unrealistic chloride input values for the four salt source categories, so these two gaging stations were removed from the calculations entirely.

At each gaging station, the total chloride burden was assumed to be equal to the river chloride burden derived from measured August 2001 concentration and gaging data (Table 10.2). At gaging stations immediately below diversion dams, the total chloride burden was assumed to be equal to the river chloride burden plus the chloride burdens of the diversions. Total chloride burden at San Marcial was assumed to be equal to the sum of the burdens of the river and the Conveyance Channel.

Between the headwaters and San Acacia, natural tributaries were assumed to play the largest role in chloride burden increase. Therefore, the chloride contribution by natural tributaries was calculated as the difference between the measured river chloride burden and the sum of estimated wastewater and deep ground water contributions. Tributary chloride burdens calculated

for the detailed mass balance model generally corresponded to the river burden increases, but they were not used in these generalizing calculations because they did not exactly match river increases. Between San Marcial and El Paso, deep ground water was assumed to have the major role in chloride addition. At the outlet of Caballo Reservoir (841.0 km), Leasburg (919.5 km), and Sunland Park (1013.8 km), deep ground water additions were calculated as the difference between the measured river chloride burden and the sum of the chloride burdens of the other three salt source categories, minus the chloride burden lost to seepage. All of these values correspond well with the ground water chloride fluxes calculated using the detailed mass balance model (Figure 10.8). Estimated deep ground water chloride additions included half of the chloride burden of the Conveyance Channel. Because half of the chloride concentration increase in the Conveyance Channel at San Marcial was due to input from the Luis Lopez Drain A salts via the Socorro Drain in August 2001, half of the chloride burden of the Conveyance Channel at San Marcial was attributed to deep ground water input. Downstream of Elephant Butte Reservoir, deep ground water input at each gaging station was calculated as the difference between the measured river chloride burden and the sum of all other inputs at that station. The chloride burden of the Closed Basin Canal was also included in the ground water category because its waters originate from wells of much higher TDS, chloride concentration, and Cl/Br ratio than the river. The large chloride burden decrease at San Acacia due to riverbed seepage prevented direct calculation of deep ground water input at that location, so the deep ground water chloride burden at San Acacia was estimated from the deep ground water fluxes calculated using the mass balance model (Table H.1). Throughout these

chloride burden calculations, the chloride burdens of wastewater effluent were derived from data used for the August 2001 detailed mass balance model.

Chloride contributed by Elephant Butte Reservoir dynamics was calculated as the chloride burden unaccounted for by the increase in discharge between San Marcial (731.1 km) and the reservoir outlet (801.3 km). Because the discharge below the reservoir was three times that of the total discharge at San Marcial (river + Conveyance Channel), each of the chloride burdens attributed to the other three salt contribution categories at San Marcial was multiplied by three in order to obtain the salt contribution values at the outlet of Elephant Butte Reservoir. (Water leaving the reservoir was assumed to have the same fractions of salts derived from the three categories as the water entering the reservoir.) The difference between the measured river chloride burden at the reservoir outlet and the burden calculated as just described was attributed to reservoir dynamics. Admittedly, this calculation greatly simplifies the movement of water and salts within the reservoir.

After performing these calculations, the percentages of chloride burden added by each source with distance downstream were calculated relative to sum of the cumulative chloride burden and the seepage at El Paso (1021.6 km). These calculations indicate that 25% of chloride addition between the headwaters and El Paso was due to natural tributary input in August 2001 (Tables 10.3 - 10.4, Figure 10.9). Wastewater effluent accounted for 26% of chloride addition. Reservoir dynamics (transient salt release effects) added 9% of river chloride burden, and deep ground water added 37%. Of this 37%, salts from the Conveyance Channel/Luis Lopez Drain A accounted for 22%. Therefore,

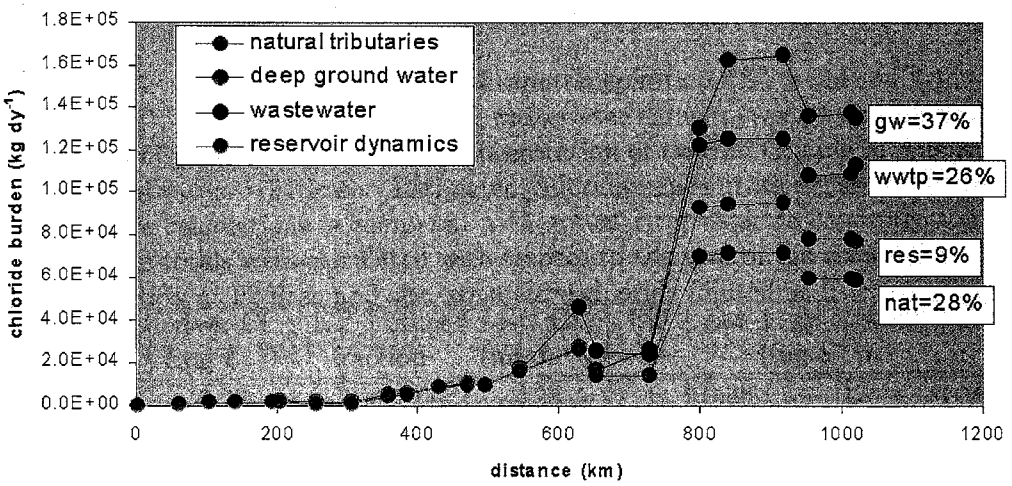

Figure 10.9: Stacked graph of cumulative chloride addition by natural tributaries, wastewater effluent, deep ground water, and Elephant Butte Reservoir dynamics, August 2001.

the Luis Lopez Drain A contributed 8% (37% * 22%) of the total salt burden between the headwaters and El Paso in August 2001.

10.7 Cumulative effect of important salinization processes on river chloride concentration, August 2001

Calculations similar to those implemented in the previous section were performed for chloride concentration. Using August 2001 data, concentration increases were accumulated by gaging interval into four categories including evapotranspiration (ET), natural tributaries, deep ground water, and wastewater effluent (Table 10.5). The major influence of Elephant Butte Reservoir on chloride concentration was assumed to be due to evaporation, and "reservoir dynamics" in this sense are included in the ET category. Concentration

Table 10.5: Cummulative effects of evapotranspiration (ET), natural tributaries (nat), deep ground water (gw), wastewater effluent (wwtp) and natural tributary dilution (dil) on chloride concentration of the Rio Grande in August 2001, headwaters - El Paso. Estimated chloride concentration based on the cumulative calculations is compared with actual river chloride concentration. Percentage totals were calculated with respect to the sum of the river chloride concentration at El Paso and the cumulative chloride diluted at El Paso.

distance (km)	river Cl (mg L^{-1})	ET fraction	other fraction	est. Cl (mg L^{-1})	ET (mg L^{-1})	nat (mg L^{-1})	gw (mg L^{-1})	wwtp (mg L^{-1})	dil (mg L^{-1})
3.2	0.28	0.00	1.00	0.28		0.28			
61.7	0.37	0.00	1.00	0.37		0.37			
104.1	0.68	0.56	0.44	0.68	0.17	0.50			
141.2	0.65	0.00	1.00	0.65	0.17	0.50			0.02
192.8	3.44	1.00	0.00	3.44	2.96	0.50			0.02
203.1	6.98	0.50	0.50	6.98	4.73	0.50	1.77		0.02
256.9	8.97	1.00	0.00	8.97	6.72	0.50	1.77		0.02
306.7	4.22	0.00	1.00	4.22	6.72	0.50	1.77		4.78
359.3	7.11	0.77	0.23	7.11	8.95	1.17	1.77		4.78
384.5	6.37	0.00	1.00	6.37	8.95	1.17	1.77		5.52
430.9	6.53	0.00	1.00	6.53	9.48	1.17	1.77		5.89
471.0	4.87	1.00	0.00	4.87	9.48	1.17	1.77		7.54
496.4	5.34	0.00	1.00	5.34	9.95	1.17	1.77		7.54
547.5	9.07	0.00	1.00	9.07	9.95	3.03	1.77	1.87	7.54
630.7	22.6	0.44	0.56	22.6	15.9	3.03	1.77	9.45	7.54
655.3	27.1	0.03	0.97	27.1	16.0	3.03	6.08	9.45	7.54
731.1	49.8	0.13	0.87	49.8	19.0	3.03	25.9	9.45	7.54
801.3	52.3	1.00	0.00	52.3	21.5	3.03	25.9	9.45	7.54
841.0	54.3	0.50	0.50	54.3	22.5	3.03	26.8	9.45	7.54
899.4	60.6	1.00	0.00	60.6	28.8	3.03	26.8	9.45	7.54
919.5	62.7	0.35	0.65	62.7	29.5	3.03	28.2	9.5	7.54
955.1	65.2	0.54	0.46	65.2	30.9	3.03	28.2	10.6	7.54
987.6	80.4	0.94	0.06	80.4	45.2	3.03	29.1	10.6	7.54
1013.8	85.3	0.94	0.06	85.3	49.8	3.03	29.4	10.6	7.54
1021.6	98.7	0.63	0.37	98.7	58.2	3.03	31.5	13.4	7.54
			TOTALS (%):		55	3	30	13	100

decreases also occurred with distance downstream, generally due to inflow of dilute tributaries in the headwaters region. These decreases were accumulated in a dilution category. Simple linear mixing calculations were performed at locations of chloride concentration increase in order to determine how much of the increase was due to due to known inputs (Tables 10.6 - 10.7):

$$C_{RG}V_{RG} + C_I V_I = C_{RG,d}V_{RG,d} \tag{10.1}$$

where C_{RG} is the river chloride concentration at the gaging station closest to the input in mg L^{-1}, V_{RG} is the discharge of the river at the gaging station closest to the input in m^3 s^{-1}, C_I is the chloride concentration of the input in mg L^{-1}, V_I is the discharge of the input in m^3 s^{-1}, $C_{RG,d}$ is the estimated chloride concentration of the river downstream of the input, and $V_{RG,d}$ is the estimated discharge of the river downstream of the input (for simplicity, this value was assumed to be equal to $V_{RG,u} + V_I$). This equation was rearranged and solved for $C_{RG,d}$, using data for all other values.

Table 10.6: Data for simple mixing calculations used to determine the effects evapotranspiration, natural tributaries, deep ground water, wastewater effluent and dilution of natural tributaries on river chloride concentration, August 2001. See text for variable descriptions and details. Concentration averages for multiple inputs considered as one are flow-weighted. See Table 10.7 for results of calculations.

distance (km)	input	C_{RG} (mg L^{-1})	V_{RG} (m^3 s^{-1})	C_I (mg L^{-1})	V_I (m^3 s^{-1})	$V_{RG,d}$ (m^3 s^{-1})
104.1	headwaters streams	0.37	21.1	1	5.3	26.4
203.1	Closed Basin Canal	3.44	2.7	13	0.6	3.3
306.7	dilute recharge	8.97	1.8	0.50	2.2	4
359.3	headwaters tribs	4.22	4	5.78	3	7
430.9	Chama+S.Cruz	6.37	10	5.59	9.06	19.1
547.5	RRWWTP 2	5.34	21.8	57	0.4	22.2
547.5	RRWWTP 3	5.34	21.8	380	0.13	21.9
547.5	Jemez	5.34	21.8	166	0.65	22.5
630.7	SWRP	9.07	23.3	90	2.42	25.7
655.3	brine	22.6	11.2	32300	0.0015	11.2
841.0	brine	52.3	45.3	2000	0.4	45.7
919.5	brine	60.6	35.6	1707	0.030	35.6
955.1	LCWWTP	62.7	44.3	200	0.38	44.7
987.6	Del Rio+La Mesa D	65.2	16.8	127	3.17	20.0
1013.8	East D	80.4	18.8	130	1.13	19.9
1021.6	NWWWTP	85.3	24.3	275	0.37	24.7
1021.6	Montoya D	85.3	24.3	208	3.20	27.5

Table 10.7: Results of simple mixing calculations used to determine the effects evapotranspiration, natural tributaries, deep ground water, wastewater effluent and dilution of natural tributaries on river chloride concentration, August 2001. See text for variable descriptions and details. See Table 10.6 for data used for calculations. "d" indicates a diluting input that caused the river chloride concentration to decrease.

distance (km)	input	$C_{RG,d}$ (mg L^{-1})	C actual (mg L^{-1})	Cl input (fraction)	gw contribution (fraction)
104.1	headwaters streams	0.52	0.70	0.44	
203.1	Closed Basin Canal	5.23	6.98	0.51	0.51
306.7	dilute recharge	4.31	4.22	1.00	
359.3	headwaters tribs	4.89	7.11	0.23	
430.9	Chama+S.Cruz	6.00	6.53	d	
547.5	RRWWTP 2	6.27	9.04	0.25	
547.5	RRWWTP 3	7.56	9.04	0.60	
547.5	Jemez	9.99	9.04	1.00	
630.7	SWRP	16.68	22.60	0.56	
655.3	brine	26.94	27.06	0.97	
841.0	brine	69.40	54.26	1.00	
919.5	brine	61.95	62.68	0.65	
955.1	LCWWTP	63.87	65.23	0.46	
987.6	Del Rio+La Mesa D	74.94	80.40	0.64	0.06
1013.8	East D	83.21	85.30	0.57	0.06
1021.6	NWWWTP	88.15	98.70	0.21	
1021.6	Montoya D	99.58	98.70	1.00	0.16

Based on this simple mixing calculation, river chloride concentration increases immediately downstream of wastewater treatment plants were assumed to be partially due to effluent input (Tables 10.6 - 10.7). The chloride concentration increase that could not be accounted for with mixing calculations was assumed to be evapotranspirative increase. Chloride concentration changes due to natural tributaries were calculated in the same way, including calculations of the diluting effects of ground water recharge from the headwaters mountains near Cerro (306.7 km) and dilutions due to other headwaters rivers at Taos Junction bridge (359.3 km) and Otowi (430.9 km).

Chloride concentration increases due to deep ground water input directly to the river was estimated using the mixing equation along with the assumed deep ground water end member concentrations and estimated deep ground water discharges calculated using the detailed mass balance model (Table H.1). In this way (Tables 10.6 - 10.7), most of the chloride concentration increase at San Acacia (655.3 km) was attributed to deep ground water input. The chloride concentration increase between the outlets of Elephant Butte (801.3 km) and Caballo (841.0 km) Reservoirs was calculated to be 100% due to deep ground water input directly to the river at T or C/Williamsburg (806.6 km). However, ET could also account for all of the chloride concentration increase in this interval, as calculated by dividing the pan evaporation value at Caballo Reservoir (6.91 $m^3 s^{-1}$) by the river discharge at the same location to obtain the percentage of evapotranspirative concentration (13%). Because it was not otherwise possible to reconcile these overlapping calculations, half of the chloride concentration increase at the outlet of Caballo Reservoir was attributed to ET, and half was attributed to deep groundwater. Deep ground

water input at Selden canyon/Leasburg (919.5 km) was calculated to account for 65% of chloride concentration increase. Ground water input directly to the river at Sunland Park (1013.8 km) was not considered due to the fact that calculations of wastewater effluent and drain input at this location were thought to be more important, and the estimated sum of these two inputs (see below) fully accounted for the total river chloride concentration increase.

Several agricultural drains were assumed to have a deep ground water component. The Closed Basin Canal was treated as a deep ground water input, for reasons described in the previous section. At San Marcial (731.1 km), the total chloride concentration was assumed to be a flow-weighted average of the river and the Conveyance Channel. The 3 mg L^{-1} increase between San Acacia and the input of the Conveyance Channel (772.4 km) was assumed to be due to ET, and the remaining concentration increase was attributed to deep ground water input from the Conveyance Channel (Tables 10.6 - 10.7). The Garfield and Hatch Drains were not considered to be significant in salinization because neither the river chloride concentration nor the Cl/Br ratio increased downstream of their input from the in August 2001, and no ground water component was calculated.

To estimate the amount of deep ground water contributed by Mesilla valley drains, the chloride concentration in the drains due to consumptive use of water was estimated using the following equation:

$$C_e = \frac{C_o}{\left(1 - \left(\frac{V_o - V_e}{V_o}\right)\right)} \tag{10.2}$$

where C_e is the drain chloride concentration after evapotranspiration in mg L^{-1}, C_o is the original concentration of diversions in mg L^{-1}, V_o is the original

drain flow before evapotranspiration in m ^{3} s^{-1}, and V_e is the drain flow after ET. Using this equation, the evaporated chloride concentration in Mesilla valley drains was estimated to be 166 mg L^{-1}, based on the loss of flow of diversions at the Mesilla diversion dam (V_o= 19.2 m^3 s^{-1}) and the return flows of the corresponding Del Rio, La Mesa, East, and Montoya Drains (V_e= 7.5 m^3 s^{-1}), and considering the original chloride concentration of the diversions (C_o= 65.2 mg L^{-1}, identical to that of the river at Mesilla). The chloride concentrations of the Del Rio, La Mesa, and East Drains were less than 166 mg L^{-1}, implying that all of their chloride concentration increases could be attributed to evapotranspirative concentration. However, their Cl/Br ratios were over 30% higher than the diversions at the Mesilla diversion dam. Based on these elevated Cl/Br ratios, a minimum of 10% of the chloride concentration increases in these drains was assumed to be due to interception of deep brines. This estimation was not meant to reflect accurate chloride and bromide mixing calculations, which would not be particularly meaningful in this case since the deep brine end member chemistry is not well-constrained. Furthermore, although the river seems to receive input from low Cl/Br-ratio brine at the distal end of the Mesilla basin, it is possible that the drains intercept brines of slightly different sources that have higher Cl/Br ratios.

On the other hand, the chloride concentration of the Montoya Drain was 207 mg L^{-1}, 25% higher than the estimated concentration of evaporated Mesilla valley diversions; its Cl/Br ratio was 60% higher than that of the Mesilla diversions. Using the simple mixing equation, it was determined that a 20% contribution of a brine with a chloride concentration of 3000 mg L^{-1} to an evaporated drain with a concentration of 166 mg L^{-1} could explain the

elevated Montoya Drain chloride concentration. Therefore, 20% of the chloride concentration of the Montoya Drain was attributed to deep ground water. The simple mixing calculations were used to determine the fraction of river chloride concentration increases that were due to input of each of these drains. These fractions were multiplied by the ground water fraction assumed for each drain in order to estimate the amount of chloride concentration increase that was due to deep brines intercepted by drains. Though the Montoya Drain input was calculated to account for the total river chloride increase between Sunland Park (1013.8 km) and El Paso (1021.6 km) (Tables 10.6 - 10.7), it was also calculated that wastewater effluent from the Northwest wastewater treatment plant increased the chloride concentration 21% in this reach. For this reason, the Montoya Drain was assumed to have caused 80% of the total concentration increase, and the resulting deep ground water contribution from this drain was calculated to be 16% (80% * 20%).

To verify the chloride chloride concentration increases that were attributed to ET, evapotranspirative concentration of chloride was calculated where possible using an equation similar to Equation 10.2:

$$C_{added} = \frac{C_o}{\left(1 - \left(\frac{V_o - V_e}{V_o}\right)\right) - C_o} \tag{10.3}$$

where are variables are defined as in Equation 10.2 and C_{added} is the increase in chloride concentration due to ET, in mg L^{-1}. (Note that C_{added} is not the final chloride concentration after ET.) Locations of ET calculation did not include gaining reaches of the river or losing reaches where riverbed seepage was thought to be the main reason for flow loss. These calculations assumed that the total flow at gaging stations immediately below diversion dams was equal

Table 10.8: Calculated increases in chloride concentration at selected gaging stations based on flow loss. Flow loss was calculated as the difference between the total gaged flow at the station of interest and the total gaged flow at the upstream gaging station. "na" indicates that calculations were not performed at this station and the total gaged flow is only presented in the table to elucidate the calculations at the next gaging station downstream. See text for details.

distance (km)	flow ($m^3\ s^{-1}$)	evap frac.	Cl increase ($mg\ L^{-1}$)
104.1	26.4	na	na
192.8	5.4	0.80	2.6
203.1	3.9	0.28	1.3
256.9	1.8	0.54	8.3
899.4	50.6	na	na
919.5	44.3	0.12	8.6
955.1	36.0	0.19	14.4
987.6	18.8	0.48	60.0
1013.8	27.7	na	na
1021.6	24.3	0.12	11.9

to the sum of the flows of the river and the diversions. Comparing these calculated ET-driven chloride increases (Table 10.8) with the chloride increases attributed to ET using the mixing calculation (Tables 10.6 - 10.7) indicate that the mixing calculation and the independent ET calculations agree fairly well in the headwaters region and at El Paso. Between Lobatos (256.9 km) and Anthony (987.6 km), the ET calculations obviously overestimate chloride concentration increase, as the calculations result in concentration increases several times those that were observed in the river in August 2001. The overestimation is probably due to poor constraint on the water balance for these simple calculations. Overall, it was calculated that only 3% of the increase in chloride concentration with distance downstream in August 2001 was due to tributary

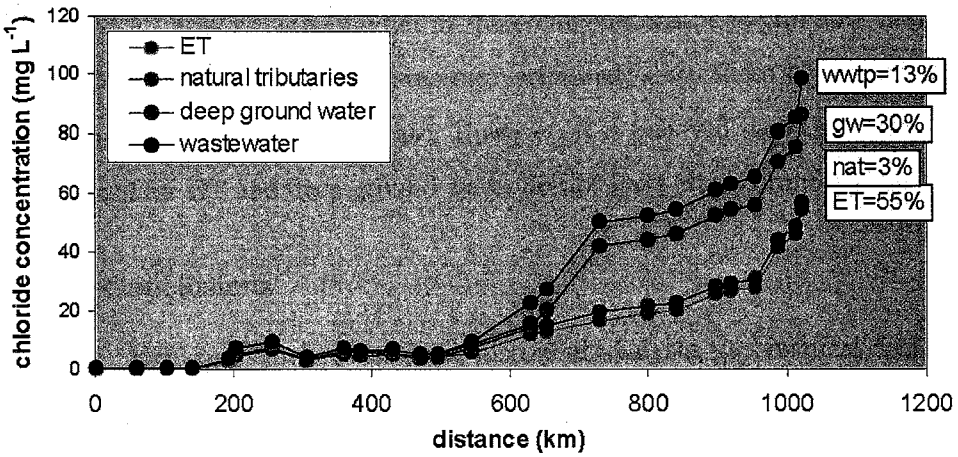

Figure 10.10: Stacked graph of cumulative salinizing effects of evapotranspiration, natural tributaries, deep ground water, and wastewater effluent on river chloride concentration, August 2001.

inflow (Table 10.5), Figure 10.10). This low value is expected because tributaries are generally dilute. Wastewater treatment plant effluent was calculated to cause 13% of the chloride concentration increase between the headwaters and El Paso, with 56% of which was due to SWRP effluent in Albuquerque. Deep ground water input was determined to cause 30% of chloride concentration increase, and sixty-three percent of that ground water input was due to increase in chloride concentration from input of high chloride concentration Conveyance Channel water originating from the Luis Lopez Drain A. This indicates that 19% of the total increase in chloride concentration between the headwaters and El Paso is due to high concentration waters from the Luis Lopez Drain A. Finally, ET was calculated to account for the majority of chloride concentration increase, or 55%. This is less than but generally consistent with the calculation of water loss of 60-75% between the headwaters and El Paso (see chapter 7).

If in fact ET was underestimated in these calculations, it is probable that the deep ground water component was overestimated, since these two parameters were the most difficult to separate. However, it is believed that the two values calculated for ET and deep ground water do not have errors of more than 10%.

10.8 Conclusions

Environmental tracer data, historical analysis, geochemical data and hydrogeologic information from the literature all suggest that deep saline ground waters surface at San Acacia, in the southern Socorro basin, at Truth or Consequences, in Selden Canyon, and at El Paso. Input from these ground waters accounts for the largest increase in chloride concentration aside from evapotranspiration and for about one-third of total salt addition between the headwaters and El Paso. In response to previous research that has attributed salinization of the Rio Grande to the effects of irrigated agriculture, in light of this study it would be possible to concede that they were correct, in both an expected and an unexpected way. As asserted by scientists throughout the previous century, this thesis confirms that evapotranspiration accounts for the greatest increase in chloride concentration with distance downstream. However, salt addition due to geologic processes bringing deep brines and geothermal waters to the surface seems to account for the most important addition of salt. In addition to direct addition of deep ground water to the river, a significant percentage of this salt enters the river by way of ground water interception by the drainage system and delivery to the river. Natural tributaries and wastewater treatment plants both have small effects in terms of increasing the river chloride concentration, though they have more significant effects in terms of salt addition to

the river. The long-term transient processes that occur within Elephant Butte Reservoir are a factor that cannot be neglected in considering the salt balance of the river at any time scale.

Bibliography

Anderholm, S. K., Hydrogeology of the Socorro and La Jencia basins, Socorro County, New Mexico, *U. S. Geological Survey Water-Resources Investigations Report 84-4342,* 62 pp. plus plates, 1987.

Barroll, M. W., and M. Reiter, Hydrogeothermal investigation of the Bosque del Apache, New Mexico, *New Mexico Geology*, *17*, 1–7, 1995.

Berner, K., and R. A. Berner, *Global Environment: Water, Air, and Geochemical Cycles*, Prentice Hall, Upper Saddle River, New Jersey, 376 pp., 1996.

Bexfield, L. M., Occurrence and sources of arsenic in ground water of the middle Rio Grande basin, central New Mexico, M. S. thesis, 143 pp., New Mexico Institute of Mining and Technology, Socorro, New Mexico, 2001.

Bullard, T. F., and S. G. Wells, Hydrology of the middle Rio Grande from Velarde to Elephant Butte reservoir, New Mexico, *United States Fish and Wildlife Service Resource Publication 179, Washington, D.C., 46 pp.*, 1992.

Campbell, A. R., and P. B. Larson, Introduction to stable isotope applications in hydrothermal systems, in *Techniques in Hydrothermal Ore Deposit Geology*, edited by J. P. Richards and P. B. Larson, vol. 10 of *Reviews in Economic Geology*, pp. 173–193, Society of Economic Paleontologists and Mineralogists, Socorro, New Mexico, 1998.

CDWR, *Rio Grande overview*, Colorado's Decision Support Systems, Colorado Division of Water Resources, http://cdss.state.co.us/overview/rgdss/rgdss.asp#San_Luis_Valley_Project, 2003.

Clark, I. D., and P. Fritz, *Environmental Isotopes in Hydrogeology*, CRC Press, 328 pp., Boca Raton, Florida, 1997.

Cornett, R. J., H. R. Andrews, L. A. Chant, W. G. Davies, B. F. Greiner, Y. Imahori, V. T. Koslowsky, J. D. Milton, and G. M. Milton, Is chlorine-36 from weapons test fallout still cycling in the atmosphere?, *National Instrument Methods and Physics Research, B123*, 378–381, 1997.

Craig, H., Isotopic variations in meteoric waters, *Science*, *133*, 1702–1703, 1961.

Crouch, T. M., Potentiometric surface, 1980, and water-level changes, 1969-80, in the unconfined valley-fill aquifers of the San Luis basin, Colorado and New Mexico, *U. S. Geological Survey Hydrologic Investigations Atlas HA-683, Denver, Colorado, 2 plates*, 1985.

Dansgaard, W., Stable isotopes in precipitation, *Tellus*, *16*, 436–468, 1964.

Davis, S. N., D. O. Whittemore, and J. Fabryka-Martin, Uses of chloride/bromide ratios in studies of potable water, *Ground Water*, *36*, 338–350, 1998.

Desaulniers, D. E., J. A. Cherry, and P. Fritz, Origin, age, and movement of

pore water in argillaceous Quaternary deposits at four sites in southwestern Ontario, *Journal of Hydrology*, *50*, 231–257, 1981.

EPA, *STORET data warehouse*, Environmental Protection Agency, http://www.epa.gov/STORET/dw_home.html, 2003.

EPID, *Irrigation District Terminology*, El Paso Improvement District No. 1, http://www.epcwid1.org/html/terminology.html, 2003.

Fattah, Q. N., and S. J. A. Baki, Effect of drainage systems on water quality in major Iraqi rivers, in *Proceedings of the Helsinki Symposium*, IAHS publication no. 130, pp. 265-269, Helsinki, Finland, 1980.

Feth, J. H., Chloride in natural continental water, *U. S. Geological Survey Water Supply Paper 2167*, 36 pp., 1981.

Flury, M., and A. Papritz, Bromide in the natural environment: occurrence and toxicity, *Journal of Environmental Quality*, *22*, 747–758, 1993.

Frenzel, P. F., C. A. Kaehler, and S. K. Anderholm, Geohydrology and simulation of ground-water flow in the Mesilla basin, Dona Ana County, New Mexico and El Paso County, Texas, *U. S. Geological Survey Professional Paper 1407C*, 105 pp. plus plates, 1992.

Gerritse, R. G., and R. J. George, The role of soil organic matter in the geochemical cycling of chloride and bromide, *Journal of Hydrology*, *101*, 83–95, 1988.

Ghassemi, F., A. J. Jakeman, and H. A. Nix, *Salinisation of land and water resources*, University of New South Wales Press Ltd., 526 pp., 1995.

Hanna, T. M., and E. J. Harmon, An overview of the historical, stratigraphic, and structural setting of the aquifer system of the San Luis valley, in *Water in the valley: a 1989 perspective on water supplies, issues, and solutions in the San Luis Valley, Colorado*, edited by E. J. Harmon, Colorado Ground-Water Association, 294 pp., Lakewood, CO, 1989.

Hanor, J. S., Origin of saline fluids in sedimentary basins, in *Geofluids: Origin, Migration, and Evolution of Fluids in Sedimentary Basins, Geological Society Special Publication No. 78*, edited by J. Parnell, pp. pp. 151–174, 1994.

Hawley, J. W., and R. P. Lozinsky, Hydrogeologic framework of the Mesilla basin in New Mexico and western Texas, *New Mexico Bureau of Mines and Mineral Resources Open-File Report 323, Socorro, New Mexico, 55 pp. plus plates*, 1992.

Hendrickx, J. M. H., *Water quality protection for El Paso County Water Improvement District No. 1*, Draft report to the El Paso County Water Improvement District No. 1, 32 pp. plus appendices., 1998.

IAEA, *Isotope techniques in hydrogeological assessment of potential sites of the disposal of high-level radioactive wastes, Chp. 6: Stable isotopes of hydrogen and oxygen.*, International Atomic Energy Agency Technical Report 228, 1983.

IBWC, *About Us*, International Boundary and Water Commission, http://www.ibwc.state.gov/html/about_us.html, 2003a.

Johnson, P. S., and J. W. Shomaker, *New Mexico's water: perceptions, reality, and imperatives, background report for the 28th New Mexico First Town Hall*, New Mexico First, 76 pp., Albuquerque, New Mexico, 2002.

Keller, G. R., and S. M. Cather, *Basins of the Rio Grande rift: structure, stratigraphy, and tectonic setting*, Geological Society of America Special Paper 291, 304 pp., Boulder, Colorado, 1994.

Kelly, T., and H. E. Taylor, Concentrations of loads of selected trace elements and other constituents in the Rio Grande in the vicinity of Albuquerque, New Mexico, 1994, *U. S. Geological Survey Open-File Report 96-126, 45 pp.*, 1996.

LANL, Hydrogeochemical data for thermal and nonthermal waters and gases of the Valles Caldera-southern Jemez mountains region, New Mexico, *Los Alamos National Laboratory report LA-10923-OBES*, 1987.

Levings, G. W., D. F. Healy, S. F. Richey, and L. F. Carter, Water quality in the Rio Grande valley, Colorado, New Mexico and Texas, 1992-95, *U. S. Geological Survey Circular 1162, 39 pp.*, 1998.

Lippincott, J. B., Southwest border water problems, *Journal of the American Water Works Association*, *31*, 1–28, 1939.

McAda, D. A., and P. Barroll, Simulation of ground-water flow in the middle Rio Grande basin between Cochiti and San Acacia, New Mexico, *U. S. Geological Survey Water-Resources Investigations Report 02-4200, 81 pp.*, 2002.

Moore, S. J., and S. K. Anderholm, Spatial and temporal variations in streamflow, dissolved solids, nutrients, and suspended sediment in the Rio Grande valley study unit, Colorado, New Mexico, and Texas, 1993-95, *Water-Resources Investigations Report 02-4224, 52 pp.*, 2002.

MRGCD, *About the district: the Middle Rio Grande Conservancy District*, Middle Rio Grande Conservancy district, http://www.mrgcd.com/, 2003.

Newton, B. T., S. Kuhn, P. Johnson, and D. L. Hathaway, Investigation of flow and seepage conditions on a critical reach of the Rio Grande, New Mexico, in *Ground Water/Surface Water Interactions, AWRA 2002 Summer Specialty Conference Proceedings*, edited by J. F. Kenny, pp. 581–586, American Water Resources Association, Middleburg, Virginia, 2002.

Nickerson, E. L., Selected hydrologic data for the Mesilla ground water basin, 1987-1992 water years, Dona Ana County, New Mexico, and El Paso County, Texas, *U. S. Geological Survey Open-File Report 95-111, 123 pp.*, 1995.

NRC, *Regional Planning Report part VI, Rio Grande joint investigation in the upper Rio Grande basin in Colorado, New Mexico, and Texas, 1936-1937*, National Resources Committee, U. S. Government Printing Office, 566 pp., Washington, D.C., 1938.

OSE, *What is adjudication? fact sheet*, New Mexico Office of the State Engineer - Interstate Stream Commission, http://www.seo.state.nm.us/water-info/NMWaterPlanning/fact-sheets/adjudication.pdf, 2003.

Papadopulos, S. S., and I. Associates, *Middle Rio Grande Water Supply Study*, Report prepared for the U. S. Army Corps of Engineers Albuquerque district

and the New Mexico Interstate Stream Commission, 70 pp. plus tables and figures, 2000.

Papadopulos, S. S., and I. Associates, *Assessment of flow conditions and seepage on the Rio Grande and adjacent channels, Isleta to San Marcial, summer 2001*, Unpublished report prepared with Mussetter Engineering, Inc. for the New Mexico Interstate Stream Commission, 24 pp. plus appendices, 2002a.

Papadopulos, S. S., and I. Associates, *Middle Rio Grande Conservancy District efficiency and metering program*, Report prepared for the New Mexico Interstate Stream Commission, 105 pp. plus figures and appendices, 2002b.

Phillips, F. M., Chlorine-36, in *Environmental Tracers in Subsurface Hydrology*, edited by P. Cook and A. L. Herczeg, pp. 299–248, Kluwer Academic, Dordrecht, 2000.

Phillips, F. M., J. F. Hogan, S. K. Mills, and J. M. H. Hendrickx, Environmental tracers applied to quantifying causes of salinity in arid-region rivers: preliminary results from the Rio Grande, southwestern USA, in *Water Resources Perspectives: Evaluation, Management and Policy*, edited by A. S. Alsharhan and p. .-. Wood, W. W., Elsevier, Amsterdam, 2003.

Plummer, M. A., Secular variation of cosmogenic nuclide production from chlorine-36 in fossil pack rat middens: implications for cosmogenic nuclide dating and potential application as a groundwater tracer, M. S. thesis, 161 pp., New Mexico Institute of Mining and Technology, 1996.

Postel, S., *Pillar of sand: can the irrigation miracle last?*, W. W. Norton and Company, 313 pp., London, 1999.

Powell, W. J., Ground-water resources of the San Luis valley, Colorado, *U. S. Geological Survey Water-Supply Paper 1379, 284 pp. plus plates*, 1958.

Rao, U., U. Fehn, R. T. D. Teng, and F. Goff, Sources of chloride in hydrothermal fluids from the Valles caldera, New Mexico: a chlorine-36 study, *Journal of Volcanology and Geothermal Research*, *72*, 59–70, 1996.

Reiter, M., Hydrogeothermal studies in the albuquerque basin - a geophysical investigation of ground water flow characteristics, *New Mexico Bureau of Geology and Mineral Resources Circular 211, 74 pp., Socorro, New Mexico*, 2003.

Scurlock, D., *From the rio to the sierra: an environmental history of the middle Rio Grande basin*, General Technical Report 5 (RMRS-GTR-5), U.S. Department of Agriculture, Forest Service, Rocky Mountain Research Station, 440 pp., 1998.

Stabler, H., Some stream waters of the western United States, *U. S. Geological Survey Water Supply Paper 274, 188 pp.*, 1911.

Stueber, A. M., A. H. Saller, and e. al., Origin, migration, and mixing of brines in the Permian basin: geochemical evidence from the eastern central basin platform, Texas., *American Association of Petroleum Geologists Bulletin*, *82*, 1652–1672, 1998.

Trock, W. L., P. C. Huszar, G. E. Radosevich, G. V. Skogerboe, and E. C. Vlachos, *Socio-economic and institutional factors in irrigation return flow quality control volume III: middle Rio Grande valley case study*, report EPA-600/2-78-174c, Environmental Protection Agency, 1978.

USACE, *Albuquerque District Recreational Resources: Reservoirs and Projects: Cochiti Lake*, United States Army Corps of Engineers, http://www.spa.usace.army.mil/recreation/default.htm, 2003.

USBR, *Cochiti Lake Operations Fact Sheet*, Albuquerque Area Office, United States Bureau of Reclamation, http://www.usbr.gov/uc/albuq/water/SanJuanChama/Reservoirs/cochiti/sjc_cochiti.html, 2003a.

USBR, *Middle Rio Grande Conservancy District Gage Schematic*, River Systems and Meteorology Group, Policy, Management and Technical Services, United States Bureau of Reclamation, http://www.usbr.gov/pmts/rivers/awards/Nm/rg/RioG/gage/schematic/SCHEMATICnorth.html and http://www.usbr.gov/pmts/rivers/awards/Nm/rg/RioG/gage/schematic/SCHEMATICsouth.html, 2003b.

USBR, *Dams, Projects, and Power Plants: Rio Grande Project Fact Sheet*, Dataweb, United States Bureau of Reclamation, http://www.usbr.gov/dataweb/html/riogrande.html#general, 2003c.

USGS, *NWISWeb data for the nation*, United States Geological Survey, http://waterdata.usgs.gov/nwis, 2003.

USGS, *Historical Rio Grande flow conditions*, International Boundary and Water Commission, http://www.ibwc.state.gov/wad/histflo1.htm, 2003b.

vanDenburgh, A. S., and J. H. Feth, Solute erosion and chloride balance in selected river basins of the western conterminous United States, *Water Resources Research*, *1*, 537–541, 1965.

Veenhuis, J. E., Summary of flow loss between selected cross sections on the Rio Grande in and near Albuquerque, New Mexico, *U. S. Geological Survey Water-Resources Investigations Report 02-4131, 30 pp.*, 2002.

Wilcox, L. V., Analysis of salt balance and salt-burden data on the Rio Grande, in *Problems of the Upper Rio Grande: an Arid Zone River, Publication No. 1*, edited by P. C. Duisberg, pp. 39–44, U. S. Commission for Arid Resource Improvement and Development, Socorro, New Mexico, 1957.

Wilkins, D. W., Summary of the southwest alluvial basins regional aquifer-system analysis in parts of Colorado, New Mexico, and Texas, *U. S. Geological Survey Professional Paper 1407A, 49 pp.*, 1998.

Williams, J. H., Salt balance in the Rio Grande Project from San Marcial, New Mexico to Fort Quitman, Texas, M. S. thesis, 80 pp., New Mexico State University, 2001.

Wilson, C. A., R. R. White, B. R. Orr, and G. R. Roybal, *Water resources of the Rincon and Mesilla Valleys and adjacent areas, New Mexico*, New Mexico State Engineer Technical Report 43, 66 pp., Santa Fe, New Mexico, 1981.

Winograd, I. J., *Ground-water conditions and geology of Sunshine Valley and western Taos County, New Mexico*, New Mexico State Engineer Technical Report 12, 70 pp., Santa Fe, New Mexico, 1959.

Witcher, J. C., *A geothermal resource database of New Mexico*, Southwest Technology Development Institute, 28 pp., Las Cruces, New Mexico, 1995.

APPENDIX A

RESERVOIR RESIDENCE TIME CALCULATIONS

As first discussed in Chapter 3, average residence times for Cochiti, Elephant Butte, and Caballo Reservoirs were calculated for four different time periods: the entire period of record for each reservoir, 2001-2002, January's of 2001-2002, and August's of 2001-2002. It should be kept in mind that these residence time calculations are calculated from averages of transient reservoir conditions and allow only a qualitative look at the relative effects of reservoir storage and release on the movement of water and salts. Average residence times were calculated as the average of the monthly residence times for the time period of interest. Monthly residence times were calculated using the equation below:

$$t_{res} = \frac{S}{q_{out}} \tag{A.1}$$

where t_{res} is the residence time, S is the average monthly reservoir storage, and q_{out} is the average monthly outflow from the reservoir. The average storage and outflows reported in the tables below Table A.1 and Table A.2) were calculated as the averages of the entire period of interest. Residence times are presented in both days and years (Table A.3 and Table A.4).

Table A.1: Average reservoir outflow (m^3 s^{-1}).

reservoir	historical	2001-2002	Jan 01+Jan 02	Aug 01+Aug 02
Cochiti	40.16	22.2	16.11	22.1
Elephant Butte	28.54	31.56	6.25	47.68
Caballo	26.6	36.54	0.07	53.43

Table A.2: Average reservoir storage (m^3).

reservoir	historical	2001-2002	Jan 01+Jan 02	Aug 01+Aug 02
Cochiti	7.78E+07	6.18E+07	6.25E+07	6.08E+07
Elephant Butte	1.20E+09	1.29E+09	1.59E+09	1.12E+09
Caballo	1.06E+08	6.45E+07	4.68E+07	5.11E+07

Table A.3: Average reservoir residence time (days).

reservoir	historical	2001-2002	Jan 01+Jan 02	Aug 01+Aug 02
Cochiti	22	32	45	32
Elephant Butte	487	472	2944	273
Caballo	46	20	7523	11

Table A.4: Average reservoir residence time (years).

reservoir	historical	2001-2002	Jan 01+Jan 02	Aug 01+Aug 02
Cochiti	0.061	0.088	0.123	0.087
Elephant Butte	1.33	1.29	8.06	0.747
Caballo	0.126	0.056	20.6	0.030

APPENDIX B

SIMPLIFIED SCHEMATIC OF THE MIDDLE RIO GRANDE CONSERVANCY DISTRICT SYSTEM

Though there are numerous agricultural systems in the Rio Grande basin, a digital diagram was only available for the Middle Rio Grande Conservancy District (MRGCD). It is presented here as an excerpt from *Papadopulos and Associates* [2002b]. The entire report is available online at http://www.ose.state.nm.us/water-info/MRGCD-efficiency/index.html.

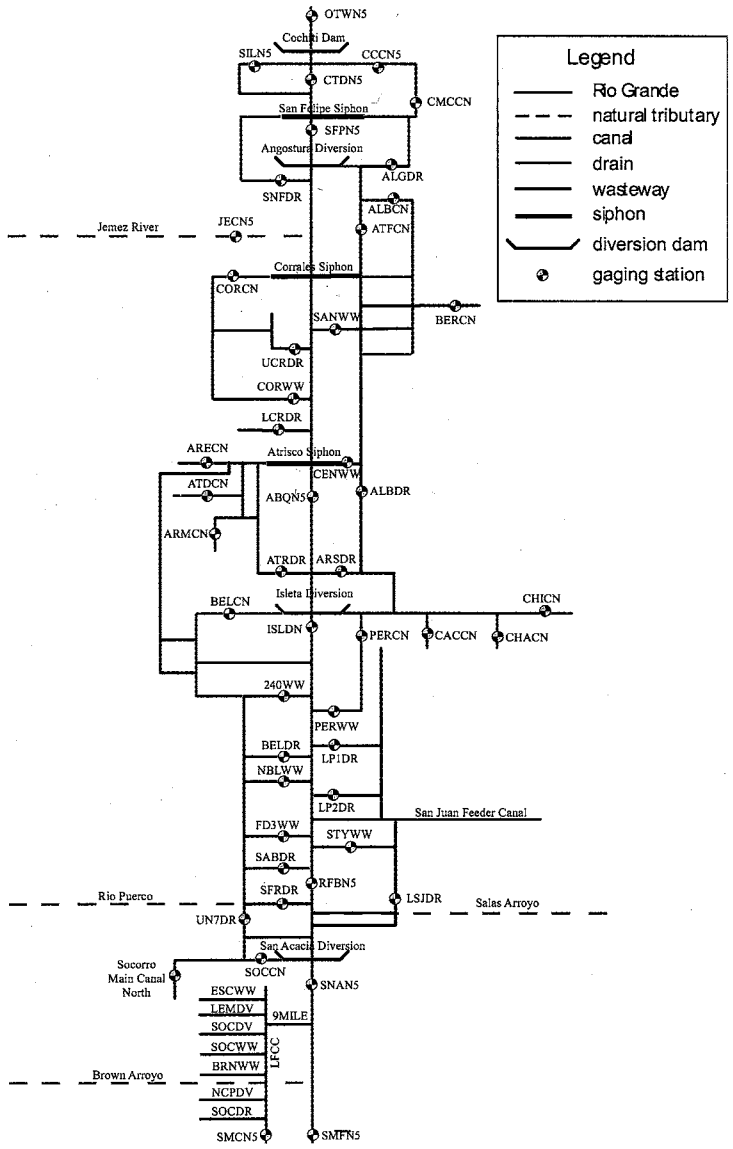

Figure B.1: Simplified schematic of the MRGCD system [*Papadopulos and Associates*, 2002b]. See Figure B.2 and Figure B.3 for tables containing the key to abbreviations.

Existing and Planned Gaging Stations for Monitoring Key MRGCD Irrigation System Flows

Table 3.3 Cochiti Division

Gage Name	Gage ID	Operator	Gage Purpose	Period of Record
Cochiti East Side Main Canal	CCCN5	USGS	Canal Heading	1954 - present
Sili Main Canal	SILN5	USGS	Canal Heading	1954 - present
Approximately 10 - 14 return flow points	.....	.....	Returns to River	TBD
Cochiti Main at San Felipe	CMCCN	MRGCD	mid-reach	(1954) 1974 - present

Table 3.4 Albuquerque Division

Gage Name	Gage ID	Operator	Gage Purpose	Period of Record
Albuquerque Main Canal	ALBCN	MRGCD	Canal Heading	1974 - present
Atrisco Feeder Canal	ATFCN	MRGCD	Canal Heading	1974 - present
Algodones Riverside Drain	ALGDR	MRGCD	Return from Cochiti Div.	1974 - present
Arenal Main Canal	ARECN	MRGCD	Central Ave. X-Section	1974 - present
Arroijo Acequia	ARMCN	MRGCD	Central Ave. X-Section	1958 - present
Atrisco Ditch	ATDCN	MRGCD	Central Ave. X-Section	1958 - present
Albuquerque Riverside Drain @ Central Avenue	ALBDR	MRGCD	Central Ave. X-Section	1954 - present
Corrales Main Canal	CORCN	MRGCD	Secondary Canal	1974 - present
Upper Corrales Riverside Drain	UCRDR	MRGCD	Drain to River	2001 - present
Corrales Main Canal Wasteway	CORWW	MRGCD	Wasteway to River	1997 - present
Central Avenue Wasteway	CENWW	MRGCD	Wasteway to River	2000 - present
Atrisco Riverside Drain	ATRDR	MRGCD	Drain to River	1997 - present
Lower Corrales Riverside Drain	LCRDR	MRGCD	Drain to River	2000 - present
Albuquerque Riverside Drain	ARSDR	MRGCD	Drain to River	1997 - present
Sandia Lakes Wasteway	SANWW	MRGCD	Wasteway to River	2000 - present
Bernalillo Acequia	BERCN	MRGCD	Secondary Canal	2001 - present

[1] This gage also forms the basis for estimating return flow to the river from this drain.
[2] Diversions from the Low Flow Conveyance Channel gaged intermittently by USGS.
[3] MRGCD has a new gage here beginning 2001.
TBD - the installation date has not yet been established.

Figure B.2: Key to abbreviations for the simplified schematic of the MRGCD system, part 1 [*Papadopulos and Associates*, 2002b].

Existing and Planned Gaging Stations for Monitoring Key MRGCD Irrigation System Flows

Table 3.5 Belen Division

Gage Name	Gage ID	Operator	Gage Purpose	Period of Record
Belen Highline Canal	BELCN	MRGCD	Canal Heading	1974 - present
Peralta Main Canal	PERCN	MRGCD	Canal Heading	1974 - present
Chical Lateral	CHICN	MRGCD	Canal Heading	1974 - present
Chical Acequia	CHACN	MRGCD	Canal Heading	1974 - present
Cacique Acequia	CACCN	MRGCD	Canal Heading	1974 - present
Lower San Juan Riverside Drain	LSJDR	MRGCD	Bernardo X-Section[1]	1974 - present
Isleta Drain Outfall	ISLDR	----------	Drain to River	TBD
Barr-Chical Canal	BCHCN	----------	Return from Alb. Division	1997; 2002 planned
Peralta Main Wasteway	PERWW	MRGCD	Wasteway to River	1999 - present
Feeder #3 Wasteway	FD3WW	MRGCD	Wasteway to River	2000 - present
240 Wasteway	240WW	MRGCD	Wasteway to River	2002 planned
Belen Riverside Drain	BELDR	MRGCD	Drain to River	2000 - present
New Belen Acequia Wasteway	NBLWW	MRGCD	Wasteway to River	2002 planned
Lower Peralta Riverside Drain #1	LP1DR	MRGCD	Drain to River	2001 - present
Lower Peralta Riverside Drain #2	LP2DR	MRGCD	Drain to River	2002 planned
Sabinal Riverside Drain	SABDR	MRGCD	Drain to River	2001 - present
Stoney Wasteway	STYWW	MRGCD	Wasteway to River	2002 planned
San Francisco Riverside Drain	SFRDR	MRGCD	Drain to River	2002 planned
Unit 7 Drain	UN7DR	MRGCD	Return to Socorro Division	2001 - present

Table 3.6 Socorro Division

Gage Name	Gage ID	Operator	Gage Purpose	Period of Record
Socorro Main Canal	SOCCN	USGS/MRGCD[3]	Canal Heading	2001 - present
San Acacia Wasteway	SNAWW	MRGCD	Wasteway to LFCC	2002 planned
Escondida Wasteway off Socorro Main Canal	ESCWW	MRGCD	Wasteway to LFCC	2002 planned
Socorro Wasteway	SOCWW	MRGCD	Wasteway to LFCC	2002 planned
Brown Arroyo Wasteway	BRNWW	MRGCD	Wasteway to Brn. Arroyo	2002 planned
Socorro Riverside Drain at Bosque del Apache	SOCDR	MRGCD	end of MRGCD reach	2002 planned
Socorro Main Canal South at Bosque del Apache	SMSCN	MRGCD	end of MRGCD reach	2002 planned
San Antonio Ditch at Bosque del Apache	SADCN	MRGCD	end of MRGCD reach	2002
Elmendorf Drain at Bosque del Apache	ELMDR	MRGCD	end-reach	2002 planned
Lemitar Diversion	LEMDV	MRGCD	Diversion from LFCC[2]	TBD
Socorro Diversion	SOCDV	MRGCD	Diversion from LFCC[2]	TBD
Neil-Cupp Diversion	NCPDV	MRGCD	Diversion from LFCC[2]	TBD

[1] This gage also forms the basis for estimating return flow to the river from this drain.
[2] Diversions from the Low Flow Conveyance Channel gaged intermittently by USGS.
[3] MRGCD has a new gage here beginning 2001.
TBD - the installation date has not yet been established.

Figure B.3: Key to abbreviations for the simplified schematic of the MRGCD system, part 2 [*Papadopulos and Associates*, 2002b].

APPENDIX C

PROCEDURE FOR ISOLATING CHLORIDE FROM WATER SAMPLES FOR ^{36}CL ANALYSIS BY AMS

Written by Fred M. Phillips and others at New Mexico Tech; edited by Suzanne K. Mills. The LabCalcs Excel workbook used in Section 1 can be obtained from the Hydrology Program at New Mexico Tech. To prepare final AgCl samples for shipment in Section 6, the Purdue Rare Isotope (PRIME) laboratory at Purdue University in West Lafayette, Indiana should be contacted to determine the sample wrapping procedure.

1. Determine the appropriate masses of water sample and ^{35}Cl spike to use

   (a) The amount of sample and spike used will depend on the sample composition and age. Use the LabCalcs Excel workbook to determine the appropriate masses of water to use and spike to add.

   (b) LABCALCS: at the top of the SPIKE addition page, fill in the box concerning Cl ppm concentration and the box concerning estimated ^{36}Cl/Cl ratio. (This assumes the Cl concentration of the water sample has been measured or can be well-estimated.) If you are using this procedure for the first time, assume an efficiency of 10-30%.

   (c) Read the information included on the side of the charts. The values highlighted in green meet all the constraints and will most often be

used though they are not necessarily optimal for that parameter. The values highlighted in red do not meet the constraints.

(d) Basically, first you want the Stable/Stable ratio (S/S) to be close to six (6). Second, you want to maximize the $^{36}Cl/Cl$ ratio (R/S). Third, maximize the AgCl mass recovered, preferably at least 10 mg but definitely no less than 3 mg. NOTE: never use less than 20 g of sample.

2. Acid-wash the appropriate lab ware

Before using, all Teflon and glassware to be used in this procedure that will contact the AgCl needs to be "acid-washed."

(a) Rinse lab ware in dilute NH_4OH from a squeeze bottle. Follow this with a rinse in 18 MΩ DI water from a squeeze bottle.

i. For glassware

A. Place the glassware in a metal pitcher. After the pitcher has been filled with the glassware to be acid-washed, fill the pitcher with HNO_3. Place the pitcher on a hot plate (under the hood) so that the contents of the pitcher are thoroughly heated for 30 minutes.

B. Turn off the hot plate to let the pitcher and its contents cool for at least 30 minutes. Then pour off the HNO_3 into a storage container (it can be re-used multiple times for acid-washing). Finally, thoroughly rinse the glassware in 18 MΩ DI water from a squeeze bottle.

ii. For Teflon

A. Fill the Teflon bottles/beakers with HNO_3 to within 1/2 inch of full. Loosely cap the bottles or put Teflon covers over the beakers, and place them on a hot plate (under the hood) with a setting of 3 for 1 hour. Teflon ware should become warm, but does not need to become hot (risks melting the Teflon).

B. Turn off the hot plate and let the HNO_3 cool for 30 minutes, then pour it off into a storage container (it can be re-used for multiple acid-washings). Rinse the Teflon in 18 MΩ DI water from a squeeze bottle.

3. Separation of Cl from water sample by precipitation of AgCl

(a) Weigh the appropriate amount of water sample, as determined from the LabCalcs program, into a tared, clean (does not need to be acid-washed) beaker.

(b) Using a standard vacuum filtration set-up, filter the water sample using 0.45 μm (or finer) filter paper. (Equipment used for vacuum filtration does not need to be acid-washed.)

(c) Transfer the filtered sample into a tared, acid-washed Teflon beaker (or 1-L bottle if the sample is large). Record the sample weight in your lab book.

(d) Exactly weigh the amount of spike determined from LabCalcs into an acid-washed 10-mL beaker. Record the mass, concentration, and

the identification code of the spike in your lab book. Add the spike to the sample and rinse the beaker several times with 18 MΩ DI water, adding the rinse to the sample also. Swirl the sample.

(e) (NOTE: All of the remaining steps in this procedure must be performed under the hood) Acidify the sample to a pH of 2 using concentrated HNO_3. Use pH paper to determine sample pH while adding the acid.

(f) Add 10 mL of 0.2 m $AgNO_3$ to the solution in the Teflon beaker, or bottle, using an acid washed 10-mL beaker (this doesn't have to be exact). Cover the Teflon beakers with Teflon covers or loosely cap the bottles, place on a warm hot plate (setting of 1-3), and leave for approximately 12 hours (overnight). Do not leave the samples longer than this: if the liquid completely evaporates from the beaker while the hot plate is still on, the AgCl will burn.

4. Purification of AgCl

(a) Transfer the solution and precipitate into acid-washed 250-mL Teflon bottles (transparent bottles are best so you can see the precipitate more easily), balance the bottles with 18 MΩ DI water, and centrifuge the bottles for about 15 minutes. Using the Teflon beaker in which the AgCl was first precipitated (or another acid-washed Teflon beaker), transfer the liquid from the 250 mL bottles into a waste bucket and the precipitate into acid washed 50-mL centrifuge tubes, using 18 MΩ DI water to facilitate the transfer.

(b) Balance the tubes using 18 MΩ DI water and cover with parafilm. Centrifuge for at least 10 minutes at approximately 2000 rpm.

(c) Decant the solution into the waste bucket used previously. Rinse the samples in 18 MΩ DI water, balance the tubes, cover with parafilm, and centrifuge again.

(d) Decant the water down the drain in the sink. Add enough NH_4OH (a few mL) to dissolve the white powder sample containing the AgCl (Strange looking precipitate may form here). Add the NH_4OH a small amount at a time, swirling the tube after each addition. Do not add more than you need to dissolve the powder. NOTE: you may need to use an acid washed, glass stir rod on some samples to assure that the chloride is in solution.

(e) Balance the tubes (using dilute NH_4OH), cover with parafilm, and centrifuge for at least 10 minutes.

(f) Decant the liquid, containing the chloride, into another acid-washed 50-mL glass centrifuge tube. SLOWLY drip concentrated HNO3 from the squeeze bottle down the inside of the tube (CAUTION: reaction may be violent at first) until AgCl precipitate begins to form (liquid turns milky white). The solution will have a tendency to "boil over" if the HNO_3 is added too fast, thus losing chloride to the outside of the tube. When completed, balance the tubes using HNO_3, cover with parafilm, and centrifuge for at least 10 minutes.

(g) Dump the solution down the drain with the faucet running, being careful not to lose any precipitate.

(h) Rinse the sample in 18 MΩ DI water, balance, and centrifuge again.

5. Sulfur removal

(a) Pour off the solution, and as described in step 4d, add enough NH_4OH to dissolve the AgCl sample (a few mL). Balance the tubes using dilute NH_4OH, then add 1 mL of $Ba(NO_3)_2$, to precipitate $BaSO_4$. Cover the tubes with parafilm and leave the solution in a dark place for at least 8 hours (24 to 48 hours is preferable for the initial sulfur removal step if time allows).

(b) Centrifuge the sample for at least 30 minutes at approximately 2000 rpm (longer centrifuge times sometimes aids in removal of the solution). Carefully remove the solution with a clean glass pipette. (Label appropriately a sufficient number of pipettes. The pipettes should be rinsed in dilute nitric acid and then 18 MΩ DI water. They can be stored in a clean glass beaker (tips up), rinsed thoroughly after each use, and used for each particular sample until the procedure is complete.) If the "clump" of precipitate in the bottom of the tube begins to come apart, re-centrifuge the sample. Eventually it will stay in one coherent mass in the bottom of the tube. The solution may be placed in a 10 mL test tube that has been cleaned as described above if the sample is small, otherwise use 50-mL tubes.

(c) Add enough HNO_3 to precipitate AgCl as in step 3f, (CAUTION: reaction may be violent at first) balance the tubes using HNO_3, and cover with parafilm. Let stand for 2 hours, then centrifuge and pour

off the acidic solution (down the drain). Rinse the AgCl sample in 18 MΩ DI water and centrifuge again. Repeat the sulfur removal procedures at least once more. If the sample is suspected of having a high sulfur content, repeat the procedure 3 times (^{36}S is an isobar of ^{36}Cl and interferes with AMS analysis).

(d) When all the sulfur has been removed, rinse the sample which has been precipitated in HNO3 at least 3 times in 18 MΩ DI water, centrifuging each time. The pH of the final solution should be about 7. Store the clean sample in 18 MΩ DI water in a tightly covered test tube (parafilm) in a dark place until it needs to be sent away, however, drying the sample and wrapping it in weighing paper is preferred (see below).

6. Preparation for shipping

(a) Label a set of watch glasses that have been cleaned as described earlier. Decant as much water from the tubes as possible. Pour each sample into its prelabeled watchglass using 18 MΩ DI water to facilitate complete transfer. Very carefully remove excess water from the watch glass with a clean glass pipette. Prepare and label pieces of aluminum foil that are large enough to cover the watch glasses. Very carefully, cover the watch glass with the aluminum foil. Very carefully, place samples in the oven for about 24 hours at a temperature of about 60°C. (Note: leaving the sample in the oven for more than 24 hours may facilitate removal of the dried sample from the watch glass in the following steps.)

(b) According to PRIME's instructions, fold an unused piece of weighing paper to hold the sample.

(c) Fold another unused piece of weighing paper in half along one axis. Calibrate the digital balance then weigh and tare the weighing paper. Very carefully transfer the sample from the watch glass to the weighing paper. Weigh the sample and record the weight in your lab book. Carefully transfer the sample from the weighing paper into the appropriately folded weighing paper. Wrap parafilm around the weighing paper containing the AgCl as if you were wrapping a gift. Using labeling tape and a fine-point Sharpee marker, label the package with the sample ID and sample mass.

(d) Store the packages in a ziplock bag until ready to send them to be analyzed.

APPENDIX D

CHLORIDE, BROMIDE, AND CHLORINE-36 MIXING CALCULATIONS

Calculated chloride, bromide, and chlorine-36 values presented in mixing figures in Chapter 7 are presented in the following two tables.

Table D.1: Calculated chloride and bromide concentrations and Cl/Br ratios of a meteoric water progressively mixed with brine. The chloride concentrations and Cl/Br ratios presented here are plotted as the mixing curve in Figure 7.18. Calculations assume a meteoric end member equivalent to the Rio Grande headwaters and a brine end member equivalent to the San Acacia pool (Table 7.7).

brine fraction	Cl (mg L^{-1})	Br (mg L^{-1})	Cl/Br (wt/wt)
0	0.283	0.002	118.888
0.00001	0.606	0.003	227.837
0.0001	3.513	0.005	678.292
0.001	32.583	0.030	1072.614
0.01	323.280	0.282	1144.940
0.02	646.277	0.562	1149.281
0.03	969.274	0.842	1150.737
0.04	1292.272	1.122	1151.466
0.05	1615.269	1.402	1151.904
0.08	2584.260	2.242	1152.561
0.1	3230.255	2.802	1152.781
0.2	6460.226	5.602	1153.220
0.3	9690.198	8.402	1153.366
0.4	12920.170	11.201	1153.440
0.5	16150.141	14.001	1153.484
0.6	19380.113	16.801	1153.513
0.7	22610.085	19.601	1153.534
0.8	25840.057	22.400	1153.549
0.9	29070.028	25.200	1153.562

Table D.2: Calculated chloride-bromide and chlorine-36 parameters of a meteoric water progressively mixed with brine. The Cl/Br and $^{36}Cl/Cl$ ratios are plotted as the mixing curve in Figure 7.20. Calculations assume a meteoric end member equivalent to the Rio Grande headwaters and a brine end member equivalent to the San Acacia pool (Table 7.7). The units of mg L^{-1} * 10^{-15} atoms are used for the ^{36}Cl term for convenience in the mixing equation.

brine fraction	Cl (mg $^{-1}$)	Br (mg $^{-1}$)	Cl/Br (wt/wt)	^{36}Cl *see caption for units*	$^{36}Cl/Cl$ *10^{15} (atoms)
0	0.283	0.002	118.888	732	2587
0.00001	0.606	0.003	227.837	743	1226
0.00002	0.929	0.003	316.029	754	812
0.00005	1.898	0.004	502.200	788	415
0.00007	2.544	0.004	586.272	811	319
0.0001	3.513	0.005	678.292	845	240
0.00015	5.128	0.007	779.444	901	176
0.0003	9.973	0.011	925.250	1071	107
0.0006	19.663	0.019	1025.287	1410	72
0.001	32.583	0.030	1072.614	1861	57
0.002	64.882	0.058	1111.485	2991	46
0.003	97.182	0.086	1125.156	4121	42
0.005	161.781	0.142	1136.367	6381	39
0.01	323.280	0.282	1144.940	12029	37
0.02	646.277	0.562	1149.281	23327	36
0.1	3230.255	2.802	1152.781	113709	35
0.5	16150.141	14.001	1153.484	565616	35
0.8	25840.057	22.400	1153.549	904546	35
0.9	29070.028	25.200	1153.562	1017523	35

APPENDIX E

DATA SOURCES, CHLORIDE, BROMIDE, AND FLOW DATA, AND BURDEN CALCULATIONS FOR TRIBUTARIES AND DIVERSIONS FOR THE DETAILED MASS BALANCE MODEL

Data sources, chloride, bromide, and flow data, and chloride burden calculations for modeled tributaries and diversions during August 2001 and January 2002 are presented here. For further explanation, see Chapter 9. For all data for the August 2001 and January 2002 sampling seasons, see Appendices I-J.

Table E.1: Sources of discharge and chemistry data for modeled tributaries, headwaters (62.7 km) - Albuquerque (541.3 km). Bolded entries in the chemistry source column indicate that the tributary was sampled; unbolded entries indicate the sample chemistry that was used in the models for unsampled tributaries.

distance (km)	station name	station identifier	discharge	chemistry
62.7	Goose Creek	GOOWAGCO	CDWR	TRIB-85.7-X01
85.7	South Fork	8219500	USGS	**TRIB-85.7-X01**
114.0	Pinos Creek	PINDELCO	CDWR	TRIB-85.7-X01
195.0	Closed Basin Canal	CBPALACO	CDWR	**RG-200-X01**
225.6	Conejos River	8249000	USGS	**RG-225.6-X01**
306.7	286.1-306.7 seepage		Winograd (1959)	RG-306.7-X01
318.9	306.7-318.9 seepage		Winograd (1959)	RG-306.7-X01
318.9	Red River	8266820	USGS	**RG-318.9-X01**
332.5	Rio Hondo	8267500	USGS	**RG-332.5-X01**
356.2	Rio Pueblo de Taos	8276300	USGS	historical average
380.6	Embudo Creek	8279000	USGS	**RG-380.6-X01**
409.2	Rio Chama	8290000	USGS	**RG-409.2-X01**
415.4	Santa Cruz River	8291000	USGS	**RG-415.4-X01**
507.8	Jemez River	8329000	USGS	historical average
522.5	Rio Rancho WWTP Outfall 2		RRWWTP	8/14/2001 data
522.5	Rio Rancho WWTP Outfall 3		RRWWTP	8/14/2001 data
530.0	Sandia Lakes Wasteway	SANWW	MRGCD	RG-494.6-X01
533.3	Upper Corrales Riverside Drain	UCRDR	MRGCD	DRAIN-555.6-X01b
538.0	Corrales Wasteway	CORWW	MRGCD	DRAIN-555.6-X01b
541.3	Central Avenue Wasteway	CENWW	MRGCD	DRAIN-555.6-X01a

Table E.2: Sources of discharge and chemistry data for modeled tributaries, Albuquerque (550.0 km) - Fabens (1080.3 km). See Table E.1 for detailed explanation.

distance (km)	station name	station identifier	discharge	chemistry
550.0	Southside WWTP		SSWWTP	7/1/2002 sampling
569.9	Albuquerque Riverside Drain	ARSDR	MRGCD	**DRAIN-555.6-X01a**
569.9	Atrisco Riverside Drain	ATRDR	MRGCD	**DRAIN-555.6-X01b**
598.0	Peralta Main Canal Wasteway	PERWW	MRGCD	RG-570.0-X01
601.0	Lower Peralta Drain 1	LP1DR	MRGCD	**DRAIN-601.1-X01a**
603.0	Belen Riverside Drain Outfall	BELDR	MRGCD	**DRAIN-601.1-X01b**
612.5	Feeder 3 Wasteway	FD3WW	MRGCD	RG-570.0-X01
623.0	Sabinal Drain	SABDR	MRGCD	DRAIN-601.1-X01a
637.1	Rio Puerco	8353000	USGS	**TRIB-637.1-X01**
640.0	Lower San Juan Riverside Drain	LSJDR	MRGCD	DRAIN-630.7-X01
772.0	Conveyance Channel	8358300	USGS	RGCC-731.1-X01
874.8	Garfield Drain		EBID	**DRAIN-874.8-X01**
888.2	Hatch Drain		EBID	**DRAIN-888.2-X01**
945.0	Las Cruces WWTP		LCWWTP	3/28/2003 sampling
973.6	Del Rio Drain		EBID	**DRAIN-973.6-X01**
982.8	La Mesa Drain		EBID	**DRAIN-982.8-X01**
991.7	East Drain		EBID	**DRAIN-991.7-X01**
1014.0	Montoya Drain		EPID	**DRAIN-1014.0-X01**
1021.0	Northwest WWTP		NWWWTP	3/28/2003 sampling
1033.8	Ascarate Wasteway		USBR	RG-1021.6-X01
1080.3	Fabens Waste Channel		EPID	**DRAIN-1080.3-X01**

Table E.3: Sources of discharge and chemistry data for modeled diversions, headwaters (90.0 km) - La Joya (642.7 km). See Chapter 9 for detailed explanation of data sources.

distance (km)	station name	station identifier	discharge	chemistry
90.0	Anaconda Ditch	511	CDWR	RG-79.5-X01
92.5	Minor Ditch	752	CDWR	RG-79.5-X01
114.0	Rio Grande Canal	812	CDWR	RG-115.3-X01
130.1	Prairie Ditch	798	CDWR	RG-130.0-X01
131.0	Monte Vista Canal	753	CDWR	RG-130.0-X01
131.0	Rio Grande and Piedra Valley Ditch	811	CDWR	RG-130.0-X01
153.5	Centennial Ditch	566	CDWR	RG-155.6-X01
156.0	Excelsior Ditch	627	CDWR	RG-155.6-X01
193.0	Westside Ditch	903	CDWR	RG-192.8-X01
195.0	Chicago Ditch	575	CDWR	RG-192.8-X01
470.9	Sili Main Canal (Cochiti diversions)	SILN5	USGS	RG-471.0-X01
470.9	Cochiti Main Canal (Cochiti diversions)	CCCN5	USGS	RG-471.0-X01
507.0	Angostura diversions		MRGCD	RG-496.4-X01
546.5	Arenal Main Canal	ARECN	MRGCD	RG-547.5-X01
569.9	Isleta diversions		MRGCD	RG-570.0-X01
582.9	570.0-582.9 seepage		Papadopulos (2002a)	RG-570.0-X01
601.1	582.9-601.1 seepage		Papadopulos (2002a)	RG-582.9-X01
614.7	601.1-614.7 seepage		Papadopulos (2002a)	RG-601.1-X01
630.7	614.7-630.7 seepage		Papadopulos (2002a)	RG-614.7-X01
642.9	630.7-642.9 seepage		Papadopulos (2002a)	RG-630.7-X01

Table E.4: Sources of discharge and chemistry data for modeled diversions, San Acacia (655.2 km) - El Paso (1021.4 km). See Chapter 9 for detailed explanation of data sources.

distance (km)	station name	station identifier	discharge	chemistry
655.2	San Acacia diversions	SNADV	MRGCD	RG-655.3-X01
655.3	642.9-655.3 seepage		Papadopulos (2002a)	RG-642.9-X01
671.8	655.3-671.8 seepage		Newton et al. (2002)	RG-655.3-X01
679.3	671.8-679.3 seepage		Newton et al. (2002)	RG-671.8-X01
686.3	679.3-686.3 seepage		Newton et al. (2002)	RG-679.3-X01
696.4	686.3-696.4 seepage		Newton et al. (2002)	RG-686.3-X01
723.6	696.4-723.6 seepage		Newton et al. (2002)	RG-696.4-X01
731.1	723.6-731.1 seepage		Newton et al. (2002)	RG-723.6-X01
738.8	731.1-738.8 seepage		Newton et al. (2002)	RG-731.1-X01
747.5	738.8-747.5 seepage		Newton et al. (2002)	RG-738.8-X01
845.5	Arrey Canal (Percha diversion)		EBID	RG-845.6-X01
919.0	Leasburg Canal (Leasburg diversion)		EBID	RG-919.5-X01
955.0	Eastside Canal (Mesilla diversions)		EBID	RG-955.1-X01
955.0	Westside Canal (Mesilla diversions)		EBID	RG-955.1-X01
955.1	944.7-955.1 seepage		Wilson et al. (1981)	RG-944.7-X01
987.6	973.6-987.6 seepage		Wilson et al. (1981)	RG-979.6-X01
1013.8	987.6-1013.8 seepage		Wilson et al. (1981)	RG-1013.8-X01
1017.0	American Canal	8364500	IBWC	RG-1021.6-X01
1021.4	Acequia Madre	8365500	IBWC	RG-1021.6-X01

Table E.5: Discharge of modeled tributaries, August 2001, Wagon Wheel Gap (61.7 km) - Bernardo (630.7 km). Only gaging intervals with modeled tributaries are shown.

gaging interval (km)	distance (km)	station name	flow (m^3 s^{-1})
61.7 - 104.1	62.7	Goose Creek	1.73
	85.7	South Fork	3.00
		sector sums	**4.73**
104.1 - 141.2	114.0	Pinos Creek	**0.76**
192.8 - 203.1	195.0	Closed Basin Canal	**0.59**
203.1 - 256.9	225.6	Conejos River	**0.04**
256.9 - 306.7	306.7	286.1-306.7 seepage	**2.26**
306.7 - 359.3	318.9	306.7-318.9 seepage	0.45
	318.9	Red River	1.87
	332.5	Rio Hondo	0.71
	356.2	Rio Pueblo de Taos	0.42
		sector sums	**3.45**
359.3 - 384.5	380.6	Embudo Creek	**2.18**
384.5 - 430.9	409.2	Rio Chama	7.70
	415.4	Santa Cruz River	1.36
		sector sums	**9.06**
496.4 - 547.5	507.8	Jemez River	0.65
	522.5	Rio Rancho WWTP Outfall 2	0.09
	522.5	Rio Rancho WWTP Outfall 3	0.03
	530.0	Sandia Lakes Wasteway	1.89
	533.3	Upper Corrales Riverside Drain	1.34
	538.0	Corrales Wasteway	0.02
	541.3	Central Avenue Wasteway	1.47
		sector sums	**5.49**
547.5 - 630.7	550.0	Southside WWTP	2.42
	569.9	Albuquerque Riverside Drain	4.49
	569.9	Atrisco Riverside Drain	1.32
	598.0	Peralta Main Canal Wasteway	1.58
	601.0	Lower Peralta Drain 1	1.79
	603.0	Belen Riverside Drain Outfall	0.28
	612.5	Feeder 3 Wasteway	0.17
	623.0	Sabinal Drain	0.14
		sector sums	**12.19**

Table E.6: Discharge of modeled tributaries, August 2001, Bernardo (630.7 km) - Ft. Quitman (1149.0 km). Only gaging intervals with modeled tributaries are shown.

gaging interval (km)	distance (km)	station name	flow ($m^3\ s^{-1}$)
630.7 - 655.3	637.1	Rio Puerco	0.48
	640.0	Lower San Juan Riverside Drain	3.77
		sector sums	**4.25**
731.1 - 801.3	772.0	Conveyance Channel	**8.12**
841.0 - 899.4	874.8	Garfield Drain	0.20
	888.2	Hatch Drain	0.40
		sector sums	**0.59**
944.7 - 955.1	945.0	Las Cruces WWTP	**0.38**
955.1 - 987.6	973.6	Del Rio Drain	1.87
	982.8	La Mesa Drain	1.30
		sector sums	**3.17**
987.6 - 1013.8	991.7	East Drain	**1.13**
1013.8 - 1021.6	1014.0	Montoya Drain	3.20
	1021.0	Northwest WWTP	0.37
		sector sums	**3.57**
1021.6 - 1149.0	1033.8	Ascarate Wasteway	0.74
	1080.3	Fabens Waste Channel	2.46
		sector sums	**3.20**

Table E.7: Discharge of modeled diversions, August 2001, Wagon Wheel Gap (61.7 km) - Bernardo (630.7 km). Only gaging intervals with modeled diversions are shown.

gaging interval (km)	distance (km)	station name	flow (m^3 s^{-1})
61.7-104.1	90.0	Anaconda Ditch	0.33
	92.5	Minor Ditch	0.56
		sector sums	**0.90**
104.1 - 141.2	114.0	Rio Grande Canal	13.1
	130.1	Prairie Ditch	0.08
	131.0	Monte Vista Canal	3.91
	131.0	RG and Piedra Valley Ditch	1.26
		sector sums	**18.3**
141.2 - 192.8	153.5	Centennial Ditch	1.43
	156.0	Excelsior Ditch	1.22
		sector sums	**2.65**
192.8 - 203.1	193.0	Westside Ditch	0.46
	195.0	Chicago Ditch	0.74
		sector sums	**1.21**
430.9 - 471.0	470.9	Sili Main Canal	2.09
	470.9	Cochiti Main Canal	3.79
		sector sums	**5.89**
496.4 - 547.5	507.0	Angostura diversions	8.64
	546.5	Arenal Main Canal	2.21
		sector sums	**10.9**
547.5 - 630.7	569.9	Isleta diversions	11.8
	582.9	570.0-582.9 seepage	1.50
	601.1	582.9-601.1 seepage	2.11
	614.7	601.1-614.7 seepage	0.12
	630.7	614.7-630.7 seepage	0.14
		sector sums	**15.7**

Table E.8: Discharge of modeled diversions, August 2001, Bernardo (630.7 km) - Ft. Quitman (1149.0 km). Only gaging intervals with modeled diversions are shown.

gaging interval (km)	distance (km)	station name	flow (m^3 s^{-1})
630.7 - 655.3	642.9	630.7-642.9 seepage	0.24
	655.2	San Acacia diversions	0.56
	655.3	642.9-655.3 seepage	0.39
		sector sums	**1.19**
655.3 - 731.1	671.8	655.3-671.8 seepage	0.51
	679.3	671.8-679.3 seepage	0.58
	686.3	679.3-686.3 seepage	0.87
	696.4	686.3-696.4 seepage	1.76
	723.6	696.4-723.6 seepage	2.34
	731.1	723.6-731.1 seepage	0.41
		sector sums	**6.46**
731.1 - 801.3	738.8	731.1-738.8 seepage	0.26
	747.5	738.8-747.5 seepage	0.70
		sector sums	**0.96**
841.0 - 899.4	845.5	Arrey Canal	**7.08**
899.4 - 919.5	919.0	Leasburg Canal	**8.72**
944.7 - 955.1	955.0	Eastside Canal	6.08
	955.0	Westside Canal	13.2
	955.1	944.7-955.1 seepage	0.46
		sector sums	**19.7**
955.1 - 987.6	987.6	973.6-987.6 seepage	**0.25**
987.6 - 1013.8	1013.8	987.6-1013.8 seepage	**0.46**
1013.8 - 1021.6	1017.0	American Canal	18.3
	1021.4	Acequia Madre	5.65
		sector sums	**24.0**

Table E.9: Discharge of modeled tributaries, January 2002, Wagon Wheel Gap (61.7 km) - Bernardo (630.7 km). Only gaging intervals with modeled tributaries are shown.

gaging interval (km)	distance (km)	station name	flow ($m^3\ s^{-1}$)
61.7-104.1	62.7	Goose Creek	0.37
	85.7	South Fork	0.74
		sector sums	**1.10**
104.1 - 141.2	114.0	Pinos Creek	**0.14**
192.8 - 256.9	195.0	Closed Basin Canal	0.79
	225.6	Conejos River	0.96
		sector sums	**1.75**
256.9 - 306.7	306.7	286.1-306.7 seepage	**2.26**
306.7 - 359.3	318.9	306.7-318.9 seepage	0.45
	318.9	Red River	0.93
	332.5	Rio Hondo	0.28
	356.2	Rio Pueblo de Taos	0.00
		sector sums	**3.93**
359.3 - 384.5	380.6	Embudo Creek	**0.93**
384.5 - 430.9	409.2	Rio Chama	na
	415.3	Santa Cruz River	0.20
		sector sums	**0.20**
496.4 - 547.5	507.8	Jemez River	0.22
	522.5	Rio Rancho WWTP Outfall 2	0.13
	522.5	Rio Rancho WWTP Outfall 3	0.04
	530.0	Sandia Lakes Wasteway	0.00
	533.3	Upper Corrales Riverside Drain	0.00
	538.0	Corrales Wasteway	0.00
	541.3	Central Avenue Wasteway	0.00
		sector sums	**0.38**
547.5 - 630.7	550.0	Southside WWTP	2.26
	569.9	Albuquerque Riverside Drain	0.68
	569.9	Atrisco Riverside Drain	0.00
	598.0	Peralta Main Canal Wasteway	0.00
	601.0	Lower Peralta Drain 1	0.06
	603.0	Belen Riverside Drain Outfall	0.00
	612.5	Feeder 3 Wasteway	0.00
	623.0	Sabinal Drain	0.00
		sector sums	**3.00**

Table E.10: Discharge of modeled tributaries, January 2002, Bernardo (630.7 km) - Ft. Quitman (1149.0 km). Only gaging intervals with modeled tributaries are shown.

gaging interval (km)	distance (km)	station name	flow ($m^3\ s^{-1}$)
630.7 - 655.3	637.1	Rio Puerco	0.00
	640.0	Lower San Juan Riverside Drain	1.23
		sector sums	**1.23**
731.1 - 801.3	772.0	Conveyance Channel	**6.17**
841.0 - 899.4	874.8	Garfield Drain	0.00
	888.2	Hatch Drain	0.00
		sector sums	**0.00**
944.7 - 955.1	945.0	Las Cruces WWTP	**0.31**
955.1 - 987.6	973.6	Del Rio Drain	0.71
	982.8	La Mesa Drain	0.25
		sector sums	**0.96**
987.6 - 1013.8	991.7	East Drain	**0.23**
1013.8 - 1021.6	1014.0	Montoya Drain	0.79
	1021.0	Northwest WWTP	0.31
		sector sums	**1.10**
1021.6 - 1149.0	1033.8	Ascarate Wasteway	0.00
	1080.3	Fabens Waste Channel	2.55
		sector sums	**2.55**

Table E.11: Discharge of modeled diversions, January 2002, Wagon Wheel Gap (61.7 km) - Bernardo (630.7 km). Only gaging intervals with modeled diversions are shown.

gaging interval (km)	distance (km)	station name	flow (m^3 s^{-1})
61.7 - 104.1	90.0	Anaconda Ditch	0.00
	92.5	Minor Ditch	0.00
		sector sums	**0.00**
104.1 - 141.2	114.0	Rio Grande Canal	0.00
	130.1	Prairie Ditch	0.00
	131.0	Monte Vista Canal	0.00
	131.0	RG and Piedra Valley Ditch	0.00
		sector sums	**0.00**
141.2 - 192.8	153.5	Centennial Ditch	0.00
	156.0	Excelsior Ditch	0.00
		sector sums	**0.00**
192.8 - 256.9	193.0	Westside Ditch	0.00
	195.0	Chicago Ditch	0.00
		sector sums	**0.00**
430.9 - 471.0	470.9	Sili Main Canal	0.00
	470.9	Cochiti Main Canal	0.00
		sector sums	**0.00**
496.4 - 547.5	507.0	Angostura diversions	0.00
	546.5	Arenal Main Canal	0.00
		sector sums	**0.00**
547.5 - 630.7	569.9	Isleta diversions	0.00
	582.9	570.0-582.9 seepage	1.50
	601.1	582.9-601.1 seepage	2.11
	614.7	601.1-614.7 seepage	0.12
	630.7	614.7-630.7 seepage	0.14
		sector sums	**3.87**

Table E.12: Discharge of modeled diversions, January 2002, Bernardo (630.7 km) - Ft. Quitman (1149.0 km). Only gaging intervals with modeled diversions are shown.

gaging interval (km)	distance (km)	station name	flow ($m^3\ s^{-1}$)
630.7 - 655.3	642.9	630.7-642.9 seepage	0.24
	655.2	San Acacia diversions	0.00
	655.3	642.9-655.3 seepage	0.39
		sector sums	**0.63**
655.3 - 731.1	671.8	655.3-671.8 seepage	0.22
	679.3	671.8-679.3 seepage	0.35
	686.3	679.3-686.3 seepage	0.57
	696.4	686.3-696.4 seepage	3.47
	712.4	696.4-712.4 seepage	1.09
	723.6	712.4-723.6 seepage	0.76
	731.1	723.6-731.1 seepage	1.05
		sector sums	**7.51**
731.1 - 801.3	738.8	731.1-738.8 seepage	0.01
	747.5	738.8-747.5 seepage	0.19
		sector sums	**0.20**
841.0 - 899.4	845.5	Arrey Canal	**0.00**
899.4 - 919.5	919.0	Leasburg Canal	**0.00**
944.7 - 955.1	955.0	Eastside Canal	0.00
	955.0	Westside Canal	0.00
	955.1	944.7-955.1 seepage	0.46
		sector sums	**0.46**
955.1 - 987.6	987.6	973.6-987.6 seepage	**0.25**
987.6 - 1013.8	1013.8	987.6-1013.8 seepage	**0.46**
1013.8 - 1021.6	1017.0	American Canal	0.10
	1021.4	Acequia Madre	0.00
		sector sums	**0.10**

Table E.13: Chloride and bromide data and calculated chloride burdens for modeled tributaries, August 2001, Rio Grande Reservoir (61.7 km) - Bernardo (630.7 km). See Table E.5 for flow data and gaging intervals.

distance (km)	station name	Cl (mg L^{-1})	Br (mg L^{-1})	Cl/Br (wt/wt)	Cl burden (kg dy^{-1})
62.7	Goose Creek	1.1	0.005	226	164
85.7	South Fork	1.1	0.005	226	285
	sector sums				**448**
114.0	Pinos Creek	1.1	0.005	226	**72**
195.0	Closed Basin Canal	13.3	0.126	106	**683**
225.6	Conejos River	1.5	0.017	88	**5**
306.7	286.1-306.7 seepage	4.2	0.039	109	**825**
318.9	306.7-318.9 seepage	4.2	0.039	109	165
318.9	Red River	5.3	0.666	8	859
332.5	Rio Hondo	5.8	0.052	110	353
356.2	Rio Pueblo de Taos	7.8	na	na	285
	sector sums				**1662**
380.6	Embudo Creek	3.2	0.013	247	**604**
409.2	Rio Chama	5.8	0.015	392	3854
415.4	Santa Cruz River	4.4	0.028	159	514
	sector sums				**4368**
507.8	Jemez River	166	na	na	9335
522.5	Rio Rancho WWTP Outfall 2	57.0	0.190	300	447
522.5	Rio Rancho WWTP Outfall 3	380	1.267	300	988
530.0	Sandia Lakes Wasteway	5.3	0.025	214	870
533.3	Upper Corrales Riverside Drain	7.8	0.037	211	904
538.0	Corrales Wasteway	7.8	0.037	211	13
541.3	Central Avenue Wasteway	9.0	0.041	218	1149
	sector sums				**16914**
550.0	Southside WWTP	90.0	0.300	300	18801
569.9	Albuquerque Riverside Drain	9.0	0.041	218	3502
569.9	Atrisco Riverside Drain	7.8	0.037	211	888
598.0	Peralta Main Canal Wasteway	19.2	0.075	255	2632
601.0	Lower Peralta Drain 1	28.8	0.127	228	4447
603.0	Belen Riverside Drain Outfall	22.8	0.101	226	559
612.5	Feeder 3 Wasteway	19.2	0.075	255	282
623.0	Sabinal Drain	28.8	0.127	228	352
	sector sums				**31463**

Table E.14: Chloride and bromide data and calculated chloride burdens for modeled tributaries, August 2001, Bernardo (630.7 km) - Ft. Quitman (1149.0 km). See Table E.6 for flow data and gaging intervals.

distance (km)	station name	Cl (mg L^{-1})	Br (mg L^{-1})	Cl/Br (wt/wt)	Cl burden (kg dy^{-1})
637.1	Rio Puerco	11.0	0.022	511	459
640.0	Lower San Juan Riverside Drain	27.7	0.112	248	9024
	sector sums				**9483**
772.0	Conveyance Channel	67.0	0.168	398	**47022**
874.8	Garfield Drain	142	0.290	491	2433
888.2	Hatch Drain	136	0.254	535	4657
	sector sums				**7089**
945.0	Las Cruces WWTP	200	0.240	833	**6585**
973.6	Del Rio Drain	113	0.208	544	18256
982.8	La Mesa Drain	147	0.259	567	16526
	sector sums				**34782**
991.7	East Drain	130	0.229	569	**12747**
1014.0	Montoya Drain	209	0.312	671	57814
1021.0	Northwest WWTP	275	0.310	887	8773
	sector sums				**66587**
1033.8	Ascarate Wasteway	98.7	0.200	495	6273
1080.3	Fabens Waste Channel	309	0.323	955	65647
	sector sums				**71919**

Table E.15: Chloride and bromide data and calculated chloride burdens for modeled diversions, August 2001, Rio Grande Reservoir (61.7 km) - Bernardo (630.7 km). See Table E.7 for flow data and gaging intervals.

distance (km)	station name	Cl ($mg\ L^{-1}$)	Br ($mg\ L^{-1}$)	Cl/Br (wt/wt)	Cl burden ($kg\ dy^{-1}$)
90.0	Anaconda Ditch	0.5	0.003	161	13
92.5	Minor Ditch	0.5	0.003	161	22
	sector sums				**35**
114.0	Rio Grande Canal	0.6	0.006	105	684
130.1	Prairie Ditch	0.8	0.010	78	6
131.0	Monte Vista Canal	0.8	0.010	78	262
131.0	RG and Piedra Valley Ditch	0.8	0.010	78	84
	sector sums				**1035**
153.5	Centennial Ditch	1.6	0.008	189	197
156.0	Excelsior Ditch	1.6	0.008	189	168
	sector sums				**365**
193.0	Westside Ditch	3.4	0.047	74	137
195.0	Chicago Ditch	3.4	0.047	74	221
	sector sums				**359**
470.9	Sili Main Canal	4.9	0.032	154	880
470.9	Cochiti Main Canal	4.9	0.032	154	1594
	sector sums				**2474**
507.0	Angostura diversions	5.3	0.025	214	3987
546.5	Arenal Main Canal	9.1	0.037	244	1730
	sector sums				**5717**
569.9	Isleta diversions	19.2	0.075	255	19629
582.9	570.0-582.9 seepage	19.2	0.075	255	2489
601.1	582.9-601.1 seepage	20.1	0.080	251	3669
614.7	601.1-614.7 seepage	21.7	0.098	222	233
630.7	614.7-630.7 seepage	21.0	0.079	267	246
	sector sums				**26266**

Table E.16: Chloride and bromide data and calculated chloride burdens for modeled diversions, August 2001, Bernardo (630.7 km) - Ft. Quitman (1149.0 km). See Table E.8 for flow data and gaging intervals.

distance (km)	station name	Cl (mg L^{-1})	Br (mg L^{-1})	Cl/Br (wt/wt)	Cl burden (kg dy^{-1})
642.9	630.7-642.9 seepage	22.6	0.082	277	465
655.2	San Acacia diversions	27.1	0.113	240	1312
655.3	642.9-655.3 seepage	23.5	0.105	225	788
	sector sums				**2564**
671.8	655.3-671.8 seepage	27.1	0.113	240	1188
679.3	671.8-679.3 seepage	26.7	0.110	243	1339
686.3	679.3-686.3 seepage	28.4	0.102	279	2134
696.4	686.3-696.4 seepage	27.5	0.116	238	4191
723.6	696.4-723.6 seepage	28.1	0.104	270	5672
731.1	723.6-731.1 seepage	31.2	0.103	304	1100
	sector sums				**15623**
738.8	731.1-738.8 seepage	30.5	0.096	319	684
747.5	738.8-747.5 seepage	29.1	0.096	304	1756
	sector sums				**2440**
845.5	Arrey Canal	58.0	0.144	401	**35434**
919.0	Leasburg Canal	62.7	0.150	417	**47202**
955.0	Eastside Canal	65.2	0.154	423	34293
955.0	Westside Canal	65.2	0.154	423	74168
955.1	944.7-955.1 seepage	65.4	0.150	436	2598
	sector sums				**111058**
987.6	973.6-987.6 seepage	73.2	0.165	444	**1566**
1013.8	987.6-1013.8 seepage	85.3	0.177	482	**3416**
1017.0	American Canal	98.7	0.200	495	156004
1021.4	Acequia Madre	98.7	0.200	495	48165
	sector sums				**204170**

Table E.17: Chloride and bromide data and calculated chloride burdens for modeled tributaries, January 2002. See Tables E.9 - E.10 for flow data and gaging intervals. Only flowing tributaries are shown. Although the Rio Chama was observed to be flowing, its gage was frozen and no discharge data is available for modeling.

distance (km)	station name	Cl (mg L^{-1})	Br (mg L^{-1})	Cl/Br (wt/wt)	Cl burden (kg dy^{-1})
62.7	Goose Creek	1.2	0.004	274	39
85.7	South Fork	1.2	0.004	274	77
	sector sums				**116**
114.0	Pinos Creek	1.2	0.004	274	**15**
195.0	Closed Basin Canal	15.6	0.135	115	1066
225.6	Conejos River	1.2	0.004	263	96
	sector sums				**1163**
306.7	286.1-306.7 seepage	4.7	0.021	227	**916**
318.9	306.7-318.9 seepage	4.7	0.021	227	183
318.9	Red River	5.4	0.044	123	434
332.5	Rio Hondo	4.8	0.038	128	115
	sector sums				**732**
380.6	Embudo Creek	4.0	0.066	62	**327**
415.3	Santa Cruz River	5.7	0.023	246	**100**
507.8	Jemez River	213	na	na	3955
522.5	Rio Rancho WWTP Outfall 2	50.0	0.167	300	543
522.5	Rio Rancho WWTP Outfall 3	360	1.200	300	1129
	sector sums				**5628**
550.0	Southside WWTP	90.0	0.300	300	17608
569.9	Albuquerque Riverside Drain	13.0	0.059	219	761
601.0	Lower Peralta Drain 1	26.2	0.117	225	128
	sector sums				**18498**
640.0	Lower San Juan Riverside Drain	28.6	0.120	238	**3037**
772.0	Conveyance Channel	105	0.177	595	**56012**
945.0	Las Cruces WWTP	200	0.240	833	**5298**
973.6	Del Rio Drain	120	0.223	540	7350
982.8	La Mesa Drain	177	0.379	468	3900
	sector sums				**11250**
991.7	East Drain	349	0.488	715	**6826**
1014.0	Montoya Drain	342	0.530	645	23400
1021.0	Northwest WWTP	275	0.310	887	7253
	sector sums				**30653**
1080.3	Fabens Waste Channel 247	313	0.387	811	**68963**

Table E.18: Chloride and bromide data and calculated chloride burdens for modeled diversions, January 2002. See Tables E.11 - E.12 for flow data and gaging intervals. Only flowing diversions are shown.

distance (km)	station name	Cl (mg L^{-1})	Br	Cl/Br (wt/wt)	Cl burden (kg dy^{-1})
582.9	570.0-582.9 seepage	20.0	0.087	229	2597
601.1	582.9-601.1 seepage	28.7	0.040	717	5238
614.7	601.1-614.7 seepage	24.4	0.092	265	262
630.7	614.7-630.7 seepage	23.1	0.097	238	271
	sector sums				**8368**
642.9	630.7-642.9 seepage	27.8	0.104	267	572
655.2	San Acacia diversions	dry			
655.3	642.9-655.3 seepage	24.2	0.100	241	811
	sector sums				**1382**
671.8	655.3-671.8 seepage	47.4	0.137	347	888
679.3	671.8-679.3 seepage	37.2	0.120	311	1139
686.3	679.3-686.3 seepage	36.1	0.109	332	1777
696.4	686.3-696.4 seepage	35.1	0.109	321	10519
712.4	696.4-712.4 seepage	35.1	0.109	321	3305
723.6	712.4-723.6 seepage	33.2	0.116	285	2191
731.1	723.6-731.1 seepage	35.9	0.122	295	3252
	sector sums				**23071**
738.8	731.1-738.8 seepage	38.5	0.121	318	37
747.5	738.8-747.5 seepage	32.6	0.108	303	534
	sector sums				**572**
955.1	944.7-955.1 seepage	183	0.307	596	**7273**
987.6	973.6-987.6 seepage	161	0.242	666	3443
1013.8	987.6-1013.8 seepage	187	0.416	451	7509
1017.0	American Canal	280	0.588	477	2422
	sector sums				**2422**

APPENDIX F

SMALL-SCALE PIPE DIAGRAMS OF CHLORIDE BURDEN FOR AUGUST 2001 AND JANUARY 2002

The chloride burden pipe diagrams in Chapter 9 are all to a single scale in order to portray the effects of salinization at the basin-scale. The pipe diagrams in this appendix divide the river into three sections and use different scales for each in order to show detail at the local level. Small-scale diagrams are presented here for both August 2001 (Figure F.1, Figure F.2, and Figure F.3) and January 2002 (Figure F.4, Figure F.5, and Figure F.6). Chloride burdens were calculated for gaging stations of the main stem Rio Grande as well as major tributaries and diversions considered in the mass balance modeling.

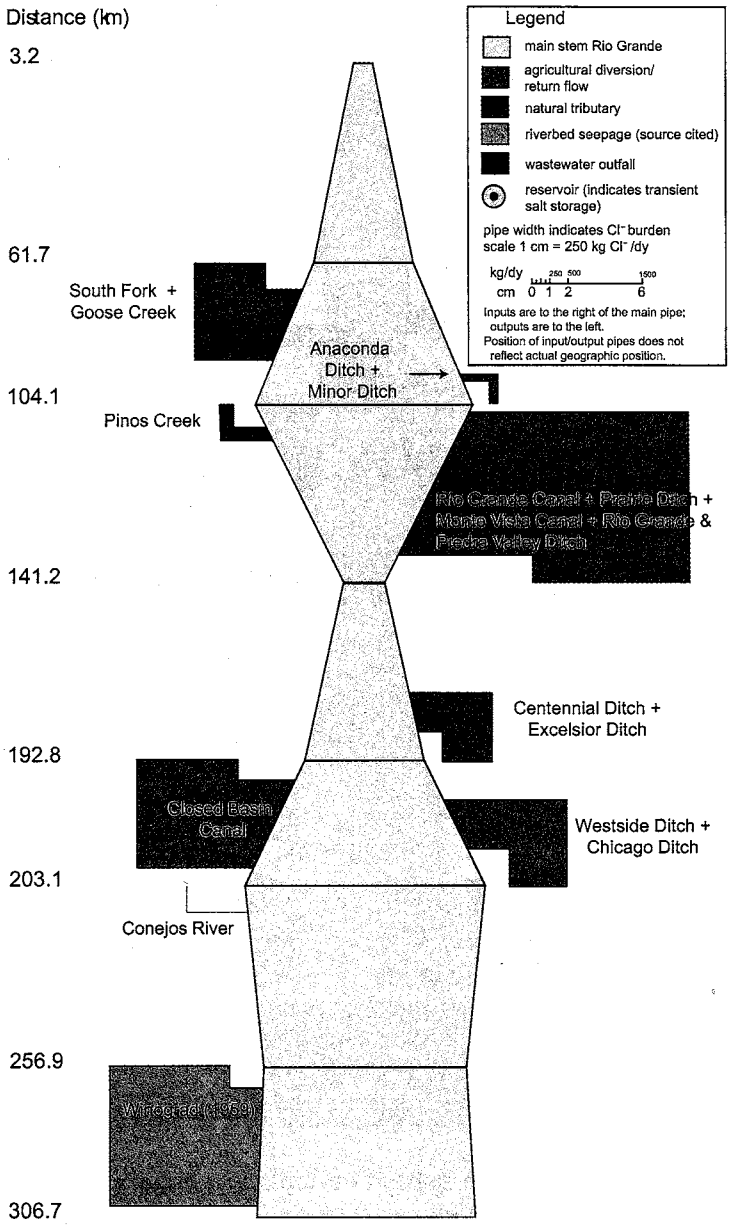

Figure F.1: Pipe diagram of chloride burden of the Rio Grande, its modeled tributaries and diversions, August 2001 (kg dy^{-1}). River distance 3.2 - 306.7 km.

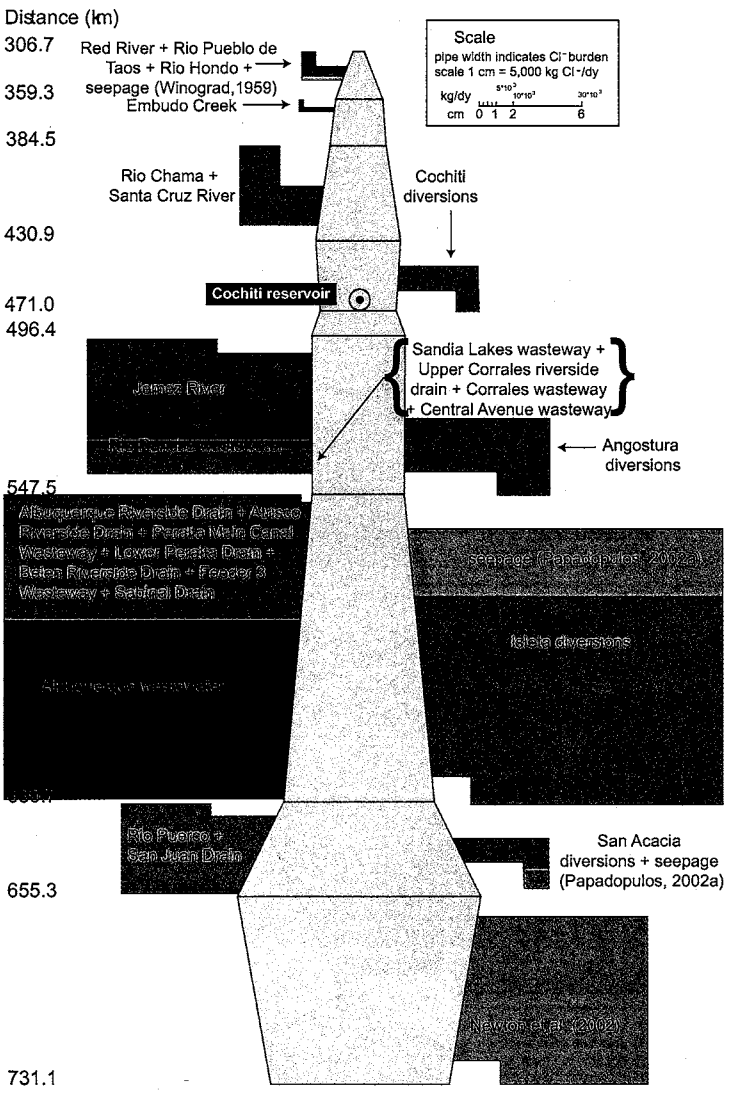

Figure F.2: Pipe diagram of chloride burden of the Rio Grande, its modeled tributaries and diversions, August 2001 (kg dy^{-1}). River distance 306.7 - 731.1 km. See Figure F.1 for full legend.

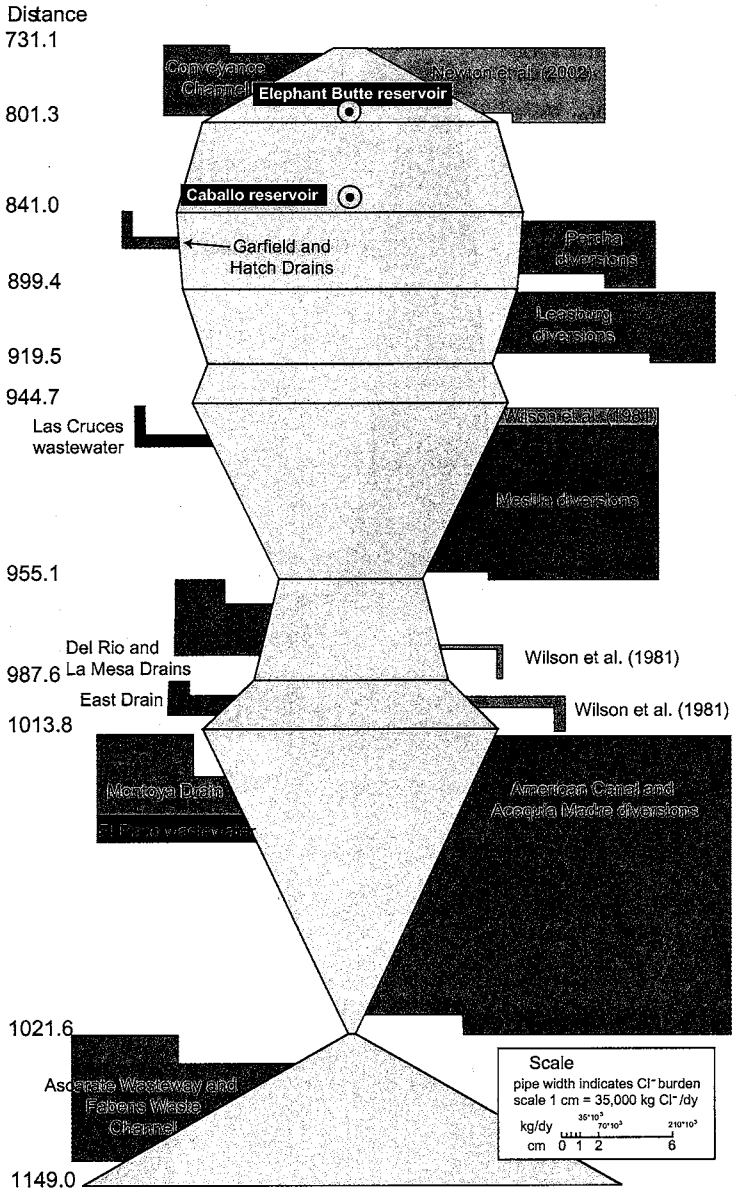

Figure F.3: Pipe diagram of chloride burden of the Rio Grande, its modeled tributaries and diversions, August 2001 (kg dy^{-1}). River distance 731.1 - 1149.0 km. See Figure F.1 for full legend.

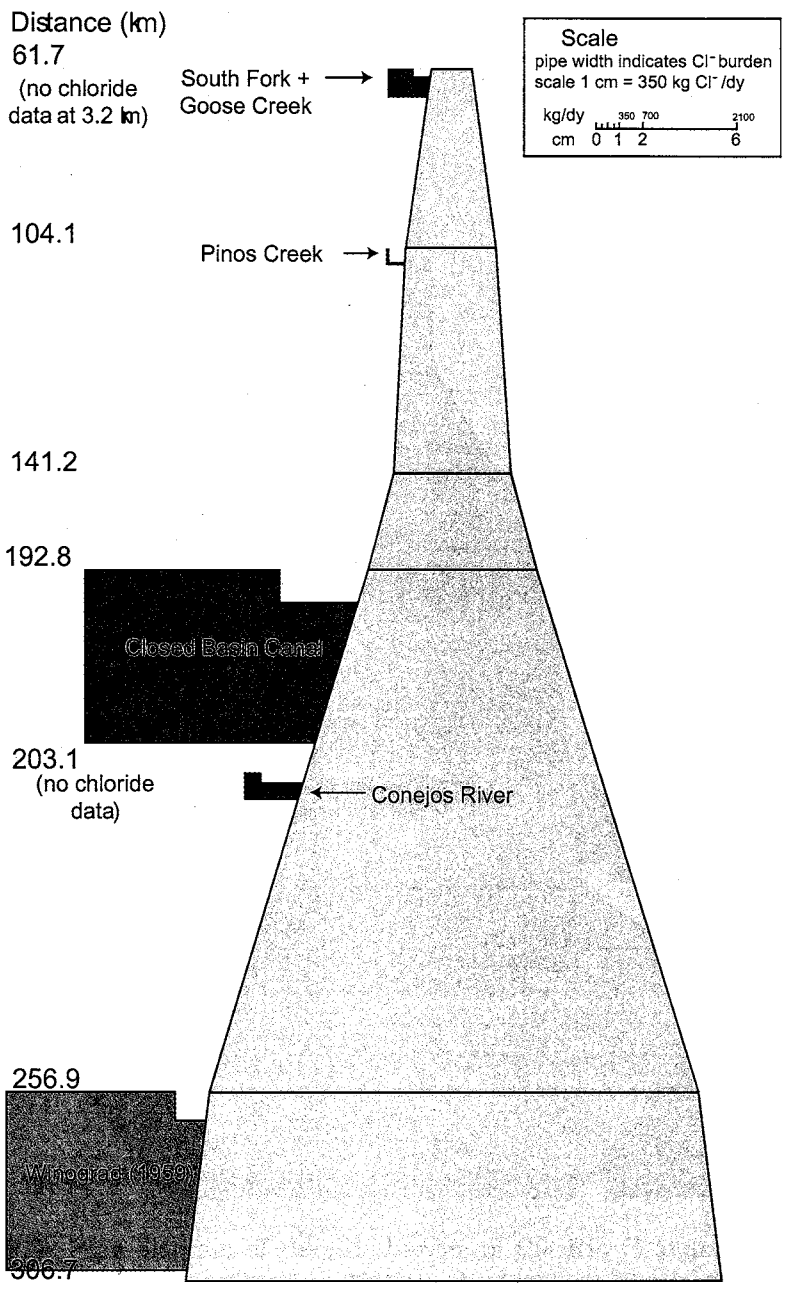

Figure F.4: Pipe diagram of chloride burden of the Rio Grande, its modeled tributaries and diversions, January 2002 (kg dy^{-1}). River distance 3.2 - 306.7 km.

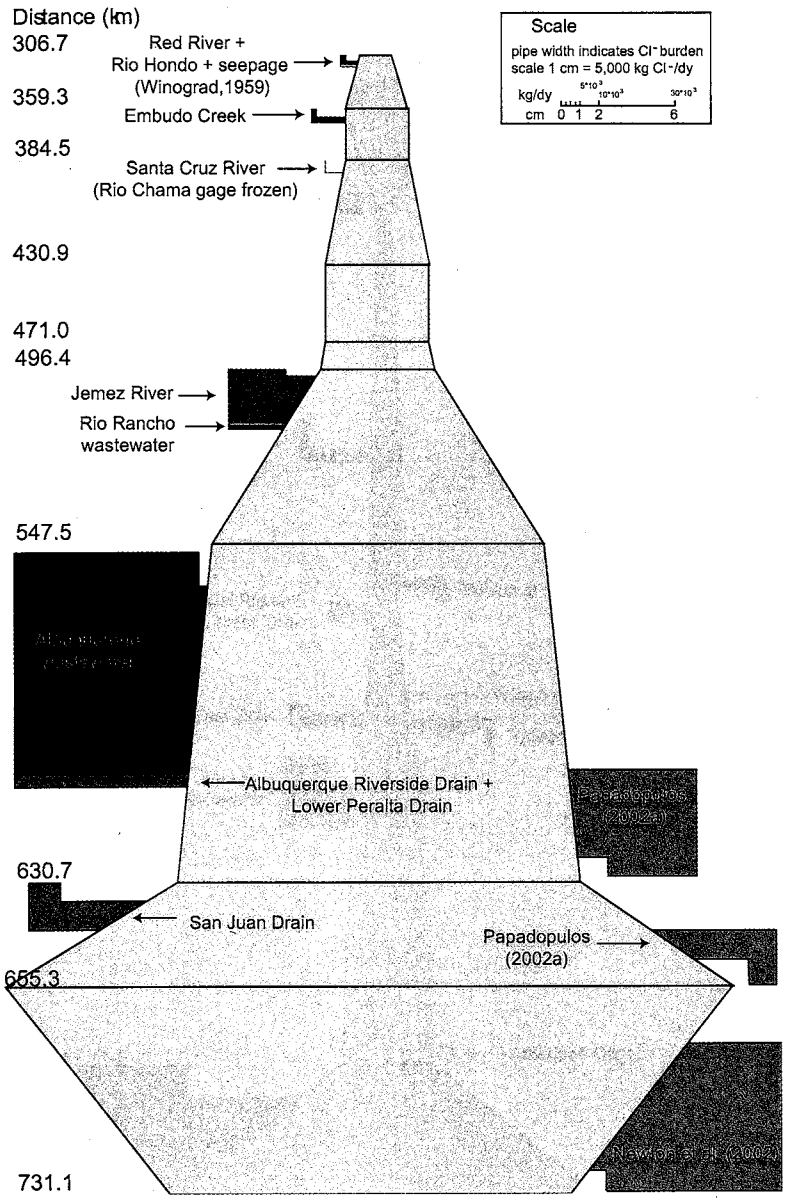

Figure F.5: Pipe diagram of chloride burden of the Rio Grande, its modeled tributaries and diversions, January 2002 (kg dy^{-1}). River distance 306.7 - 731.1 km. The chloride burden at San Acacia (655.3 km) is diminished with respect to the other chloride burdens in the diagram in order to fit on the page. See Figure F.1 for full legend.

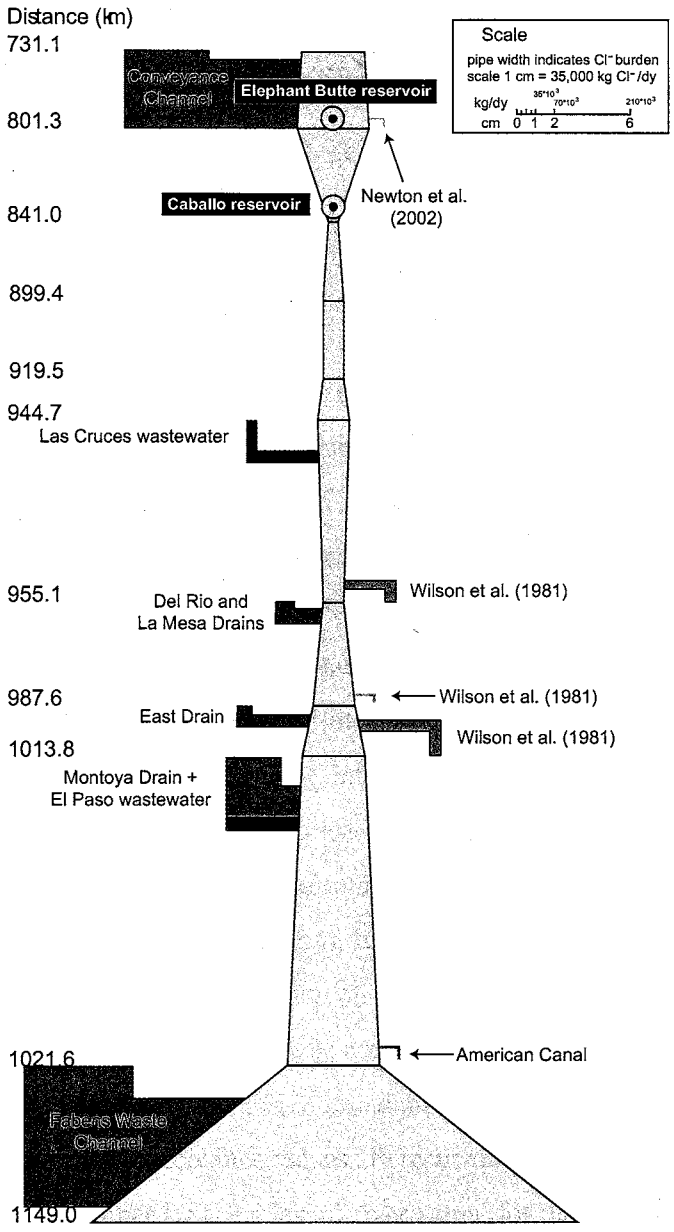

Figure F.6: Pipe diagram of chloride burden of the Rio Grande, its modeled tributaries and diversions, January 2002 (kg dy^{-1}). River distance 731.1 - 1149.0 km. See Figure F.1 for full legend.

APPENDIX G

CALCULATED WATER AND CHLORIDE BURDEN IMBALANCES FOR THE DETAILED MASS BALANCE MODELS

This appendix contains August 2001 and January 2002 river discharges, river chloride burdens, and water and chloride burden imbalances calculated using the equations described in Chapter 9. Water imbalances were the calculated residuals of the water balance equation (V_n) at each gaging station. A positive imbalance indicates an excess; a negative imbalance indicates a lack. For most gaging intervals, V_n was assumed to be the amount of evapotranspiration within the interval, and should be greater than zero to make sense in the mass balance equation. For gaging intervals terminating at reservoir outlets (471.0, 801.3 and 841.0), pan evaporation data was used as the evapotranspiration term and V_n was assumed to be equivalent to the stored water released into (or removed from) the river. Gaging interval burden imbalances were calculated as the sum of all sampling interval imbalances within the gaging interval. A positive imbalance indicates a lack; a negative imbalance indicates an excess. Note that the signs of the chloride imbalance values follow the opposite convention as the water imbalance values. Percent imbalances were calculated by dividing the imbalance by the relevant river value (for discharge or burden) and multiplying by 100. Discharge at El Paso (1021.6 km) was calculated by subtracting gaged Acequia Madre diversions from the gaged river discharge below

American dam (1017.0 km). Discharge at this location was calculated so that the discharge data would correspond with the sampling location at 1021.6 km. Detailed tributary and diversion flow and chloride burden data is presented in Appendix E.

Table G.1: August 2001 river discharge, tributaries, and diversions (and pan evaporation at reservoirs) and calculated water imbalances by gaging interval. Empty boxes in the tributary/diversion columns indicate that there were no modeled tributaries/diversions within the gaging interval.

distance (km)	discharge ($m^3\ s^{-1}$)	tributaries ($m^3\ s^{-1}$)	diversions ($m^3\ s^{-1}$)	pan evap ($m^3\ s^{-1}$)	V_n ($m^3\ s^{-1}$)	percent imbalance
3.2	5.8					
61.7	21.1				-15.28	-72
104.1	25.5	4.73	0.90		-0.53	-2
141.2	5.1	0.76	18.32		2.79	54
192.8	2.7		2.65		-0.27	-10
203.1	2.7		1.21		-1.15	-43
256.9	1.8	0.04			0.95	53
306.7	4.0	0.04			-2.22	-55
359.3	8.4	3.45			-0.91	-11
384.5	10.4	2.18			0.14	1
430.9	16.6	9.06			2.86	17
471.0	19.2		5.89	0.33	8.79	46
496.4	21.8				-2.55	-12
547.5	12.4	5.49	10.85		4.01	32
630.7	8.2	12.19	15.69		0.74	9
655.3	11.2	4.25	1.19		-0.02	0
731.1	7.2		6.46		-2.42	-34
801.3	45.3	8.12	0.96	6.96	37.89	84
841.0	50.7			1.53	6.91	14
899.4	43.5	0.59	7.08		0.65	1
919.5	35.6		8.72		-0.76	-2
944.7	38.7				-3.17	-8
955.1	16.8	0.38	19.70		2.61	16
987.6	18.8	3.17			1.22	6
1013.8	27.7	1.13			-7.81	-28
1021.6	0.3	3.57	23.95		7.02	2339
1149.0	5.1	3.20	5.63		-7.20	-142

Table G.2: January 2002 discharge, tributaries, and diversions (and pan evaporation at reservoirs) and calculated water imbalances by gaging interval. Empty boxes in the tributary/diversion columns indicate that there were no modeled tributaries/diversions within the gaging interval.

distance (km)	discharge ($m^3\ s^{-1}$)	tributaries ($m^3\ s^{-1}$)	diversions ($m^3\ s^{-1}$)	pan evap ($m^3\ s^{-1}$)	V_n ($m^3\ s^{-1}$)	percent imbalance
3.2	0.1				na	na
61.7	3.1				-3.04	-98
104.1	4.5	1.10			-0.31	-7
141.2	4.4	0.14			0.28	6
192.8	4.7				-0.28	-6
256.9	6.7	1.75			-0.23	-3
306.7	7.2	2.26			1.73	24
359.3	12.3	1.66			-3.46	-28
384.5	12.5	0.93			0.71	6
430.9	15.8	0.20			-3.02	-19
471.0	15.3			0.09	-0.42	-3
496.4	17.1				-1.87	-11
547.5	15.5	0.38			1.96	13
630.7	16.1	3.00	3.87		-1.44	-9
655.3	19.8	1.23	0.63		-3.08	-16
731.1	13.6		7.51		-1.35	-10
801.3	9.4	6.17	0.20	2.10	-8.09	-86
841.0	1.0			0.22	-8.15	-800
899.4	1.2				-0.20	-16
919.5	1.2				0.03	2
944.7	1.2				-0.03	-2
955.1	1.0	0.31	0.46		0.02	2
987.6	2.1	0.96	0.25		-0.30	-15
1013.8	2.4	0.23	0.46		-0.58	-24
1021.6	2.8	1.10	0.10		0.65	23
1149.0	4.6	2.55			0.70	15

Table G.3: August 2001 calculated chloride burden and chloride imbalances by sampling and gaging interval, Rio Grande Reservoir (3.2 km) - Albuquerque (547.5 km).

distance (km)	river burden (kg dy^{-1})	sampling imbalance (kg dy^{-1})	gaging imbalance (kg dy^{-1})	percent imbalance
3.2	142	na		
23.8		333		
40.8		10		
50.3		1095		
61.7	667	-914	525	79
79.5		56		
104.1	1486	350	406	27
115.3		-210		
130.0		150		
141.2	289	-174	-234	-81
155.6		424		
192.8	816	468	892	109
203.1	1621	480	480	30
225.2		461		
243.5		-459		
256.9	1382	-245	-244	-18
306.7	1474	-732	-732	-50
332.5		1587		
359.3	5165	442	2029	39
384.5	5745	-24	-24	0
393.9		-354		
407.4		-304		
415.3		-270		
430.9	9384	199	-730	-8
471.0	8078	1168	1168	14
496.4	10038	1960	1960	20
514.8		-4862		
533.4		-172		
547.5	9714	-3279	-8313	-86

Table G.4: August 2001 calculated chloride burden and chloride imbalances by sampling and gaging interval, Albuquerque (555.6 km) - Caballo Reservoir (841.0 km).

distance (km)	river burden (kg dy^{-1})	sampling imbalance (kg dy^{-1})	gaging imbalance (kg dy^{-1})	percent imbalance
555.6		-16543		
564.9		12014		
570.0		5510		
582.9		410		
601.1		-279		
614.7		-652		
630.7	15928	557	1017	6
642.9		-194		
655.3	26270	3617	3423	13
671.8		807		
679.3		2179		
686.3		-322		
696.4		1014		
723.6		2988		
731.1	18967	1654	8320	44
738.8		-2715		
747.5		-1522		
772.4		-10120		
780.2		-13783		
791.4		-5755		
797.2		-1756		
801.3	204765	176866	141217	69
806.6		-19347		
813.0		40917		
830.2		1931		
838.5		-10370		
841.0	237497	19600	32732	14

Table G.5: August 2001 calculated chloride burden and chloride imbalances by sampling and gaging interval, Arrey (845.6 km) - Ft. Quitman (1149.0 km).

distance (km)	river burden (kg dy^{-1})	sampling imbalance (kg dy^{-1})	gaging imbalance (kg dy^{-1})	percent imbalance
845.6		15989		
852.3		4467		
858.7		-3929		
874.3		2745		
891.3		7458		
899.4	227745	-8137	18593	8
912.3		7678		
919.5	192640	4419	12097	6
929.9		11861		
935.5		4641		
944.7	218870	9728	26230	12
955.1	94743	-19654	-19654	-21
966.1		1876		
979.6		-2810		
987.6	130387	3363	2429	2
997.6		26311		
1005.4		21940		
1013.8	204179	16210	64461	32
1021.6	2557	-64039	-64039	-2504
1034.5		22900		
1047.0		235686		
1060.1		779351		
1072.9		2.15E+06		
1085.8		1.29E+07		
1098.8		3.22E+07		
1112.5		3.46E+08		
1126.0		8.87E+08		
1139.1		2.00E+09		
1149.0	371887	-3.29E+09	297410	80

Table G.6: January 2002 calculated chloride burden and chloride imbalances by sampling and gaging interval, Rio Grande Reservoir (3.2 km) - Albuquerque (547.5 km).

distance (km)	river burden (kg dy^{-1})	sampling imbalance (kg dy^{-1})	gaging imbalance (kg dy^{-1})	percent imbalance
3.2	na	na	na	
23.8		na		
40.8		na		
50.3		na		
61.7	197	na	na	
79.5		108		
104.1	493	71	179	36
115.3		18		
130.0		-3		
141.2	629	107	122	19
155.6		71		
192.8	971	270		
203.1	na	na	na	na
225.2		343		
256.9	2644	168	853	32
306.7	2910	-651	-651	-22
332.5		1038		
359.3	5969	1289	2327	39
384.5	5807	-489	-489	-8
393.9		586		
407.4		352		
415.3		1376		
430.9	10292	2072	4385	43
471.0	10109	-183	-183	-2
496.4	11402	1293	1293	11
514.8		-3037		
533.4		8852		
547.5	31627	8782	14597	46

Table G.7: January 2002 calculated chloride burden and chloride imbalances by sampling and gaging interval, Albuquerque (555.6 km) - Caballo Reservoir (841.0 km).

distance (km)	river burden (kg dy^{-1})	sampling imbalance (kg dy^{-1})	gaging imbalance (kg dy^{-1})	percent imbalance
555.6		-22230		
564.9		2497		
570.0		2532		
582.9		13603		
601.1		-5116		
614.7		-1292		
630.7	38736	6985	-3021	-8
642.9		-2074		
655.3	81092	42776	40702	50
671.8		-16372		
679.3		-1453		
686.3		-1350		
696.4		-2123		
712.6		915		
723.6		3666		
731.1	45254	3949	-12767	-28
738.8		-7579		
747.5		251		
772.4		-762		
780.2		-11734		
791.4		500		
797.2		-708		
801.3	45598	-35064	-55096	-121
806.6		23862		
813.0		22705		
830.2		-19589		
838.5		25737		
841.0	7315	-32432	20283	277

Table G.8: January 2002 calculated chloride burden and chloride imbalances by sampling and gaging interval, Arrey (845.6 km) - Ft. Quitman (1149.0 km).

distance (km)	river burden (kg dy^{-1})	sampling imbalance (kg dy^{-1})	gaging imbalance (kg dy^{-1})	percent imbalance
845.6		5489		
852.3		14674		
858.7		7774		
874.3		5080		
891.3		14496		
899.4	12736	-100658	-53145	-417
912.3		528		
919.5	14293	1029	1557	11
929.9		4215		
935.5		353		
944.7	19246	384	4953	26
955.1	16306	-965	-965	-6
966.1		1874		
979.6		3413		
987.6	29615	215	5502	19
997.6		4200		
1005.4		3009		
1013.8	39040	2900	10109	26
1021.6	64414	-437	-437	-1
1034.5		-5577		
1047.0		-11663		
1060.1		14597		
1072.9		-408		
1085.8		-619		
1098.8		-231		
1112.5		148415		
1126.0		-16128		
1139.1		-1967		
1149.0	328467	45813	172231	52

APPENDIX H

ANALYSIS OF THE DETAILED INSTANTANEOUS MASS BALANCE MODELS

After solving the equations for the detailed water, chloride, and bromide mass balance models for August 2001 and January 2002 (see Chapter 9), the resulting chloride imbalances were systematically examined at each sampling station with distance downstream in an attempt to determine their causes. The chloride, bromide, and gaging data were kept in mind as clues indicating salinization processes. Here the imbalances are analyzed by hydrogeologic region with distance downstream. Imbalances within 2-5% of the local river chloride burden were generally considered to be within the error of the gaging and chloride measurements.

H.1 Colorado headwaters - San Luis valley

Between the first sample below Rio Grande Reservoir (3.2 km) and Del Norte (104.1 km), river discharge increased 5-fold in August 2001 and increased by over an order of magnitude in January 2002. The chloride and bromide concentrations remained relatively constant through this reach and chloride imbalances were largely positive during August 2001, suggesting that low-chloride water addition was unaccounted for. Although they were smaller in magnitude, chloride imbalances were also positive for this reach during January 2002, though with little consistent trend in chloride or bromide concentrations.

Goose Creek and the South Fork of the Rio Grande were the only gaged inputs, and there were small gaged agricultural diversions into the Anaconda Ditch and the Minor Ditch during August 2001. The water imbalance term was particularly high in August 2001. It is likely that chloride imbalances here were due to input of ungaged headwaters tributaries. Such tributaries would have high flows during the summer but would probably have little runoff during the winter, which could explain the seasonal differences in the magnitude of the water and chloride imbalances.

Between Del Norte (104.1 km) and Monte Vista (141.2 km), river discharge decreased by 80% in August 2001 due to agricultural diversions. During January 2002, no agricultural diversions took place and river discharge remained nearly constant. The chloride and bromide concentrations remained stable in both seasons. It is possible that the negative chloride imbalances in August 2001 represented excess chloride due to ungaged agricultural diversions, though this probably did not explain most of the error. More likely, the error was the effect of model sensitivity to the large change in river discharge. Furthermore, the high water imbalance in August 2001 resulted in estimation of a large evapotranspiration component (e), which may have over-concentrated chloride in the model and caused a negative balance. The salt and water balances were smaller in magnitude in January 2002 when the water balance was better constrained. In both seasons, part of the negative imbalance may have been due to ungaged seepage out of the river [*Crouch*, 1985].

Between Monte Vista (141.2 km) and Alamosa (192.8 km), river discharge decreased by half in August 2001, mostly due to agricultural diversions.

The chloride concentration doubled in August 2001, and it increased by 30% in January 2002 when the discharge remained nearly constant. The Cl/Br ratio remained nearly constant in August 2001, though it dropped by 50% in January 2002. This suggests a high-chloride, low-Cl/Br input, but without any gaged tributaries in this reach, it was difficult to attribute the positive chloride balance during both seasons to any particular cause. Part of the chloride imbalance may have been due to shallow ground water movement into the river [*Crouch*, 1985].

Input of the high-chloride, low-Cl/Br waters of the Closed Basin Canal was evident between Alamosa (192.8 km) and Lobatos (256.9 km) in both seasons, with the chloride concentration doubling but the Cl/Br ratio remaining relatively unchanged in August 2001 and decreasing in January 2002. Positive chloride imbalances between Alamosa (192.8 km) and the river just upstream of the head of the Rio Grande gorge (225.2 km) and a significant increase in chloride concentration during both winter and summer suggest ground water input in this region of the San Luis valley where shallow groundwater discharges to the surface [*Crouch*, 1985]. Negative chloride imbalances between the head of the Rio Grande gorge (243.5) and Lobatos (256.9 km) in August 2001 indicate chloride losses that were unaccounted for, which could have been due to river loss to shallow ground water as the river begins incising into the Taos plateau. It is unclear why chloride imbalances were positive near Lobatos in January 2002.

H.2 Lobatos - Cochiti Lake

Lobatos (256.9 km) to Cerro (306.7 km) was a gaining reach August 2001, with discharge doubling during August 2001 and increasing less dramatically during January 2002. Seepage into the river of shallow, rapidly moving dilute ground waters that are recharged in the surrounding Jemez and Sangre de Cristo mountains was documented by *Winograd* [1959]. Seepage calculations based on this observation were consistent with the drop in chloride concentration during August 2001, and they accounted for most of the chloride mass flux in the river during that sampling season. However, the chloride concentration remained constant through this reach in January 2002 and there was a negative salt balance that was difficult to explain given the lack of gaged inputs or outputs.

Between Cerro (306.7 km) and the Taos Junction bridge (359.3 km), river discharge significantly increased in January and August, though chloride concentration only increased during the summer. Several tributaries entered the river in this reach, although it was difficult to explain the August 2001 increase in chloride concentration because the tributaries had low chloride concentrations. *Winograd* [1959] noted shallow groundwater seepage into the river in this reach as well. Though a seepage calculation based on *Winograd* [1959] was performed for this reach, salt imbalances were positive in both seasons and the calculation may not have accounted for the total shallow ground water recharge. The chloride concentration increase and marked decrease in the Cl/Br ratio just below the confluence of the Rio Hondo (332.5 km) during both seasons may have been due to mixing of river water with geothermal waters sur-

facing in springs along the banks of the river. Though the Cl/Br ratios of these springs are unknown, *Witcher* [1995] noted the presence of local low-Cl/Br, high-bromide hot springs at Ojo Caliente, 30 km west.

Between the Taos Junction bridge (359.3 km) and Embudo Station (384.5 km), chloride and bromide concentrations did not change systematically during either field season, though discharge increased during both. The chloride imbalance was negative for both seasons, though the error was fairly small (1-8%).

There was little net change in the chloride concentration or Cl/Br ratio between Embudo Station (384.5 km) and Otowi (430.9 km) during August 2001, though river discharge nearly doubled due to the input of the Rio Chama, the largest tributary of the Rio Grande. The local 25% increase in Cl/Br ratio between San Juan Pueblo and Santa Cruz in August 2001 was probably also due to the relatively high-Cl/Br Rio Chama input. Though there were certainly ungaged summer agricultural diversions in this region in August 2001, the negative salt balance during this time was probably due to model sensitivity to the large water input without a corresponding increase in chloride concentration. In January 2002, chloride concentration increased nearly 50% in this distance with little systematic change in the Cl/Br ratio, though there was a 30% discharge increase that was mostly due to the Rio Chama. It was unclear why the Cl/Br ratio locally increased upstream of the input of the Rio Chama in January 2002. Rio Chama input could not be included in the January 2002 model because the Rio Chama gage was frozen and gaging data was unavailable, though the river was observed to be flowing. The positive chlo-

ride imbalance during January 2002 was one-third of the Rio Chama chloride burden in August 2001, indicating that the January imbalance was probably partly an artifact of missing data.

Between Otowi (430.9 km) and the outlet of Cochiti Lake (471.0 km), discharge increased 20% but chloride concentration decreased 30% in August 2001. The low chloride value at the reservoir outlet may have been due to release of dilute pre-irrigation season headwater recharge, though the residence time of the reservoir during 2001 and 2002 was calculated to be only about 1 month (see Chapter 3). The positive chloride imbalance during August 2001 was probably due to model sensitivity to this anomalously low value. During January 2002 the chloride concentration, Cl/Br ratio, and discharge were nearly constant through this reach, and the chloride mass balance was nearly satisfied.

H.3 Cochiti Lake - Bernardo

Between Cochiti Lake (471.0 km) and San Felipe (496.4 km), river discharge increased by 10% and chloride concentration remained nearly constant in both August 2001 and January 2002. The Cl/Br ratio increased by 25% in August 2001. In both seasons, 2 m^3 s^{-1} of water entering the Rio Grande in this reach were unaccounted for, and there was corresponding 10-20% positive chloride imbalance. Many ungaged agricultural drains returned to the river in this region, which probably could have accounted for this missing chloride and water. Increase in the Cl/Br ratio in the summer may have indicated that drain return flows brought a small amount of brine-influenced waters into the river.

From San Felipe (496.4 km) to Albuquerque (547.5 km) in August 2001, the river lost about half of its discharge, though its chloride concentration doubled. There was only a 10% decrease in discharge between these two gaging stations in January 2002, though chloride concentration also doubled. The water imbalance was high (20-30% of the river discharge in the summer; 15% in the winter) in this reach during both seasons. The negative chloride balance at Bernalillo (514.8 km) during both seasons may have reflected a water and chloride loss through riverbed seepage, as the river is known to be losing there [*Veenhuis*, 2002]. Furthermore, the models were sensitive to the estimation of the chloride addition of the Jemez River: reducing the estimated chloride concentration by 30% from 166 mg L^{-1} to 103 mg L^{-1} accounted for 80% of the excess chloride between San Felipe (496.4 km) and Bernalillo (514.8 km) in the August 2001 model. Given the high variability of Jemez River chloride concentration, it is likely that the estimated Jemez River burdens caused part of the large negative chloride imbalances.

The chloride concentration increased during both seasons between Bernalillo (514.8 km) and Alameda (533.4 km) downstream of the input of the Rio Rancho wastewater treatment plant effluent, though the increase was more pronounced during January 2002. This effluent input did not account for all of the winter chloride concentration increase, resulting in a positive chloride imbalance in January 2002. On the other hand, in August 2001 the chloride imbalance downstream of the wastewater effluent was negative, indicating that too much chloride was accounted for upstream of Alameda (533.4 km). Though the chloride burden contributed by wastewater effluent was estimated from the historical record, the model calculations were not sensitive to this estimation

and it is unlikely that it was the cause of the salt imbalance in either season. Additionally, the August 2001 model was not particularly sensitive to the estimated chloride concentrations of the agricultural return flows, and there were no gaged flowing drains returning to the river between San Felipe and Albuquerque in January 2002. This leaves the cumulative chloride imbalances between these two gaging stations difficult to explain in either season, particularly since they were of opposite signs in the summer and winter.

Between Albuquerque (547.5 km) and Bernardo (630.7 km), the chloride concentration doubled and the Cl/Br ratio increased by 25%. In January 2002, chloride concentration increased by 20% and the Cl/Br ratio remained nearly constant. Discharge decreased by 30% in the summer and remained stable in the winter. In this gaging interval, most water and chloride outputs occurred by agricultural diversion at the Isleta diversion dam as well as by riverbed seepage [*Papadopulos and Associates*, 2002a]. Chloride additions to the river were dominated by input from the Southside Water Reclamation Plant (SWRP), with agricultural return flows accounting for about half of the chloride input. During August 2001, the addition of chloride to the river by the SWRP in Albuquerque was not observed at the sampling station immediately below its input location just south of the Rio Bravo bridge (550.0 km). However, the chloride concentration in the river doubled and the Cl/Br ratio increased by 30% between the Route 550 bridge (555.6 km) and the Route 25 bridge (564.9 km). This was probably due to lack of mixing in the river. In the August 2001 model, a negative chloride burden (indicating an excess of salt) persisted downstream of the wastewater plant, even when it was assumed that the effluent entered the river between the Rt. 550 and Rt. 25 bridges rather

than at its actual discharge point upstream of the Rio Bravo bridge. Closer examination of the estimated chloride burden of the effluent showed that its value of almost 19,000 kg dy^{-1} is at the high end of the range of effluent chloride burden values from 1999-2003 (see Chapter 5). It is likely that the effluent chloride contribution to the river was overestimated for August 2001. During January 2002, a negative chloride balance of the same magnitude exists between Albuquerque (547.5 km) and the Rt. 25 bridge because the effluent chloride signal was not seen in the river until Los Lunas (582.9 km). It was difficult to determine the change in the Cl/Br ratio in the river due to the effluent in January 2002 because of analytical errors in the bromide analysis at Los Lunas.

Between Isleta (570.0 km) and Belen (601.1 km) in August 2001, the chloride concentration and the Cl/Br ratio remained essentially constant. This reach showed chloride imbalances on the order of the seepage calculations that were included in the model based on *Papadopulos and Associates* [2002a]. The model was sensitive to the estimations of seepage flow out of the river here, which probably caused the imbalances. During January 2002, the chloride imbalance of this reach was positive and of the same magnitude as the SWRP effluent, again reflecting an artifact of sampling the unmixed river.

At Bernardo (630.7 km) in January 2002, there was a positive chloride imbalance much larger than the order of magnitude of the seepage calculations. With no notable chloride concentration or Cl/Br increase, it is difficult to explain this chloride deficiency at Bernardo. Examining the terms in the chloride balance equation individually, it seems that the biggest error in chloride im-

balance at Bernardo in both seasons was caused by incorrect calculation of evapotranspirative concentration of chloride. It is unclear why this calculation should be so erroneous since the water imbalance is only 10% of river discharge throughout the gaging interval.

H.4 Bernardo - Elephant Butte Reservoir

Between Bernardo (630.7 km) and La Joya (642.9 km), there was no significant change in the chloride concentration or Cl/Br ratio during August 2001; chloride concentration and Cl/Br ratio decreased by 10% in January 2002. The imbalance was negative in both seasons, though is was only 1-5% of the total river chloride burden. The model is in fact highly sensitive to the estimated chloride concentration of the Lower San Juan Riverside Drain that enters the river above La Joya, and changing its concentration by several mg L^{-1} easily rectifies the imbalance.

Between La Joya and San Acacia (655.3 km), there was a significant (20% in August 2001; 50% in January 2002) jump in chloride concentration in both seasons that was sustained downstream. The Cl/Br ratio increased as well: 10% in August 2001 and 30% in January 2002. This resulted in a large positive chloride imbalance between La Joya (642.9 km) and San Acacia (655.3 km) during both August 2001 and January 2002. Given that San Acacia is a known location of ground water discharge [*Anderholm*, 1987; *Wilkins*, 1998] and given the discovery of the San Acacia pool (see Chapter 7), this imbalance was probably due to addition of subsurface brine.

Brine addition was estimated in two ways. The discharge of water

necessary to account for the chloride imbalance at San Acacia was first calculated using a simple equation:

$$V_{gw} = \frac{I_x}{C_{gw}} \tag{H.1}$$

where V_{gw} is the groundwater discharge and C_{gw} is the assumed chloride concentration of ground water. I_x is the chloride flux imbalance at river sampling location x. I_x is also the ground water chloride mass flux in this model, which assumes that the entire mass flux imbalance is due to brine input. This V_{gw} was compared to the ground water discharge calculated by simultaneously solving the chloride and bromide equations of the detailed mass balance model (Chapter 9). The ground water chloride mass flux was calculated from this model by multiplying the estimated ground water discharge by the assumed end member chloride concentration. In the simple model, the brine chloride concentration is directly proportional to the ground water chloride flux, and increasing the brine end member chloride concentration results in higher brine chloride mass fluxes. In the complex model, the Cl/Br ratio of the brine end member must be changed in order to change the calculated ground water chloride mass flux.

Both methods of solving for the ground water discharge were performed several times assuming different chloride and bromide concentrations of the ground water end member. (Table H.1).

Table H.1: Ground water discharges and chloride fluxes calculated for August 2001 (X01) and January 2002 (W02) at locations of documented ground water discharge, using simple and complex models (see text). SanAc= San Acacia, TorC= Truth or Consequences, Wburg= Williamsburg, Seldon= Seldon canyon, Lburg=Leasburg, and Sunland= Sunland Park. Ground water chemistries were estimated based on published and field values, indicated on the table by a citation (SAP= San Acacia Pool; W(1995)= *Witcher* [1995], W(1981)= *Wilson et al.* [1981]). Modifications of the published values were used to show the range of possible ground water fluxes.

location	season	river Cl imbalance (kg dy^{-1})	chemistry source	ground water chemistry Cl (mg L^{-1})	Br (mg L^{-1})	Cl/Br (wt/wt)	gw discharge simple (m^3 s^{-1})	gw discharge complex (m^3 s^{-1})	gw Cl burden (kg dy^{-1})
SanAc	X01	3617	SAP	32300	28	1154	0.001	0.001	2017
SanAc	X01	3617		20000	17	1154	0.002	0.001	2017
SanAc	X01	3617		20000	47	430	0.002	0.002	3614
SanAc	W02	42776	SAP	32300	28	1154	0.015	0.008	21939
SanAc	W02	42776		20000	17	1154	0.025	0.013	21935
SanAc	W02	42776		20000	37	540	0.025	0.025	42976
TorC	W02	23862	W(1995)	1339	0.91	1477	0.206	0.286	33051
TorC	W02	23862		1339	0.67	2000	0.206	0.249	28794
TorC	W02	23862		1339	0.74	1800	0.206	0.259	30006
Wburg	X01	39899	W(1995)	1339	0.91	1477	0.354	0.492	56860
Wburg	X01	39899		1339	0.67	2000	0.354	0.449	51887
Wburg	W02	22705	W(1995)	1339	0.91	1477	0.196	0.535	61911
Wburg	W02	22705		2000	1.0	2000	0.131	0.280	48403
Seldon	W02	528	W(1995)	1709	1.07	1604	0.004	0.001	152
Seldon	W02	528		1707	3.4	502	0.004	0.004	517
Lburg	X01	4419	W(1995)	1707	1.1	965	0.030	-0.061	-9039
Lburg	W02	1029	W(1995)	1709	1.07	1604	0.007	0.040	5839
Lburg	W02	1029		1707	0.85	2000	0.007	0.036	5350
Sunland	X01	16210	W(1981)	3000	7.8	385	0.063	0.062	16171
Sunland	W02	2900	W(1981)	3000	11	268	0.011	0.011	2947

The brine end member was first assumed to have a chemistry equivalent to that of the San Acacia pool. Because the brine in this pool has probably been significantly evaporated since its discharge from the subsurface, a second less-concentrated end member with the same Cl/Br ratio as the San Acacia pool was tried. A third brine end member with a lower Cl/Br ratio was used as well. Using these three end members in both models, calculations of ground water discharge varied between 0.001 and 0.025 $m^3\ s^{-1}$.

For a given end member chemistry, the ground water fluxes calculated from the simple model compared favorably with those calculated using the complex model. Ground water discharges were calculated to be an order of magnitude greater in the winter than in the summer. By definition, the ground water chloride mass fluxes calculated by the simple model account for 100% of the chloride imbalance at San Acacia. Using a relatively low Cl/Br ratio for the ground water end member, the chloride mass fluxes calculated with the complex model could accounted for 100% of the river chloride burden imbalance as well. The magnitudes of groundwater inflows calculated using both models are small, which are the expected magnitude of deep ground water seepage to the surface. The calculated brine chloride mass flux in the summer is about the same magnitude as a local drain input, although the estimated brine chloride mass flux in the winter is greater than the output of the Southside Wastewater Reclamation Plant.

River flow at San Acacia in January 2002 was twice as high as flow in August 2001, but the chloride concentration and Cl/Br increase was greater in January 2002 than in August 2001. If the discharge of brine were relatively

constant year-long, it would be expected that higher river flows would dilute the brine inflow and that river salinization would be higher at this location in the summer. The fact that the reverse is true suggests that brine discharge to the river may vary with river flow or other parameters.

Between San Acacia (655.3 km) and San Marcial (731.1 km) in August 2001, the chloride concentration and remained nearly unchanged though the Cl/Br ratio increased by 30%. River discharge decreased by nearly half, and the positive water imbalance was 25-40% of the river discharge. There was a net positive chloride imbalance as well. The chloride imbalances between individual sampling stations from Pueblito (671.8 km) and Tiffany (723.6 km) are also positive, and the imbalance calculations in this reach were of the same order of magnitude as seepage losses. However, the imbalance calculations were not particularly sensitive to the seepage estimates of water and chloride removal based on *Newton et al.* [2002]. This suggests that these imbalances are probably in part due to effects of the large water imbalance in this reach. The negative imbalances between San Marcial (731.1 km) and the Corral site (747.5 km) during August 2001 are probably the artifact of an even larger water imbalance.

Aside from modeling sensitivities, it is likely that the imbalances in this region partially reflect the ungaged water pumped from the Conveyance Channel into the Rio Grande in order to maintain river flows for the silvery minnow. Ungaged pumps are located at Tiffany (723.6 km) and Ft. Craig (738.8 km). Field sampling (Chapter 7) reveals that the Conveyance Channel was a relatively high chloride, high Cl/Br input, and its inflow could explain

the summer increase in river Cl/Br ratio in this reach. The January 2002 data showed little increase in the river chloride concentration or Cl/Br ratio in this area, and net chloride imbalance was negative and greater in magnitude than in the summer. The change from positive to negative chloride balances at San Marcial (731.1 km) during both seasons may partially be an artifact of the change in water imbalance from negative to positive at San Marcial and the accompanying change in evapotranspiration calculations.

The chloride concentration doubled in the Elephant Butte Reservoir narrows (772.4 km) at the upstream end of the reservoir in both seasons, and the Cl/Br ratio increased by about 30% as well. This increase can be attributed mainly to the input of the Conveyance Channel above this point. Salinization of the Conveyance Channel is probably due to interception of geothermal or other subsurface waters upwelling in the southern Socorro basin [*Anderholm*, 1987], as discussed in more detail in Chapter 7.

H.5 Elephant Butte Reservoir - Caballo Reservoir

August 2001 and January 2002 chloride imbalances at the outlet of Elephant Butte Reservoir (801.3 km) reflected transient chloride and water storage effects as explained in Chapter 5. The river chloride burden increased at the outlet of Elephant Butte Reservoir during both seasons. During both August 2001 and January 2002, reservoir storage volume was in a period of decline (Chapter 10) and the reservoir could be expected to have exported stored chloride during this time. Chloride imbalances at the reservoir outlet are due to these unquantified reservoir dynamics.

At Truth or Consequences (806.6 km), the chloride concentration and Cl/Br ratio increased by 50% during January 2002, and the Cl/Br ratio increased by 10% in August 2001. "Hot Springs" was the original name of this town, and it is likely that geothermal waters mix with river waters in this vicinity. *Witcher* [1995] observed geothermal springs with Cl/Br ratios between 546 and 1827 in Truth or Consequences (T or C). Mixing with high chloride, high Cl/Br waters is consistent with positive chloride imbalance in January 2002. As there are no observed low-chloride, low-bromide geothermal waters in the T or C area [*Witcher*, 1995], it is likely that the decrease in chloride and bromide concentrations observed in August 2001 between the outlet of Elephant Butte Reservoir and T or C were anomalous. Instead, it is possible that in August 2001, the geothermal signature was not picked up in the sampling record until Williamsburg, though the further increase in chloride concentration and Cl/Br ratio and the positive chloride imbalance in Williamsburg in January 2002 suggest geothermal mixing may continue downstream of T or C. Estimations of this geothermal input at Williamsburg (August 2001 and January 2002) and Truth or Consequences (January 2002 only) were performed using the two models used for ground water input calculations at San Acacia described above (Table H.1). The geothermal end member chemistry was assumed to be similar to the average of five hot springs and hot wells in T or C for which chloride and bromide data were available [*Witcher*, 1995]. August 2001 calculations at Williamsburg assumed that the bromide concentration at T or C was 0.15 mg L^{-1} (as were all other observed bromide concentrations between Elephant Butte and Caballo Reservoirs during this field season) and the Cl/Br ratio was 324 so that the observed chloride concentration at T or C was preserved.

Calculations at Williamsburg indicated that geothermal inflow ranged between 0.35 - 0.5 $m^3 s^{-1}$ in August 2001, which was about 1% of river flow. In January 2002, estimated geothermal inflow at Williamsburg was 0.13 - 0.54 $m^3 s^{-1}$ or about 3-5% of river flow. Geothermal addition at T or C in January 2002 was calculated to be about 0.2 $m^3 s^{-1}$, which was about 3% of winter river flow. Using these calculated geothermal discharge values, the geothermal chloride mass flux at Williamsburg was overestimated by the complex model by about 30-50%. Geothermal chloride mass flux was overestimated by about 20-30% at T or C. Geothermal input at both locations was consistent with an end member of a higher Cl/Br ratio than the waters observed by *Witcher* [1995].

Downstream of the geothermal input, the chloride concentration remained nearly constant through Caballo Reservoir in August 2001, and there was no consistent chloride concentration or Cl/Br ratio change in January 2002 along this distance. River discharge remained about the same between the outlet of Elephant Butte Reservoir and the outlet of Caballo Reservoir during August 2001 because Caballo Reservoir is a flow-through structure during the irrigation season. River discharge during January 2002 decreased between the two reservoirs, as releases from Elephant Butte Reservoir for hydropower generation were being stored in Caballo Reservoir for the following irrigation season. During January 2002, releases from Caballo were minimal and river discharge decreased 80%. Chloride imbalances in and at the outlet of Caballo Reservoir (841.0 km) most likely reflected transient chloride and water storage effects in both seasons. Given the short residence time of Caballo Reservoir (Chapter 3), its chloride imbalance was more closely related to input and output of water and salts within the previous season rather than to inputs or

outputs on a longer time scale.

H.6 Outlet of Caballo Reservoir - Leasburg

Between the outlet of Caballo Reservoir (841.0 km) and Haynor Ranch (899.4 km), the chloride concentration and the Cl/Br ratio remained fairly constant in August 2001. River discharge decreased by 10% due to agricultural diversions at the Percha diversion dam. The cumulative chloride imbalance in this gaging interval was less than 1%, and chloride imbalances between sampling stations were minimal as well. However, the water imbalance was 15%, suggesting that water input to the river was not accounted for in the model. In January 2002, the river discharge increased by 20% and the chloride concentration steadily increased by 50%, though Cl/Br ratio dropped by 25% between the outlet of Caballo Reservoir (841.0 km) and Placitas (874.3 km). With the major drains (Garfield and Hatch) dry during this season and no significant known ungaged inputs, it is possible that shallow groundwater seepage with a chemistry similar to the Rio Grande could have brought water into the river through this reach during the winter to satisfy the large positive imbalances, with the local decrease in Cl/Br being an anomaly.

Between Haynor Ranch (899.4 km) and the bridge below Leasburg diversion dam (919.5 km), river discharge decreased by 25% in August 2001 due to agricultural diversions. River discharge remained constant in this reach during January 2002. The chloride concentration and Cl/Br ratio remained fairly constant in this gaging interval in August 2001, though in January 2002 the chloride concentration increased nearly 20% and the Cl/Br ratio increased by over 25%. Chloride imbalances were positive at Selden canyon and Leasburg

in January 2002, suggesting an input of salt even where discharge did not seem to increase. Additionally, *Wilson et al.* [1981] and *Nickerson* [1995] observed that this is a gaining reach of the river during the low-flow season, making it a likely place for addition of highly saline waters such as geothermally-influenced waters noted at Radium Springs by *Witcher* [1995].

Ground water addition calculations for January 2002 (Table H.1) indicated that total geothermal input between Selden canyon and Leasburg was 0.001 - 0.04 $m^3 s^{-1}$, about 1-5% of river flow. The geothermal chloride mass flux at Selden canyon in January 2002 was consistent with an input of lower Cl/Br ratio water than the Cl/Br ratios of the waters observed by *Witcher* [1995]. Input of a high-chloride water with a Cl/Br ratio of 502, which is well within the range of common geothermal waters, could account for almost the entire chloride imbalance at Selden canyon. The geothermal chloride flux was significantly overestimated at Leasburg using end members from *Witcher* [1995], and chloride addition there was consistent with addition of higher Cl/Br ratio waters instead. This difference was due to the fact that the chloride concentration and the Cl/Br ratio did not increase by the same percentages at Selden canyon and Leasburg. Though the chloride imbalance was positive at Leasburg in August 2001 and addition of geothermal water was estimated to be about 1% of river flow, geothermal addition was inconsistent with the chloride and bromide mass balance model. The chloride imbalance was negative at Selden canyon in August 2001, which was also inconsistent with geothermal addition. It is possible that high river flow suppresses seepage into the river [*Nickerson*, 1995] such that deep ground water addition was minimal in August 2001 in comparison with January 2002.

H.7 Leasburg - Mesilla

During August 2001, the chloride concentration increased steadily between Leasburg (919.5 km) and Las Cruces (944.7 km). River discharge and the Cl/Br ratio remained nearly constant. The positive chloride imbalances at Hill (929.9 km) and Las Cruces could have been partially accounted for by ungaged drain return flows that entered in this reach, though ungaged flows in the Elephant Butte Irrigation District are generally thought to be small and are not expected to be particularly saline [*James Narvaez,* personal communication 2003]. During January 2002 the chloride concentration increased by 25% and the Cl/Br jumped by 10% at Hill, and the Cl/Br increased another 10% between Hill and Las Cruces. A positive chloride imbalance persisted through the gaging interval during both the summer and winter, though the chloride imbalance was greater in the summer. With no known major tributaries in this reach and no evidence that this is an area of ground water discharge, it is difficult to explain the chloride concentration and the Cl/Br increases in the winter and the positive chloride imbalances in both seasons.

Between Las Cruces and Mesilla (955.1 km), river discharge decreased by 50% in August 2001 due to diversions at the Mesilla diversion dam. The chloride concentration increased slightly and the Cl/Br ratio increased by 10% in January 2002 due to effluent inflow from the Las Cruces wastewater treatment plant, though no noticeable chemistry changes occurred in this reach in August 2001. A negative chloride imbalance was calculated during August 2001, which was probably due to model sensitivity to seepage calculations based on *Wilson et al.* [1981] performed in this reach. The model was insensi-

tive to changes in the estimate of the chloride concentration of the wastewater treatment plant effluent. In January 2002 the chloride concentration decreased slightly, which caused calculation of a negative chloride imbalance in this reach. The winter imbalance was much smaller in magnitude than the summer imbalance, indicating that the seepage estimations were more appropriate for winter conditions. This is expected since the seepage runs of *Wilson et al.* [1981], upon whose work the calculations are based, were performed in the winter as well.

H.8 Mesilla - El Paso

Between Mesilla and Anthony (987.6 km), the chloride concentration increased by 30% and the Cl/Br ratio increased by 10% in August 2001. This was due to return flow from the Del Rio and La Mesa Drains in this reach, both of which had chloride concentrations twice as high as the river and Cl/Br ratios 15% higher than the river. The positive chloride imbalance at Mesquite (966.1) reflected the unexplained increase in chloride concentration and Cl/Br between Mesilla and Mesquite. The chloride imbalances at Berino (979.6 km) and Anthony were negligible. In January 2002, the chloride concentration and the Cl/Br ratio decreased. The Del Rio and La Mesa Drains also ran during this season, though they had a low chloride concentration and low Cl/Br ratio relative to the river during the winter (when the river was undiluted by releases from Elephant Butte Reservoir). Input of these drains probably caused most of the decrease in river chloride concentration and Cl/Br in this reach in January. Positive water and chloride imbalances in this reach in January 2002 suggest that some inputs to the river remained unaccounted for.

Chloride concentration increased slightly between Anthony and Sunland Park (1013.8 km) in August 2001, though the Cl/Br ratio remained nearly constant. River discharge increased about 50%, although the only known input in this gaging interval was the East Drain which accounted for only 10% of inflow. In January 2002, the chloride concentration also increased slightly, though the Cl/Br ratio decreased by 20% over the gaging interval. River discharge increased 10% in the winter, and the water imbalance for both seasons was 25% of river discharge. Input of the East Drain, which had a significantly higher chloride concentration and Cl/Br ratio than the river in both seasons, was probably the cause of increases in river chloride concentration and Cl/Br ratio between Anthony and Canutillo (997.6 km). The positive chloride imbalances in both seasons at Sunland Park, in combination with the increases in chloride concentration and the decreases in Cl/Br ratio, suggest input of saline, low-Cl/Br waters. Ungaged agricultural return flows may have entered in this reach, though in this area the gaged, sampled drains (i.e. the East Drain and Montoya Drain) tended to have higher Cl/Br ratios than the river. *Frenzel et al.* [105 pp. plus plates, 1992] identified this area at the southern end of the Mesilla basin as a region of ground water discharge. Discharging ground waters are known to be saline, though it is unclear whether they are so due to evapotranspirative concentration [*Wilson et al.*, 1981] or to contribution by deep basin brines or geothermal waters [*Frenzel et al.*, 105 pp. plus plates, 1992]. Evapotranspired waters are most likely to have the high chloride concentration and low Cl/Br ratio of the water that seems to be mixing with the Rio Grande near Sunland Park. Using the same two models of ground water addition that have been used at San Acacia, Truth or Consequences, and Selden canyon,

the contribution of a evapotranspired ground water was estimated (Table H.1). The ground water was assumed to have a chloride concentration of 3000 mg L^{-1} as observed in the southern Mesilla basin by *Wilson et al.* [1981], and a Cl/Br ratio 25-50% lower than that of the river. The estimated ground water input for both seasons by both the simple and the complex model was 0.06 - 0.1 $m^3\ s^{-1}$, which was less than 1% of August 2001 river flow and was about 5% of river flow in January 2002. These ground water discharge estimations resulted in ground water chloride mass fluxes that nearly all of the river chloride imbalances. Whether the ground water end member is evaporatively concentrated or has a deeper source, it is very likely that a high-chloride, low Cl/Br water enters the river at Sunland Park.

Between Sunland Park and El Paso (1021.6 km), the chloride concentration increased by 15% during August 2001. The river was nearly emptied in this reach in August 2001, when water was being diverted into the American Canal and the Acequia Madre. In January 2002, the chloride concentration increased by 50%, and river discharge increased by 15%. The Cl/Br ratio remained relatively unchanged in both seasons. The Montoya Drain and the Northwest wastewater treatment plant contributed salt and water to the river in this reach, and during both seasons their chloride concentrations and Cl/Br ratios were higher than that of the river. The large negative chloride imbalance in August 2001 in this gaging interval was probably due to model sensitivity to removal of nearly all water from the system. The chloride imbalance in January 2002 is unaffected by such an artifact and is negligible.

H.9 El Paso - Ft. Quitman

Below El Paso, the chloride concentration tripled in January 2002 and increased by an order of magnitude in August 2001, though the chloride concentration at Ft. Quitman was about the same in both seasons. River discharge increased by 50% (January 2002) - 150% (August 2001) in this reach. Large chloride and water imbalances were calculated between sampling stations in this entire region in August 2001, but no attempt is made to explain them because of the dearth of agricultural return flow gaging data. This makes calculation of a reasonable water balance nearly impossible, and evapotranspiration estimates from the residual of the water balance equations are very much overestimated in August 2001. The chloride imbalances during January 2002 also may be the effect of lack of chloride burden data for saline drains in the area that may still flow in winter.

APPENDIX I

AUGUST 2001 AND JANUARY 2002 DATA ANALYZED IN THIS STUDY

The tables in this appendix include the August 2001 and January 2002 data analyzed in this thesis. The tables here include chloride concentration, bromide concentration, Cl/Br ratio, $\delta^{18}O$, δD, and $^{36}Cl/Cl$ data. Dry sample sites are not included. The "type" category indicates whether a sample location was on the main stem Rio Grande (RG), a drain (D), the Conveyance Channel (CC), or a natural tributary (T). In several headwaters locations in August 2001, identical $^{36}Cl/Cl$ values are reported for multiple sample locations, indicating samples were combined for analysis. Bolded values were below threshold. Blank cells in the tables indicate that data was not collected for that particular parameter. See Appendix J for detailed information about the sample locations as well as field parameters and other analyzed constituents for January 2000 - August 2003. Appendix E includes data used for the August 2001 and January 2002 detailed mass balance models that were not collected during the sampling seasons.

Table I.1: August 2001 data analyzed in this thesis.

type	distance (km)	Cl (mg L^{-1})	Br (mg L^{-1})	Cl/Br (wt/wt)	$\delta^{18}O$ (per mille)	δD (per mille)	$^{36}Cl/Cl * 10^{15}$ (atoms)	^{36}Cl error
RG	3.2	0.28	0.0024	119	-14.2	-98		
RG	23.8	0.49	0.0029	167	-14.1	-101		
RG	40.8	0.28	0.0031	91	-13.9	-98		
RG	50.3	0.65	0.0041	160	-14.1	-100		
RG	61.7	0.37	0.0030	124	-14.1	-99		
RG	79.5	0.45	0.0028	161	-14.1	-100		
RG	104.1	0.68	0.0041	164	-14.0	-98		
RG	115.3	0.61	0.0058	105	-13.6	-99		
RG	130.0	0.78	**0.01**	78	-14.0	-100		
RG	141.2	0.65	0.0057	114	-14.0	-98		
RG	155.6	1.59	0.0084	189	-13.6	-98		
RG	192.8	3.44	0.047	74	-12.8	-95		
RG	203.1	6.98	0.059	119	-12.3	-94		
RG	225.2	10.5	0.075	141	-11.9	-90		
RG	243.5	9.14	0.072	127	-11.3	-87	2587	53
RG	256.9	8.97	0.076	119	-11.2	-86	2587	53
RG	306.7	4.22	0.039	109	-11.8	-90		
RG	332.5	6.54	0.21	31	-13.1	-96		
RG	359.3	7.11	0.052	136	-13.0	-95	2136	59
RG	384.5	6.37	0.035	185	-12.7	-91		
RG	393.9	6.33	0.044	143	-12.7	-90	2136	59
RG	407.4	6.49	0.046	142	-12.6	-92	2136	59
RG	415.3	6.27	0.035	181	-12.0	-88	1318	23
RG	430.9	6.53	0.035	187	-12.1	-88	1318	23

type	distance (km)	Cl (mg L^{-1})	Br (mg L^{-1})	Cl/Br (wt/wt)	$\delta^{18}O$ (per mille)	δD (per mille)	$^{36}Cl/Cl * 10^{15}$ (atoms)	^{36}Cl error
RG	471.0	4.87	0.032	154	-11.8	-86		
RG	496.4	5.34	0.025	214	-11.8	-87		
RG	514.8	9.47	0.027	351	-11.5	-85		
RG	533.4	10.4	0.041	254	-11.6	-86		
RG	547.5	9.07	0.037	244	-11.5	-86	1840	19
RG	555.6	9.41	0.045	208	-11.1	-85		
RG	564.9	19.0	0.064	295	-10.8	-86		
RG	570.0	19.2	0.075	255	-11.5	-86		
RG	582.9	20.1	0.080	251	-11.3	-85	844	18
RG	601.1	21.7	0.10	222	-11.3	-86		
RG	614.7	21.0	0.079	267	-11.1	-86		
RG	630.7	22.6	0.082	277	-10.9	-83		
RG	642.9	23.5	0.10	225	-10.4	-81		
RG	655.3	27.1	0.11	240	-10.4	-81	844	17
RG	671.8	26.7	0.11	243	-10.6	-81		
RG	679.3	28.4	0.10	279	-10.5	-81		
RG	686.3	27.5	0.12	238	-10.1	-81		
RG	696.4	28.1	0.10	270	-10.2	-80		
RG	723.6	31.2	0.10	304	-9.9	-78		
RG	731.1	30.5	0.10	319	-9.8	-77		
RG	738.8	29.1	0.10	304	-10.0	-77		
RG	747.5	29.4	0.10	305	-9.6	-76		
RG	772.4	66.9	0.18	376	-8.8	-73	369	10
RG	780.2	54.0	0.16	348	-7.6	-67		

type	distance (km)	Cl (mg L^{-1})	Br (mg L^{-1})	Cl/Br (wt/wt)	$\delta^{18}O$ (per mille)	δD (per mille)	$^{36}Cl/Cl * 10^{15}$ (atoms)	^{36}Cl error
RG	791.4	53.5	0.16	340	-7.4	-66		
RG	797.2	54.7	0.15	365	-7.2	-65		
RG	801.3	52.3	0.15	356	-7.6	-68	376	10
RG	806.6	47.6	0.12	412	-7.6	-66		
RG	813.0	58.4	0.15	396	-7.6	-67		
RG	830.2	59.8	0.15	388	-7.5	-66		
RG	838.5	57.5	0.15	379	-7.2	-65		
RG	841.0	54.3	0.14	379	-7.2	-64	364	10
RG	845.6	58.0	0.14	401	-7.2	-65		
RG	852.3	59.2	0.14	411	-7.2	-65		
RG	858.7	58.3	0.15	386	-7.1	-64		
RG	874.3	59.2	0.15	406	-7.1	-65		
RG	891.3	62.5	0.17	377	-7.2	-65		
RG	899.4	60.6	0.16	367	-7.2	-64	391	10
RG	912.3	61.9	0.14	429	-7.1	-64		
RG	919.5	62.7	0.15	417	-7.1	-63	356	13
RG	929.9	64.2	0.16	410	-7.3	-64		
RG	935.5	64.4	0.16	415	-7.2	-64		
RG	944.7	65.4	0.15	436	-6.9	-63	372	10
RG	955.1	65.2	0.15	423	-7.0	-64		
RG	966.1	68.2	0.16	438	-7.0	-63		
RG	979.6	73.2	0.16	444	-7.0	-64		
RG	987.6	80.4	0.16	490	-7.1	-64		
RG	997.6	85.1	0.17	508	-7.1	-63		

type	distance (km)	Cl (mg L^{-1})	Br (mg L^{-1})	Cl/Br (wt/wt)	$\delta^{18}O$ (per mille)	δD (per mille)	$^{36}Cl/Cl * 10^{15}$ (atoms)	^{36}Cl error
RG	1005.4	85.5	0.17	494	-6.9	-63		
RG	1013.8	85.3	0.18	482	-7.0	-65	324	10
RG	1021.6	98.7	0.20	495	-7.0	-66		
RG	1034.5	103.3	0.20	511	-6.8	-62		
RG	1047.0	259.5	0.37	696	-8.4	-68		
RG	1060.1	292.8	0.43	686	-8.7	-70		
RG	1072.9	262.0	0.37	712	-8.2	-68	151	7
RG	1085.8	379.3	0.46	821	-7.6	-67		
RG	1098.8	329.1	0.37	896	-7.1	-65		
RG	1112.5	748.3	0.53	1421	-7.5	-67		
RG	1126.0	686.4	0.49	1389	-7.3	-66		
RG	1139.1	507.6	0.43	1185	-7.0	-64		
RG	1149.0	849.0	0.66	1295	-7.1	-65	118	5.0
D	166.0	3.11	0.023	134	-13.4	-97		
D	195	13.3	0.13	106	-12.1	-91		
D	547.5	7.82	0.037	211	-11.8	-89		
D	547.5	9.02	0.041	218	-11.7	-88		
D	601.1	22.8	0.10	226	-11.7	-87		
D	601.1	28.8	0.13	228	-11.6	-87		
D	630.7	27.7	0.11	248	-11.5	-88		
D	696.4	118.9	0.18	678	-11.3	-86		
D	874.8	142.1	0.29	491	-7.8	-68		
D	888.2	136.0	0.25	535	-7.8	-67		
D	973.6	113.1	0.21	544	-7.8	-67		

type	distance (km)	Cl (mg L^{-1})	Br (mg L^{-1})	Cl/Br (wt/wt)	$\delta^{18}O$ (per mille)	δD (per mille)	$^{36}Cl/Cl * 10^{15}$ (atoms)	^{36}Cl error
D	982.8	146.9	0.26	567	-8.2	-72		
D	991.7	130.3	0.23	569	-7.0	-63		
D	1014.0	209.2	0.31	671	-7.7	-67		
D	1080.3	308.6	0.32	955	-7.3	-65		
D	1139.6	966.4	0.92	1050	-7.3	-66		
D	1140.1	1609.7	0.91	1772	-7.0	-65		
CC	671.8	32.1	0.12	274	-11.1	-83		
CC	679.3				-11.1	-85		
CC	686.3	33.6	0.12	281	-11.2	-85		
CC	696.4				-11.3	-85		
CC	712.6	50.0	0.12	410	-11.0	-85		
CC	723.6				-10.8	-84		
CC	731.1	67.0	0.17	398	-10.8	-83	641	18
CC	738.8				-11.0	-85		
T	85.7	1.10	0.0049	226	-14.0	-98		
T	214.6	7.75	0.081	96	-8.9	-78		
T	225.6	1.53	0.017	88	-11.3	-88		
T	318.9	5.33	0.67	8	-13.7	-96		
T	332.5	5.78	0.052	110	-13.6	-95		
T	380.6	3.21	0.013	247	-12.0	-82		
T	409.2	5.80	0.015	392	-11.3	-84		
T	415.3	4.38	0.028	159	-11.5	-81		
T	450.3	4.15	0.011	384	-11.2	-75		
T	637.1	11.0	0.022	511	-4.6	-35		

Table I.2: January 2002 data analyzed in this thesis.

type	distance (km)	Cl (mg L^{-1})	Br (mg L^{-1})	Cl/Br (wt/wt)	$\delta^{18}O$ (per mille)	δD (per mille)
RG	50.3	0.69	0.0059	117		
RG	61.7	0.73	0.0050	147		
RG	79.5	1.09	0.0134	81		
RG	104.1	1.26	0.0076	165	-15.2	-107
RG	115.3	1.33	0.0064	207	-15.1	-106
RG	130.0	1.35	0.0063	214		
RG	141.2	1.66	0.0079	210		
RG	155.6	1.82	0.0089	205	-15.0	-106
RG	192.8	2.41	0.01	227	-15.1	-106
RG	225.2	4.92	0.03	157		
RG	256.9	4.60	0.03	175	-14.8	-105
RG	306.7	4.68	0.02	227	-14.8	-105
RG	332.5	4.95	0.03	170		
RG	359.3	5.61	0.04	144		
RG	384.5	5.36	0.05	119		
RG	393.9	5.63	0.03	163		
RG	407.4	5.55	0.03	190		
RG	415.3	6.40	0.03	185		
RG	430.9	7.56	0.04	170	-13.8	-100
RG	471.0	7.67	0.05	166	-13.2	-96
RG	496.4	7.71	0.05	145		
RG	514.8	8.58	0.06	155		
RG	533.4	16.44	0.07	237		
RG	547.5	23.56	0.08	287	-12.4	-91

type	distance (km)	Cl (mg L^{-1})	Br (mg L^{-1})	Cl/Br (wt/wt)	$\delta^{18}O$ (per mille)	δD (per mille)
RG	555.6	17.40	0.08	222		
RG	564.9	18.82	0.07	264		
RG	570.0	20.05	0.09	229		
RG	582.9	28.67	**0.05**	573	-12.4	-91
RG	601.1	24.37	0.09	265		
RG	614.7	23.08	0.10	238		
RG	630.7	27.84	0.10	267	-12.2	-90
RG	642.9	24.20	0.10	241		
RG	655.3	47.45	0.14	347	-11.8	-89
RG	671.8	37.21	0.12	311		
RG	679.3	36.10	0.11	332		
RG	686.3	35.06	0.11	321		
RG	696.4	33.20	0.12	285		
RG	712.6	33.30	0.11	308		
RG	723.6	35.93	0.12	295		
RG	731.1	38.48	0.12	318	-12.1	-89
RG	738.8	32.58	0.11	303		
RG	747.5	33.44	0.11	307		
RG	772.4	59.36	0.15	398	-11.3	-86
RG	780.2	52.74	0.16	326	-7.8	-68
RG	791.4	54.40	0.15	359	-7.0	-65
RG	797.2	54.63	0.16	343	-7.1	-64
RG	801.3	56.17	0.15	365	-7.0	-65
RG	806.6	85.84	0.16	533	-7.4	-67

type	distance (km)	Cl (mg L^{-1})	Br (mg L^{-1})	Cl/Br (wt/wt)	$\delta^{18}O$ (per mille)	δD (per mille)
RG	813.0	114.33	0.15	762	-7.2	-65
RG	830.2	90.96	0.16	570	-7.1	-64
RG	838.5	123.83	0.17	720	-6.6	-62
RG	841.0	83.10	0.20	422	-7.5	-66
RG	845.6	88.67	0.20	440	-7.6	-65
RG	852.3	104.57	0.22	482		
RG	858.7	111.64	0.32	348		
RG	874.3	111.87	0.35	318		
RG	891.3	121.40	0.29	423		
RG	899.4	121.14	0.31	387	-7.3	-67
RG	912.3	128.07	0.33	390		
RG	919.5	139.18	0.27	507	-7.4	-66
RG	929.9	178.47	0.31	568		
RG	935.5	180.92	0.33	543		
RG	944.7	183.05	0.31	596	-7.5	-66
RG	955.1	180.23	0.29	621		
RG	966.1	182.96	0.27	674		
RG	979.6	160.91	0.24	666		
RG	987.6	165.91	0.29	573		
RG	997.6	185.30	0.32	583		
RG	1005.4	183.64	0.39	475		
RG	1013.8	187.49	0.42	451	-7.8	-68
RG	1021.6	280.27	0.59	477		
RG	1034.5	263.63	0.43	617		

type	distance (km)	Cl (mg L^{-1})	Br (mg L^{-1})	Cl/Br (wt/wt)	$\delta^{18}O$ (per mille)	δD (per mille)
RG	1047.0	218.86	0.37	597		
RG	1060.1	290.83	0.41	705		
RG	1072.9	296.50	0.42	712	-9.1	-74
RG	1085.8	311.58	0.45	699		
RG	1098.8	319.26	0.49	653		
RG	1112.5	697.45	0.81	861		
RG	1126.0	675.39	0.80	842		
RG	1139.1	688.24	0.72	951		
RG	1149.0	824.66	0.84	986	-8.2	-69
D	166.0	19.67	0.19	106		
D	195.0	15.57	0.14	115	-13.8	-99
D	547.5	13.23	0.06	235		
D	547.5	13.02	0.06	219		
D	601.1B	25.61	0.12	217		
D	601.1A	26.18	0.12	225		
D	630.7	28.59	0.12	238		
D	696.4	110.72	0.17	665	-11.3	-85
D	888.2	141.61	0.35	408	-8.1	-68
D	973.6	120.24	0.22	540	-7.9	-69
D	982.8	177.22	0.38	468	-8.7	-73
D	991.7	348.95	0.49	715	-8.5	-71
D	1014.0	341.80	0.53	645	-8.6	-71
D	1080.3	313.38	0.39	811	-9.8	-73
D	1139.6	687.75	0.83	828		

type	distance (km)	Cl (mg L^{-1})	Br (mg L^{-1})	Cl/Br (wt/wt)	$\delta^{18}O$ (per mille)	δD (per mille)
D	1140.1	1325.50	1.37	971		
CC	671.8	99.19	0.17	570		
CC	679.3	47.25	0.15	310		
CC	686.3	40.52	0.16	254		
CC	696.4	49.89	0.14	359		
CC	712.6	54.25	0.14	388		
CC	723.6	96.27	0.17	553		
CC	731.1	105.08	0.18	595	-11.2	-85
CC	738.8	103.72	0.20	525		
T	85.7	1.22	0.0044	274	-15.1	-106
T	225.6	1.16	0.00	263	-14.9	-105
T	318.9	5.38	0.04	123	-14.1	-99
T	332.5	4.82	0.04	128		
T	380.6	4.05	0.07	62	-13.0	-90
T	409.2	13.39	0.05	262	-11.5	-85
T	415.3	5.69	0.02	246		
T	450.3	2.90	**0.01**	290	-11.5	-81

APPENDIX J

DATA FROM SAMPLING SEASONS, JANUARY 2000 - AUGUST 2003

This appendix contains field data and laboratory analyses from January 2000 - August 2003 synoptic sampling trips. The author participated in sample collection from August 2001 - August 2003. Data reported for January 2000 - January 2001 are the results of sample collection by other New Mexico Tech students and some of the details of the data are unclear to the author. In particular, some determinations of distances for January 2000 and August 2000 are thought to be slightly inconsistent with later data. Due to lack of information about this data, it is presented without any attempt to correct such inconsistencies. The San Acacia pool (see Chapter 7) was sampled only once during March 2002, and chemistry data for the pool is included in the August 2002 data tables. San Acacia pool chlorine-36 data is presented in Chapter 7.

Table J.1: Description of sampling locations, latitude, longitude and elevation for January 2000. Latitude, longitude, and elevation of sample RG1 was measured; all other coordinates are estimated from sample maps and the TopoUSA program by DeLorme. All stations are on the main stem Rio Grande.

Distance			Latitude			Longitude			Elevation
(km)	ID	location	Deg	Min.	Sec.	Deg	Min.	Sec.	(m)
766.0	RG1	EB - Red Rock	33	26	25.05	107	9	50.76	1360
772.4	RG2	EB Res. - China Canyon	33	23	1.54	107	10	3.78	1358
774.9	RG3	EB Res. - Mitchell Pt	33	21	58.23	107	10	40.68	1355
780.2	RG4	EB Res. - Monticello Pt	33	18	57.88	107	11	39.4	1356
786.7	RG5	EB Res.	33	15	47.75	107	11	30.22	1360
791.4	RG6	EB Res - Rock Canyon	33	13	43.06	107	12	51.48	1359
797.2	RG7	Elephant Butte dam	33	10	9.78	107	12	12.65	1355
799.4	RG8	EB Spillway	33	9	12.84	107	11	28.75	1351
801.3	RG9	RG - Below Spillway	33	8	49.69	107	12	28.13	1301
806.6	RG10	Tor C	33	7	42.35	107	14	37.02	1292
808.5	RG11	T or C	33	7	5.6	107	15	19.12	1299
813.0	RG12	Williamsburg - off Rt187	33	6	28.85	107	17	52.83	1291
825.4	RG13	Caballo Res.	33	1	36.97	107	17	38.32	1290
832.7	RG14	Caballo Res.	32	57	44.99	107	18	40.86	1290
836.3	RG16	Caballo Res.	32	55	48.58	107	18	25.91	1277
838.5	RG15	Caballo park	32	54	38.9	107	18	29.19	1289
840.2	RG17	Caballo Dam	32	53	49.83	107	17	29.47	1302
841.0	RG18	Below Caballo Dam	32	53	25.4	107	17	29.22	1273
845.6	RG19	Arrey	32	51	21.56	107	17	57.04	1263
852.3	RG20	Arrey - Rt 187	32	48	32.67	107	18	13.72	1256
858.7	RG21	Garfield	32	45	52.5	107	17	2.71	1252
863.1	RG22	S. of Garfield off RT 390	32	44	1.61	107	16	25.86	1247

Distance (km)	ID	location	Latitude			Longitude			Elevation (m)
			Deg	Min.	Sec.	Deg	Min.	Sec.	
867.0	RG23	off Rt 390	32	42	26.87	107	15	21.73	1246
869.6	RG24	Salem - Off Rt 390	32	41	43.74	107	14	2.96	1241
874.3	RG25	Hatch - Rt 187 Bridge	32	40	58.71	107	11	22.45	1236
882.6	RG26	Hatch - Rt 26 Bridge	32	40	44.47	107	9	20.55	1233
886.4	RG27	Hatch - Rt 154 Bridge	32	40	4.54	107	7	11.33	1232
891.3	RG28	Rincon - Rt 140	32	39	17.59	107	4	34.92	1228
895.3	RG29	Off Rt 393	32	38	24.7	107	2	26.24	1224
899.4	RG30	Bridge Between Rt 185 and 393	32	36	48.46	107	1	13.6	1221
904.4	RG31	Off Rt 185	32	34	29.32	106	59	57.25	1220
909.2	RG32	Off Rt 185	32	32	16.13	106	59	11.15	1215
914.0	RG33	Off Rt 185	32	30	46.91	106	57	24.6	1215
916.2	RG34	Off Rt 185	32	30	1.66	106	56	36.49	1213
917.5	RG35	Radium Springs - Off 185	32	29	57.83	106	55	48.13	1213
922.9	RG36	Off 185	32	28	1.42	106	54	21.51	1206
926.9	RG37	Off 185	32	26	6.07	106	53	25.62	1201
932.3	RG38	Near Hill	32	23	51.39	106	51	44.7	1197
937.1	RG39	Dona Ana	32	22	31.31	106	50	23.97	1194
941.7	RG40	Dona Ana	32	20	17.47	106	50	10.41	1189
944.7	RG41	Rt 70 Las Cruces	32	18	37.84	106	49	39.5	1188
950.1	RG42	La Mesilla	32	15	49.81	106	49	30.74	1183
955.1	RG43	At Mesilla Diverson	32	13	42.35	106	47	57.04	1181
959.5	RG45	RT 28 Bridge	32	12	23.12	106	45	33.67	1177
966.1	RG46	San Miguel - Rt 192? Bridge	32	9	43.58	106	43	1.08	1171
973.6	RG47	Vado RT 189	32	6	49.17	106	40	6.98	1165

Distance (km)	ID	location	Latitude			Longitude			Elevation (m)
			Deg	Min.	Sec.	Deg	Min.	Sec.	
974.9	RG49	S. of Vado off Rt 478	32	6	15.82	106	39	39.64	1164
975.4	RG50	S. of Vado off Rt 478	32	6	4.03	106	39	26.85	1164
979.6	RG51	RT 226 Bridge	32	3	55.44	106	39	47.61	1162
981.8	RG54	Near La Union Drain	32	2	43.45	106	39	43.22	1160
984.6	RG52	Rt 186 near Anthony	32	1	22.8	106	38	56.92	1159
987.6	RG55	Rt 225 Near Anthony	31	59	56.9	106	38	9.18	1157
991.3	RG57	Off Rt 20 Near Vinton	31	58	12.46	106	36	28.94	1155
992.7	RG58	Vinton Ave Bridge	31	57	32.3	106	36	17.19	1153
997.6	RG59	Bridge in Canutillo	31	54	53.94	106	36	6.72	1150
1000.9	RG60	Borderland Rd	31	53	8.88	106	35	55.99	1145
1005.4	RG61	Rt 260 Bridge	31	50	47.36	106	36	21.1	1144
1011.6	RG62	Near Medow Vista	31	48	8.54	106	34	38.36	1138
1013.8	RG65	Rt 498 Bridge	31	47	56.18	106	33	17.66	1138
1015.0	RG64	power plant	31	48	18.43	106	32	41.12	1137
1015.4	RG63	Rt 273 Bridge	31	48	9.93	106	32	29.12	1137
1044.0	RG66	Zaragoza bridge	31	40	19.03	106	20	17.69	1119
1057.5	RG67	San Elizario	31	33	43.83	106	16	49.2	1110
1078.3	RG69	Rt 1109 Bridge - Tornillo	31	25	50.19	106	8	36.92	1096
1115.0	RG68	Fort Hancock	31	16	24	105	51	14	1076

Table J.2: Field parameters for January 2000. The "Day" column indicates the numbered day of the month. See Table J.1 for detailed sample locations.

Distance (km)	Day	Time	Temp (C)	EC (μS cm^{-1})	TDS (mg L^{-1})
766.0	28	12:00	11.1	603	298
772.4	28	13:20	9.6	597	296
774.9	28	14:10	9.5	590	292
780.2	28	15:10	16.6	564	279
786.7	28	16:00	11.5	577	286
791.4	28	16:20	10.8	583	289
797.2	29	17:00	10.4	606	300
799.4	29	10:25	9.3	624	309
801.3	29	10:50	9.2	626	310
806.6	29	12:20	10.2	645	319
808.5	29	12:40	10.5	692	342
813.0	29	13:30	10.4	672	333
825.4	29	14:00	9.6	693	343
832.7	29	15:00	9.7	716	354
836.3	31	11:00	10.7	864	422
838.5	29	15:30	9.9	872	427
840.2	31	11:30	9.5	873	427
841.0	31	11:50	12.3	993	486
845.6	31	12:50	13.8	1018	500
852.3	31	13:05	13.1	1131	557
858.7	31	13:30	14.3	1308	646
863.1	31	13:45	14.6	1317	651

Distance (km)	Day	Time	Temp (C)	EC (μS cm^{-1})	TDS (mg L^{-1})
867.0	31	14:15	13.5	1293	639
869.6	31	14:30	12.1	1281	633
874.3	31	14:50	13.1	1325	656
882.6	31	15:15	13.0	1308	647
886.4	31	15:30	12.2	1320	653
891.3	31	15:45	12.5	1316	651
895.3	1	10:15	8.5	1318	651
899.4	1	10:45	7.2	1318	652
904.4	1	11:25	7.5	1293	642
909.2	1	12:10	8.3	1322	653
914.0	1	13:00	8.5	1307	646
916.2	1	13:15	8.5	1283	635
917.5	1	13:35	8.9	1278	631
922.9	1	15:50	9.3	1330	659
926.9	1	14:45	8.9	1320	653
932.3	1	15:05	9.1	1387	685
937.1	1	15:25	9.7	1417	703
941.7	1	15:40	9.6	1364	676
944.7	1	16:00	9.2	1361	674
950.1	2	9:55	4.7	1371	679
955.1	2	10:15	5.2	1349	668
959.5	2	10:35	5.5	1333	660
966.1	2	11:00	5.8	1306	646
973.6	2	11:20	7.5	1260	623

Distance (km)	Day	Time	Temp (C)	EC (μS cm^{-1})	TDS (mg L^{-1})
974.9	2	11:45	6.7	1263	624
975.4	2	12:00	8.9	1286	635
979.6	2	12:50	9.4	1269	627
981.8	2	14:00	10.8	1276	631
984.6	2	14:10	10.5	1317	652
987.6	2	14:40	11.7	1318	652
991.3	2	14:50	11.5	1297	643
992.7	2	15:15	11.7	1368	677
997.6	2	15:30	11.2	1346	667
1000.9	3	9:40	5.3	1376	679
1005.4	3	10:10	6.1	1364	676
1011.6	3	10:40	7.2	1334	666
1013.8	3	12:10	9.0	1347	666
1015.0	3	11:50	9.0	1570	782
1015.4	3	11:15	8.6	1670	833
1044.0	3	13:40	14.8	1533	763
1057.5	3	14:45	14.6	1531	762
1078.3	3	12:00	11.5	1665	831
1115.0	3	10:25	8.8	2900	1481

Table J.3: Description of sampling locations for August 2000. RG= Rio Grande, T= natural tributary. Distances were estimated from January 2001 sample locations and sample maps using the TopoUSA program by DeLorme.

Type	Distance (km)	location
RG	na	Upstream of Rio Grande Reservoir
RG	na	Rio Grande Reservoir (Inlet)
RG	0.0	Rio Grande Reservoir (Outlet)
RG	1.1	Rio Grande Reservoir (Downstream) near NF campsite
RG	3.2	Rio Grande Reservoir (Downstream) Bridge at "Little Squaw Resort"
RG	5.1	Beginning of Weminuche Wilderness
RG	19.3	(522) Bridge over RG
RG	31.8	See Map (on ranch land)
RG	38.1	Next to (149)
RG	40.8	Marshall Park Entrance (near 149)
RG	50.3	San Juan National Forrest [Bridge over (806)]
RG	59.1	Private Road (before Wagon Wheel Gap) near bridge
RG	61.7	(149) Bridge over RG
RG	72.9	Entrance to Collier Wildlife Area
RG	79.5	Exit Collier Wildlife Area (at Masonic Park Exit)
RG	87.6	Short Distance South from North River Road
RG	95.9	Public Fishing Area, Short Distance from North River Road
RG	107.5	Private Ranch (follow road back to river)
RG	116.0	Park at Bridge over RG near Del Norte, walk east to river fork
RG	130.0	At Bridge near (5W)
RG	134.5	At (3W) Bridge over RG
RG	141.2	At (285) Bridge over RG, sign "Rio Grande River"
RG	148.6	At (3N) Bridge over RG (near homelake)
RG	156.4	Off (6E) Bridge over RG (hike east to flood gate)

Type	Distance (km)	location
RG	179.7	Near (105) at River Bend
RG	192.8	At "Cole Park," downtown Alamosa, near (160) bridge over RG
RG	203.1	Alamosa National Wildlife Refuge near visitor's center
RG	214.2	At end of (137S) near bridge, exit from (112S) at Rancher's Gate
RG	222.2	Enter ranch gate off Z-road north, park and hike to river
RG	225.2	At (Z-road) bridge over RG
RG	236.1	At lake area, park near cemetary off (28-Rd)
RG	243.5	At (142) bridge over RG
RG	253.8	River Bend, park at fence and hike to RG
RG	265.8	Runoff Channel Inflow, hike to bottom of canyon
RG	294.1	Canyon Bottom
RG	327.7	Canyon Bottom (near Carlson National Forrest Campsite)
RG	332.5	Bridge over RG near Arroyo Hondo (downstream from inflow)
RG	339.6	Taos Bridge (64)
RG	356.6	(567 and 570) Taos Junction Campground
RG	366.0	Near Pilar, just off road
RG	375.7	Embudo Station (park area), just off road
RG	393.9	Bridge near Lyden? (exit at 582, Junct. 68)
RG	404.6	Reservation (San Juan Pueblo) road below Alcalde
RG	430.9	At (502-W) Bridge over RG
RG	471.0	At (22-W) Bridge (Cochiti Lake Outflow)
RG	482.4	Off 22, cattle guard gate btwn Cochiti and Santo Domingo Pueblos
RG	514.8	At (550) Bridge over RG near Bernalillo
RG	533.4	At (528) Bridge over RG, near Alameda
RG	545.1	At (I-40-W) Bridge over RG

Type	Distance (km)	location
RG	555.6	On (500-W) Bridge over RG, Rio Bravo Exit
RG	564.9	On (I-25-S)
RG	570.0	At (47) Bridge over RG
RG	582.9	(6) Bridge over RG near Los Lunas
RG	596.6	Off (Manzano)
RG	601.1	At (309) Bridge over RG near Belen
RG	610.1	Bridge on NM 346
RG	614.7	At (346-W) Bridge over RG
RG	630.7	At (60) Bridge over RG near Bernardo
RG	639.3	Backroad near LaJoya
RG	655.3	At San Acacia, just off road
RG	671.8	At Bridge near PueblitoTake (408) toward Escondida Lake
RG	679.3	Take Chaparrel Dr. to Riverside Park
RG	686.3	Riverside Park above Luis Lopez
RG	696.4	At (380) Bridge over RG near San Antonio
RG	712.6	Bosque Del Apache (take 2nd trail w/ steps at far end of Refuge – look for weather tower)
RG	723.6	South of Bosque Del Apache (nr service road near canal/pumps)
RG	731.1	Railroad Bridge over RG
RG	738.8	Pipeline Trail (on pipeline road)
RG	747.5	Inflow to Elephant Butte Reservoir
RG	763.1	(I-25) Exit, 1st road to Reservoir
RG	766.0	(I-25) Exit, 2nd road to Reservoir
RG	772.4	Follow Upper Narrows Road to Reservoir

Type	Distance (km)	location
RG	774.9	Follow Lower Narrows Road to Reservoir
RG	780.2	Follow Monticello Road to Reservoir
RG	784.6	3 Sisters Cove Area – road ends at reservoir
RG	791.4	Rock Canyon Road (Rock Canyon Marina)
RG	796.1	Main Marina Area (Pay Area)
RG	797.2	Near Dam, Reservoir Exit
RG	801.3	Follow (51) to park area, approx. 1mi from Reservoir Dam
RG	806.6	Off East Riverside Drive in Truth or Consequences
RG	813.0	(HW-187) Near I-25 exit
RG	827.0	Off (HW-187) Cow Pasture
RG	830.2	Off (HW-187) near north end of Caballo Lake
RG	838.5	Caballo Lake State Park – boat launch
RG	840.2	Caballo Lake State Park – entrance near (25) – boat launch
RG	841.0	Caballo Lake State Park – gated area w/ small door
RG	845.6	Bridge over RG near Arrey
RG	852.3	At (HW-187) Bridge over RG past Arrey
RG	858.2	Take Paved Road near (436) at Catholic Church on Loma Parda
RG	874.3	At (HW-187) Bridge over RG before Hatch
RG	891.3	At (HW-140) Bridge over RG near Rincon
RG	896.6	Off (HW-185) at River Bend
RG	900.4	Off (HW-185) at River Bend
RG	912.3	Off (HW-185) at River Bend
RG	919.5	At (HW-185) Bridge over RG near Ft. Seldon State Monument Sign

Type	Distance (km)	location
RG	929.9	(185-S and 158-E) Intersection, follow road right to river edge
RG	937.1	At (320) intersection (neighborhood area, road leads to RG)
RG	944.7	At (70-W) Bridge over RG
RG	959.5	At (HW-28) Bridge over RG
RG	966.1	At (HW-192) Bridge over RG
RG	973.6	At (HW-189) Bridge over RG near Vado
RG	987.6	At (TX-1905) Bridge over RG, near Anthony
RG	1000.9	At (Borderlands Rd.) Bridge over RG South of Canutillo
RG	1005.4	At (NM-184) Bridge on Texas / New Mexico Border
RG	1013.8	At HW-498 (also Racetrack Rd) Bridge at Roadside Park
RG	1030.4	Levee Rd.
RG	1037.2	Levee Rd.
RG	1047.0	Levee Rd.
RG	1060.1	Levee Rd.
RG	1073.4	Levee Rd. (Fabens Port of Entry)
RG	1084.8	Levee Rd – 4mi from Fabens Port of Entry
RG	1097.9	Levee Rd – 12mi from Fabens Port of Entry
RG	1110.1	Levee Rd – 20mi from Fabens Port of Entry
RG	1120.5	Levee Rd – 28mi from Fabens Port of Entry
RG	1133.3	Levee Rd – 37mi from Fabens Port of Entry
RG	1142.0	Levee Rd – 46 mi from Fabens Port of Entry
T	16.3	Ranch Stream Inflow
T	16.5	"Texas Creek" Inflow
T	16.8	"Clear Creek Inflow" (from Wilderness)
T	66.3	"Blue Creek" Inflow, across from Blue Creek Lodge on (149)

Table J.4: Latitude, longitude, elevation, and sample IDs of sampling locations for August 2000. Coordinates are estimated from January 2001 data. See Table J.3 for detailed sample locations.

Type	Distance (km)	ID	Latitude			Longitude			Elevation (m)
			Deg	Min.	Sec.	Deg	Min.	Sec.	
RG		RG-A-P	37	45	54.02	107	21	20.14	2904
RG		RG-0.0-P	37	45	12.67	107	20	9.49	2856
RG	0.0	RG-8.4-P	37	43	15.98	107	15	58.49	2859
RG	1.1	RG-9.6-P	37	43	29.71	107	15	15.02	2827
RG	3.2	RG-11.4-P	37	43	43.38	107	14	3.11	2808
RG	5.1	RG-13.5-P	37	44	3.30	107	12	57.68	2802
RG	19.3	RG-26.7-P	37	44	44.46	107	6	11.09	2708
RG	31.8	RG-39.5-P	37	43	55.54	107	0	48.16	2674
RG	38.1	RG-44.9-P	37	46	46.87	107	0	5.56	2670
RG	40.8	RG-48.3-P	37	47	33.21	106	58	54.13	2660
RG	50.3	RG-57.8-P	37	49	1.21	106	54	54.55	2608
RG	59.1	RG-B-P	37	47	42.66	106	51	7.52	2584
RG	61.7	RG-69.0-P	37	46	39.11	106	50	12.10	2554
RG	72.9	RG-80.0-P	37	44	11.29	106	44	9.23	2528
RG	79.5	RG-87.0-P	37	42	2.85	106	41	8.41	2511
RG	87.6	RG-95.0-P	37	40	43.49	106	36	58.48	2475
RG	95.9	RG-102.0-P	37	41	34.72	106	32	18.53	2445
RG	107.5	RG-114.0-P	37	41	8.52	106	25	45.83	2409
RG	116.0	RG-123.0-P	37	41	13.35	106	20	27.13	2381
RG	130.0	RG-136.1-P	37	38	50.85	106	14	25.73	2359
RG	134.5	RG-140.5-P	37	37	28.06	106	12	15.43	2333
RG	141.2	RG-144.3-P	37	36	30.81	106	8	56.95	2306

Type	Distance (km)	ID	Latitude			Longitude			Elevation (m)
			Deg	Min.	Sec.	Deg	Min.	Sec.	
RG	148.6	RG-155.0-P	37	34	56.43	106	5	38.42	2312
RG	156.4	RG-162.0-P	37	34	11.10	106	1	51.19	2303
RG	179.7	RG-179.4-P	37	30	38.98	105	56	3.45	2283
RG	192.8	RG-190.7-P	37	28	13.16	105	51	43.20	2284
RG	203.1	RG-197.6-P	37	26	16.71	105	48	7.91	2279
RG	214.2	RG-207.2-P	37	22	20.62	105	46	18.89	2291
RG	222.2	RG-214.5-P	37	19	26.50	105	44	46.52	2277
RG	225.2	RG-217.5-P	37	18	23.87	105	44	19.85	2276
RG	236.1	RG-227.6-P	37	14	22.64	105	44	28.97	2268
RG	243.5	RG-235.3-P	37	10	49.54	105	43	44.42	2264
RG	253.8	RG-245.0-P	37	6	9.80	105	44	25.49	2254
RG	265.8	RG-259.5-P	37	1	26.41	105	44	53.59	2277
RG	294.1	RG-284.4-P	36	49	48.86	105	41	34.13	2262
RG	327.7	RG-316.0-P	36	34	24.28	105	41	59.72	2013
RG	332.5	RG-E-P	36	32	5.42	105	42	30.80	1966
RG	339.6	RG-TB-P	36	28	35.15	105	44	8.22	2117
RG	356.6	RG-343.1-P	36	20	10.13	105	44	1.32	1845
RG	366.0	RG-352.9-P	36	16	25.18	105	47	14.50	1813
RG	375.7	RG-366.5-P	36	13	19.00	105	52	12.02	1788
RG	393.9	RG-377.8-P	36	8	45.07	105	59	50.71	1714
RG	404.6	RG-389.5-P	36	4	44.84	106	4	14.85	1705
RG	430.9	RG-417.1-P	35	52	27.20	106	8	27.18	1654
RG	471.0	RG-457.6-P	35	37	0.87	106	19	30.19	1603
RG	482.4	RG-465.5-P	35	32	1.66	106	21	58.55	1581
RG	514.8	RG-501.2-P	35	19	17.94	106	33	17.92	1519

Type	Distance (km)	ID	Latitude			Longitude			Elevation (m)
			Deg	Min.	Sec.	Deg	Min.	Sec.	
RG	533.4	RG-519.4-P	35	11	52.93	106	38	39.03	1508
RG	545.1	RG-530.9-P	35	6	22.28	106	41	30.93	1506
RG	555.6	RG-541.2-P	35	1	38.49	106	40	20.56	1481
RG	564.9	RG-550.5-P	34	57	0.64	106	40	54.17	1479
RG	570.0	RG-562.1-P	34	54	22.03	106	41	11.48	1489
RG	582.9	RG-572.1-P	34	48	19.03	106	43	13.25	1454
RG	596.6	RG-F-P	34	41	26.41	106	44	36.98	1431
RG	601.1	RG-584.7-P	34	39	10.58	106	44	16.78	1439
RG	610.1	RG-597.5-P	34	34	57.04	106	45	33.35	1438
RG	614.7	RG-610.6-P	34	32	42.33	106	45	55.27	1422
RG	630.7	RG-616.4-P	34	25	3.42	106	47	51.75	1400
RG	639.3	RG-624.7-P	34	21	22.15	106	50	54.21	1417
RG	655.3	RG-640.7-P	34	15	20.33	106	53	45.49	1408
RG	671.8	RG-656.0-P	34	7	15.56	106	53	8.08	1382
RG	679.3	RG-663.0-P	34	3	40.23	106	52	31.96	1382
RG	686.3	RG-671.2-P	34	0	8.79	106	52	16.29	1373
RG	696.4	RG-680.2-P	33	55	7.45	106	51	5.12	1371
RG	712.6	RG-692.7-P	33	47	15.39	106	52	42.16	1370
RG	723.6	RG-706.0-P	33	42	28.91	106	55	48.27	1353
RG	731.1	RG-716.0-P	33	40	51.62	106	59	35.39	1343
RG	738.8	RG-736.0-P	33	37	21.37	107	0	23.35	1335
RG	747.5	RG-743.4-P	33	34	11.20	107	4	16.98	1326
RG	763.1	RG-G-P	33	27	52.04	107	9	40.41	1337
RG	766.0	RG-746.9-P	33	26	36.16	107	9	39.19	1326

Type	Distance (km)	ID	Latitude			Longitude			Elevation (m)
			Deg	Min.	Sec.	Deg	Min.	Sec.	
RG	772.4	RG-753.2-P	33	23	1.01	107	10	0.34	1326
RG	774.9	RG-757.6-P	33	21	39.42	107	10	34.99	1337
RG	780.2	RG-761.7-P	33	18	58.53	107	11	2.91	1337
RG	784.6	RG-770.1-P	33	16	51.39	107	10	47.23	1316
RG	791.4	RG-776.0-P	33	13	33.94	107	12	23.60	1335
RG	796.1	RG-782.3-P	33	10	46.52	107	12	17.53	1338
RG	797.2	RG-784.5-P	33	10	14.42	107	12	18.46	1345
RG	801.3	RG-786.9-P	33	8	52.02	107	12	24.62	1288
RG	806.6	RG-791.5-P	33	7	44.25	107	14	35.96	1258
RG	813.0	RG-798.0-P	33	6	36.58	107	17	54.30	1275
RG	827.0	RG-808.0-P	33	0	42.88	107	16	47.86	1257
RG	830.2	RG-818.1-P	32	59	2.99	107	17	19.16	1266
RG	838.5	RG-823.2-P	32	54	40.46	107	18	23.45	1258
RG	840.2	RG-827.0-P	32	53	54.82	107	17	31.11	1281
RG	841.0	RG-827.5-P	32	53	41.44	107	17	26.74	1251
RG	845.6	RG-834.0-P	32	51	19.63	107	17	55.48	1270
RG	852.3	RG-839.3-P	32	48	30.48	107	18	10.23	1238
RG	858.2	RG-846.1-P	32	46	4.21	107	17	15.61	1223
RG	874.3	RG-861.8-P	32	40	57.11	107	11	21.79	1211
RG	891.3	RG-868.9-P	32	39	23.07	107	4	34.74	1205
RG	896.6	RG-887.1-P	32	37	48.01	107	2	21.62	1199
RG	900.4	RG-H-P	32	36	15.78	107	1	11.08	1206
RG	912.3	RG-896.7-P	32	30	57.17	106	58	17.14	1231

Type	Distance (km)	ID	Latitude			Longitude			Elevation (m)
			Deg	Min.	Sec.	Deg	Min.	Sec.	
RG	919.5	RG-900.3-P	32	29	8.14	106	55	29.57	1180
RG	929.9	RG-910.3-P	32	25	8.25	106	52	2.23	1171
RG	937.1	RG-919.2-P	32	22	30.01	106	50	22.38	1168
RG	944.7	RG-926.9-P	32	18	45.39	106	49	40.77	1174
RG	959.5	RG-941.7-P	32	12	25.40	106	45	35.36	1156
RG	966.1	RG-948.3-P	32	9	41.63	106	43	3.05	1136
RG	973.6	RG-955.7-P	32	6	49.49	106	40	7.21	1124
RG	987.6	RG-971.8-P	31	59	58.28	106	38	7.17	1124
RG	1000.9	RG-983.5-P	31	53	9.65	106	35	56.21	1120
RG	1005.4	RG-987.9-P	31	50	46.75	106	36	23.54	1116
RG	1013.8	RG-999.2-P	31	47	57.80	106	33	25.61	1108
RG	1030.4	RG-BORD-P	31	45	15.74	106	25	53.17	1099
RG	1037.2	RG-BORD2-P	31	43	17.49	106	22	30.79	1105
RG	1047.0	RG-BORD3-P	31	38	53.97	106	19	22.04	1102
RG	1060.1	RG-BORD4-P	31	33	0.03	106	15	24.13	1090
RG	1073.4	RG-BORD5-P	31	27	31.13	106	10	54.91	1078
RG	1084.8	RG-BORD6-P	31	24	10.81	106	5	10.10	1068
RG	1097.9	RG-BORD7-P	31	21	57.10	105	57	46.22	1063
RG	1110.1	RG-BORD8-P	31	17	30.67	105	53	42.31	1052
RG	1120.5	RG-BORD9-P	31	14	1.81	105	49	15.01	1045
RG	1133.3	RG-BORD10-P	31	9	42.03	105	44	12.18	1034
RG	1142.0	RG-BORD11-P	31	7	16.23	105	39	47.37	1038
T	16.3	RG-23.8-P	37	45	54.51	107	7	7.07	2719
T	16.5	RG-24.1-P	37	45	50.08	107	7	0.26	2732
T	16.8	RG-24.4-P	37	45	38.14	107	6	51.83	2733
T	66.3	RG-C-P	37	46	8.02	106	47	51.65	2545

Table J.5: Field parameters, chloride and bromide for August 2000. The "Day" column indicates the numbered day of the month. Bolded values are below threshold. Cl- and Br- analyses performed at the New Mexico Bureau of Geology and Mineral Resources. Samples are listed by ID rather than by distance due to inconsistencies in distance determinations with post-2000 data. See Table J.3 for detailed sample locations.

ID	Day	Time	pH	Temp (°C)	EC (μS cm^{-1})	TDS (mg L^{-1})	Cl (mg L^{-1})	Br (mg L^{-1})
RG-A-P	6	16:17	7.40	19.8	121.2	58	na	na
RG-0.0-P	6	17:26	7.53	20.2	90.2	42.3	0.27	**0.02**
RG-8.4-P	6	18:07	7.59	19.5	65.1	31.2	0.36	**0.02**
RG-9.6-P	7	7:15	7.63	10.3	66.2	31.2	0.3	**0.02**
RG-11.4-P	7	7:54	7.54	9.4	68.2	32.6	0.35	**0.02**
RG-13.5-P	7	8:31	7.01	14.2	67.4	31.7	na	na
RG-26.7-P	7	11:23	7.46	16.2	67.3	31.6	0.3	**0.02**
RG-39.5-P	7	12:24	5.70	20.2	110.6	52.4	0.84	**0.02**
RG-44.9-P	7	13:56	7.49	19.3	93.5	44.1	0.4	**0.02**
RG-48.3-P	7	14:27	8.20	19.7	87.3	41.3	na	na
RG-57.8-P	7	14:48	7.61	21.5	92.2	43.7	0.43	**0.02**
RG-B-P	7	15:17	7.74	20.4	67.9	32	na	na
RG-69.0-P	7	15:42	8.24	20.8	100.8	47.7	0.68	**0.02**
RG-80.0-P	7	16:16	8.16	20.4	104.1	48.9	na	na
RG-87.0-P	7	16:48	8.23	20.5	104.9	50	0.79	**0.02**
RG-95.0-P	7	17:07	8.18	21.7	104.9	49.8	na	na
RG-102.0-P	8	7:41	7.77	13.9	106.5	50.5	0.88	**0.02**
RG-114.0-P	8	8:50	7.43	15.8	122.9	58.1	na	na
RG-123.0-P	8	9:38	7.83	16.9	121.5	57.7	0.86	**0.02**
RG-136.1-P	8	11:18	6.00	19.7	120.3	57.2	1.1	**0.02**
RG-140.5-P	8	11:41	5.35	22.3	118.3	56.1	na	na
RG-144.3-P	8	12:01	7.29	21.9	121.1	57.4	1.1	**0.02**

ID	Day	Time	pH	Temp (°C)	EC (μS cm^{-1})	TDS (mg L^{-1})	Cl (mg L^{-1})	Br (mg L^{-1})
RG-155.0-P	8	12:42	7.51	23.2	139.8	66.7	1.7	**0.02**
RG-162.0-P	8	13:22	8.14	25.3	146.6	70	na	na
RG-179.4-P	8	15:15	8.09	28.1	280	134.8	4.6	0.05
RG-190.7-P	8	14:37	8.31	24.9	309	148.4	5.5	0.09
RG-197.6-P	8	16:21	8.43	32.1	504	244	na	na
RG-207.2-P	9	6:43	7.77	14.5	473	229	15	0.1
RG-214.5-P	9	7:50	8.24	15.0	560	271	na	na
RG-217.5-P	9	8:11	5.67	14.7	560	271	17	0.24
RG-227.6-P	9	9:02	6.45	18.2	477	231	na	na
RG-235.3-P	9	9:30	8.53	18.6	488	236	14	0.24
RG-245.0-P	9	11:04	7.50	23.3	445	215	na	na
RG-259.5-P	9	12:26	8.11	24.0	455	222	16	0.23
RG-284.4-P	9	15:12	7.77	20.0	266	127.6	na	na
RG-316.0-P	10	8:13	6.58	16.7	286	137.6	6.7	0.09
RG-E-P	10	9:36	7.18	17.8	311	150	6.1	**0.02**
RG-TB-P	10	11:24	6.40	21.1	293	140.6	6.8	0.1
RG-343.1-P	10	13:24	7.37	20.8	296	141.3	na	na
RG-352.9-P	10	13:42	6.77	24.5	296	143	7.2	**0.02**
RG-366.5-P	10	14:09	8.26	24.9	293	140.8	na	na
RG-377.8-P	10	15:13	6.60	26.3	324	155.7	7.2	**0.02**
RG-389.5-P	10	16:14	6.68	28.6	378	182	na	na
RG-417.1-P	10	17:30	7.34	24.3	303	145.1	3.4	**0.02**
RG-457.6-P	12	7:47	7.44	22.3	308	148.2	3.4	**0.02**
RG-465.5-P	12	8:26	7.31	19.5	467	226	na	na
RG-501.2-P	12	8:58	7.66	21.7	321	154	3.9	**0.02**

ID	Day	Time	pH	Temp (^{o}C)	EC (μS cm^{-1})	TDS (mg L^{-1})	Cl (mg L^{-1})	Br (mg L^{-1})
RG-519.4-P	12	9:48	7.94	23.6	335	161.6	4.9	**0.02**
RG-530.9-P	12	10:35	7.45	23.7	327	157	4.6	**0.02**
RG-541.2-P	12	11:01	6.88	25.7	336	161.9	na	na
RG-550.5-P	12	11:34	7.19	27.1	363	175	9.7	**0.02**
RG-562.1-P	12	12:21	7.61	27.3	368	176.9	na	na
RG-572.1-P	12	12:47	8.12	30.9	411	198.4	14	0.07
RG-F-P	12	13:18	7.28	27.5	410	198	na	na
RG-584.7-P	12	13:40	7.65	28.0	470	228	18	0.22
RG-597.5-P	12	15:03	8.18	31.7	423	204	na	na
RG-610.6-P	12	15:29	7.46	31.8	433	209	16	0.16
RG-616.4-P	13	6:45	8.57	22.7	449	217	16	0.08
RG-624.7-P	13	8:15	7.63	24.0	516	250	20	0.17
RG-640.7-P	13	9:18	7.94	24.5	538	261	27	0.28
RG-656.0-P	13	9:48	8.47	24.1	506	245	23	0.09
RG-663.0-P	13	10:06	8.34	24.9	525	254	25	0.17
RG-671.2-P	13	13:00	7.52	28.7	531	257	26	0.22
RG-680.2-P	13	13:19	7.79	31.0	526	256	25	0.28
RG-692.7-P	13	14:01	7.31	32.4	522	254	27	0.25
RG-706.0-P	13	17:04	8.40	33.4	523	253	28	0.38
RG-716.0-P	13	16:26	8.04	33.4	538	261	29	0.26
RG-736.0-P	13	16:05	7.54	33.5	548	265	na	na
RG-743.4-P	13	15:52	7.91	35.0	610	296	37	0.23
RG-G-P	14	9:22	7.94	26.4	759	368	na	na

ID	Day	Time	pH	Temp (°C)	EC (μS cm^{-1})	TDS (mg L^{-1})	Cl (mg L^{-1})	Br (mg L^{-1})
RG-746.9-P	14	10:02	7.60	28.4	597	289	39	0.24
RG-753.2-P	14	10:43	6.77	28.5	686	335	52	0.3
RG-757.6-P	14	12:02	6.55	29.6	669	326	50	0.32
RG-761.7-P	14	12:40	5.42	31.7	679	330	45	0.11
RG-770.1-P	14	13:03	6.99	31.4	663	321	na	na
RG-776.0-P	14	13:31	7.72	31.0	625	303	44	0.29
RG-782.3-P	14	14:46	7.16	30.5	644	313	na	na
RG-784.5-P	14	14:36	7.27	30.1	637	310	45	0.34
RG-786.9-P	14	15:25	8.50	19.1	631	307	na	na
RG-791.5-P	14	15:38	8.41	19.4	652	315	46	0.27
RG-798.0-P	14	16:01	6.64	21.2	663	323	na	na
RG-808.0-P	14	16:41	6.40	23.6	655	318	48	0.36
RG-818.1-P	14	18:05	7.80	27.9	727	354	na	na
RG-823.2-P	14	18:23	8.61	25.9	644	313	46	0.35
RG-827.0-P	14	18:41	8.33	26.7	644	313	na	na
RG-827.5-P	14	18:51	8.28	27.4	654	318	48	0.36
RG-834.0-P	14	19:22	8.47	24.4	646	315	na	na
RG-839.3-P	14	19:37	8.57	24.6	652	318	48	0.26
RG-846.1-P	14	20:00	8.63	25.7	656	319	na	na
RG-861.8-P	14	20:23	8.74	25.6	681	332	48	0.28
RG-868.9-P	14	20:42	8.66	25.9	691	337	na	na
RG-887.1-P	15	8:46	8.03	23.2	683	335	49	0.38
RG-H-P	15	8:59	7.30	23.6	686	334	na	na
RG-896.7-P	15	9:20	7.87	24.9	689	335	na	na

ID	Day	Time	pH	Temp (°C)	EC (μS cm^{-1})	TDS (mg L^{-1})	Cl (mg L^{-1})	Br (mg L^{-1})
RG-900.3-P	15	9:30	7.77	24.3	704	343	50	0.33
RG-910.3-P	15	9:55	6.54	25.8	714	348	52	0.31
RG-919.2-P	15	10:17	8.07	26.3	716	349	na	na
RG-926.9-P	15	10:52	7.75	25.2	715	348	52	0.32
RG-941.7-P	15	11:21	7.43	25.7	725	353	54	0.37
RG-948.3-P	15	11:34	6.57	27.6	724	352	na	na
RG-955.7-P	15	11:55	8.22	26.7	727	355	54	0.28
RG-971.8-P	15	12:35	7.77	27.2	805	392	63	0.29
RG-983.5-P	15	13:15	8.51	27.4	851	416	67	0.37
RG-987.9-P	15	13:57	7.72	27.4	829	404	na	na
RG-999.2-P	15	14:23	7.75	27.6	850	415	68	0.39
RG-BORD-P	15	15:02	8.17	30.3	970	477	83	0.38
RG-BORD2-P	15	15:23	8.40	30.6	928	456	na	na
RG-BORD3-P	15	15:43	8.60	28.0	1021	502	88	0.12
RG-BORD4-P	15	16:21	8.02	30.1	1199	592	118	**0.02**
RG-BORD5-P	15	16:43	7.99	29.3	1528	760	145	0.41
RG-BORD6-P	16	9:57	7.20	24.3	1682	840	190	0.61
RG-BORD7-P	16	10:15	7.18	25.9	1818	910	220	0.69
RG-BORD8-P	16	10:38	6.24	24.7	3880	2010	660	1.3
RG-BORD9-P	16	10:54	7.94	24.8	3810	1972	660	1.2
RG-BORD10-P	16	11:15	6.96	25.9	3760	1945	650	1.3
RG-BORD11-P	16	11:30	7.76	25.1	5300	2790	1000	1.9
RG-23.8-P	7	10:10	6.75	16.8	77.6	36.6	na	na
RG-24.1-P	7	9:53	6.94	15.4	68.7	32.4	0.51	**0.02**
RG-24.4-P	7	10:52	5.68	14.9	62	29.4	na	na
RG-C-P	7	15:55	7.60	18.0	132.8	63.3	0.98	**0.02**

Table J.6: Major cations for August 2000. Bolded values are below threshold. Analyses performed at the New Mexico Bureau of Geology and Mineral Resources. See Table J.3 for detailed sample locations.

ID	Ca (mg L-1)	K (mg L-1)	Mg (mg L-1)	Na (mg L-1)	Sr (mg L-1)
RG-144.3-P	16	2.8	2.5	6	0.22
RG-190.7-P	34	6	6.5	24	0.47
RG-217.5-P	50	8.2	9.7	67	0.71
RG-316.0-P	19	4	7.1	22	0.43
RG-457.6-P	44	3	6.2	15	0.54
RG-530.9-P	45	3.3	6.8	18	0.6
RG-572.1-P	53	5.2	7.2	30	0.67
RG-616.4-P	53	5.5	7.9	35	0.73
RG-640.7-P	66	6.2	10	47	1.1
RG-716.0-P	59	6.3	9.1	50	0.96
RG-753.2-P	46	7.2	12	79	1.1
RG-776.0-P	40	6.8	12	73	1.1
RG-839.3-P	53	6.8	12	72	1.1
RG-955.7-P	60	7.4	13	76	1.2
RG-999.2-P	68	8.8	14	96	1.4
RG-BORD3-P	77	9.2	15	127	1.7
RG-BORD5-P	115	12	23	170	2.5
RG-BORD7-P	115	13	28	229	2.9
RG-BORD8-P	228	15	43	504	6.1
RG-BORD10-P	218	16	44	463	6.1
RG-BORD11-P	292	18	67	744	8.6

Table J.7: Major anions for August 2000. Analyses performed at the New Mexico Bureau of Geology and Mineral Resources. See Table J.3 for detailed sample locations.

ID	HCO3 (mg L-1)	F (mg L-1)	NO3 (mg L-1)	PO4 (mg L-1)	SO4 (mg L-1)
RG-144.3-P	64	**0.1**	**0.1**	**0.5**	8
RG-190.7-P	160	0.18	0.59	**0.5**	20
RG-217.5-P	240	0.98	**0.1**	**0.5**	74
RG-316.0-P	91	0.86	1.6	**0.5**	40
RG-457.6-P	117	0.15	**0.1**	**0.5**	57
RG-530.9-P	141	0.24	**0.1**	**0.5**	59
RG-572.1-P	155	0.43	0.22	**0.5**	68
RG-616.4-P	171	0.35	**0.1**	**0.5**	72
RG-640.7-P	188	0.52	0.39	**0.5**	98
RG-716.0-P	174	0.56	**0.1**	**0.5**	95
RG-753.2-P	149	0.62	**0.1**	**0.5**	134
RG-776.0-P	132	0.63	**0.1**	**0.5**	122
RG-839.3-P	165	0.58	**0.1**	**0.5**	119
RG-955.7-P	172	0.63	**0.1**	**0.5**	133
RG-999.2-P	192	0.62	**0.1**	**0.5**	161
RG-BORD3-P	222	0.66	1.2	**0.5**	194
RG-BORD5-P	302	0.63	**0.1**	**0.5**	216
RG-BORD7-P	259	0.62	**0.1**	**0.5**	306
RG-BORD8-P	273	1.10	2.1	**0.5**	572
RG-BORD10-P	232	1.10	0.31	**0.5**	576
RG-BORD11-P	297	1.00	**0.1**	**0.5**	864

Table J.8: Description of sampling locations for January 2001. RG= Rio Grande, T= natural tributary.

Type	Distance (km)	location
RG	16.3	Above the Ranch Stream Inflow
RG	31.9	on ranch land
RG	40.8	Marshall Park Entrance near 149
RG	50.3	San Juan National Forest, bridge over 806
RG	61.7	149 bridge over RG
RG	79.5	Collier Wildlife Area at Masonic Park Exit
RG	95.9	Public Fishing Area, near North River Road
RG	115.3	Park at Bridge over RG near Del Norte, walk east to river fork
RG	130.0	At Bridge near 5W
RG	141.2	At 285 Bridge over RG
RG	148.6	At 3N Bridge over RG (near homelake)
RG	179.7	Near (105) at River Bend
RG	192.8	At "Cole Park," downtown Alamosa, near (160) bridge over RG
RG	214.2	At end of (137S) near bridge, exit from (112S) at Rancher's Gate
RG	225.2	At (Z-road) bridge over RG
RG	243.5	At (142) bridge over RG
RG	256.9	Bridge on G Road
RG	306.7	Chifio Trail
RG	332.5	Bridge over RG near Arroyo Hondo (downstream from inflow)
RG	356.6	Bridge North of Pilar in campground
RG	366.0	Near Pilar, just off road
RG	384.5	Embudo Station (park area), just off road
RG	393.9	Bridge near Lyden (exit at 582, Junct. 68)

Type	Distance (km)	location
RG	415.3	US RT 84 Bridge in Espanola
RG	430.9	At (502-W) Bridge over RG
RG	471.0	At (22-W) Bridge (Cochiti Lake Outflow)
RG	514.8	US Rt 550 Bridge, Bernalillo
RG	533.4	At (528) Bridge over RG, near Alameda
RG	545.1	At (I-40-W) Bridge over RG
RG	550.5	Bridge Blvd Bridge over RG
RG	564.9	On (I-25-S)
RG	570.0	At (147) Bridge over RG, Isleta
RG	582.9	(6) Bridge over RG near Los Lunas
RG	601.1	At (309) Bridge over RG near Belen
RG	614.7	Bridge on NM 346
RG	630.7	At (60) Bridge over RG near Bernardo
RG	642.9	La Joya Refuge
RG	655.3	At San Acacia, just off road
RG	671.8	At Bridge near PueblitoTake (408) toward Escondida Lake
RG	679.3	Take Chaparrel Dr. to Riverside Park
RG	686.3	Riverside Park above Luis Lopez
RG	696.4	At (380) Bridge over RG near San Antonio
RG	712.6	Bosque Del Apache (take 2nd trail w/ steps at far end of Refuge – look for weather tower)
RG	723.6	South of Bosque Del Apache (look for service road near canal and pumps)
RG	731.1	Railroad Bridge over RG

Type	Distance (km)	location
RG	738.8	Pipeline Trail (on pipeline road)
RG	747.5	Inflow to Elephant Butte Reservoir
RG	766.0	(I-25) Exit, 2nd road to Reservoir
RG	772.4	Follow Upper Narrows Road to Reservoir
RG	780.2	Follow Monticello Road to Reservoir
RG	784.6	3 Sisters Cove Area – road ends at reservoir
RG	791.4	Rock Canyon Road (Rock Canyon Marina)
RG	796.1	Main Marina Area (Pay Area)
RG	797.2	Near Dam, Reservoir Exit
RG	801.3	Follow (51) to park area, approx. 1mi from Reservoir Dam
RG	806.6	Off East Riverside Drive in Truth or Consequences
RG	813.0	(HW-187) Near I-25 exit
RG	825.4	Off (HW-187) Cow Pasture
RG	830.2	Off (HW-187) near north end of Caballo Lake
RG	838.5	Caballo Lake State Park – boat launch
RG	840.2	Caballo Lake State Park – entrance near (25) – boat launch
RG	841.0	Caballo Lake State Park – gated area w/ small door
RG	845.6	Bridge over RG near Arrey
RG	852.3	At (HW-187) Bridge over RG past Arrey
RG	858.7	Take Paved Road near (436) at Catholic Church on Loma Parda
RG	874.3	At (HW-187) Bridge over RG before Hatch
RG	891.3	At (HW-140) Bridge over RG near Rincon
RG	904.4	Off (HW-185) at River Bend
RG	912.3	Off (HW-185) at River Bend
RG	919.5	At (HW-185) Bridge over RG near Ft. Seldon State Monument Sign

Type	Distance (km)	location
RG	929.9	(185-S and 158-E) Intersection, follow road right to river edge
RG	937.1	At (320) intersection (neighborhood area, road leads to RG)
RG	944.7	At (70-W) Bridge over RG
RG	959.5	At (HW-28) Bridge over RG
RG	966.1	At (HW-192) Bridge over RG
RG	979.6	At (HW-189) Bridge over RG near Vado
RG	987.6	At (TX-1905) Bridge over RG, near Anthony
RG	1000.9	At (Borderlands Rd.) Bridge over RG South of Canutillo
RG	1005.4	At (NM-184) Bridge on Texas / New Mexico Border
RG	1013.8	At HW-498 (also Racetrack Rd) Bridge at Roadside Park
RG	1021.6	Levee Rd.
RG	1034.5	Levee Rd.
RG	1047.0	Levee Rd.
RG	1060.1	Levee Rd.
RG	1072.9	Levee Rd. (Fabens Port of Entry)
RG	1085.8	Levee Rd – 4mi from Fabens Port of Entry
RG	1098.8	Levee Rd – 12mi from Fabens Port of Entry
RG	1112.5	Levee Rd – 20mi from Fabens Port of Entry
RG	1123.0	Levee Rd – 28mi from Fabens Port of Entry
RG	1139.1	Levee Rd – 37mi from Fabens Port of Entry
RG	1152.4	Levee Rd – 46 mi from Fabens Port of Entry
T	16.3	Ranch Stream Inflow
T	16.5	"Texas Creek" Inflow
T	16.8	"Clear Creek Inflow" (from Wilderness)
T	66.3	"Blue Creek" Inflow, across from Blue Creek Lodge on 149

Table J.9: Latitude, longitude, and elevation of sampling locations for January 2001. See Table J.8 for detailed sample locations.

		Latitude			Longitude			
Type	Distance (km)	Deg	Min.	Sec.	Deg	Min.	Sec.	Elevation (m)
RG	16.3	37	45	54.51	107	7	7.07	2719
RG	31.9	37	44	16.33	107	0	51.68	2676
RG	40.8	37	47	33.68	106	58	51.58	2663
RG	50.3	37	49	1.69	106	54	54.78	2609
RG	61.7	37	46	39.11	106	50	12.10	2554
RG	79.5	37	42	4.01	106	41	7.16	2473
RG	95.9	37	41	27.23	106	32	27.30	2440
RG	115.3	37	41	9.39	106	21	1.81	na
RG	130.0	37	38	48.99	106	14	22.53	2355
RG	141.2	37	36	31.34	106	8	58.04	2313
RG	148.6	37	34	59.43	106	5	38.70	2298
RG	179.7	37	30	41.99	105	55	57.34	2283
RG	192.8	37	28	13.64	105	51	45.84	2287
RG	214.2	37	22	19.38	105	46	19.59	2297
RG	225.2	37	18	24.76	105	44	16.81	2262
RG	243.5	37	10	49.65	105	43	43.18	na
RG	256.9	37	4	43.82	105	45	26.79	2252
RG	306.7	36	44	34.05	105	40	56.70	2170
RG	332.5	36	32	5.42	105	42	30.80	1966
RG	356.6	36	20	8.21	105	44	0.10	1843
RG	366.0	36	16	25.66	105	47	13.76	1801
RG	384.5	36	12	26.96	105	57	37.71	1751
RG	393.9	36	8	45.07	105	59	50.71	1714

Type	Distance (km)	Latitude			Longitude			Elevation (m)
		Deg	Min.	Sec.	Deg	Min.	Sec.	
RG	415.3	35	59	25.75	106	4	24.77	1632
RG	430.9	35	52	27.20	106	8	27.18	1654
RG	471.0	35	37	2.05	106	19	29.50	1575
RG	514.8	35	19	22.30	106	33	34.99	1537
RG	533.4	35	11	52.93	106	38	39.03	1508
RG	545.1	35	6	22.17	106	41	32.68	1479
RG	550.5	35	4	10.73	106	39	46.37	1467
RG	564.9	34	57	0.63	106	40	54.70	1486
RG	570.0	34	54	22.03	106	41	11.48	1489
RG	582.9	34	48	15.09	106	42	58.40	1457
RG	601.1	34	39	10.91	106	44	11.79	1448
RG	614.7	34	32	41.94	106	45	44.68	1438
RG	630.7	34	25	3.42	106	47	51.75	1400
RG	642.9	34	19	39.60	106	51	30.05	1422
RG	655.3	34	15	19.09	106	53	43.03	1402
RG	671.8	34	7	15.56	106	53	8.08	1382
RG	679.3	34	3	40.23	106	52	31.96	1382
RG	686.3	34	0	8.33	106	52	16.51	1374
RG	696.4	33	55	7.64	106	51	11.47	1398
RG	712.6	33	47	13.09	106	52	30.35	1362
RG	723.6	33	42	27.51	106	55	50.36	1355
RG	731.1	33	40	51.42	106	59	35.93	1352
RG	738.8	33	37	21.95	107	0	25.08	1313
RG	747.5	33	34	11.79	107	4	16.92	1349

Type	Distance (km)	Latitude			Longitude			Elevation (m)
		Deg	Min.	Sec.	Deg	Min.	Sec.	
RG	766.0	33	26	36.75	107	9	40.94	1328
RG	772.4	33	23	6.54	107	9	58.29	1330
RG	780.2	33	18	53.11	107	11	16.72	1298
RG	784.6	33	16	51.39	107	10	47.23	1316
RG	791.4	33	13	32.61	107	12	23.79	1317
RG	796.1	33	10	52.37	107	12	16.36	1315
RG	797.2	33	10	14.76	107	12	17.93	1329
RG	801.3	33	8	51.79	107	12	25.04	1289
RG	806.6	33	7	44.07	107	14	35.03	1268
RG	813.0	33	6	37.07	107	17	54.43	1258
RG	825.4	33	1	32.14	107	16	12.24	1260
RG	830.2	32	59	6.47	107	17	20.50	1267
RG	838.5	32	54	39.21	107	18	26.39	1276
RG	840.2	32	53	55.19	107	17	30.02	1264
RG	841.0	32	53	35.41	107	17	32.94	1242
RG	845.6	32	51	23.08	107	17	56.30	1247
RG	852.3	32	48	32.61	107	18	18.25	1231
RG	858.7	32	45	46.07	107	16	59.34	1225
RG	874.3	32	40	56.21	107	11	20.59	1221
RG	891.3	32	39	14.21	107	4	34.46	1211
RG	904.4	32	34	26.07	106	59	55.92	1206
RG	912.3	32	30	57.25	106	58	19.22	1185
RG	919.5	32	29	8.14	106	55	29.57	1180
RG	929.9	32	25	8.25	106	52	2.23	1171

Type	Distance (km)	Latitude			Longitude			Elevation (m)
		Deg	Min.	Sec.	Deg	Min.	Sec.	
RG	937.1	32	22	26.76	106	50	17.94	1172
RG	944.7	32	18	36.66	106	49	36.54	1167
RG	959.5	32	12	25.31	106	45	34.87	1142
RG	966.1	32	9	40.41	106	42	57.31	1154
RG	979.6	32	3	55.23	106	39	50.69	1141
RG	987.6	31	59	58.66	106	38	7.33	1142
RG	1000.9	31	53	10.56	106	35	55.01	1130
RG	1005.4	31	50	46.59	106	36	24.12	1132
RG	1013.8	31	47	57.80	106	33	25.61	1108
RG	1021.6	31	45	41.20	106	30	25.49	1118
RG	1034.5	31	44	20.03	106	23	35.08	1101
RG	1047.0	31	38	53.39	106	19	22.21	1092
RG	1060.1	31	32	58.55	106	15	25.53	1074
RG	1072.9	31	27	35.46	106	11	13.95	1066
RG	1085.8	31	23	54.58	106	4	40.50	1068
RG	1098.8	31	21	52.79	105	57	11.10	1061
RG	1112.5	31	17	26.44	105	52	17.82	1055
RG	1123.0	31	11	54.77	105	46	59.21	1034
RG	1139.1	31	7	50.58	105	41	32.50	1036
RG	1152.4	31	3	49.10	105	35	36.37	1028
T	16.3	37	45	54.51	107	7	7.07	2719
T	16.5	37	45	48.56	107	7	1.66	2716
T	16.8	37	45	40.96	107	6	49.99	2693
T	66.3	37	46	8.78	106	47	51.64	2544

Table J.10: Field parameters, chloride and bromide for January 2001. The "Day" column indicates the numbered day of the month. Bolded values are below threshold. See Table J.8 for detailed sample locations.

Type	Distance (km)	Day	Time	Temp (°C)	pH	EC (μS cm^{-1})	TDS (mg L^{-1})	Cl (mg L^{-1})	Br (mg L^{-1})
RG	16.3	5	8:40	0.9	7.66	80.7	38.2	0.49	**0.01**
RG	31.9	5	10:10	0.4	8.61	90.4	42.8	0.59	**0.01**
RG	40.8	5	10:31	1.7	7.18	100.7	47.8	0.67	**0.01**
RG	50.3	5	10:52	2.2	7.22	101.6	48.2	0.66	**0.01**
RG	61.7	5	11:10	2.6	7.48	119.1	56.8	0.7	**0.01**
RG	79.5	5	11:42	1.1	7.77	120.3	57.3	1.1	**0.01**
RG	95.9	5	12:32	2.1	7.44	117.2	55.7	1.1	**0.01**
RG	115.3	5	1:07	4.2	7.92	139.5	66.6	1.3	**0.01**
RG	130.0	5	1:30	2.1	7.83	141.2	67.4	1.3	**0.01**
RG	141.2	5	1:45	1.4	7.70	138.5	66.1	1.4	**0.01**
RG	148.6	5	2:02	2.8	7.23	178.4	86.3	3.8	0.016
RG	179.7	5	2:52	3.2	7.01	167.1	79.5	2.8	0.014
RG	192.8	5	3:35	2.5	7.82	166	79.2	2.6	0.01
RG	214.2	5	4:11	2.5	8.03	230	110.2	5.1	0.038
RG	225.2	5	4:45	2.6	8.32	231	111	5.8	0.039
RG	243.5	5	5:22	1.7	8.52	218	104.2	4.4	0.035
RG	256.9	6	8:00	0.1	7.98	208	99.7	4.4	0.035
RG	306.7	6	9:39	1.3	8.30	230	110.2	4.8	0.043
RG	332.5	6	10:25	3.9	8.46	250	119.8	5.3	**0.01**
RG	356.6	6	11:51	5.1	8.28	273	131.5	5.9	0.048
RG	366.0	6	12:09	5.0	8.68	262	125.7	5.8	0.048
RG	384.5	6	12:35	5.0	8.47	273	131	na	na
RG	393.9	6	1:19	5.1	8.62	288	138.1	6	0.05

Type	Distance (km)	Day	Time	Temp (°C)	pH	EC (μS cm^{-1})	TDS (mg L^{-1})	Cl (mg L^{-1})	Br (mg L^{-1})
RG	415.3	6	1:45	5.3	8.57	317	152.2	7.3	0.04
RG	430.9	6	2:10	5.9	8.78	326	157.2	7.6	0.055
RG	471.0	6	3:18	5.7	8.40	348	167.7	7.4	0.054
RG	514.8	6	4:02	6.4	8.18	368	177.6	8.1	0.054
RG	533.4	6	4:30	8.2	8.81	368	177.3	8.9	0.06
RG	545.1	7	7:22	1.7	8.48	400	193.1	10	0.059
RG	550.5	7	7:35	1.8	8.39	402	193.7	na	na
RG	564.9	7	8:04	4.3	8.30	455	220	23	0.011
RG	570.0	7	8:30	4.9	8.35	463	224	na	na
RG	582.9	7	8:47	5.0	8.47	489	236	27	0.11
RG	601.1	7	9:15	5.8	8.36	506	245	25	0.12
RG	614.7	7	9:40	5.1	8.57	512	248	27	0.11
RG	630.7	7	10:02	4.4	8.48	503	243	26	0.1
RG	642.9	7	10:38	5.0	8.64	527	256	27	0.12
RG	655.3	7	11:04	5.8	8.51	596	289	39	0.13
RG	671.8	7	11:20	6.4	8.60	578	280	37	0.13
RG	679.3	7	11:45	6.5	8.55	579	281	37	0.12
RG	686.3	8	8:30	2.3	8.62	587	285	36	0.13
RG	696.4	8	8:54	2.2	8.15	583	282	36	0.13
RG	712.6	8	9:33	4.1	8.45	573	278	37	0.12
RG	723.6	8	10:19	4.1	8.66	584	283	37	0.15
RG	731.1	8	10:55	4.9	8.65	584	284	37	0.12
RG	738.8	8	11:15	5.0	8.68	578	281	36	0.11
RG	747.5	8	11:35	5.4	8.53	579	281	36	0.1

Type	Distance (km)	Day	Time	Temp (°C)	pH	EC (μS cm^{-1})	TDS (mg L^{-1})	Cl (mg L^{-1})	Br (mg L^{-1})
RG	766.0	8	2:13	12.6	8.82	815	399	57	0.15
RG	772.4	8	3:00	7.7	8.88	737	359	59	0.15
RG	780.2	8	3:37	11.0	8.70	656	319	51	0.12
RG	784.6	8	3:55	11.6	8.75	656	321	na	na
RG	791.4	8	4:15	10.8	8.58	645	314	50	0.13
RG	796.1	8	4:32	10.3	8.78	654	318	na	na
RG	797.2	8	4:40	10.9	8.76	653	318	50	0.12
RG	801.3	8	4:58	11.9	8.79	655	318	50	0.13
RG	806.6	8	5:05	12.2	8.70	1260	622	215	0.19
RG	813.0	9	8:00	8.7	7.67	1686	841	360	0.2
RG	825.4	9	8:33	8.1	8.03	1466	727	305	0.18
RG	830.2	9	8:55	6.1	8.38	1467	723	290	0.15
RG	838.5	9	9:17	6.2	8.70	812	397	95	0.13
RG	840.2	9	9:25	6.1	8.74	805	393	95	0.13
RG	841.0	9	9:37	7.6	8.24	848	415	86	0.14
RG	845.6	9	9:50	9.2	7.98	1011	498	85	0.15
RG	852.3	9	10:10	8.1	8.08	1212	598	98	0.21
RG	858.7	9	10:20	8.4	8.11	1350	668	105	0.24
RG	874.3	9	10:40	8.1	8.25	1370	679	115	0.27
RG	891.3	9	11:00	8.5	8.38	1449	719	130	0.21
RG	904.4	9	11:25	8.4	8.30	1451	720	140	0.3
RG	912.3	9	11:40	8.1	8.45	1435	712	135	0.11
RG	919.5	9	11:55	8.0	8.37	1442	715	140	0.28
RG	929.9	9	12:05	7.6	8.12	1602	798	175	0.33

Type	Distance (km)	Day	Time	Temp (^{o}C)	pH	EC (μS cm^{-1})	TDS (mg L^{-1})	Cl (mg L^{-1})	Br (mg L^{-1})
RG	937.1	9	12:27	11.5	7.91	2440	1237	250	0.51
RG	944.7	9	1:05	9.5	7.60	1600	798	180	0.31
RG	959.5	9	1:40	10.8	8.35	1518	754	185	0.32
RG	966.1	9	1:55	10.4	8.38	1538	765	190	0.31
RG	979.6	9	2:21	11.1	8.47	1483	736	170	0.3
RG	987.6	9	2:35	11.3	8.37	1548	770	180	0.32
RG	1000.9	9	3:02	12.7	8.44	1618	802	195	0.34
RG	1005.4	9	3:15	12.4	8.38	1613	805	195	0.34
RG	1013.8	9	3:37	11.7	8.47	1620	806	195	0.34
RG	1021.6	10	8:15	7.9	7.82	2000	1010	270	0.46
RG	1034.5	10	8:47	6.8	8.11	2030	1018	275	0.47
RG	1047.0	10	9:03	13.2	7.05	1732	865	220	0.38
RG	1060.1	10	9:32	11.4	7.38	1916	962	285	0.46
RG	1072.9	10	9:45	9.9	7.67	2000	1006	295	0.44
RG	1085.8	10	10:12	8.9	7.53	1957	982	290	0.48
RG	1098.8	10	10:30	8.2	7.68	2200	1107	340	0.52
RG	1112.5	10	10:51	8.2	7.60	2880	1473	510	0.64
RG	1123.0	10	11:10	8.3	7.57	2800	1427	495	0.61
RG	1139.1	10	11:18	8.4	7.52	2800	1429	490	0.72
RG	1152.4	10	11:50	8.6	7.44	3320	1760	655	0.87
T	16.3	5	8:40	1.5	7.59	609	296	12	0.11
T	16.5	5	9:14	0.2	7.66	62.9	29.6	0.47	**0.01**
T	16.8	5	8:54	1.3	7.23	42.1	67.8	1.3	0.069
T	66.3	5	11:24	1.3	7.52	146.9	70	1.5	0.018

Table J.11: January 2001 major cations and $^{87}Sr/^{86}Sr$ for the main stem Rio Grande. Samples analyzed by the New Mexico Bureau of Geology and Mineral Resources. See Table J.8 for detailed sample locations.

Distance (km)	Ca (mg L^{-1})	K (mg L^{-1})	Mg (mg L^{-1})	Na (mg L^{-1})	Sr (mg L^{-1})	$^{87}Sr/^{86}Sr$	$^{87}Sr/^{86}Sr$ error
141.2	18	2.3	2.9	7.1	**0.25**		
148.6	21	5.3	3.3	9.8	**0.25**		
225.2	25	4.6	4.2	18	0.29		
356.6	31	3.8	6.2	19	0.36	0.708936	0.000013
545.1	49	4.1	8.1	27	0.61		
582.9	54	5.9	7.9	42	0.69		
630.7	56	5.8	8.5	42	0.77		
655.3	61	6	9.5	57	0.88		
731.1	61	6.2	11	59	0.89	0.710079	0.000011
772.4	68	7.1	13	81	1.1		
801.3	51	7.1	13	77	1.1		
813.0	128	17	22	211	3.52		
845.6	70	6.8	19	117	1.4		
891.3	97	8.4	26	170	2.6		
919.5	83	9.3	24	166	2.4		
937.1	137	10	33	287	3.1		
979.6	109	14	26	185	2.5		
1013.8	98	16	29	218	2.65		
1034.5	123	15	30	310	3		
1072.9	144	14	28	284	3.4		
1112.5	188	16	34	398	4.7		
1152.4	225	17	50	493	5.9	0.709863	0.000013

Table J.12: January 2001 major anions for the main stem Rio Grande. Samples analyzed by the New Mexico Bureau of Geology and Mineral Resources. See Table J.8 for detailed sample locations.

Distance (km)	HCO_3 (mg L^{-1})	F (mg L^{-1})	NO_3 (mg L^{-1})	PO_4 (mg L^{-1})	SO_4 (mg L^{-1})
141.2	71	**0.1**	**0.1**	**0.5**	13
148.6	77	**0.1**	7.9	**0.5**	13
225.2	104	0.23	4.2	**0.5**	25
356.6	119	0.52	2.3	**0.5**	35
545.1	168	0.46	0.42	**0.5**	60
582.9	169	0.71	3.4	**0.5**	72
630.7	181	0.58	2.3	**0.5**	77
655.3	195	0.57	0.71	**0.5**	97
731.1	190	0.56	2	**0.5**	96
772.4	202	0.79	**0.1**	**0.5**	135
801.3	165	0.72	**0.1**	**0.5**	129
813.0	208	1.4	10	0.64	164
845.6	238	0.77	2.3	**0.5**	164
891.3	175	0.59	1.7	**0.5**	349
919.5	131	0.32	1.3	**0.5**	358
937.1	125	0.22	**0.1**	**0.5**	688
979.6	214	0.42	9.3	**0.5**	338
1013.8	186	0.43	7.2	**0.5**	374
1034.5	271	0.49	8	0.55	453
1072.9	319	0.79	7.3	1.9	365
1112.5	315	0.85	11	1.9	530
1152.4	311	0.86	8.5	2.3	586

Table J.13: Description of sampling locations for August 2001 - August 2003. RG= Rio Grande, D=Drain, CC=Conveyance Channel, T=natural tributary, SAP=San Acacia pool (which was sampled only once in March 2002).

Type	Distance (km)	Location	Road
RG	3.2	Headwaters	Bridge/Little Squaw Resort
RG	23.8	Along Road	Rt 149
RG	40.8	Marshall Bridge	Rt 149
RG	50.3	Creede	Bridge CR 806 (Deep Creek Road)
RG	61.7	Wagon Wheel Gap	Bridge on 149
RG	79.5	Masonic Park	Bridge
RG	104.1	Del Norte	Cr17
RG	115.3	Del Norte	Rt 112
RG	130.0	Del Norte	Five Mile Road Bridge
RG	141.2	Monte Vista	US Rt 285
RG	155.6	Monte Vista	Bridge CR6 (CR9/CR100)
RG	192.8	Alamosa	Cole Park
RG	203.1	Alamosa NWR	main parking lot
RG	225.2		Z Road Bridge
RG	243.5		Rt 142 Bridge
RG	256.9	Lobatos	CR H (or G) Bridge
RG	306.7	Cerro	Chiflo Trail off of SR 378
RG	332.5	Arroyo Hondo	Bridge near Arroyo Hondo
RG	359.3	Below Taos Jct Bridge	Off of SR RT 570
RG	384.5	Embudo Station	Off of SR RT 68
RG	393.9	Lyden	SR RT 582 Bridge
RG	407.4	San Juan Pueblo	SR 74 Bridge
RG	415.3	Santa Cruz	Rt 84 Bridge

Type	Distance (km)	Location	Road
RG	430.9	Otowi	Rt 502 Bridge
RG	471.0	Cochiti Dam	SR 22 Bridge
RG	496.4	San Felipe	Bridge BIA85
RG	514.8	Bernalillo	SR44 Bridge
RG	533.4	Alameda	SR 528 Bridge
RG	547.5	Albuquerque	Cental Ave Bridge
RG	555.6	Albuquerque	Rt 550 Bridge
RG	564.9	Albuquerque	I-25 Bridge
RG	570.0	Isleta	Rt 147, at diversion dam
RG	582.9	Los Lunas	Rt 6
RG	601.1	Belen	Rt 309
RG	614.7	Bosque	RT 346 Bridge
RG	630.7	Bernardo	US RT 60 Bridge
RG	642.9	La Joya	La Joya Refuge - Exit 169 I-25
RG	655.3	San Acacia	Cross RR Tracks walk down to river
RG	671.8	Pueblito	Pueblito Bridge
RG	679.3	Socorro	Take Chaparral Dr. to Riverside Park
RG	686.3	Luiz Lopez	Bridge near Riverside Park
RG	696.4	San Antonio	US RT 380 Bridge
RG	712.6	Bosque del Apache	take 2nd trail w/ steps at far end of Refuge – look for weather tower
RG	723.6	Tiffany	Tiffany Pumps

Type	Distance (km)	Location	Road
RG	731.1	San Marcial	at RR Bridge
RG	738.8	Fort Craig	Fort Craig Pumping Site
RG	747.5	Corral Site	end of road - RG near road
RG	772.4	Elephant Butte Reservoir	Upper Narrows Road
RG	780.2	Elephant Butte Reservoir	Monticello Point
RG	791.4	Elephant Butte Reservoir	Rock Canyon Marina
RG	797.2	Elephant Butte Reservoir	on dam
RG	801.3	below Elephant Butte dam	Park below Spillway
RG	806.6	T or C	Along E. Riverside Drive
RG	813.0	Williamsburg	Along Rt 187
RG	830.2	Caballo Reservoir	Seco Creek area
RG	838.5	Caballo Reservoir	Boat Launch
RG	841.0	below Caballo dam	Picnic Area
RG	845.6	Arrey	CR-B38 Bridge
RG	852.3	Arrey	Rt 187 Bridge
RG	858.7	Garfield	Take paved road (Walnut Grove?) near 436 at Catholic Church on Loma Parda
RG	874.3	Placitas	Rt 187 Bridge
RG	891.3	Rincon	Rt 140 Bridge
RG	899.4	Haynor Ranch	Tonuco Bridge
RG	912.3	Seldon Canyon	River Bend off of Rt185
RG	919.5	Leasburg	Rt 185 Bridge below diversion dam

Type	Distance (km)	Location	Road
RG	929.9	Hill	(185-S and 158-E) Intersection, follow road to river
RG	935.5	Dona Ana	Bridge CRD052 (Shalem Colony Trl)
RG	944.7	Las Cruces	US RT 70 Bridge
RG	955.1	Mesilla	Bridge SRR 374 (Mesilla Dam Road) at div. dam
RG	966.1	Mesquite	Rt 192 Bridge
RG	979.6	Berino	Rt 226 Bridge
RG	987.6	Anthony	Rt255 Bridge
RG	997.6	Canutillo	Rt 259 Bridge
RG	1005.4	Montoya	Country Club Rd (Ranch 260)
RG	1013.8	Sunland Park	Rt 490 Bridge
RG	1021.6	El Paso	Entrance to Levee Rd below American dam
RG	1034.5	El Paso	Levee Rd -8 miles along
RG	1047.0	Socorro	Levee Rd
RG	1060.1	Clint	Levee Rd
RG	1072.9	Fabens	Levee Rd
RG	1085.8	Tornillo	Levee Rd
RG	1098.8		Levee Rd
RG	1112.5	Ft. Hancock	Levee Rd
RG	1126.0		Levee Rd
RG	1139.1		Levee Rd
RG	1149.0	Ft. Quitman Gage	Levee Rd
D	166.0	Rio Grande Drain	Stanley Road

Type	Distance (km)	Location	Road
D	195.0	Closed Basin Canal	5.5 miles east of Alamosa on US160
D	555.6	Atrisco Riverside Drain	Rt 550 Bridge - West Side
D	555.6	Albuquerque Drain	Rt 550 Bridge - East Side
D	601.1	Lower Belen Riverside Drain	Rt 309 - West Side
D	601.1	Lower Peralta Riverside Drain	Rt 309 - East Side
D	630.7	San Francisco Riverside Drain	US Rt 60 Bridge
D	696.4	Socorro Riverside Drain	US RT 380 Bridge
D	874.8	Garfield Drain	Bridge on RT 187 near sample below
D	888.2	Hatch Drain	Bridge on Rt 185
D	973.6	Del Rio Drain	Bridge near Vado
D	982.8	La Mesa Drain	Rt 226 Bridge
D	991.7	East Drain	South of Anthony off of Rt20
D	1014.0	Montoya Drain	Bridge Rt 498
D	1080.3	Fabens Waste Channel	on Levee Road
D	1139.6	River Drain	on Levee Road
D	1140.1	Lower Drain	on Levee Road
CC	655.3	San Acacia	below diversion dam
CC	671.8	Pueblito	Pueblito Bridge
CC	679.3	Socorro	Take Chaparral Dr. to Riverside Park
CC	686.3	Luiz Lopez	Bridge near Riverside Park
CC	696.4	San Antonio	US RT 380 Bridge
CC	712.6	Bosque del Apache	take 2nd trail w/ steps at far end of Refuge – look for weather tower

Type	Distance (km)	Location	Road
CC	723.6	Tiffany	Tiffany Pumps
CC	731.1	San Marcial	RR Bridge
CC	738.8	Fort Craig	Fort Craig Pumping Site
T	85.7	South Fork of Rio Grande	US Rt. 160 - 1 Mile from Jct W/ SR149
T	214.6	La Jara Creek	Bridge on CR 122S
T	224.3	Trinchera Creek	Bridge on Sec. Road / Just North of Z Road
T	225.6	Conjeos River	Bridge on 28 Rd
T	273.6	Costilla Creek	SSR516 Near CO/NM Boundry
T	318.9	Red River	Bridge on SR515 at Fish Hatchery
T	332.5	Rio Hondo	near above sample
T	356.2	Rio Pueblo de Taos	Off Los Cordovas Rd / 2mi SW of Los Cordovas
T	380.6	Embudo Creek at Dixon	Near Jct of Rt 75/68
T	409.2	Rio Chama	US RT 285 Bridge
T	UChama	Upper Rio Chama	Bridge on SR 554
T	OjoCal	Rio Ojo Caliente	Bridge on SR 111
T	415.3	Santa Cruz River	Rt 84 Bridge near Rt 369
T	418.3	Santa Clara Creek	SR 30 Bridge - 2.5 km S of US 84
T	450.3	Rito de los Frijoles	Bandelier Nat'l Mnt. Rd - off of SR4
T	473.7	Santa Fe River	Bridge on SR 22 - N of jct. w/ SR16
T	482.8	Galisteo Creek	Bridge on SR 22 - Santo Domingo Pueblo
T	637.1	Rio Puerco	I-25 Exit 175 / Old Hwy 85 Bridge
T	650.0	Rio Salado	I-25 bridge
SAP	655.0	San Acacia pool	east side of butte next to San Acacia graveyard

Table J.14: Correlations of August 2001 - August 2003 sampling locations with USGS gaging stations and NAWQA sampling sites as well as latitude, longitude, and elevation of sampling locations. Latitude, longitude and elevation coordinates were not obtained at Rito de los Frijoles due to interference from trees. Coordinates were not recorded for stations that were dry in August 2001 nor for the San Acacia pool. See Table J.13 for detailed sample explanations.

Type	Distance (km)	Notes	Latitude		Longitude		Elevation (m)
			Deg	Min.	Deg	Min.	
RG	3.2		37	43.7467	107	14.0513	2807
RG	23.8		37	44.1880	107	4.3340	2699
RG	40.8		37	47.5475	106	58.9140	2630
RG	50.3		37	49.0313	106	54.9022	2607
RG	61.7	USGS 08217500	37	46.6459	106	50.2166	2562
RG	79.5		37	42.0604	106	41.1189	2503
RG	104.1	USGS 08220000/NAWQA Site 1	37	41.2953	106	27.5850	2425
RG	115.3		37	41.0705	106	21.0601	2394
RG	130.0		37	38.8326	106	14.4625	2342
RG	141.2		37	36.5207	106	8.5804	2313
RG	155.6		37	34.2541	106	2.3838	2297
RG	192.8		37	28.2273	105	51.7640	2287
RG	203.1		37	26.3060	105	48.1690	2275
RG	225.2	NAWQA Site 4	37	18.4071	105	44.2771	2276
RG	243.5		37	10.8200	105	43.7240	2255
RG	256.9	USGS 08251500/NAWQA Site 6	37	4.6816	105	45.3577	2258
RG	306.7	USGS 08263500	36	44.5047	105	40.8309	2258
RG	332.5		36	32.0925	105	42.5138	1961
RG	359.3	USGS 08276500/NAWQA Site 7	36	19.1867	105	45.2635	1826
RG	384.5	USGS 08279500	36	12.4344	105	57.6443	1754
RG	393.9		36	8.7499	105	59.8466	1722

Type	Distance (km)	Notes	Latitude		Longitude		Elevation (m)
			Deg	Min.	Deg	Min.	
RG	407.4		36	3.4205	106	4.7440	1695
RG	415.3		35	59.4062	106	4.5557	1704
RG	430.9	USGS 08313000/NAWQA Site 9	35	52.5510	106	8.5707	1676
RG	471.0	USGS 08317400	35	37.0358	106	19.4857	1577
RG	496.4	USGS 08319000	35	26.3987	106	26.6376	1544
RG	514.8		35	19.3730	106	33.5792	1536
RG	533.4		35	11.8830	106	38.6477	1502
RG	547.5	USGS 08330000	35	5.4774	106	40.7688	1496
RG	555.6		35	1.6082	106	40.4588	1491
RG	564.9		34	57.0101	106	40.9176	1505
RG	570.0	NAWQA Site 12	34	54.3742	106	41.0065	1463
RG	582.9		34	48.3223	106	43.2143	1460
RG	601.1		34	39.1463	106	44.1839	1447
RG	614.7		34	32.7097	106	45.9224	1450
RG	630.7	USGS 08332010	34	25.0459	106	48.1007	1435
RG	642.9		34	19.6382	106	51.6364	1403
RG	655.3	USGS 08354900	34	15.3309	106	53.7673	1402
RG	671.8		34	7.2478	106	53.2864	1387
RG	679.3		34	3.6695	106	52.5346	1378
RG	686.3		34	0.1353	106	52.2730	1373
RG	696.4		33	55.1617	106	51.4360	1365

Type	Distance (km)	Notes	Latitude		Longitude		Elevation (m)
			Deg	Min.	Deg	Min.	
RG	712.6		na	na	na	na	na
RG	723.6		33	42.5411	106	55.9658	1349
RG	731.1	USGS 08358400/NAWQA Site 15	33	40.8546	106	59.5932	1341
RG	738.8		33	37.3689	107	0.3890	1330
RG	747.5		33	34.1981	107	4.2840	1339
RG	772.4		33	23.0367	107	9.8829	1312
RG	780.2		33	18.7406	107	11.5232	1334
RG	791.4		33	13.5261	107	12.4082	1331
RG	797.2		33	13.5431	107	12.3990	1334
RG	801.3	USGS 08361000	33	8.8595	107	12.4145	1271
RG	806.6		33	7.7471	107	13.9501	1273
RG	813.0		33	6.6130	107	17.9055	1276
RG	830.2		32	59.0493	107	17.3073	1255
RG	838.5		32	54.6558	107	18.4169	1270
RG	841.0	USGS 08362500	32	53.6289	107	17.5753	1236
RG	845.6		32	51.3903	107	17.9355	1245
RG	852.3		32	48.5071	107	18.1797	1234
RG	858.7		32	45.9196	107	17.0316	1231
RG	874.3		32	40.9105	107	11.3366	1221
RG	891.3		32	39.2378	107	4.5668	1204
RG	899.4		32	36.7898	107	1.1839	1196

Type	Distance (km)	Notes	Latitude		Longitude		Elevation (m)
			Deg	Min.	Deg	Min.	
RG	912.3		32	30.9575	106	58.2950	1203
RG	919.5	NAWAQ Site 16	32	29.2291	106	55.5494	1186
RG	929.9		32	25.1409	106	52.0365	1176
RG	935.5		32	22.5368	106	51.3189	1169
RG	944.7		32	18.6052	106	49.6009	1156
RG	955.1		32	13.7275	106	47.9192	1150
RG	966.1		32	9.6669	106	42.9558	1147
RG	979.6		32	3.9381	106	39.7357	1133
RG	987.6		31	59.9731	106	38.1784	1124
RG	997.6		31	54.9515	106	36.1495	1128
RG	1005.4		31	50.7933	106	36.4017	1123
RG	1013.8	USGS 0836400	31	47.9638	106	33.1992	1122
RG	1021.6		31	45.6878	106	30.4275	1114
RG	1034.5		31	44.3591	106	23.5827	1106
RG	1047.0		31	38.5011	106	18.9954	1099
RG	1060.1		31	33.0043	106	15.4026	1086
RG	1072.9		31	27.5555	106	11.0508	1074
RG	1085.8		31	23.8903	106	4.3966	1059
RG	1098.8		31	21.8009	105	57.1330	1055
RG	1112.5		31	17.5231	105	52.5655	1064
RG	1126.0		31	12.0953	105	47.4837	1061

Type	Distance (km)	Notes	Latitude		Longitude		Elevation (m)
			Deg	Min.	Deg	Min.	
RG	1139.1		31	7.8429	105	41.5381	1039
RG	1149.0	IBWC Ft. Quitman Gage	31	5.2458	105	36.5522	1037
D	166.0		37	34.4626	105	58.4566	2286
D	195.0		37	28.4299	105	45.9952	2299
D	555.6		35	1.6082	106	40.4588	1491
D	555.6		35	1.6073	106	40.1509	1492
D	601.1		34	39.1805	106	44.4293	1447
D	601.1		34	39.1463	106	44.1839	1447
D	630.7		34	25.0459	106	48.1007	1435
D	696.4		33	55.1617	106	51.4360	1365
D	874.8		32	41.2243	107	11.5149	1219
D	888.2		32	39.0635	107	6.6321	1213
D	973.6		32	6.9069	106	39.9750	1139
D	982.8		32	3.7311	106	40.4150	1135
D	991.7		31	58.1533	106	36.3468	1125
D	1014.0		31	48.1299	106	32.8882	1121
D	1080.3		31	25.4980	106	7.4428	1065
D	1139.6		31	7.7964	105	41.3046	1051
D	1140.1		31	7.4552	105	40.2295	1045
CC	655.3	USGS 08354800	na	na	na	na	na
CC	671.8		34	7.2478	106	53.2864	1387

Type	Distance (km)	Notes	Latitude		Longitude		Elevation (m)
			Deg	Min.	Deg	Min.	
CC	679.3		34	3.6695	106	52.5346	1378
CC	686.3		34	0.1353	106	52.2730	1373
CC	696.4		33	55.1617	106	51.4360	1365
CC	712.6		33	47.6816	106	52.3974	1353
CC	723.6		33	42.5411	106	55.9658	1349
CC	731.1	USGS 08358300/NAWQA Site 14	33	40.8546	106	59.5932	1341
CC	738.8		33	37.3689	107	0.3890	1330
T	85.7	USGS 08219500	37	39.6967	106	38.8127	2469
T	214.6		37	22.2859	105	49.2437	2282
T	224.3		na	na	na	na	na
T	225.6	USGS 08249000/NAWQA Site 5	37	17.4997	105	44.8438	2278
T	273.6	USGS 08252500	na	na	na	na	na
T	318.9	USGS 08266820	36	41.0343	105	39.1427	2157
T	332.5	USGS 08267500	36	32.0925	105	42.5138	1961
T	356.2	USGS 08276300	na	na	na	na	na
T	380.6	USGS 08279000	36	12.6025	105	54.6359	1778
T	409.2	USGS 08290000/NAWQA Site 8	36	4.3935	106	6.7525	1705
T	UChama	USGS 08287000	36	13.0240	106	14.9025	1769
T	OjoCal	USGS 08289000	36	20.8319	106	2.6144	1927
T	415.3	USGS 08291000	35	59.3820	106	4.0265	1694
T	418.3		na	na	na	na	na

Type	Distance (km)	Notes	Latitude		Longitude		Elevation (m)
			Deg	Min.	Deg	Min.	
T	450.3	NAWQA Site 10	na	na	na	na	na
T	473.7	USGS 08317200 / NAWQA Site 11	na	na	na	na	na
T	482.8	USGS 08317950	na	na	na	na	na
T	637.1	USGS 08353000 / NAWQA Site 13	34	24.5993	106	51.1728	1419
T	650.0	USGS 08354000	na	na	na	na	na

Table J.15: August 2001 field parameters. Bolded values indicate the instrument was unstable. The "Day" column indicates the numbered day of the month. "sfas"= samples were filtered after several hours of sitting within 24 hours of sample collection. "nfs"= no filtered samples available. See Table J.13 for detailed sampling station locations.

Type	Distance (km)	Day	Time	Temp (°C)	pH	EC (μS cm^{-1})	TDS (mg L^{-1})	Notes
RG	3.2	16	8:30	12.5	5.87	68.0	31.7	
RG	23.8	16	10:10	13.6	**3.31**	59.4	28.1	
RG	40.8	16	10:45	13.4	**5.50**	62.0	29.0	
RG	50.3	16	11:25	14.7	**4.90**	67.7	31.9	
RG	61.7	16	11:50	15.7	5.38	67.6	31.9	
RG	79.5	16	12:20	16.0	5.17	70.3	33.2	
RG	104.1	16	13:45	17.1	5.90	76.1	36.0	
RG	115.3	16	14:40	18.1	6.98	94.1	44.5	
RG	130.0	16	15:05	18.9	7.12	91.0	43.1	
RG	141.2	16	15:25	20.4	7.24	90.6	42.9	
RG	155.6	16	16:00	20.6	7.35	113.7	54.1	
RG	192.8	16	17:00	23.1	6.84	198.6	95.0	
RG	203.1	16	17:50	22.7	7.57	278.0	133.6	
RG	225.2	17	8:35	14.6	7.19	370.0	178.3	
RG	243.5	17	9:55	16.0	7.22	378.0	182.3	
RG	256.9	17	10:45	18.0	7.15	348.0	167.2	
RG	306.7	17	12:45	21.5	7.56	301.0	144.7	
RG	332.5	17	14:45	20.4	7.04	300.0	144.4	
RG	359.3	17	16:30	21.0	7.62	315.0	151.4	
RG	384.5	17	17:20	22.8	8.01	308.0	148.4	
RG	393.9	17	17:45	22.9	7.42	318.0	152.9	

Type	Distance (km)	Day	Time	Temp (C)	pH	EC (μS cm^{-1})	TDS (mg L^{-1})	Notes
RG	407.4	17	18:15	24.2	8.12	329.0	158.3	
RG	415.3	18	10:30	19.8	7.64	359.0	173.2	
RG	430.9	18	11:35	20.6	7.70	362.0	174.3	
RG	471.0	18	15:00	23.5	7.01	321.0	154.6	
RG	496.4	18	16:00	25.9	7.59	335.0	160.9	
RG	514.8	18	16:30	25.9	7.32	368.0	177.5	
RG	533.4	19	9:05	20.9	7.27	367.0	176.7	
RG	547.5	19	9:50	21.8	8.17	365.0	176.2	
RG	555.6	19	10:30	24.8	7.87	365.0	175.6	
RG	564.9	19	11:30	26.9	7.44	407.0	196.5	
RG	570.0	19	12:10	24.6	7.29	420.0	203.0	
RG	582.9	19	12:45	28.9	7.31	440.0	213.0	
RG	601.1	19	14:00	25.5	7.62	500.0	242.0	
RG	614.7	19	15:30	28.7	7.22	470.0	227.0	
RG	630.7	19	16:05	30.2	8.53	491.0	238.0	
RG	642.9	19	17:15	27.4	7.62	544.0	264.0	
RG	655.3	19	18:05	26.9	7.58	558.0	270.0	sfas
RG	671.8	20	12:30	26.9	7.60	562.0	273.0	
RG	679.3	20	13:45	27.3	7.66	572.0	278.0	
RG	686.3	20	14:35	27.9	7.64	573.0	278.0	
RG	696.4	20	15:35	27.9	7.63	578.0	280.0	
RG	712.6	20	na	na	na	na	na	dry
RG	723.6	20	18:00	26.4	7.77	613.0	297.0	sfas

Type	Distance (km)	Day	Time	Temp (C)	pH	EC (μS cm^{-1})	TDS (mg L^{-1})	Notes
RG	731.1	20	18:40	25.7	7.74	609.0	296.0	sfas
RG	738.8	20	19:15	25.7	7.93	615.0	299.0	sfas
RG	747.5	20	15:30	26.6	7.69	631.0	307.0	sfas
RG	772.4	21	11:00	24.0	8.02	790.0	386.0	
RG	780.2	21	13:05	25.0	8.07	664.0	323.0	
RG	791.4	21	13:35	26.1	7.79	669.0	325.0	
RG	797.2	21	14:05	25.7	7.54	674.0	328.0	
RG	801.3	21	14:20	17.7	7.32	695.0	338.0	
RG	806.6	21	15:05	17.7	7.51	706.0	344.0	
RG	813.0	21	15:30	17.8	7.39	711.0	346.0	
RG	830.2	23	8:45	19.1	7.64	731.0	357.0	
RG	838.5	21	16:15	23.9	7.97	708.0	345.0	
RG	841.0	21	16:35	23.3	7.42	716.0	349.0	
RG	845.6	21	16:55	23.5	8.14	716.0	349.0	
RG	852.3	21	17:15	24.5	8.00	726.0	354.0	
RG	858.7	21	17:30	24.7	8.23	729.0	355.0	
RG	874.3	21	18:00	24.8	7.82	732.0	356.0	
RG	891.3	21	18:50	24.9	8.31	770.0	375.0	
RG	899.4	21	19:15	24.4	7.55	754.0	368.0	
RG	912.3	21	20:00	24.0	7.92	763.0	372.0	
RG	919.5	22	7:40	22.0	8.16	767.0	375.0	
RG	929.9	22	8:00	22.0	8.23	784.0	382.0	
RG	935.5	22	8:15	21.9	7.92	781.0	381.0	

Type	Distance (km)	Day	Time	Temp (C)	pH	EC (μS cm^{-1})	TDS (mg L^{-1})	Notes
RG	944.7	22	8:45	22.8	7.88	784.0	382.0	
RG	955.1	22	9:20	22.9	**7.85**	783.0	382.0	
RG	966.1	22	9:45	23.3	7.65	795.0	388.0	
RG	979.6	22	10:45	23.6	7.78	861.0	421.0	
RG	987.6	22	11:05	24.3	8.29	916.0	448.0	
RG	997.6	22	12:05	25.0	8.22	956.0	469.0	
RG	1005.4	22	12:35	26.0	8.01	952.0	467.0	
RG	1013.8	22	13:00	26.2	7.83	945.0	463.0	
RG	1021.6	22	14:15	28.6	8.48	1022.0	502.0	
RG	1034.5	22	14:45	29.9	8.23	1009.0	495.0	
RG	1047.0	22	15:15	26.7	7.34	1325.0	657.0	
RG	1060.1	22	15:40	31.7	7.78	1318.0	652.0	
RG	1072.9	22	16:00	32.9	8.03	1262.0	623.0	
RG	1085.8	22	16:45	34.4	8.68	2290.0	1142.0	
RG	1098.8	22	17:10	32.2	8.11	2300.0	1164.0	
RG	1112.5	22	17:35	29.0	7.88	3970.0	2060.0	
RG	1126.0	22	18:05	30.5	8.05	3640.0	1882.0	
RG	1139.1	22	18:30	31.2	8.20	2950.0	1509.0	
RG	1149.0	22	19:10	28.9	8.13	4320.0	2250.0	
D	166.0	16	16:20	21.7	7.38	168.5	80.5	
D	195.0	16	17:20	21.1	8.13	378.0	182.2	
D	555.6	19	10:30	20.9	7.36	357.0	172.0	
D	555.6	19	11:05	22.5	7.33	369.0	177.9	

Type	Distance (km)	Day	Time	Temp (C)	pH	EC (μS cm^{-1})	TDS (mg L^{-1})	Notes
D	601.1	19	14:00	25.9	7.28	675.0	329.0	
D	601.1	19	14:00	24.4	7.48	522.0	252.0	
D	630.7	19	16:05	26.3	7.58	628.0	305.0	
D	696.4	20	15:35	23.8	8.30	1167.0	575.0	
D	874.8	21	18:10	25.0	8.14	1624.0	809.0	
D	888.2	21	18:30	23.5	7.65	1654.0	825.0	
D	973.6	22	10:07	21.9	7.45	1274.0	629.0	
D	982.8	22	10:27	21.1	7.54	1555.0	773.0	
D	991.7	22	11:45	25.5	8.11	1259.0	620.0	
D	1014.0	22	13:45	25.8	7.60	1928.0	966.0	
D	1080.3	22	16:20	26.9	7.94	1528.0	760.0	
D	1139.6	22	18:40	29.1	8.12	5030.0	2640.0	sfas
D	1140.1	22	18:50	29.5	8.05	7280.0	3880.0	sfas
CC	655.3	19	na	na	na	na	na	dry
CC	671.8	20	12:30	24.4	7.70	623.0	302.0	
CC	679.3	20	13:45	23.3	**8.10**	610.0	296.0	nfs
CC	686.3	20	14:35	23.0	7.88	636.0	309.0	
CC	696.4	20	15:35	21.7	8.23	686.0	334.0	nfs
CC	712.6	20	16:55	22.4	7.67	718.0	346.0	
CC	723.6	20	18:00	22.9	7.55	834.0	400.0	nfs
CC	731.1	20	18:40	24.4	7.64	844.0	413.0	
CC	738.8	20	19:15	24.0	7.65	828.0	405.0	nfs
T	85.7	16	13:10	17.1	5.38	65.7	31.0	

Type	Distance (km)	Day	Time	Temp (°C)	pH	EC (μS cm^{-1})	TDS (mg L^{-1})	Notes
T	214.6	17	7:50	15.7	7.40	580.0	282.0	
T	224.3	17	na	na	na	na	na	dry
T	225.6	17	9:10	17.4	6.73	195.6	93.5	
T	273.6	17	na	na	na	na	na	dry
T	318.9	17	13:55	19.7	7.00	370.0	178.3	
T	332.5	17	15:00	22.5	7.57	320.0	154.1	
T	356.2	17	na	na	na	na	na	dry
T	380.6	17	17:04	22.6	8.15	315.0	151.6	
T	409.2	18	8:30	16.5	7.36	399.0	192.5	
T	UChama	18	9:00	16.0	7.94	374.0	180.2	
T	OjoCal	18	9:50	17.5	7.81	952.0	467.0	
T	415.3	18	11:00	21.1	8.26	327.0	157.1	
T	418.3	18	na	na	na	na	na	dry
T	450.3	18	12:20	18.2	6.41	117.3	55.8	
T	473.7	18	na	na	na	na	na	dry
T	482.8	18	na	na	na	na	na	dry
T	637.1	19	16:45	29.0	7.91	1380.0	683.0	sfas
T	650.0	20	na	na	na	na	na	dry

Table J.16: August 2001 stable isotopes, ammonium, total dissolved nitrate (TDN), dissolved organic carbon (DOC), nitrate, and sulfate. See Table J.13 for detailed sampling station locations. Analyses performed at the University of Arizona.

Type	Distance (km)	$\delta^{18}O$ (per mille)	δD (per mille)	NH_4 (mg L^{-1})	TDN (mg L^{-1})	DOC (mg L^{-1})	NO_3 (mg L^{-1})	SO_4 (mg L^{-1})
RG	3.2	-14.2	-98	0.001	0.200	2.611	0.000	4.06
RG	23.8	-14.1	-101	0.003	0.230	3.46	0.054	2.82
RG	40.8	-13.9	-98	0.002	0.180	2.828	0.000	3.82
RG	50.3	-14.1	-100	0.000	0.270	2.774	0.057	4.15
RG	61.7	-14.1	-99	0.000	0.180	3.574	0.015	5.83
RG	79.5	-14.1	-100	0.002	0.130	2.815	0.000	6.93
RG	104.1	-14.0	-98	0.000	0.270	3.419	0.037	5.53
RG	115.3	-13.6	-99	0.001	0.180	3.196	0.000	6.13
RG	130.0	-14.0	-100	0.001	na	na	0.000	6.11
RG	141.2	-14.0	-98	0.001	0.370	3.271	0.000	5.59
RG	155.6	-13.6	-98	0.002	0.390	3.287	1.794	6.59
RG	192.8	-12.8	-95	0.007	0.250	4.149	0.468	12.1
RG	203.1	-12.3	-94	0.004	0.560	4.173	1.781	19.2
RG	225.2	-11.9	-90	0.002	0.420	4.512	0.998	43.7
RG	243.5	-11.3	-87	0.004	0.330	4.076	0.000	44.8
RG	256.9	-11.2	-86	0.061	0.200	4.044	0.000	38.7
RG	306.7	-11.8	-90	0.004	0.170	3.401	0.277	16.7
RG	332.5	-13.1	-96	0.002	0.340	2.393	1.080	47.6
RG	359.3	-13.0	-95	0.005	0.370	4.255	1.100	51.2
RG	384.5	-12.7	-91	0.001	0.270	4.026	0.534	37.7
RG	393.9	-12.7	-90	0.001	0.350	3.924	0.282	37.4

Type	Distance (km)	$\delta^{18}O$ (per mille)	δD (per mille)	NH_4 (mg L^{-1})	TDN (mg L^{-1})	DOC (mg L^{-1})	NO_3 (mg L^{-1})	SO_4 (mg L^{-1})
RG	407.4	-12.6	-92	0.004	0.360	3.933	0.245	39.1
RG	415.3	-12.0	-88	0.000	0.220	3.849	0.171	57.6
RG	430.9	-12.1	-88	0.000	0.230	na	0.124	56.4
RG	471.0	-11.8	-86	0.007	0.310	4.466	0.326	58.5
RG	496.4	-11.8	-87	0.006	0.240	4.329	0.033	59.8
RG	514.8	-11.5	-85	0.001	0.260	4.211	0.037	66.4
RG	533.4	-11.6	-86	0.004	0.170	3.968	0.194	64.6
RG	547.5	-11.5	-86	0.005	0.200	3.731	0.265	62.5
RG	555.6	-11.1	-85	0.002	0.240	4.48	0.384	63.2
RG	564.9	-10.8	-86	0.003	1.310	4.662	6.327	64.1
RG	570.0	-11.5	-86	0.011	1.610	4.226	6.137	64.6
RG	582.9	-11.3	-85	0.002	1.180	3.95	6.082	65.6
RG	601.1	-11.3	-86	0.012	1.080	3.837	3.985	77.0
RG	614.7	-11.1	-86	0.008	1.490	4.732	5.783	74.1
RG	630.7	-10.9	-83	0.007	1.010	3.907	5.364	78.1
RG	642.9	-10.4	-81	0.008	1.120	5.046	4.527	101.3
RG	655.3	-10.4	-81	0.011	1.530	4.467	5.289	99.7
RG	671.8	-10.6	-81	0.030	1.250	4.246	4.713	102.0
RG	679.3	-10.5	-81	0.008	1.250	4.248	4.725	106.1
RG	686.3	-10.1	-81	0.003	0.880	4.013	4.744	103.2
RG	696.4	-10.2	-80	0.015	1.370	4.55	5.148	105.9
RG	723.6	-9.9	-78	0.023	1.270	4.73	5.175	120.0
RG	731.1	-9.8	-77	0.037	1.310	5.214	5.250	125.7

Type	Distance (km)	$\delta^{18}O$ (per mille)	δD (per mille)	NH_4 (mg L^{-1})	TDN (mg L^{-1})	DOC (mg L^{-1})	NO_3 (mg L^{-1})	SO_4 (mg L^{-1})
RG	738.8	-10.0	-77	0.010	1.110	4.322	5.272	126.6
RG	747.5	-9.6	-76	0.003	1.450	4.895	5.618	135.9
RG	772.4	-8.8	-73	0.012	0.340	4.81	0.021	147.7
RG	780.2	-7.6	-67	0.005	0.230	4.946	0.023	129.9
RG	791.4	-7.4	-66	0.005	0.250	4.664	0.004	129.3
RG	797.2	-7.2	-65	0.013	0.200	4.631	0.007	132.8
RG	801.3	-7.6	-68	0.171	0.640	4.118	0.017	127.7
RG	806.6	-7.6	-66	0.131	0.360	4.18	0.036	110.8
RG	813.0	-7.6	-67	0.093	0.410	4.883	0.243	129.1
RG	830.2	-7.5	-66	0.051	0.360	4.154	0.189	133.0
RG	838.5	-7.2	-65	0.021	0.340	4.471	0.011	129.2
RG	841.0	-7.2	-64	0.024	0.310	4.233	0.018	123.3
RG	845.6	-7.2	-65	0.040	0.350	4.152	0.050	129.0
RG	852.3	-7.2	-65	0.030	0.320	4.219	0.082	131.8
RG	858.7	-7.1	-64	0.047	0.320	3.991	0.119	130.3
RG	874.3	-7.1	-65	0.015	0.340	4.202	0.031	133.9
RG	891.3	-7.2	-65	0.009	0.230	4.161	0.177	143.3
RG	899.4	-7.2	-64	0.008	0.310	4.529	0.168	136.9
RG	912.3	-7.1	-64	0.000	0.360	4.105	0.171	140.0
RG	919.5	-7.1	-63	0.002	0.310	4.171	0.170	140.9
RG	929.9	-7.3	-64	0.018	0.360	na	0.334	143.9
RG	935.5	-7.2	-64	0.014	0.320	4.475	0.323	142.5

Type	Distance (km)	$\delta^{18}O$ (per mille)	δD (per mille)	NH_4 (mg L^{-1})	TDN (mg L^{-1})	DOC (mg L^{-1})	NO_3 (mg L^{-1})	SO_4 (mg L^{-1})
RG	944.7	-6.9	-63	0.004	0.280	4.686	0.304	145.3
RG	955.1	-7.0	-64	0.023	0.400	na	0.668	143.4
RG	966.1	-7.0	-63	0.039	0.350	4.024	1.056	148.3
RG	979.6	-7.0	-64	0.005	0.490	4.122	1.175	161.7
RG	987.6	-7.1	-64	0.009	0.470	3.862	1.159	206.1
RG	997.6	-7.1	-63	0.036	0.610	4.777	1.140	183.7
RG	1005.4	-6.9	-63	0.021	0.410	4.309	0.758	185.9
RG	1013.8	-7.0	-65	0.013	0.330	4.439	0.609	183.1
RG	1021.6	-7.0	-66	0.063	0.390	4.271	0.589	208.5
RG	1034.5	-6.8	-62	0.087	0.400	3.862	0.363	209.4
RG	1047.0	-8.4	-68	0.705	1.530	4.45	0.376	310.7
RG	1060.1	-8.7	-70	0.365	1.380	4.927	0.675	316.3
RG	1072.9	-8.2	-68	0.108	1.550	5.035	3.118	307.1
RG	1085.8	-7.6	-67	0.011	0.900	4.957	0.028	401.2
RG	1098.8	-7.1	-65	0.045	1.780	5.363	5.021	464.6
RG	1112.5	-7.5	-67	0.029	1.920	6.342	5.139	664.2
RG	1126.0	-7.3	-66	0.042	1.910	6.602	4.902	638.9
RG	1139.1	-7.0	-64	0.086	1.940	5.432	4.969	528.0
RG	1149.0	-7.1	-65	0.073	2.040	7.153	4.481	730.5
D	166.0	-13.4	-97	0.017	0.350	4.026	0.640	12.9
D	195.0	-12.1	-91	0.002	0.330	3.913	0.011	50.6
D	555.6	-11.8	-89	0.007	0.170	3.267	0.010	62.1

Type	Distance (km)	$\delta^{18}O$ (per mille)	δD (per mille)	NH_4 (mg L^{-1})	TDN (mg L^{-1})	DOC (mg L^{-1})	NO_3 (mg L^{-1})	SO_4 (mg L^{-1})
D	555.6	-11.7	-88	0.007	0.120	4.475	0.010	54.0
D	601.1	-11.7	-87	0.015	0.910	3.909	3.582	80.8
D	601.1	-11.6	-87	0.012	0.520	3.868	1.768	124.4
D	630.7	-11.5	-88	0.011	0.780	3.617	3.211	109.8
D	696.4	-11.3	-86	0.077	0.590	4.268	0.713	193.3
D	874.8	-7.8	-68	0.058	0.990	4.222	2.697	370.2
D	888.2	-7.8	-67	0.102	1.380	4.222	4.887	407.3
D	973.6	-7.8	-67	0.043	1.310	5.243	3.890	270.2
D	982.8	-8.2	-72	0.131	1.280	4.834	3.465	352.0
D	991.7	-7.0	-63	0.078	1.150	4.167	2.456	239.1
D	1014.0	-7.7	-67	0.074	1.040	6.543	2.265	427.2
D	1080.3	-7.3	-65	0.064	2.180	6.381	8.347	472.7
D	1139.6	-7.3	-66	0.141	1.390	6.507	1.450	910.6
D	1140.1	-7.0	-65	0.242	1.980	7.065	2.892	1320.8
CC	671.8	-11.1	-83	0.042	1.120	3.993	3.924	113.4
CC	679.3	-11.1	-85	na	na	na	na	na
CC	686.3	-11.2	-85	0.052	0.420	3.221	1.229	117.1
CC	696.4	-11.3	-85	na	na	na	na	na
CC	712.6	-11.0	-85	0.007	0.520	4.367	1.232	124.6
CC	723.6	-10.8	-84	na	na	na	na	na
CC	731.1	-10.8	-83	0.026	0.610	4.246	2.102	151.9
CC	738.8	-11.0	-85	na	na	na	na	na

Type	Distance (km)	$\delta^{18}O$ (per mille)	δD (per mille)	NH_4 (mg L^{-1})	TDN (mg L^{-1})	DOC (mg L^{-1})	NO_3 (mg L^{-1})	SO_4 (mg L^{-1})
T	85.7	-14.0	-98	0.003	0.120	3.254	0.121	3.21
T	214.6	-8.9	-78	0.010	0.590	8.401	0.014	134.6
T	225.6	-11.3	-88	0.002	0.190	4.106	0.000	11.8
T	318.9	-13.7	-96	0.050	0.320	1.58	1.053	108.8
T	332.5	-13.6	-95	0.009	0.400	2.779	1.433	20.6
T	380.6	-12.0	-82	0.003	0.195	4.232	0.135	19.1
T	409.2	-11.3	-84	0.021	na	4.138	0.116	88.0
T	UChama	-11.4	-87	0.004	0.260	4.489	0.138	87.8
T	OjoCal	-12.3	-90	0.001	0.100	4.505	0.000	121.7
T	415.3	-11.5	-81	0.000	0.160	4.567	0.310	7.57
T	450.3	-11.2	-75	0.000	na	2.605	0.057	2.19
T	637.1	-4.6	-35	0.010	2.050	6.745	2.250	141.1

Table J.17: Hardness ($CaCO_3$), major cations, and alkalinity (HCO_3) for selected August 2001 samples. See Table J.13 for detailed sampling station locations. Analyses performed at the New Mexico Bureau of Geology and Mineral Resources.

Type	Distance (km)	$CaCO_3$ (mg L^{-1})	Ca (mg L^{-1})	K (mg L^{-1})	Mg (mg L^{-1})	Na (mg L^{-1})	Sr (mg L^{-1})	HCO_3 (mg L^{-1})
RG	141.2	38	12	2	1.9	4.4	0.11	na
RG	192.8	72	22	4.7	4.1	16	0.3	na
RG	256.9	109	33	6.1	6.4	35	0.45	na
RG	359.3	121	36	3.9	7.5	21	0.51	na
RG	430.9	154	49	3.5	7.6	22	0.73	na
RG	471.0	129	40	3.4	7.1	19	0.55	na
RG	547.5	148	48	4.1	6.9	24	0.77	na
RG	582.9	160	52	5.9	7.3	36	0.81	na
RG	655.3	194	63	6.3	9	52	1.1	na
RG	731.1	210	66	6.2	11	59	1.4	na
RG	772.4	215	63	7.7	14	91	1.5	191
RG	801.3	203	60	7	13	81	1.5	187
RG	841.0	196	57	7.1	13	85	1.4	189
RG	899.4	210	61	7.6	14	88	1.5	198
RG	919.5	215	63	7.7	14	86	1.6	198
RG	944.7	222	66	7.4	14	87	1.6	na
RG	1013.8	257	75	9.2	17	110	1.9	221
RG	1072.9	438	136	12	24	261	3.6	340
RG	1149.0	898	272	17	53	615	7.7	na
CC	731.1	na	57	6.2	12.6	93	0.8	na
T	637.1	406	128	7.7	21	217	3.2	261

Table J.18: $\delta^{34}S$ and $^{87}Sr/^{86}Sr$ for selected August 2001 samples. See Table J.13 for detailed sampling station locations. Analyses performed at the University of Arizona.

Type	Distance (km)	$\delta^{34}S$ (per mille)	$^{87}Sr/^{86}Sr$	$^{87}Sr/^{86}Sr$ error
RG	430.9	-3.3	na	na
RG	471.0	-3.1	0.709607	0.000011
RG	496.4	-5.2	na	na
RG	547.5	-3.1	0.709672	0.000011
RG	582.9	-2	0.709815	0.000014
RG	655.3		0.709818	0.000017
RG	723.6	-1.7	na	na
RG	731.1		0.709856	0.000016
RG	747.5	-2	na	na
RG	772.4	2.8	0.710062	0.000014
RG	801.3		0.710033	0.000016
RG	806.6	1.8	na	na
RG	841.0		0.710175	0.000013
RG	997.6	1.2	na	na
RG	1005.4	1.8	na	na
RG	1021.6	1.9	na	na
RG	1047.0	2.5	na	na
RG	1060.1	3.3	na	na
RG	1149.0	4	na	na
CC	731.1	na	0.710054	0.000016
T	637.1	na	0.709738	0.000014

Table J.19: January 2002 field parameters. Locations not in this table were not sampled in January 2002. Bolded values indicate the instrument was unstable. The "Day" column indicates the numbered day of the month. "sfas"= samples were filtered after several hours of sitting within 24 hours of sample collection. "nfs"= no filtered samples available. See Table J.13 for detailed sampling station locations.

Type	Distance (km)	Day	Time	Temp (°C)	pH	EC (μS cm^{-1})	TDS (mg L^{-1})	Notes
RG	40.8	4	na	na	na	na	na	frozen
RG	50.3	4	9:10	-0.6	7.20	89	58	
RG	61.7	4	9:35	-0.9	6.97	46	30	
RG	79.5	4	10:05	0.6	**6.80**	133	87	
RG	104.1	4	11:20	2.4	6.93	126	83	
RG	115.3	4	11:40	1.9	6.87	126	84	
RG	130.0	4	12:00	1.7	6.95	150	99	
RG	141.2	4	12:45	0.2	7.10	150	100	
RG	155.6	4	1:25	2.7	6.90	162	106	
RG	192.8	4	2:10	1.8	6.60	197	128	
RG	203.1	4	na	na	na	na	na	frozen
RG	225.2	4	na	0.2	7.04	264	174	
RG	243.5	4	na	na	na	na	na	frozen
RG	256.9	5	8:45	-0.8	7.33	232	155	
RG	306.7	5	10:10	0.2	7.71	251	168	
RG	332.5	5	12:00	1.9	7.82	296	196	
RG	359.3	5	2:30	4.0	7.96	280	151	
RG	384.5	5	3:12	3.4	8.20	292	193	
RG	393.9	5	3:30	2.9	8.11	299	196	

Type	Distance (km)	Day	Time	Temp (C)	pH	EC (μS cm^{-1})	TDS (mg L^{-1})	Notes
RG	407.4	5	3:50	3.7	8.26	292	193	
RG	415.3	5	4:15	3.6	8.05	323	212	
RG	430.9	5	4:50	2.8	7.81	337	222	
RG	471.0	6	10:45	3.8	7.58	356	232	
RG	496.4	6	11:20	4.5	7.86	367	243	
RG	514.8	6	12:00	4.2	7.90	386	253	
RG	533.4	6	12:30	4.7	7.83	420	278	
RG	547.5	6	1:25	5.6	8.04	472	310	
RG	555.6	6	2:10	7.5	7.87	426	278	
RG	564.9	6	2:45	8.7	7.86	448	292	
RG	570.0	6	3:00	9.2	7.78	461	306	
RG	582.9	6	3:30	7.7	7.94	502	331	
RG	601.1	6	4:05	7.5	8.09	414	273	
RG	614.7	6	4:40	6.4	7.99	518	337	
RG	630.7	6	5:10	5.9	8.07	535	351	
RG	642.9	7	11:15	5.5	7.29	546	360	
RG	655.3	7	na	8.0	7.91	667	438	
RG	671.8	7	12:50	7.7	8.05	616	403	
RG	679.3	7	1:20	8.8	7.96	570	375	
RG	686.3	7	2:15	8.7	8.24	601	393	
RG	696.4	7	2:55	8.4	8.13	592	391	
RG	712.6	7	3:50	9.8	8.17	602	393	
RG	723.6	7	4:35	7.1	8.22	600	397	
RG	731.1	7	5:00	6.0	8.09	624	412	

Type	Distance (km)	Day	Time	Temp (C)	pH	EC (μS cm^{-1})	TDS (mg L^{-1})	Notes
RG	738.8	8	8:30	3.5	8.11	599	399	
RG	747.5	8	8:55	3.4	7.64	610	400	
RG	772.4	8	10:50	6.3	8.5	785	520	
RG	780.2	8	11:55	10.6	7.98	729	481	
RG	791.4	8	na	12.5	8.21	689	457	
RG	797.2	8	12:55	11.6	8.17	719	473	
RG	801.3	8	1:10	11.1	8.42	724	481	
RG	806.6	8	1:30	12.5	8.40	838	549	
RG	813.0	8	2:00	12.7	8.44	920	611	
RG	830.2	8	na	17.7	9.22	833	547	
RG	838.5	8	2:50	12.9	8.65	973	639	
RG	841.0	8	3:05	13.6	8.10	993	653	
RG	845.6	8	3:25	15.9	8.21	1112	737	
RG	852.3	8	3:50	14.4	8.10	1285	845	
RG	858.7	8	4:05	15.1	7.85	1466	973	
RG	874.3	8	4:30	14.3	8.47	1396	919	
RG	891.3	9	10:20	8.9	8.25	1514	994	
RG	899.4	9	10:45	7.4	8.16	1512	998	
RG	912.3	9	na	7.7	8.19	1541	1020	
RG	919.5	9	11:35	9.8	8.23	1544	1020	
RG	929.9	9	11:55	10.0	8.00	1733	1140	
RG	935.5	9	12:05	10.1	8.12	1715	1130	
RG	944.7	9	12:30	10.7	8.21	1727	1130	
RG	955.1	9	12:55	13.3	8.50	1619	1070	

Type	Distance (km)	Day	Time	Temp (C)	pH	EC (μS cm^{-1})	TDS (mg L^{-1})	Notes
RG	966.1	9	1:25	13.3	8.56	1570	1020	
RG	979.6	9	2:20	14.0	8.51	1496	987	
RG	987.6	9	2:45	14.1	8.51	1613	1060	
RG	997.6	9	3:15	12.8	8.56	1694	1120	
RG	1005.4	9	3:35	12.5	8.69	1692	1120	
RG	1013.8	9	4:05	14.5	8.59	1682	1070	
RG	1021.6	10	9:00	9.7	8.13	2260	1490	
RG	1034.5	10	9:25	9.6	8.03	2070	1370	
RG	1047.0	10	9:50	12.6	7.83	1835	1200	
RG	1060.1	10	10:15	13.3	7.97	2050	1350	
RG	1072.9	10	11:00	11.7	8.05	2130	1400	
RG	1085.8	10	11:25	12.2	**7.95**	2110	1390	
RG	1098.8	10	12:00	13.1	7.86	2130	1420	
RG	1112.5	10	12:20	13.1	7.95	3020	1990	
RG	1126.0	10	12:45	12.8	8.05	3020	2010	
RG	1139.1	10	1:20	12.9	8.12	3000	1990	
RG	1149.0	10	1:50	12.5	7.97	3440	2280	
D	166.0	4	1:40	4.7	6.96	786	520	
D	195.0	4	2:35	1.1	7.13	488	325	
D	555.6	6	2:10	13.9	7.98	433	285	
D	555.6	6	2:10	12.0	7.83	439	291	
D	601.1	6	4:05	11.3	7.88	625	413	
D	601.1	6	4:05	10.9	8.02	608	404	
D	630.7	6	5:10	10.6	7.88	339	430	

Type	Distance (km)	Day	Time	Temp (C)	pH	EC (μS cm^{-1})	TDS (mg L^{-1})	Notes
D	696.4	7	2:55	12.0	7.98	1237	816	
D	874.8	8	na	na	na	na	na	dry
D	888.2	9	10:20	4.9	7.79	1818	1210	
D	973.6	9	2:00	13.9	8.20	1387	918	
D	982.8	9	2:20	14.7	8.13	1881	1230	
D	991.7	9	3:00	12.4	8.39	2600	1740	
D	1014.0	9	4:05	13.6	8.18	2620	1740	
D	1080.3	10	11:25	13.1	7.86	1950	1290	
D	1139.6	10	1:20	13.5	8.03	3040	1980	
D	1140.1	10	1:30	12.3	7.80	4930	3240	
CC	655.3	7	na	na	na	na	na	dry
CC	671.8	7	12:50	11.8	8.03	1102	727	
CC	679.3	7	1:20	13.7	7.56	723	479	
CC	686.3	7	2:15	13.8	8.04	602	397	
CC	696.4	7	2:55	12.5	7.89	753	498	
CC	712.6	7	3:50	13.6	7.96	777	512	
CC	723.6	7	4:35	12.9	7.94	987	649	
CC	731.1	7	5:00	12.2	7.96	1063	703	
CC	738.8	8	8:30	6.0	7.33	1094	723	
T	85.7	4	10:45	0.5	6.84	96	64	
T	214.6	4	na	na	na	na	na	frozen
T	225.6	4	4:10	0.0	7.29	176	116	
T	318.9	5	11:10	2.5	7.16	461	303	
T	332.5	5	11:48	3.0	7.36	269	178	

Type	Distance (km)	Day	Time	Temp (C)	pH	EC (μS cm^{-1})	TDS (mg L^{-1})	Notes
T	380.6	5	3:00	5.9	7.88	373	244	
T	409.2	3	3:00	2.7	7.85	510	337	
T	UChama	3	3:30	3.0	7.31	407	269	
T	OjoCal	3	4:05	4.1	7.63	740	488	
T	415.3	5	4:25	4.4	7.78	434	286	
T	450.3	6	na	0.5	7.07	112	74	
T	473.7	6	8:30	na	na	na	na	dry
T	482.8	6	na	na	na	na	na	dry
T	637.1	6	na	na	na	na	na	dry
T	650.0	7	na	na	na	na	na	dry

Table J.20: January 2002 stable isotopes, ammonium, total dissolved nitrate (TDN), dissolved organic carbon (DOC), nitrate, and sulfate for selected samples. Bolded values are below threshold or are uncertain. Analyses performed at the University of Arizona. See Table J.13 for detailed sampling station locations.

Type	Distance (km)	$\delta^{18}O$ (per mille)	δD (per mille)	NH_4 (mg L^{-1})	TDN (mg L^{-1})	DOC (mg L^{-1})	NO_3 (mg L^{-1})	SO_4 (mg L^{-1})
RG	50.3	na	na	0.097	na	na	**0.025**	7.3591
RG	61.7	na	na	na	na	na	0.4295	14.9367
RG	79.5	na	na	0.029	na	na	0.2736	14.0365
RG	104.1	-15.2	-107	0.021	na	na	0.2725	11.7144
RG	115.3	-15.1	-106	0.07	na	na	0.6468	11.7571
RG	130.0	na	na	0.01	na	na	0.664	**405.0885**
RG	141.2	na	na	0.162	0.390	2.024	0.5619	12.7782
RG	155.6	-15.0	-106	0.118	na	na	0.1634	12.4688
RG	192.8	-15.1	-106	0.101	0.510	2.044	1.0163	13.2916
RG	225.2	na	na	0.05	na	na	0.9554	25.878
RG	256.9	-14.8	-105	0.013	0.600	2.317	1.4309	25.8185
RG	306.7	-14.8	-105	0.06	na	na	0.7174	22.369
RG	332.5	na	na	0.005	na	na	0.6774	30.4791
RG	359.3	na	na	0.102	0.640	2.045	1.7527	33.2185
RG	384.5	na	na	0.109	na	na	0.6036	29.62
RG	393.9	na	na	0.13	na	na	0.8923	31.6817

Type	Distance (km)	$\delta^{18}O$ (per mille)	δD (per mille)	NH_4 (mg L^{-1})	TDN (mg L^{-1})	DOC (mg L^{-1})	NO_3 (mg L^{-1})	SO_4 (mg L^{-1})
RG	407.4	na	na	0.074	na	na	0.7841	32.4201
RG	415.3	na	na	0.083	na	na	0.6547	37.7061
RG	430.9	-13.8	-100	na	0.400	2.756	0.8801	35.8815
RG	471.0	-13.2	-96	0.077	0.490	3.128	0.7785	44.8547
RG	496.4	na	na	0.008	na	na	0.1892	47.9302
RG	514.8	na	na	0.061	na	na	0.1896	49.0007
RG	533.4	na	na	0.059	na	na	**0.025**	53.9459
RG	547.5	-12.4	-91	0.047	0.630	3.825	0.5504	63.3173
RG	555.6	na	na	0.013	na	na	**0.025**	59.6929
RG	564.9	na	na	0.037	na	na	3.9723	59.0349
RG	570.0	na	na	0.146	na	na	3.862	62.1984
RG	582.9	-12.4	-91	0.016	2.280	8.343	8.3325	67.553
RG	601.1	na	na	0.034	na	na	4.9656	67.6525
RG	614.7	na	na	0.04	na	na	2.8103	71.3397
RG	630.7	-12.2	-90	0.024	na	na	5.2182	71.7733
RG	642.9	na	na	0.052	na	na	1.5679	79.3607
RG	655.3	-11.8	-89	na	1.160	3.982	3.6557	101.4981
RG	671.8	na	na	0.048	na	na	3.5062	92.7952
RG	679.3	na	na	0	na	na	3.5809	91.8893
RG	686.3	na	na	na	na	na	2.862	92.7091
RG	696.4	na	na	0.003	na	na	2.5118	90.3086
RG	712.6	na	na	na	na	na	3.026	90.5058
RG	723.6	na	na	0.011	na	na	4.0787	92.5138

Type	Distance (km)	$\delta^{18}O$ (per mille)	δD (per mille)	NH_4 (mg L^{-1})	TDN (mg L^{-1})	DOC (mg L^{-1})	NO_3 (mg L^{-1})	SO_4 (mg L^{-1})
RG	731.1	-12.1	-89	0.01	1.670	4.119	5.1757	94.4216
RG	738.8	na	na	0.009	na	na	1.9866	89.6758
RG	747.5	na	na	0.027	na	na	2.726	90.9695
RG	772.4	-11.3	-86	0.043	0.840	4.910	1.3524	124.6308
RG	780.2	-7.8	-68	0.032	na	na	**0.025**	131.3923
RG	791.4	-7.0	-65	0.072	na	na	**0.025**	133.0457
RG	797.2	-7.1	-64	0.171	na	na	**0.025**	132.5735
RG	801.3	-7.0	-65	0.156	0.860	4.822	0.8792	134.3005
RG	806.6	-7.4	-67	0.065	na	na	**0.025**	135.2348
RG	813.0	-7.2	-65	0.078	na	na	2.069	136.225
RG	830.2	-7.1	-64	0.069	na	na	**0.025**	138.5609
RG	838.5	-6.6	-62	0.015	na	na	0.1333	141.6889
RG	841.0	-7.5	-66	0.005	0.340	4.170	0.0252	126.3205
RG	845.6	-7.6	-65	0.139	na	na	3.306	200.6235
RG	852.3	na	na	0.028	na	na	2.1345	259.5525
RG	858.7	na	na	0.183	na	na	4.0675	338.414
RG	874.3	na	na	0.019	na	na	1.6475	331.6845
RG	891.3	na	na	0.032	na	na	0.631	355.092
RG	899.4	-7.3	-67	0.082	0.540	4.589	0.2905	351.0305
RG	912.3	na	na	0.056	na	na	0.3275	373.9135
RG	919.5	-7.4	-66	0.091	0.370	4.259	0.358	359.5695
RG	929.9	na	na	0.06	na	na	0.2455	369.9055
RG	935.5	na	na	0.014	na	na	**0.025**	369.1465

Type	Distance (km)	$\delta^{18}O$ (per mille)	δD (per mille)	NH_4 (mg L^{-1})	TDN (mg L^{-1})	DOC (mg L^{-1})	NO_3 (mg L^{-1})	SO_4 (mg L^{-1})
RG	944.7	-7.5	-66	na	0.530	4.978	0.4115	370.1685
RG	955.1	na	na	1.539	na	na	7.4295	334.844
RG	966.1	na	na	0.448	na	na	12.476	319.358
RG	979.6	na	na	0.259	na	na	5.7825	322.375
RG	987.6	na	na	0.103	na	na	5.1045	356.2245
RG	997.6	na	na	0.124	na	na	4.0975	374.3425
RG	1005.4	na	na	0.193	na	na	4.689	359.491
RG	1013.8	-7.8	-68	0.824	2.540	5.879	5.2325	369.4435
RG	1021.6	na	na	0.64	na	na	10.713	495.277
RG	1034.5	na	na	0.444	na	na	10.0745	456.1655
RG	1047.0	na	na	0.791	na	na	1.857	324.71
RG	1060.1	na	na	0.733	na	na	0.795	335.841
RG	1072.9	-9.1	-74	5.315	3.650	9.281	1.8095	330.3285
RG	1085.8	na	na	4.896	na	na	7.18	346.767
RG	1098.8	na	na	2.996	na	na	17.17	382.4945
RG	1112.5	na	na	1.176	na	na	14.414	703.827
RG	1126.0	na	na	0.477	na	na	16.196	718.974
RG	1139.1	na	na	0.245	na	na	13.45	712.034
RG	1149.0	-8.2	-69	1.016	3.150	8.011	14.054	756.82
D	166.0	na	na	0.235	na	na	0.0426	80.503
D	195.0	-13.8	-99	0.176	na	na	0.3825	59.6701
D	555.6	na	na	0.036	na	na	**0.025**	67.2846

Type	Distance (km)	$\delta^{18}O$ (per mille)	δD (per mille)	NH_4 (mg L^{-1})	TDN (mg L^{-1})	DOC (mg L^{-1})	NO_3 (mg L^{-1})	SO_4 (mg L^{-1})
D	555.6	na	na	0.074	na	na	**0.025**	65.6475
D	601.1	na	na	0.082	na	na	0.0312	100.805
D	601.1	na	na	0.062	na	na	0.0662	92.4025
D	630.7	na	na	0.003	na	na	**0.025**	118.0188
D	696.4	-11.3	-85	na	na	na	na	222.4525
D	888.2	-8.1	-68	0.02	0.810	6.365	2.8175	433.567
D	973.6	-7.9	-69	0.207	na	na	1.9645	300.227
D	982.8	-8.7	-73	0.112	na	na	1.316	447.753
D	991.7	-8.5	-71	1.998	2.810	8.343	1.7785	513.07
D	1014.0	-8.6	-71	0.366	1.310	5.726	3.5715	586.724
D	1080.3	-9.8	-73	3.073	3.940	9.200	28.5965	300.469
D	1139.6	na	na	0.331	na	na	13.479	711.17
D	1140.1	na	na	0.213	na	na	1.972	1160.461
CC	671.8	na	na	0.011	na	na	**0.025**	208.2645
CC	679.3	na	na	0.015	na	na	**0.025**	126.7916
CC	686.3	na	na	0.034	na	na	**0.025**	123.905
CC	696.4	na	na	0	na	na	**0.025**	125.382
CC	712.6	na	na	0.048	na	na	**0.025**	130.4854
CC	723.6	na	na	na	na	na	**0.025**	155.059
CC	731.1	-11.2	-85	0.043	0.400	3.796	0.2346	172.9781
CC	738.8	na	na	0.029	na	na	**0.025**	172.699
T	85.7	-15.1	-106	na	na	na	0.7117	4.3218

Type	Distance (km)	$\delta^{18}O$ (per mille)	δD (per mille)	NH_4 (mg L^{-1})	TDN (mg L^{-1})	DOC (mg L^{-1})	NO_3 (mg L^{-1})	SO_4 (mg L^{-1})
T	225.6	-14.9	-105	0.033	na	na	**0.025**	8.9489
T	318.9	-14.1	-99	0.193	na	na	1.6161	134.7274
T	332.5	na	na	na	na	na	2.087	21.3052
T	380.6	-13.0	-90	0.051	na	na	0.4227	24.9809
T	409.2	-11.5	-85	0.034	na	na	0.0769	83.0328
T	UChama	na	na	0.07	na	na	**0.025**	77.7656
T	OjoCal	na	na	0.031	na	na	**0.025**	84.5569
T	415.3	na	na	na	na	na	0.3894	11.6479
T	450.3	-11.5	-81	0.003	na	na	**0.025**	1.9769

Table J.21: Major cations and alkalinity (HCO_3) for selected January 2002 samples. Analyses performed at the New Mexico Bureau of Geology and Mineral Resources. See Table J.13 for detailed sampling station locations.

Type	Distance (km)	Ca (mg L^{-1})	K (mg L^{-1})	Mg (mg L^{-1})	Na (mg L^{-1})	Sr (mg L^{-1})	HCO_3 (mg L^{-1})
RG	141.2	15	1.9	2.7	6.1	0.26	77
RG	192.8	17	2.4	3.1	8.5	0.24	90
RG	256.9	21	3.3	4	15	0.33	112
RG	359.3	24	2.8	5.3	15	0.36	119
RG	430.9	32	2.9	6.2	22	0.55	147
RG	471.0	35	2.9	7.2	23	0.64	153
RG	547.5	44	4	8	36	0.84	178
RG	582.9	43	5.6	7.6	44	0.88	173
RG	655.3	53	5.4	10	67	1.2	206
RG	731.1	52	5.4	9.6	58	1.1	199
RG	772.4	61	5.7	12	82	1.4	220
RG	801.3	46	6.3	13	83	1.4	176
RG	841.0	64	5.4	18	132	1.6	253
RG	899.4	125	7.2	26	166	3.4	134
RG	919.5	116	8.6	25	173	3	130
RG	944.7	125	12	26	208	3.1	119
RG	1013.8	118	13	27	211	3	275
RG	1072.9	136	11	27	298	4	444
RG	1149.0	211	14	45	517	5.7	327
CC	731.1	62	7	15	127	0.88	na

Table J.22: $\delta^{34}S$ and $^{87}Sr/^{86}Sr$ for selected January 2002 samples. Analyses performed at the University of Arizona. See Table J.13 for detailed sampling station locations.

Type	Distance (km)	$\delta^{34}S$ (per mille)	$^{87}Sr/^{86}Sr$	$^{87}Sr/^{86}Sr$ error
RG	471.0	na	0.709745	0.000016
RG	496.4	0.1	na	na
RG	547.5	na	0.709931	0.000010
RG	582.9	0.5	0.710136	0.000010
RG	655.3	na	0.709966	0.000011
RG	731.1	na	0.710000	0.000010
RG	747.5	0.7	na	na
RG	772.4	na	0.710037	0.000013
RG	780.2	0.8	na	na
RG	791.4	2.0	na	na
RG	797.2	2.2	na	na
RG	801.3	2.3	0.710052	0.000011
RG	806.6	2.7	na	na
RG	997.6	1.7	na	na
RG	1005.4	1.6	na	na
RG	1021.6	3.2	na	na
RG	1047.0	2.4	na	na
RG	1072.9	4.5	na	na
CC	731.1	0.8	0.710350	0.000017

Table J.23: August 2002 field parameters. "ncv" = no channel visible. "SAP" = San Acacia pool. See Table J.19 for detailed table explanation.

Type	Distance (km)	Day	Time	Temp (°C)	pH	EC (μS cm^{-1})	TDS (mg L^{-1})	Notes
RG	104.1	21	4:37	19.8	8.42	143	94	
RG	141.2	21	5:55	20.9	9.16	148	98	
RG	192.8	22	7:00	14.5	7.91	462	304	
RG	243.5	22	10:00	17.4	8.75	484	319	
RG	256.9	22	10:40	17.7	9.09	526	349	
RG	306.7	22	12:10	21.8	8.81	423	278	
RG	359.3	22	3:10	23.6	8.81	296	195	
RG	384.5	22	3:45	24.4	8.75	302	199	
RG	430.9	22	4:40	24.8	8.36	391	259	
RG	471.0	23	11:05	23.4	7.93	497	328	
RG	547.5	23	12:20	24.9	8.27	424	281	
RG	582.9	23	2:10	31.0	8.30	570	352	
RG	630.7	23	na	na	na	na	na	dry
RG	655.3	23	4:10	26.7	8.31	792	523	
RG	731.1	24	9:05	20.0	8.35	1110	731	
RG	772.4	24	na	na	na	na	na	ncv
RG	791.4	24	11:53	26.9	8.47	773	510	
RG	801.3	24	12:30	25.0	7.63	825	546	
RG	841.0	24	1:50	26.9	8.31	789	517	
RG	899.4	24	3:55	28.4	8.12	853	566	
RG	919.5	24	4:45	28.8	8.10	840	556	
RG	955.1	25	7:40	22.7	8.16	942	624	

Type	Distance (km)	Day	Time	Temp (^{o}C)	pH	EC (μS cm^{-1})	TDS (mg L^{-1})	Notes
RG	1013.8	25	10:20	28.9	8.31	1020	673	
RG	1112.5	25	12:50	29.4	8.08	3120	2050	
RG	1149.0	25	3:25	33.1	8.23	3350	2340	
D	195.0	22	7:35	16.1	9.03	507	337	
D	696.4	24	7:55	17.6	7.88	1073	709	
D	874.8	24	2:25	28.3	8.24	1569	1030	
D	888.2	24	3:00	35.0	9.15	747	493	
D	973.6	25	8:20	20.0	8.02	1264	834	
D	982.8	25	8:45	21.6	7.91	1605	1060	
D	991.7	25	na	23.2	8.13	1910	1260	
D	1014.0	25	10:00	24.1	8.09	2080	1370	
CC	731.1	24	9:35	20.9	8.15	1311	865	
T	225.6	22	na	na	na	na	na	dry
T	318.9	22	1:25	19.3	8.02	392	261	
T	409.2	23	9:40	19.4	7.99	496	328	
T	637.1	23	3:25	30.0	8.49	786	524	
SAP	655.0	15	3:58	20.9	8.06	72900	48700	

Table J.24: August 2002 stable isotopes, ammonium, total dissolved nitrate (TDN), dissolved organic carbon (DOC), nitrate, and sulfate. Bolded values are below threshold or are uncertain. Analyses performed at the University of Arizona, except for the San Acacia pool sample, which was analyzed at the New Mexico Bureau of Geology and Mineral Resources. See Table J.13 for detailed sampling station locations.

Type	Distance (km)	$\delta^{18}O$ (per mille)	δD (per mille)	NH_4 (mg L^{-1})	TDN (mg L^{-1})	DOC (mg L^{-1})	NO_3 (mg L^{-1})	SO_4 (mg L^{-1})
RG	104.1	-13.0	-97	0.036	0.061	1.883	**0.000**	12.70
RG	141.2	-12.3	-97	0.053	0.047	1.681	**0.000**	12.75
RG	192.8	-10.7	-89	0.037	0.167	3.168	0.000	35.18
RG	243.5	-9.1	-79	0.023	0.194	4.040	**0.001**	55.33
RG	256.9	-6.7	-69	0.026	0.234	6.049	**0.003**	58.03
RG	306.7	-12.6	-96	0.033	0.127	0.877	0.308	21.98
RG	359.3	-13.2	-99	0.040	0.194	1.496	0.182	35.95
RG	384.5	-12.8	-96	0.053	0.194	1.354	0.011	34.27
RG	430.9	-10.0	-78	0.020	0.154	2.593	0.033	84.78
RG	471.0	-10.0	-78	0.025	0.220	4.108	0.000	4.85
RG	547.5	-9.8	-79	0.019	0.180	2.770	0.025	78.73
RG	582.9	-9.8	-79	0.023	0.380	2.973	0.439	82.33
RG	655.3	-10.4	-82	0.015	0.287	2.973	0.288	127.30
RG	731.1	-9.9	-79	0.038	0.101	2.981	0.027	200.15
RG	791.4	-6.6	-63	0.177	0.154	6.277	**0.001**	141.49
RG	801.3	-7.8	-64	0.126	0.247	8.277	**0.003**	142.39
RG	841.0	-6.6	-63	0.088	0.260	4.724	**0.000**	139.83
RG	899.4	-6.5	-62	0.088	0.433	4.630	0.082	144.76
RG	919.5	-6.4	-62	0.026	0.287	8.196	0.123	146.58
RG	955.1	-6.5	-62	0.048	0.446	4.141	0.316	150.01

Type	Distance (km)	$\delta^{18}O$ (per mille)	δD (per mille)	NH_4 (mg L^{-1})	TDN (mg L^{-1})	DOC (mg L^{-1})	NO_3 (mg L^{-1})	SO_4 (mg L^{-1})
RG	1013.8	-7.8	-68	0.521	1.218	3.956	0.436	175.42
RG	1112.5	-7.2	-65	0.018	1.364	13.515	1.148	539.77
RG	1149.0	-6.4	-61	0.037	0.872	5.383	0.335	624.8
D	195.0	-12.1	-93	0.037	0.127	2.704	**0.000**	56.06
D	696.4	-10.8	-84	0.026	0.074	2.489	**0.000**	171.96
D	874.8	-6.9	-63	0.064	0.446	4.129	0.330	352.95
D	888.2	-5.9	-60	0.033	0.327	6.075	**0.001**	151.09
D	973.6	-7.2	-66	0.123	0.699	3.900	0.701	237.90
D	982.8	-7.7	-68	0.066	0.606	3.657	0.000	309.54
D	991.7	-7.0	-65	0.131	1.204	7.481	1.060	340.75
D	1014.0	-6.5	-62	0.077	1.258	4.504	0.444	434.10
CC	731.1	-10.2	-81	0.037	0.114	5.135	0.035	182.24
T	318.9	-13.7	-100	0.093	0.526	0.776	0.441	67.73
T	409.2	-9.7	-78	0.014	0.234	3.556	0.072	90.32
T	637.1	-3.9	-33	0.038	2.069	8.181	2.142	141.51
SAP	655.0	na	na	na	na	na	**0.1**	13300

Table J.25: Major cations, alkalinity (HCO_3), chloride and bromide for August 2002 samples. Bolded values are below threshold or are uncertain. Analyses performed at the University of Arizona (Cl^- and Br^-, except for San Acacia pool) and the New Mexico Bureau of Geology and Mineral Resources. See Table J.13 for detailed sampling station locations.

Type	Distance (km)	Ca (mg L^{-1})	K (mg L^{-1})	Mg (mg L^{-1})	Na (mg L^{-1})	Sr (mg L^{-1})	HCO_3 (mg L^{-1})	Cl (mg L^{-1})	Br (mg L^{-1})
RG	104.1	18	2.4	2.3	6.5	0.11	68	1.38	**0.000**
RG	141.2	20	2.4	2.9	7.1	0.13	77	1.65	**0.000**
RG	192.8	42	5.9	7.4	41	0.31	191	8.90	0.074
RG	243.5	29	6.8	6.5	65	0.25	192	17.01	0.161
RG	256.9	21	7.5	7.2	75	0.23	184	18.54	0.163
RG	306.7	24	3.2	6.4	19	0.18	117	11.44	0.062
RG	359.3	31	3.2	6.7	15	0.22	121	7.34	0.059
RG	384.5	33	3.2	6.7	24	0.24	128	7.79	0.068
RG	430.9	49	2.5	8.7	81	0.39	131	3.75	**0.770**
RG	471.0	48	3	8	19	0.4	131	0.30	0.000
RG	547.5	49	3.1	8.5	22	0.41	139	5.53	0.031
RG	582.9	56	5.6	8.5	29	0.43	170	19.74	0.088
RG	655.3	87	6.2	13	70	0.74	240	45.42	0.149
RG	731.1	93	7.3	16	137	0.96	254	120.30	0.220
RG	791.4	54	6.8	14	92	0.78	171	63.54	0.179
RG	801.3	56	6.7	14	88	0.69	174	63.61	0.177
RG	841.0	58	7.1	14	95	0.72	183	67.29	0.178
RG	899.4	61	7	15	96	0.73	187	69.15	0.170
RG	919.5	62	7	14	97	0.75	186	69.79	0.167
RG	955.1	63	7.3	15	100	0.74	192	73.69	0.178

Type	Distance (km)	Ca (mg L^{-1})	K (mg L^{-1})	Mg (mg L^{-1})	Na (mg L^{-1})	Sr (mg L^{-1})	HCO_3 (mg L^{-1})	Cl (mg L^{-1})	Br (mg L^{-1})
RG	1013.8	76	8.6	16	120	0.85	204	91.47	0.196
RG	1112.5	246	11	27	470	2.99	386	559.57	0.891
RG	1149.0	250	13	48	550	2.97	270	715.44	0.726
D	195.0	30	6.4	5.8	68	0.22	187	17.45	0.166
D	696.4	91	6.1	14	118	0.77	266	78.25	0.161
D	874.8	128	10	26	190	1.23	264	135.35	0.295
D	888.2	39	7.3	13	95	0.6	127	71.66	0.182
D	973.6	114	8.6	18	154	1.08	274	104.80	0.180
D	982.8	157	9.6	25	180	1.38	330	151.69	0.385
D	991.7	105	22	23	286	1.64	390	206.75	0.340
D	1014.0	152	8.2	26	321	1.49	378	238.90	0.360
CC	731.1	100	7.9	18	160	1.01	276	100.14	0.181
T	318.9	35	2.7	7.6	27	0.25	105	9.49	0.058
T	409.2	48	2.2	8.3	17	0.41	122	2.90	0.025
T	637.1	50	7.1	7.4	89	0.58	115	68.41	0.100
SAP	655.0	1450	310	2500	18000	43	510	32300	28

Table J.26: January 2003 field parameters. "ncv" = no channel visible. See Table J.19 for detailed table explanation.

Type	Distance (km)	Day	Time	Temp (°C)	pH	EC (μS cm^{-1})	TDS (mg L^{-1})	Notes
RG	104.1	11	4:10	0.7	7.55	78.6	118.5	
RG	141.2	11	4:50	0.5	**7.66**	88.2	134.2	
RG	192.8	12	8:20	-0.5	7.68	144	212	
RG	256.9	12	10:10	1.3	8.44	139	209	
RG	306.7	12	11:40	7.5	8.55	113	173	
RG	359.3	12	1:45	7.8	8.53	161	245	
RG	384.5	12	2:20	7.6	**8.28**	166	248	
RG	430.9	12	3:20	6.5	8.32	220	332	
RG	471.0	13	8:00	2.7	8.52	255	387	
RG	547.5	13	9:00	3.7	8.29	306	468	
RG	582.9	13	10:30	6.2	8.36	337	513	
RG	630.7	13	11:10	6.3	8.62	343	519	
RG	655.3	13	12:10	9	8.49	396	600	
RG	731.1	13	1:25	11.7	8.13	660	996	
RG	772.4	13	na	na	na	na	na	ncv
RG	791.4	14	11:20	9.1	7.97	481	727	
RG	801.3	14	11:55	9.8	8.21	481	731	
RG	841.0	14	1:00	12.3	8.21	551	834	
RG	899.4	14	2:25	14.3	8.25	830	1257	
RG	919.5	14	3:00	16.3	8.24	870	1322	
RG	955.1	14	3:45	16.5	8.59	929	1402	

Type	Distance (km)	Day	Time	Temp (°C)	pH	EC (μS cm^{-1})	TDS (mg L^{-1})	Notes
RG	1013.8	15	10:25	9.9	8.5	1000	1524	
RG	1112.5	15	11:35	14	7.93	1730	2610	
RG	1149.0	15	12:15	13.6	8.05	2190	3360	
D	195.0	12	8:05	-0.6	8.65	288	436	
D	696.4	13	12:45	13	8.08	663	1010	
D	874.8	14	na	na	na	na	na	dry
D	888.2	14	2:00	12.9	8.48	660	982	
D	973.6	15	8:45	8.6	8.15	832	1264	
D	982.8	15	9:10	7.6	8.07	1110	1678	
D	991.7	15	9:40	8.6	8.11	1780	2710	
D	1014.0	15	10:15	11	8.06	1920	2890	
CC	731.1	13	1:40	7.7	8.38	391	593	
T	225.6	12	9:25	0.4	8.19	109	165.8	
T	318.9	12	12:40	15.2	8.09	204	309	
T	409.2	12	2:50	6.8	8.31	380	577	
T	637.1	13	11:25	5.3	8.5	2080	3190	

Table J.27: January 2003 stable isotopes, ammonium, dissolved organic carbon (DOC), nitrate, sulfate, chloride and bromide. Bolded values are below threshold. Analyses performed at the University of Arizona. See Table J.13 for detailed sampling station locations.

Type	Distance (km)	$\delta^{18}O$ (per mille)	δD (per mille)	NH_4 (mg L^{-1})	DOC (mg L^{-1})	NO_4 (mg L^{-1})	SO_4 (mg L^{-1})	Cl (mg L^{-1})	Br (mg L^{-1})
RG	104.1	-14.3	-103	0.0233	0.906	0.0699	13.44	1.68	**0.0000**
RG	141.2	-14.3	-104	0.0336	0.976	0.0172	13.22	1.80	**0.0000**
RG	192.8	-14.1	-102	0.0145	1.272	0.0429	16.19	3.00	0.0217
RG	256.9	-13.8	-101	0.0595	1.333	0.0068	22.47	5.14	0.2018
RG	306.7	-13.7	-101	0.0201	1.008	0.1003	19.96	4.61	0.0453
RG	359.3	-13.7	-100	0.0152	0.843	0.3117	31.99	6.07	0.0352
RG	384.5	-13.6	-99	0.0204	0.837	0.2391	32.03	5.99	0.0414
RG	430.9	-12.7	-95	0.0241	1.376	0.1793	51.12	9.10	0.0369
RG	471.0	-11.6	-89	0.0420	1.673	0.0761	61.91	8.84	0.0391
RG	547.5	-11.1	-86	0.0193	1.260	0.0863	74.84	16.89	0.0745
RG	582.9	-11.3	-87	0.0349	2.080	1.1069	77.90	31.25	0.0827
RG	630.7	-11.1	-86	0.0303	1.662	0.5018	81.53	29.27	0.0857
RG	655.3	-11.0	-85	0.0382	2.178	0.3830	142.81	58.37	0.1293
RG	731.1	-11.0	-85	0.0501	1.950	0.2963	106.78	42.05	0.1023
RG	791.4	-7.2	-65	0.2187	3.955	0.0886	153.87	67.36	0.1791
RG	801.3	-6.9	-63	0.1069	3.690	0.0926	147.01	65.24	0.1594
RG	841.0	-6.3	-60	0.0446	2.841	0.0074	137.99	94.39	0.1673
RG	899.4	-7.1	-64	0.0114	2.837	0.0000	334.49	122.67	0.2295
RG	919.5	-6.9	-64	0.0271	2.556	0.0125	350.76	147.24	0.3495
RG	955.1	-7.4	-67	0.3152	3.257	2.0524	333.80	183.00	0.2765

Type	Distance (km)	$\delta^{18}O$ (per mille)	δD (per mille)	NH_4 (mg L^{-1})	DOC (mg L^{-1})	NO_4 (mg L^{-1})	SO_4 (mg L^{-1})	Cl (mg L^{-1})	Br (mg L^{-1})
RG	1013.8	-7.5	-67	0.0714	3.205	1.1952	371.63	198.75	0.3295
RG	1112.5	-8.1	-68	0.4778	4.293	3.0167	486.32	469.49	0.2816
RG	1149.0	-8.0	-68	1.2356	4.708	2.4488	583.68	684.40	0.5181
D	195.0	-13.2	-97	0.0448	1.701	0.0313	55.62	15.33	0.1351
D	696.4	-10.8	-84	0.0252	2.083	0.1243	200.72	102.75	0.1690
D	888.2	-8.5	-71	0.0650	4.050	0.8799	195.83	79.14	0.1720
D	973.6	-7.5	-67	0.1810	2.432	0.8380	293.58	124.35	0.1530
D	982.8	-8.4	-72	0.3233	3.067	0.6740	435.21	181.19	0.2875
D	991.7	-8.2	-69	2.1318	4.439	1.0249	506.72	363.96	0.3085
D	1014.0	-8.3	-71	0.4465	2.922	0.1385	619.23	423.53	0.5015
CC	731.1	-10.6	-83	0.0275	1.917	0.0396	185.23	117.32	0.1636
T	225.6	-14.0	-103	0.0105	0.842	0.0000	16.63	1.34	**0.0000**
T	318.9	-13.6	-99	0.0740	0.357	0.3748	68.58	10.60	0.0465
T	409.2	-10.2	-81	0.0177	2.361	0.0061	125.33	18.75	0.0911
T	637.1	-8.4	-65	0.0167	2.070	0.0883	992.36	376.58	0.7100

Table J.28: Hardness ($CaCO_3$), major cations, and alkalinity (HCO_3) for January 2003 samples. Analyses performed at the New Mexico Bureau of Geology and Mineral Resources. See Table J.13 for detailed sampling station locations.

Type	Distance (km)	$CaCO_3$ (mg L^{-1})	Ca (mg L^{-1})	K (mg L^{-1})	Mg (mg L^{-1})	Na (mg L^{-1})	Sr (mg L^{-1})	HCO_3 (mg L^{-1})
RG	104.1	49	16	1.8	2.3	6.3	0.10	62
RG	141.2	53	17	1.9	2.5	7.6	0.12	73
RG	192.8	66	20	2.5	3.9	11	0.15	94
RG	256.9	66	21	3.3	3.4	19	0.15	110
RG	306.7	71	21	2.9	4.5	18	0.15	104
RG	359.3	92	28	2.9	5.4	19	0.20	119
RG	384.5	99	30	2.9	5.9	18	0.20	128
RG	430.9	135	40	3.2	8.5	25	0.30	153
RG	471.0	150	45	3.2	9.2	28	0.36	165
RG	547.5	163	51	3.6	8.6	36	0.40	192
RG	582.9	166	50	6.2	9.9	50	0.41	201
RG	630.7	151	44	5.8	10	50	0.43	202
RG	655.3	181	57	6	9.5	69	0.55	222
RG	731.1	245	75	6.3	14	144	0.92	274
RG	791.4	181	51	7	13	92	0.70	203
RG	801.3	179	47	6.8	15	91	0.80	203
RG	841.0	226	59	6.9	19	104	0.90	252
RG	899.4	368	103	7.4	27	160	1.60	290
RG	919.5	339	98	8.8	23	166	1.50	268
RG	955.1	364	98	15	29	198	1.70	260

Type	Distance (km)	$CaCO_3$ (mg L^{-1})	Ca (mg L^{-1})	K (mg L^{-1})	Mg (mg L^{-1})	Na (mg L^{-1})	Sr (mg L^{-1})	HCO_3 (mg L^{-1})
RG	1013.8	373	103	15	28	229	1.70	304
RG	1112.5	465	140	13	28	430	2.80	333
RG	1149.0	599	174	12	40	484	3.30	344
D	195.0	91	28	5.2	5.1	59	0.21	191
D	696.4	255	79	6.9	14	142	0.88	306
D	888.2	246	77	14	13	141	0.83	367
D	973.6	351	101	9.6	24	152	1.50	317
D	982.8	474	147	9.4	26	212	1.90	380
D	991.7	373	90	39	36	463	2.90	499
D	1014.0	451	131	8.4	30	474	2.30	423
CC	731.1	181	56	5.7	10	63	0.52	210
T	225.6	60	19	3.2	3.1	9.7	0.17	91
T	318.9	111	31	2.8	8.2	27	0.24	108
T	409.2	221	62	3.1	16	43	0.56	220
T	637.1	692	160	11	71	430	3.10	314

Table J.29: August 2003 field parameters. "ncv" = no channel visible. See Table J.19 for detailed table explanation.

Type	Distance (km)	Day	Time	Temp (°C)	pH	EC (μS cm^{-1})	TDS (mg L^{-1})	Notes
RG	104.1	15	18:15	18.4	8.33	104	68.6	
RG	141.2	15	19:03	22.4	8.93	128	117	
RG	192.8	16	7:09	16.1	8.24	320	221	
RG	256.9	16	9:07	15.9	9.21	423	274	
RG	306.7	16	10:40	18.6	8.62	251	165	
RG	359.3	16	12:45	21.1	8.65	292	192	
RG	384.5	16	14:00	23	8.67	296	196	
RG	430.9	16	15:08	24.6	8.08	283	186	
RG	471.0	16	16:25	23	7.86	304	201	
RG	547.5	17	7:21	18.7	8.17	352	228	
RG	582.9	17	8:00	na	na	na	na	dry
RG	630.7	17	9:00	na	na	na	na	dry
RG	655.3	17	10:53	22.7	8.04	908	603	
RG	731.1	17	13:00	29.5	8.25	1318	867	looks like CC water
RG	772.4	17	na	na	na	na	na	ncv
RG	791.4	17	15:40	28.3	28.3	843	558	
RG	801.3	17	16:15	25.4	7.46	870	572	
RG	841.0	18	8:20	23.6	8.08	849	563	
RG	899.4	18	10:00	24.9	7.82	846	563	
RG	919.5	18	10:45	26	8	860	556	
RG	955.1	18	11:55	27.2	8.02	858	570	

Type	Distance (km)	Day	Time	Temp (°C)	pH	EC (μS cm^{-1})	TDS (mg L^{-1})	Notes
RG	1013.8	18	15:30	31.4	8.07	916	613	sample taken from Corchesne Bridge
RG	1112.5	18	18:00	34.7	8.36	3730	2460	
RG	1149.0	18	19:05	31.1	8.15	5510	3690	
D	195.0	16	7:35	16.4	9.01	1219	805	
D	696.4	17	11:50	22.4	7.91	951	629	
D	874.8	18	na	na	na	na	na	dry
D	888.2	18	9:30	24.4	8.05	962	635	
D	973.6	18	13:00	28.2	8.39	1106	729	
D	982.8	18	13:25	33	7.98	1020	676	
D	991.7	18	14:00	30.3	8.1	1502	986	
D	1014.0	18	16:36	30.7	7.74	2400	1560	
CC	731.1	17	na	na	na	na	na	dry
T	225.6	16	na	na	na	na	na	dry
T	318.9	16	11:15	18.3	7.95	382	257	
T	409.2	16	14:25	20	8.11	263	172	Storm upstream, debris in river
T	637.1	17	9:20	22	7.43	2390	1580	sfas

Table J.30: August 2003 stable isotopes, dissolved organic carbon (DOC), nitrate, sulfate, chloride and bromide. Analyses performed at the University of Arizona. See Table J.13 for detailed sampling station locations.

Type	Distance (km)	$\delta^{18}O$ (per mille)	δD (per mille)	DOC (mg L^{-1})	NO_3 (mg L^{-1})	SO_4 (mg L^{-1})	Cl (mg L^{-1})	Br (mg L^{-1})
RG	104.1	-12.8	-96	3.079	0.0182	9.896	1.027	0.008
RG	141.2	-12.7	-97	2.828	na	8.760	2.621	0.008
RG	192.8	-10.8	-88	3.478	na	24.270	5.879	0.044
RG	256.9	-7.2	-70	3.804	2.846	33.195	11.001	0.080
RG	306.7	-11.5	-89	2.623	1.051	20.756	7.259	0.060
RG	359.3	-12.7	-95	2.455	1.047	41.170	7.655	0.067
RG	384.5	-12.6	-94	2.302	0.4	39.838	7.021	0.046
RG	430.9	-11.2	-86	3.639	0.6244	47.913	3.419	0.011
RG	471.0	-11.3	-86	4.219	0.644	50.179	4.047	0.018
RG	547.5	-11.0	-85	4.219	0.3988	54.136	5.551	0.020
RG	655.3	-10.1	-81	3.762	0.7453	148.229	72.269	0.151
RG	731.1	-10.1	-81	4.798	0.019645	233.451	150.934	0.207
RG	791.4	-6.7	-63	3.3	na	158.212	79.318	0.195
RG	801.3	-6.7	-64	5.61	na	154.674	77.036	0.199
RG	841.0	-6.5	-61	5.359	na	153.897	82.278	0.197
RG	899.4	-6.4	-61	5.545	0.2199	154.526	82.628	0.193
RG	919.5	-6.3	-61	3.939	0.3831	154.364	83.059	0.188
RG	955.1	-6.3	-60	3.927	0.5954	155.438	84.405	0.202
RG	1013.8	-6.1	-59	4.851	1.3367	176.186	102.972	0.212
RG	1112.5	-5.9	-60	5.952	na	681.113	804.926	0.755
RG	1149.0	-4.2	-50	10.14	na	1110.274	1324.497	1.184

Type	Distance (km)	$\delta^{18}O$ (per mille)	δD (per mille)	DOC (mg L^{-1})	NO_3 (mg L^{-1})	SO_4 (mg L^{-1})	Cl (mg L^{-1})	Br (mg L^{-1})
D	200	-2.3	-41	20.46	na	129.382	55.790	0.535
D	696.4	-10.7	-84	3.801	0.0096	168.964	79.237	0.150
D	888.2	-6.2	-60	5.509	na	189.048	98.907	0.225
D	973.6	-7.2	-67	4.671	0.0092	230.019	117.175	0.220
D	982.8	-6.1	-60	4.69	0.2351	221.841	106.035	0.248
D	991.7	-6.4	-61	5.643	2.185585	263.422	221.328	0.305
D	1014.0	-7.2	-65	4.669	0.170886	487.046	360.323	0.465
T	318.9	-13.3	-97	1.487	1.0853	117.178	6.048	0.036
T	409.2	-11.2	-85	4.54	0.8579	49.661	2.099	0.012
T	637.1	-2.4	-19	11.03	7.311629	1028.903	89.953	0.137

Table J.31: Major cations and alkalinity (HCO_3) for August 2003 samples. Analyses performed at the New Mexico Bureau of Geology and Mineral Resources. See Table J.13 for detailed sampling station locations.

Type	Distance (km)	Ca (mg L^{-1})	K (mg L^{-1})	Mg (mg L^{-1})	Na (mg L^{-1})	Sr (mg L^{-1})	HCO_3 (mg L^{-1})
RG	104.1	12	2.1	2	5.1	0.09	46
RG	141.2	14	2.2	2.3	5.7	0.1	53
RG	192.8	30	5.3	6.6	29	0.25	157
RG	256.9	15	6.1	5.9	50	0.19	136
RG	306.7	20	3.6	6.4	25	0.18	115
RG	359.3	29	3.1	7.3	24	0.23	117
RG	384.5	32	3.1	7.2	24	0.25	127
RG	430.9	36	2.3	6.4	15	0.28	109
RG	471.0	37	2.4	6.7	16	0.3	113
RG	547.5	41	2.8	7.2	20	0.32	123
RG	655.3	76	6.8	17	103	0.84	239
RG	731.1	90	8.1	22	190	1.2	288
RG	791.4	48	6.9	17	118	0.93	176
RG	801.3	51	6.9	17	112	0.75	185
RG	841.0	53	7.4	17	119	0.76	193
RG	899.4	52	7.4	17	118	0.74	187
RG	919.5	52	7.4	17	117	0.74	193
RG	955.1	55	7.7	17	122	0.73	192
RG	1013.8	55	8.6	17	136	0.82	194
RG	1112.5	175	13	46	624	3.6	236
RG	1149.0	217	15	82	977	4.8	176

Type	Distance (km)	Ca (mg L^{-1})	K (mg L^{-1})	Mg (mg L^{-1})	Na (mg L^{-1})	Sr (mg L^{-1})	HCO_3 (mg L^{-1})
D	195.0	29	50	26	223	0.48	546
D	696.4	80	5.5	15	116	0.76	255
D	888.2	62	7.3	18	123	0.94	190
D	973.6	84	8.3	21	141	1	221
D	982.8	68	9.2	18	147	0.89	193
D	991.7	77	19	23	232	1.6	245
D	1014.0	100	8.9	30	436	1.5	362
T	318.9	50	2	12	19	0.32	90
T	409.2	36	2	5.5	12	0.27	98
T	637.1	186	12	36	374	2.4	251